University of Naples Federico II
Department of Stuctures
for Engineering and Architecture

Silvia Costanzo

CHEVRON CONCENTRICALLY BRACED FRAMES: PROPOSAL OF SEISMIC DESIGN CRITERIA FOR THE NEXT GENERATION OF EUROCODES.

PhD Thesis
XXVIII Cycle

Tutor:
Prof. Eng. R. Landolfo

Co-tutor:
PhD Eng. M. D'Aniello

Coordinator:
Prof. Eng. L. Rosati

Doctorate of Philosophy
Engineering of Construction

To my family,

To the jingles-knight,

To father, professor A. Parrella.

Alla mia famiglia,

Al cavaliere dei campanelli,

A Padre, professore A. Parrella.

There are these two young fish swimming along, and they happen to meet an older fish swimming the other way, who nods at them and says, "Morning, boys, how's the water?" And the two young fish swim on for a bit, and then eventually one of them looks over at the other and goes, "What the hell is water?"

Ci sono due giovani pesci che nuotano uno vicino all'altro e incontrano un pesce più anziano che, nuotando in direzione opposta, fa loro un cenno di saluto e poi dice "Buongiorno ragazzi. Com'è l'acqua?" I due giovani pesci continuano a nuotare per un po', e poi uno dei due guarda l'altro e gli chiede "ma cosa diavolo è l'acqua?"

D.F.W.

The measure of intelligence is the ability to change

La misura dell'intelligenza è data dalla capacità di cambiare quando è necessario.

A.E.

Memento audere semper
Remember to dare always.
Ricorda di osare sempre.

G.D.

«In una goccia d'acqua possono esserci miriadi di mondi simili.»
«Non annegano?»
«Sanno nuotare tutti»

«In a drop of water may there be myriads of similar worlds»
«Don't they drown?»
«Everybody can swim»

I.S.

Il completamento di questa tesi di dottorato rappresenta il momento conclusivo di un percorso di crescita iniziato in un punto non univocamente definito di alcuni anni fa, e costantemente caratterizzato da un mix esplosivo di emozioni contrastanti che – questo è certo – mi hanno sospinto (a volte trascinato) molto lontano da dove sono partita.
In questo momento particolare, in cui avanza la stanchezza insieme a un pizzico di elettrictià e commozione, sento di volere deporre (del tutto momentaneamente) l'armatura; di rubare cinque minuti al vorticoso procedere del tempo; un momento soltanto, per fermarmi a riflettere sulla piccola enormità di questo passaggio e ringraziare brevemente le persone che, ognuno a suo modo, sono stati gli attori e compagni di questa avventura.
Chi mi conosce, troverà alquanto inaspettato questo improvviso sentimentalismo a un passo dalla fine...
Chi mi conosce DAVVERO, sa che al di sotto della scorza dura e del sarcasmo di gomma, sotterro una tenerezza sconfinata e nascondo un rapporto con cose e persone che è puramente, solamente, profondamente emotivo.
Prima di tutto (sebbene sospetto lo troveranno piuttosto melenso) voglio ringraziare la mia famigia: i miei genitori al cui costante esempio e ai cui sacrifici, devo qualsiasi cosa di buono ho, ho fatto, e di buono sono. Lorenzo, mio primo irremovibile compagno e alleato, sangue del mio sangue. Fabiola, per essere parte di noi e ricordarci sempre quanto la propria felicità e il proprio piacere, oltre che i propri impegni, siano questioni serissime.

Immediatamente dopo, voglio dire grazie al Prof. Landolfo, alle cui doti comunicative e al cui carisma devo la scintilla che cinque anni fa ha acceso la mia passione per questa materia, avendo avuto in qualche modo il potere di cambiare le mie scelte. A lui voglio dire grazie per avere, negli anni, saputo sapientemente accogliere, rispettare e coltivare la mia curiosità, il mio impegno e devozione con illuminata sapienza. Soprattutto voglio ringraziarlo per la fiducia che ha riposto in me fin dall'inizio e per essere sempre stato presente e disponibile per aiutarmi a superare qualsiasi ostacolo e difficoltà.
A Mario D'Aniello, mio sparring-partner su questo ed altri ring, voglio dire grazie per essermi stato irremovibilmente vicino in questo percorso e nelle trincee della vita da adulti (lui adorerà la metafora militare). La sua severità, instransigenza, ma anche inaspettata dolcezza (ok, raramente) mi hanno vigorosamente impedito di attestarmi o anche solo indugiare su qualsiasi livello non fosse almeno più del meglio cui potevo aspirare. A Mario, che mi ha dolorosamente obbligato sempre al massimo che potevo, ottenendo luminosamente (spero) il massimo possibile.
A Giuseppe La Manna Ambrosino, che mi ha affiancato nel principio più primordiale di questo percorso, e che più di tutti ha saputo essere sempre forero di quella leggerezza insostenibile ma consapevole, finestra sul modo di fuori, e di quei sorrisi liberi che sono stati, nei momenti difficili, più benefici di qualsiasi parola di conforto o risultato conseguito.
A Roberto, che più di chiunque altro ha condiviso con me il senso di spaesamento, a volte persino di insoddisfazione e indeterminatezza, e che con me ha imparato a trovare la chiave di volta per combatterlo

con uno scherzo, ridendo di noi stessi e degli altri, tenendoci saldi e vicini, combattendo le paure semplicemente giocando, come eterni bambini.

A Mariana, per la sua dolcezza talmente innata e scofinata, che ha il potere di trasmettere pace persino a un tornado.

A Elvira, Tatiana, Francesco e Lucrezia e a tutti i colleghi del dip. con cui divido tutte le giornate, buone o cattive che siano.

Al Prof. De Martino, per riuscire sempre... sempre...(SEMPRE!!!) a strapparmi un sorriso.

Infine a Filippo, spuntato all'improvviso in un punto a caso e la cui confusione, agitazione, ma anche vitalità e buon umore mi hanno tenuto compagnia e sono così ingombranti che non riesco più del tutto a separarli da questi ultimi giorni di tsnunami.

Quando mi sento troppo confusa e/ spaventata e un collasso progressivo sta per cominciare a diffondersi (il pancake collapse resta comunque il mio preferito), e la terra comincia a tremare sotto i piedi, l'idea di svegliarmi e affrontare un altro banale, assolutamente comune e noioso giorno nelle trincee del dipartimento, mi restituisce sempre quella solidità che scaturisce dalla certezza che lì dentro imparo, mi diverto, mi dispero, mi arrabbio a morte, ma comunque... so esattamente dove mi trovo.

Non a caso... ci si circonda di esperti di stabilità, terremoti, eventi catastrofici di genere vario e effetti connessi.

E alla fine di tutto questo mi domando solo... chissà, se poi dopo tutto sono in grado di "cavalcare la tigre".

The accomplishment of this PhD thesis is the achievement of a growing training path started at a time not univocally fixed a few years ago, constantly characterized by an explosive mixture of contrasting emotions - that's for sure - that brought me (sometimes pushed me) very far from my starting point.

At this particular moment, when tiredness and a little bit emotion are approaching, I feel to put down my armor (just temporarily); to steel few minutes, just a moment to stop and to reflect on this huge, small step and to briefly thank the people who, each in a different way, have been actors and partners in my adventure.

Anyone knows me, probably will find quite strange such sweet and emotional approach, at the end of this path.

Anyone REALLY knows me is probably aware that under the hard exterior, endless tenderness is hidden and my actual relationship with people and things are in truth purely, solely, deeply emotional.

First of all (even though I guess they will find it too mushy) I want to thanks my family: my parents whose constant example and sacrifices, solely determined every good thing I have got, I have done, I am. Lorenzo, my first rocky allied, blood of my blood. Fabiola, to be part of us and to teach us, that our own happiness and pleasure, beside our businesses, are very serious stuff.

Immediately after that, I want to say thanks to Prof. Landolfo, whose ability to communicate and whose charisma, five years ago lighted my passion for structural engineering, having somehow the power to change my choices. As my tutor, he was always able, over the years, to embrace, respect and grow my curiosity, my efforts and devotion with illuminated wisdom. Especially, I want to thank him for trust he put in me, since the beginning and for being always available to help me in overcoming any difficulty and hurdle.

To Mario D'Aniello, my sparring-partners on this and other rings, I want to say thanks, for being always close to me during this training path and in the trenches of adult life (he will love the military metaphor). His severity, rigidity, but also unexpected sweetness (ok, quite rarely) have vigorously prevented me from accepting at any performance level lower than the best I could aspire. To Mario, who strongly forced me to achieve the maximum I could, obtaining (I hope so, at least) my maximum possible.

A Giuseppe La Manna Ambrosino, who helped me in the beginning of this path; he always brought unbearable lightness, with simple smiles that, in difficult times, have been more beneficial than any possible words of comfort or result achieved.

To Roberto, who more than anyone else has shared with me the sense of disorientation, sometimes even of dissatisfaction and uncertainty, and together with me has learned to find the key to fight all these feelings by means of a joke, kidding ourselves and others, staying close and steady, fighting our fears simply by playing as eternal children.

To Mariana, for her innate and endless sweetness, which have the power to instill peace even in a tornado.

To Elvira, Tatiana, Francesco and Lucrezia and to all the colleagues of the department I always share my days with, good or bad, as well.

Finally to Filippo, suddenly appeared at a random point; his confusion, agitation, but also vitality and good humor are huge enough that I cannot easily separate them from the latter tsunami-days.

When I feel too scared and/or confused and a progressive collapse is a to start and widespread (anyway… the pancake collapse is still my favorite), and the earth begins to tremble under my feet, the idea of waking up and to spend another trivial, absolutely ordinary and boring day in trenches of the department, always gives me the robustness that comes from the certainty that just there… I can learn, have fun, be distressed, get angry to death, but still ... I know exactly where I am.

Not by chance ... I selected my people among experts in stability, earthquakes, other catastrophic events and related induced effects.

In the end, I'm just wondering… who knows, all things considered, I can "ride the tiger".

Chapter I

INTRODUCTION

Chapter II

SEISMIC DESIGN OF STEEL STRUCTURES IN THE FRAMEWORK OF EN-1998

Chapter III

SEISMIC BEHAVIOUR OF CONCENTRICALLY BRACED FRAMES

Chapter I

Introduction

1.1 GENERALITY

The Eurocodes are the set of standards (EN) for structural design, integrating all specific National experiences and research outputs, together with the expertise of CEN Technical Committee 250 (CEN/TC250) and of International Technical and Scientific Organisations.

Nowadays, the research activity on the European scene is characterized by growing efforts within the field of the codification review and development, in which both academic institutions, and technical committees and organizations of designers and practice engineers are strongly involved.

About ten years after the official entry into force of Eurocodes, their employment in the professional practice together with the new research achievements contribute to highlight some lacks, inconsistencies and ineffectiveness of several requirements.

Therefore, the need to upgrade the current codes consistently to the advances of knowledge in structural engineering and to include the new findings from research is emerged.

With this aim, the European Commission has recently established a six year program of work devoted to develop the next generation of Eurocodes; CEN Technical Committee (CEN/TC 250 'Structural Eurocodes') will coordinate this activity, availing itself of further sub-working groups (SC/WG) of renown experts specifically established to develop the next version of each Eurocode, and eventual additional standards including new technologies. In detail WG2 deals with the seismic design of steel and composite structures (i.e. Chapters 6 and 7 of EN 1998).

In addition to the CEN Technical Committee, in Europe the TC13 (i.e. Technical Committee 13 – seismic design) of the European Convention for Constructional Steelwork (ECCS) (which is an international federation of national steelwork associations) is working on the improvement of seismic design codes for steel structures since the '70s of the last century.

One of the most interesting outcomes achieved by TC13 is the publication of the book "Assessment of EC8 Provisions for Seismic Design of Steel Structures" (Landolfo Editor, 2013) which summarizes all issues in the current version of EN 1998-1 needing clarification and/or development, aiming at contributing to a new generation of European codes.

Moreover, the Research for Coal and Steel Fund, managed by the European Commission, is currently supporting numerous research projects involving universities, research centres and private companies, also devoted to development and dissemination of several issues concerning the codification in the field of steel constructions.

1.2 MOTIVATIONS AND SCOPE OF RESEARCH

Within the framework, outlined in Section 1.1, of European research devoted to standardization review and upgrading, the research activity developed within this thesis, specifically focus the attention on steel structural buildings equipped with concentric bracings in chevron configuration (CCBs).

Chevron concentric bracings (also known as inverted-V concentric bracings) are commonly used in the seismic design of multi-storey steel buildings owing to both their architectural functionality, thus allowing the placement of doorways, windows and plants, and high structural efficiency.

Such systems are generally characterized by large lateral stiffness, which guarantees the fulfilment of both codified drift limitations and stability. On the other hand, the structural performance against strong seismic action involving large ductility demand is strongly dependent on the type of the developed plastic mechanism; experimental evidence and numerical analyses show that CCBs do not experience the expected plastic engagement and consequently exhibit poor seismic performance.

Indeed, nonlinear behaviour of chevron concentrically braced frames is still affected by several uncertainties, mainly due to the complexity of the hysteretic behaviour of bracing members under cyclic axial loading, which is not easy to be accurately predicted.

Moreover, for frames equipped with chevron bracings, the braced-intercepted beam is characterized by large displacement demand at brace intersection in the post-buckling range (Shen *et al.*, 2014, 2015; D'Aniello *et al.*, 2015) and in the most of cases, it is not possible to achieve the yielding of the braces in tension, while severe ductility demand is imposed to braces under compression.

In the light of these considerations, in Eurocode 8 the bracings in chevron configuration are expected to provide smaller energy dissipation, respect to X-CBFs. Indeed, in EN-1998 a q factor equal to 4.0 in both DCM and DCH is allowed for X-CBFs, while q = 2 and q = 2.5 are used for chevron concentrically braced frames in DCM and DCH, respectively.

However, it is worth noting that, differently from European framework, in North-American seismic codes (CSA S16-0, 2009, FEMA P-750, 2009; AISC 341-10, 2010) the response modification factor (and thus the expected dissipative capacity of the system) is independent from the bracing configuration, and the ductility class of the structure is determined only by the requirements (more strict in higher ductility classes) met at design stage.

These considerations motivated the research activity developed in this PhD thesis, which is addressed to identify the issues in the current codes needing revision and upgrading, in order to investigate the possibility to attain larger ductility capability and to define different and improved level of seismic performance.

The main objectives of this thesis can be summarized as follow:

i. to provide a critical review of existing design criteria provided by EN 1998-1 for chevron concentrically braced frames.
ii. to assess the effectiveness of codified design provisions with reference to both European and North-American framework of seismic standards.
iii. to characterize the seismic response of CCBs by identifying the main structural parameters affecting the performance against lateral loads.
iv. to develop new design criteria to improve ductility and seismic performance against seismic action of chevron bracings, for next generation of Eurocodes.

1.3 FRAMING OF THE ACTIVITY

The main goals of this thesis have been achieved by means of the constant support of a deep theoretical study, constituted by a critical analysis of the state of art, existing standard framework, *etc*, and, on the other hand, by means of a comprehensive numerical activity aimed at assessing the effectiveness of current codified provisions, at supporting the development of new design criteria and at validating their effectiveness in improving the seismic performance of chevron bracings.
In detail, the thesis is organized in 9 Chapters, whose contents can be briefly summarized as follow:

- Chapter I: Introduction

  The framework of research activity is outlined together with the motivations and scopes of the thesis.

- Chapter II: *Seismic design of steel structures in the framework of EN 1998*

  The seismic design of steel buildings in the framework of Eurocode 8 is deeply described and discussed with reference to the most common seismic resistant systems. With this regard, EN1998-1 is examined, with special focus on Section 6, dealing with the specific provisions for steel structures.

- Chapter III: *Seismic behaviour of concentrically braced frames*

  The seismic behaviour of concentrically braced frames is deeply described and discussed. The framework of existing seismic design provisions is outlined with reference to design criteria and rules provided by both European and North-American seismic codes; the hysteretic response of bracing members under axial loading is widely discussed. A critical review of existing literature on seismic design criteria devoted to improve seismic performance of concentrically braced frames is outlined. The main technological aspects to be accounted for in the design of ductile concentrically braced frames are briefly addressed.

- Chapter IV: *Brace modelling*

  The aspects related to accurate modelling of bracing members are discussed. A parametric analysis is carried out and discussed to evaluate the accuracy of modelling assumptions commonly used in literature; in detail, the influence of the initial camber, the material modelling, the type of force-based element, the number of integration points and the number of fibres are examined.

- Chapter V: *The influence of beam flexural stiffness*

  The nonlinear response of chevron concentrically braced frames is deeply influenced by the flexural behaviour of the brace-intercepted beam. In order to investigate this aspect, a comprehensive numerical parametric study is presented and described in this Chapter. In particular, the influence of beam flexural stiffness is analysed ranging the ratio between the beam flexural stiffness and the braces vertical rigidity, the beam span, the interstorey height and the brace slenderness. Analytical equations based on the regression of numerical data are proposed as design aid in order to select the optimal beam stiffness.

- Chapter VI: *Conceptual design issues and Dual-CCBs*

  Conceptual design issues concerning the use of concentrically braced frames in seismic resistant steel building are discussed, comparing the structural efficiency and the convenience of employing of both chevron and X-CBFs. In addition, the use of chevron bracings in dual-frames is discussed; with this regard, the need to investigate the influence of joints behaviour on the overall response of steel multi-storey frames emerged and suggested developing refined models in which the moment-rotation behaviour of joints is specifically accounted for.

- Chapter VII: *Assessment of codified seismic design provisions for CCBs*

  A parametric study devoted to assess the effectiveness of seismic design provisions and codified criteria given by both European (EN-1998) and North-American (AISC 341 and CSA S16-09) codes is described and discussed. With this regard, a comprehensive set of non-linear dynamic analyses is performed on low, medium and high rise residential buildings designed according to the examined codes. In addition further cases are added in order to evaluate the influence of some modifications applied to the requirements provided by EN-1998.
- Chapter VIII: *Proposal of seismic design criteria for CCBs for the next generation of Eurocodes*

  New design criteria for chevron concentrically braced frames are proposed, devoted to improve the ductility and the structural efficiency of this type of system under severe earthquake. An extensive numerical parametric study devoted to validate the design assumptions and to verify the effectiveness of proposed design criteria is shown. Low, medium and high rise residential buildings are designed according to the proposed procedure and the relevant seismic response is monitored and compared to the performance exhibited by frames designed according to EN-1998.
- Chapter IX: *Conclusion*

  Conclusive remarks are drafted.

1.4 REFERENCES

American Institute of Steel Construction, Inc. (AISC). (2010). Seismic Provisions for Structural Steel Buildings. ANSI/AISC Standard 341-10. AISC, Chicago, Illinois

CSA. (2009) Design of Steel Structures, CSA-S16-09, Canadian Standards Association, Toronto, ON

EN 1998-1-1 (2005) Eurocode 8: Design of structures for earthquake resistance – Part 1: General rules, seismic actions and rules for buildings. CEN; 2005.

FEMA P-750. (2009). Recommended Seismic Provisions for New Buildings and Other Structures. Federal Emergency Management Agency - U.S. Department of Homeland Security - Building Seismic Safety Council of the National Institute of Building Sciences

Landolfo R., editor (2013) Assessment of EC8 provisions for seismic design of steel structures. Technical Committee 13 — Seismic Design, No 131/2013. ECCS, 2013.

M. D'Aniello, S. Costanzo S., Landolfo R. (2015) The influence of beam stiffness on seismic response of chevron concentric bracings. *Journal of Constructional Steel Research,* Vol. 112, pp 305–324.

Shen J., Wen R., Akbas B., J.Shen, Doran B., Uckan E. (2014), Seismic demand on brace-intersected beams in two-story X-braced frames. *Engineering Structures*, vol.76, pp 295-312.

Shen J., Wen R., Akbas B., (2015) Mechanisms in Two-story X-braced Frames. *Journal of Constructional Steel Research*, vol. 106, pp 258-277, 2015.

Chapter II

Seismic design of steel structures in the framework of EN 1998

2.1 INTRODUCTION

EN 1998, also referred as Eurocode 8 or EC8, represents the ensemble of European codes for "Design of structures for earthquake resistance". EC8 applies to the design and construction of buildings and civil engineering in seismic areas.

The objectives of seismic design in accordance with Eurocode 8 are explicitly stated. Its purposes are to ensure that in the event of earthquakes the following design objectives are guaranteed:

- human lives are protected;
- damage is limited;
- structures important for civil protection remain

operational.
In this Section, the seismic design of steel buildings in the framework of EC8 is deeply described and discussed with reference to the most common seismic resistant systems. With this regard, EN1998-1 (General rules, seismic actions and rules for buildings) is examined hereinafter, with special focus on Section 6, which dealing with the specific provisions for steel structures. However, in order to provide a comprehensive framework of seismic design of steel structures according to EC8, also few general aspects are examined, covering material independent-rules as seismic performance levels, types of seismic action, and types of structural analysis.

2.2 GENERALITY AND MATERIAL INDEPENDENT RULES

2.2.1 *Performance requirements and compliance criteria*

According to EN 1998-1 (2005) two performance levels (each with associated objectives) should be considered in seismic design of buildings as follow:

(i) No-collapse requirement: the protection of human lives under rare seismic actions, by preventing the local or global collapse of the structure and preserving the structural integrity with a residual load capacity; in the framework of EN 1990 (basis of design) this performance level is compliant to the

Ultimate Limit State (ULS), being related to the safety of occupants and to the failure of the whole system.

(ii) Damage limitation requirement: the limitation of both structural and non-structural damage in case of frequent seismic events (namely seismic action having a larger probability of occurrence than the design seismic action), also without associated limitations of use, the costs of which would be disproportionately high in comparison with the costs of the structure itself. This second requirement is associated in the framework of EN 1990 with the Serviceability Limit State (SLS), being mainly related to functionality and economical losses.

The objectives associated to the first performance level are achieved by capacity design philosophy, namely by applying a set design and detailing rules devoted to assure a ductile global failure mechanism by mean of the strength hierarchy concept.

The second performance level is satisfied by controlling the displacements of the structure (namely by limiting the interstorey drift ratio) in order to assure the integrity of both non-structural (i.e. infill walls, claddings, plants, etc.) and structural elements under frequent earthquakes. It should be noted that some damage to non-structural parts are acceptable if no significant limitation of use of the building occurs and no severe economical efforts are needed for repairing.

According to the Performance Based Seismic Design (PBSD) the performance levels are associated to two relevant levels of intensity of seismic action. The definition of the hazard levels is referred to the national annexes; however, EN 1998 recommends the following seismic action intensity:

- *Design (ULS) earthquake*: it corresponds to a seismic action having 10% exceedance probability in 50 years (namely a mean return period equal to 475 years) for the ultimate limit state (i.e. collapse prevention). At this limit state the design seismic action for structures of ordinary importance over rock is termed "reference" seismic action.

- *Damage limitation (SLS) earthquake*: it corresponds to a seismic action having 10% exceedance probability in 10 years (namely a mean return period equal to 95 years) for the control of both structural and non-structural damage.

In case of essential or large occupancy facilities the code recommends to guarantee an enhanced performance than the case of ordinary structures. This objective is achieved by modifying the hazard level (namely the mean return period) by multiplying the reference seismic action by the importance factor, γ_I. The importance factor values are determined by the national annexes; however EN 1998-1 classifies building structures in 4 importance classes depending on: i) the consequences of collapse for human life; ii) their importance for public safety and civil protection in the immediate post-earthquake period and; iii) the social and economic consequences of collapse. Appropriate values of γ_I are associated at each building categories and both are summarized in Table 2.1.

Table 2.1 Importance factors for each building category.

Importance class	Buildings	γ_I
I	Buildings of minor importance for public safety, e.g. agricultural buildings, etc.	0,8
II	Ordinary buildings, not belonging in the other categories.	1,0
III	Buildings whose seismic resistance is of importance in view of the consequences associated with a collapse, e.g. schools, assembly halls, cultural institutions, etc.	1,2
IV	Buildings whose integrity during earthquakes is of vital importance for civil protection, e.g. hospitals, fire stations, power plants, etc.	1,4

2.2.1.1 Design for ultimate limit state

As already mentioned, the fulfillment of no-collapse requirements is mainly related to the human life safety and to avoid failure of the whole system. However, it should be noted that satisfaction of this limit state does not entails the need for the system to behave elastically under the reference seismic action; conversely, controlled inelastic deformations are acceptable/desirable if restrained in selected zones (so-called "dissipative zones") and provided the stability of the whole system.

Indeed, the selected ductile zones act as structural fuses, responsible to dissipate the incoming seismic energy, without involving too severe demand on the system. Moreover, capacity design criteria should be met in order to achieve global failure mechanism.

Therefore, the design against ULS requires verifications on both lateral resistance and energy-dissipation capacity.

2.2.1.2 Design for Damage Limitation limit state

According to EC8, the damage limitation requirement for buildings is fulfilled by limiting the interstorey drift ratio demand under the frequent (SLS) seismic action.

In general, the member size is affected by drift ratio limitations; thereby it is advisable to verify the compliance with the damage limitation requirement, before proceeding with dimensioning and detailing of members to satisfy the no-collapse requirement.

The interstorey drift ratio demand d_r for a generic storey is evaluated as the relative displacement between the storey under consideration and the one below.

It should be determined under the frequent seismic action, which is defined by multiplying the entire elastic response spectrum of the design seismic action for 5% damping by the same factor v that reflects the effect of the mean return periods of these two seismic actions.

The following limitation should be verified:

$$v \cdot d_r \geq \alpha \cdot h \tag{2.1}$$

where:

α is the limit related to the typology of non-structural elements;

d_r is the interstorey drift demand;

h is the storey height;

v is a displacement reduction factor depending on the importance class of the building, whose values are specified in the National Annex.

The limits for α depend on the type of non-structural elements and are set as follows:

- 0.5 %, if there are brittle non-structural elements attached to the structure so that they are forced to follow structural deformations (normally partitions);
- 0.75 %, if non-structural elements (partitions) attached to the structure as above are ductile;
- 1 %, if no non-structural elements are attached to the structure.

2.2.1.3 Near collapse limit-state

Beside the two performance level described above, Eurocode 8 implicitly provides a third limit state (Near Collapse Limit State or Collapse Prevention Limit State) aimed at avoiding global collapse of the whole system under very strong and rare seismic event.

This third limit state does not require specific rules for higher seismic action intensity level, but it is considered to be fulfilled by adopting in the design process specific measures to increase the reliability of the structural system.

The following prescription should be observed:

- To prefer simple, compact and regular structural layout both in plan and elevation;
- To avoid brittle failure and premature formation of unstable mechanisms;
- To design and detail the dissipative zones in order to ensure the more extent as possible plastic engagement and stable hysteretic behaviour.
- To perform structural analysis by using accurate and adequate structural models.
- To design the foundation to be stiff and strong enough to transfer uniformly the action from the super-structure to the ground.
- To properly detail design documents including all relevant information regarding materials properties, dimensions of all members, constructional details and erection instruction, if appropriate. Moreover, provisions for the necessary quality controls should also be given, specifying also the verification methods to be used for the elements of primary structural importance.

2.2.2 *Basic representation of seismic action: elastic response spectrum*

Within the scope of EN 1998 the earthquake motion at a given point on the surface is represented by an elastic ground acceleration response spectrum (see Fig. 2.2); the horizontal seismic action is described by two orthogonal components assumed as being independent and represented by the same response spectrum.

The elastic response spectrum of the design seismic action (namely that corresponding to collapse prevention) is characterized by the reference ground acceleration on rock, α_{gR}, which should be provided by national seismic-zoning maps.

The spectrum is shown in Fig. 2.1 and it is constituted by three main regions having constant properties, namely the spectral acceleration (for period T from T_B to T_C), the spectral pseudo-velocity (for period T from T_C to T_D) and spectral displacement (for period $T > T_D$).

For the horizontal components of the seismic action, the elastic response spectrum $S_e(T)$ is defined by the following expressions:

$$0 < T < T_B \qquad S_d(T) = a_g \cdot S \cdot \left(1 + \frac{T}{T_B} \cdot (\eta \cdot 2,5 - 1)\right)$$

$$T_B < T < T_C \qquad S_e(T) = a_g \cdot S \cdot \eta \cdot 2.5$$

$$T_C < T < T_D \qquad S_e(T) = a_g \cdot S \cdot \eta \cdot 2.5 \cdot \left(\frac{T_C}{T}\right)$$

$$T > T_D \qquad S_e(T) = a_g \cdot S \cdot \eta \cdot 2.5 \cdot \left(\frac{T_C \cdot T_D}{T^2}\right)$$

(2.2)

Where:

$S_e(T)$ is the elastic response spectrum;

a_g is the design ground acceleration obtained as $a_g = \gamma_I \cdot a_{gR}$

T_B is the lower limit of the period of the constant spectral acceleration branch

T_C is the upper limit of the period of the constant spectral acceleration branch

T_D is the value defining the beginning of constant displacement response range of the spectrum

S is the soil factor

η is the damping correction factor $\eta = \sqrt{10/(5+\xi)}$, being ξ the viscous damping ratio expressed as a percentage.

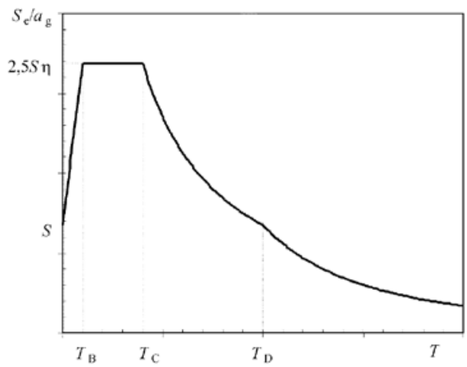

Figure 2.1 The shape of elastic acceleration response spectra in EC8.

The code recommends using two types of spectra (either described by Eq. (2.2)) depending on the earthquake magnitude:

(i) Type 1 spectrum, for low magnitude earthquakes (see Fig.

2.2a);

(ii) Type 2 spectrum, for low magnitude earthquakes with surface magnitude less than 5.5 at close distances (see Fig. 2.2b).

The values to be assumed for T_B, T_C, T_D and S in Eq. (2.2) depend on both the ground type and the spectral shape (namely type 1 or 2 spectrum), and can be found in the National Annex. However, the Eurocode provides recommended values for the spectral parameters.

In the EN1998-1(2005) five standard soil types are considered, as follows:

- Type A: rock, with an average shear wave velocity v_s in the top 30*m*, larger than 800*m*/*s*;
- Type B: very dense sand or gravel, or very stiff clay, with v_s ranging within 360 to 800*m*/*s*;
- Type C: medium-dense sand or gravel, or stiff clay, with v_s ranging within 180*m*/*s* to 360*m*/*s*;
- Type D: loose-to-medium sand or gravel, or soft-to-firm clay, with v_s lesser than 180*m*/*s*;
- Type E: 5m to 20*m* thick soil with v_s lesser than 360*m*/*s*, underlain by rock.

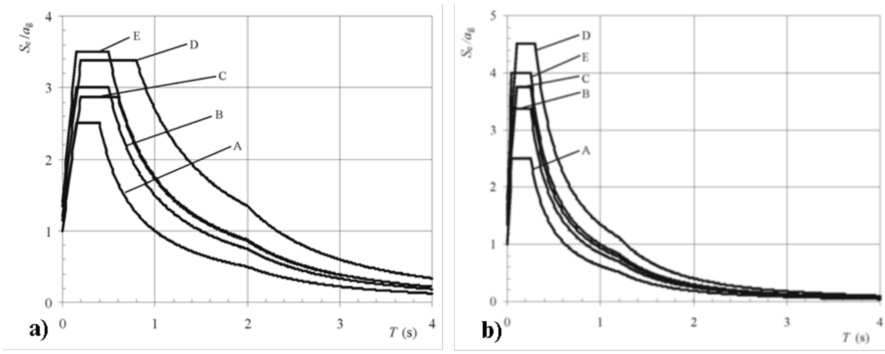

Figure 2.2 Elastic response spectra recommended in EC8: Type 1 (a) and 2 (b)

The same spectral shape is assumed for all the considered limit states; the seismic hazard level is defined by multiply the reference peak ground acceleration on bedrock a_{gR} by the importance factor γ_I, given according to the following equation to obtain the seismic demand at damage limitation and near collapse limit state:

$$\gamma_I = \left(\frac{T_{LR}}{T_L} \right)^{-1/3} \tag{2.3}$$

Where T_L is the return period and T_{LR} is the reference return period for which the reference seismic action should be computed.

2.2.3 *Design of buildings*

2.2.3.1 Design concept and ductility class

As already mentioned, EN 1998 accounts for the capability of the systems to dissipate the incoming energy through inelastic deformations of selected ductile zones.

Consistently to this approach, the code allows assuming design seismic force smaller than those related to a linear elastic response, but also avoiding sophisticated non-linear structural analyses at the design stage.

In fact, an elastic analysis based on a response spectrum reduced with respect to the elastic one, called the "design spectrum", can be performed.

The design spectrum is obtained by multiplying the elastic response spectrum by the behaviour factor q (EN 1998-1 3.2.2.5(2)), which is directly related to the dissipation capacity of the system under consideration. The q factor can be approximately intended as the ratio between the seismic forces that a single degree of freedom system equivalent to the real structure would experience if its response would be completely elastic (with 5% equivalent viscous damping) and the seismic forces that may be used in the design (EN 1998-1 3.2.2.5(3)) (see Fig. 2.3). For regular system, it is given by the following expression:

$$q = \frac{a_u}{a_1} \cdot q_0 \tag{2.4}$$

where q_o is the reference value of the behaviour factor for regular structural systems, while α_u/α_1 is the plastic redistribution parameter accounting for the system overstrength due to redundancy. The parameter α_1 is the multiplier of the horizontal seismic design action to reach the first plastic resistance in the system and α_u is the multiplier of the horizontal seismic design action corresponding to the formation of a global mechanism.

Generally, two different concepts can be applied to the design seismic resistant systems according to EN 1998:

(i) Low-dissipative structural behaviour;

(ii) Dissipative structural behaviour.

In concept (i) the seismic-induced effects can be evaluated by on the basis of an elastic global analysis neglecting the non-linear behaviour. In this case, the behaviour factor assumed in the calculation must be less than 2.

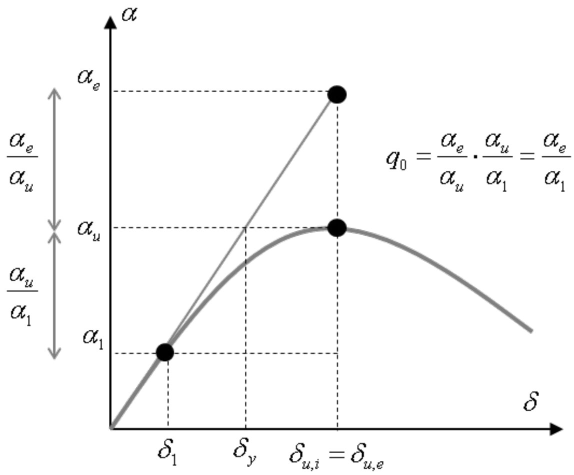

Figure 2.3 Behaviour factor defined according to EN 1998

Systems designed according to this approach, belong to Low Ductility Class (DCL); the required strength of structural members and connection are assessed according to EN 1993, without considering additional capacity design requirements. Moreover, in case of very low seismic zones ($\gamma_I \cdot S \cdot a_{gR} < 0.05\,\mathrm{g}$) EC8 allows neglecting the seismic action in design of buildings.

According to concept (ii) the capability of the system to dissipate the seismic energy through the inelastic deformation of dissipative zones is exploited. The systems designed according to concept (ii) may belong to two ductility classes, namely Medium Ductility Class (DCM) and High Ductility Class (DCH) depending on the level of expected plastic engagement.

A specific force reduction factor is correlated at each class and the Eurocode 8 prescribes specific rules at both global and local level to assure the achievement of the expected level of ductility. With this regard, EC8 adopts the EN 1993 classification for cross sections relating it to the restrictions to the value of the behaviour factor q: cross-sectional class 1, 2 or 3 is required corresponding to behaviour factors in the range [1.5, 2.0], while class 1 or 2 is required for q in a range [2.0, 4.0]; Only class 1 is allowed for DCH ($q > 4.0$).

Once fixed the behaviour factor q suitable for the structure to be calculated, the design response spectrum is obtained starting from the elastic spectrum (see Eq. 2.2) using the following equations:

$$0 < T < T_B \quad S_e(T) = a_g \cdot S \cdot \left(\frac{2}{3} + \frac{T}{T_B} \cdot \left(\frac{2.5}{q} - \frac{2}{3} \right) \right)$$

$$T_B < T < T_C \quad S_e(T) = a_g \cdot S \cdot \frac{2.5}{q}$$

$$T_C < T < T_D \quad S_e(T) \begin{cases} = a_g \cdot S \cdot \frac{2.5}{q} \cdot \frac{T_C}{T} \\ \geq \beta a_g \end{cases}$$

$$T > T_D \quad S_e(T) \begin{cases} = a_g \cdot S \cdot \frac{2.5}{q} \cdot \left(\frac{T_C \cdot T_D}{T^2} \right) \\ \geq \beta a_g \end{cases}$$

(2.5)

The parameter β is the lower bound factor for the horizontal design spectrum, whose appropriate value should be provided by the National Annex. However, EC8 recommends to assume β = 0.2.

2.2.3.2 Basic principles of conceptual design

EN 1998-1 provides a set of requirements aimed at mitigating seismic vulnerability within acceptable costs. With this regard, the following concepts and objectives, fundamental to achieve satisfactorily and safe seismic performance, should be pursued in the design process:

- structural simplicity: simply morphology must be realized both in plan and elevation in order to obtain clear and direct paths of transmission of seismic forces, thus reducing the uncertainties and allowing simply modelling and analyses.
- uniformity, symmetry and redundancy: seismic resistant

elements should be uniformly and symmetrical distributed both in plan and elevation, in order to avoid the concentrations of stress or ductility demand potentially leading to non-ductile collapse mechanisms. The redundancy of the system should be improved in order to allow the redistribution of action across the whole system.

- bi-directional resistance and stiffness: the seismic resistant elements should be located in orthogonal directions in-plan in order to provide similar lateral strength and stiffness.
- torsional resistance and stiffness: building structures should possess adequate torsional resistance and stiffness in order to limit torsional motions which tend to stress the structural systems in a non-uniform way;
- diaphragmatic behaviour at storey level: the floor slabs must behave as rigid diaphragm in order to uniformly transfer the horizontal action to the vertical structural systems
- adequate foundation: the foundations should be able to ensure that the whole building may be subjected to a uniform seismic excitation.

2.3 DESIGN CRITERIA AND DETAILING RULES IN STEEL BUILDINGS

2.3.1 *Steel seismic resistant systems and behaviour factor*

Table 2.2 summarizes the upper limits for the behaviour factors q for the steel structural schemes depicted in Fig. 2.4.

The ratio α_u/α_1 may be obtained from nonlinear static "pushover" global analysis according to EC8, but is limited to 1.6. However, Eurocode 8 proposes some reference values, as follows:

– 1 for inverted pendulum structures;

– 1.1 for one-storey frames;

– 1.2 for one-bay multistorey frames, eccentric bracing or dual systems with moment resisting frames and concentrically braced frames;

– 1.3 for multistorey multi-bay moment-resisting frames.

Hereinafter, the most common used steel seismic resistant typologies (namely moment-resisting frames and both concentrically and eccentrically braced frames) are described and the relevant design provisions and detailing rules are examined.

Table 2.2 Upper limit of reference values of behaviour factors for systems regular in elevation.

Structural type	Ductility Class	
	DCM	DCH
a) Moment resisting frame	4	$5(\alpha_u/\alpha_1)$
b) Frame with concentric bracings		
Diagonal bracings	4	4
V-bracings	2	2,5
c) Frame with eccentric bracings	4	$5(\alpha_u/\alpha_1)$
d) Inverted pendulum	2	$2(\alpha_u/\alpha_1)$
e) Structures with concrete cores or concrete walls	Are those defined for reinforced concrete structures	
f) Moment resisting frame with concentric bracings	4	$4(\alpha_u/\alpha_1)$
g) Moment resisting frames with infills		
Unconnected concrete or masonry infills, in contact with the frame	2	2
Connected reinforced concrete infills	Are those defined for composite steel – concrete buildings	
Infills isolated from moment frame (see moment frame)	4	$5(\alpha_u/\alpha_1)$

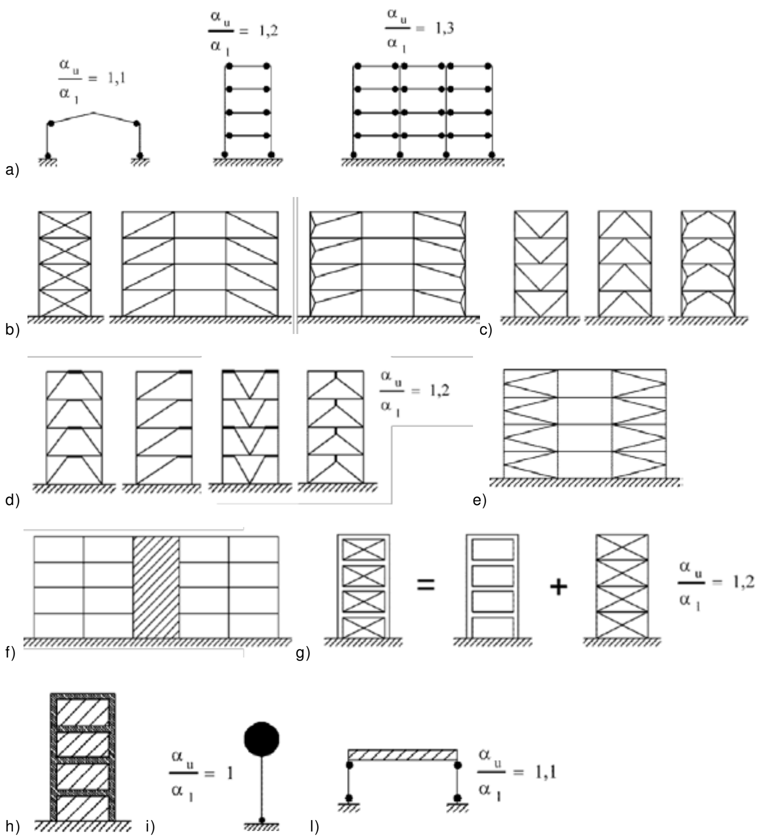

Figure 2.4 The structural schemes accounted for EC8: a) Moment resisting frames; b) Frames with concentrically diagonal bracings; c) Frame with V bracings; d) Frames with eccentric bracings e) K-braced frames (not allowed in seismic areas); f) Structures with concrete cores or concrete walls; g) Moment resisting frame combined with concentric bracing; h) Moment resisting frames combined with infills; i) Inverted pendulum with dissipative zones at the column base; l) Inverted pendulum with dissipative zones in columns.

2.3.2 *Design criteria and detailing rules for Moment Resisting Frames*

In order to assure a ductile global mechanism, Moment Resisting Frames (MRFs) are typically designed in order to restrain the inelastic deformation at the end of the beams avoiding the formation of plastic hinges in the columns, except for the base of the frame in multi-storey buildings, and also for the top storey for the single-storey frames.

Indeed, such type mechanism (often referred as "weak beam/strong column" behaviour) is expected to guarantee significant energy dissipation capacity exploiting the larger rotation capacity of the beams (see Fig. 2.5a).

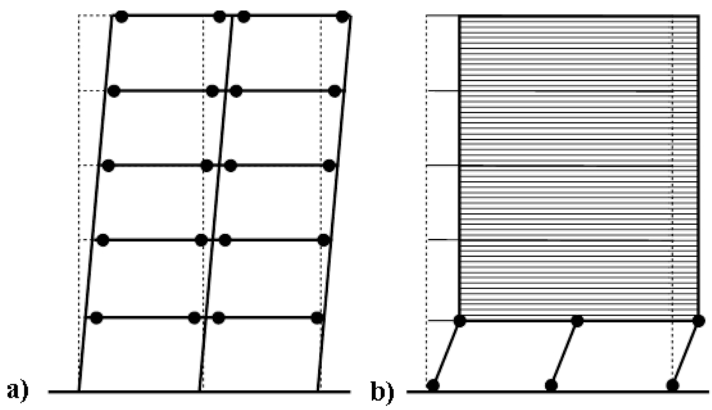

Figure 2.5 Moment Resisting frames: (a) "weak beam-strong column" mechanism; (b) soft-storey mechanism

Conversely, plasticisation of columns (namely “weak beam/strong column”) would result in premature storey collapse with consequent significant loss of lateral strength and stiffness (see Fig. 2.5b).

Aside from the requirements regarding the member cross-sectional classes related to the ductility class (see Section 2.2.3.1), the Code requires additional rules for MRFs in order to avoid that compression and shear forces acting on beams could impair the full plastic moment resistance and the rotation capacity.

To this aim, EN 1998 states that the following inequalities should be verified at the location where the formation of hinges:

$$\frac{M_{Ed}}{M_{pl,Rd}} \leq 1 \tag{2.6}$$

$$\frac{N_{Ed}}{N_{pl,Rd}} \leq 0.15 \tag{2.7}$$

$$\frac{V_{Ed}}{V_{pl,Rd}} \leq 0.5 \tag{2.8}$$

being M_{Ed}, N_{Ed} and V_{Ed} the required strengths, while $M_{\mathrm{pl,Rd}}$, $N_{\mathrm{pl,Rd}}$ and $V_{\mathrm{pl,Rd}}$ are design resistances in accordance with EN 1993.

In general, owing to the presence of floor diaphragm axial forces in beams of MRFs are negligible. Instead, shear forces could be significant and should be limited to avoid flexural-shear interaction in plastic hinge zones. Moreover, shear force demand at both beam ends should be calculated using capacity design principles as follows:

$$V_{Ed} = V_{Ed,G} + V_{Ed,M} \tag{2.9}$$

where $V_{Ed,G}$ is the shear force due to gravity forces in the seismic design situation and $V_{Ed,M}$ is the shear force corresponding to plastic hinges formed at the beam ends (namely $V_{Ed,M} = (M_{pl,A}+M_{pl,B})/L$, being $M_{pl,A}$ and $M_{pl,B}$ the beam plastic moments with opposite signs at the end sections A and B, while L is the beam length).

In order to obtain the "weak beam/strong column" behaviour, the forces acting on columns calculated by the elastic model have to be amplified by the magnification coefficient Ω, defined as:

$$\Omega = \min\left(\frac{M_{pl,Rd,i}}{M_{Ed,i}}\right) \tag{2.10}$$

where $M_{Ed,i}$ is the design value of the bending moment in beam "i" in the seismic design situation and $M_{pl,Rd,i}$ is the corresponding plastic moment. It is important to highlight that this ratio should be calculated for all beams in which dissipative zones are located.

According to the hierarchy of strengths, the columns should be verified against all resistance checks including those for element stability, according to the provisions of EC3 for the most unfavourable combination of bending moments M_{Ed}, the shear force V_{Ed} and axial forces N_{Ed} , evaluated as below (EN 1998-1 6.6.3(1)P):

$$M_{Ed} = M_{Ed,G} + 1.1 \cdot \gamma_{ov} \cdot \Omega \cdot M_{Ed,E} \tag{2.11}$$

$$V_{Ed} = V_{Ed,G} + 1.1 \cdot \gamma_{ov} \cdot \Omega \cdot V_{Ed,E} \tag{2.12}$$

$$N_{Ed} = N_{Ed,G} + 1.1 \cdot \gamma_{ov} \cdot \Omega \cdot N_{Ed,E} \tag{2.13}$$

Where:

$M_{\mathrm{Ed,G}}$, $V_{\mathrm{Ed,G}}$ and $N_{\mathrm{Ed,G}}$, are the forces in the column due to the non-seismic actions included in the combination of actions for the seismic design situation;

$M_{\mathrm{Ed,E}}$, $V_{\mathrm{Ed,E}}$ and $N_{\mathrm{Ed,E}}$ are the forces in the column due to the design seismic action;

γ_{ov} is the material overstrength factor.

In addition to the member checks based on the Ω criterion, EN 1998-1 4.4.2.3(4) requires that at every joint the following condition should be satisfied:

$$\frac{\sum M_{Rc}}{\sum M_{Rb}} \geq 1.3 \tag{2.14}$$

Where:

ΣM_{Rc} is the sum of the design values of the moments of resistance of the columns framing the joint.

ΣM_{Rb} is the sum of the design values of the moments of resistance moments of the beams framing the joint.

Eurocode 8 provides for deformation-related criteria for all building typologies; however, due to their inherent flexibility, stability matters and drift limitations often govern the design of moment-resisting frames (Elghazouli Editor, 2009).

Therefore, beside the capacity design criteria, two deformation requirements should be accounted for in order to control both second-order effects (so-called "P-Delta" effects) and interstorey drift ratios. The latter verification is referred to damage limitation limit state and it has been previously discussed in Section 2.2.12.

P-Δ effects are specified by means of an inter-storey drift sensitivity-coefficient given as:

$$\theta_i = \frac{P_{tot} \cdot d_r}{V_{tot} \cdot h_i} \tag{2.15}$$

Where:

P_{tot} is the total gravity load at the *i*-th storey;

V_{tot} is the total seismic shear at the *i*-th storey;

h_i is the storey height

d_r is the design interstorey drift (evaluated by using elastic analysis and multiplied by the behaviour facto *q*).

For $\theta_i \leq 0.1$, P-Δ effects can be neglected; for $0.1 < \theta_i \leq 0.2$ instability should be accounted for by magnify the seismic action effects by the coefficient $\frac{1}{(1-\theta)}$; $\theta_i = 0.3$ is taken as upper bound limit for the instability due to second order effects.

2.3.3 *Design criteria and detailing rules for CBFs.*

Concentrically braced frames (CBFs) are characterized by a truss behaviour due to axial forces developed in the bracing members.

Most common configurations of concentrically braced frames in seismic areas are depicted in Fig. 2.6.

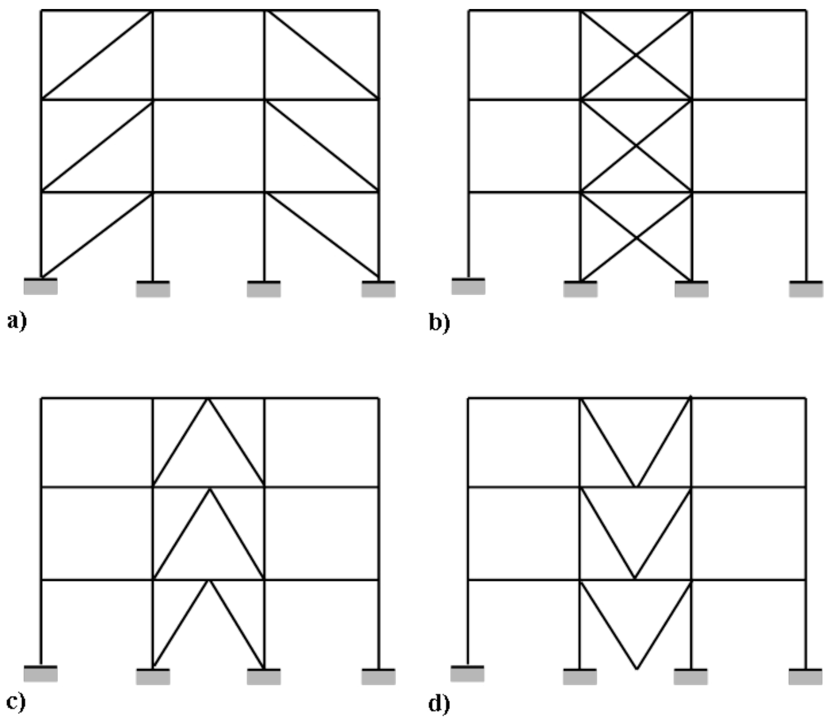

Figure 2.6 CBF common configurations: a) diagonal bracings; b) X-CBFs; c) Inverted V-CBF o Chevron bracings; d) V-CBFs

According to EN-1998 the inelastic deformation should be restrained in the diagonal members; in particular the energy dissipation is mainly provided by yielding of the braces under tension, preserving the connected elements from damage.

The response of a CBF is basically influenced by the behaviour of its bracing elements, whose role differs with the bracings configurations. Indeed, for X and Diagonal CBFs the energy dissipation capacity of braces in compression is neglected and the lateral forces are assigned to tension braces only. On the contrary, in frames with V and inverted V bracings both the tension and compression diagonals should be included in the elastic analysis of frames.

Moreover, the diagonal braces have to be designed and placed in such a way that, under seismic action reversals, the structure exhibits similar lateral load-deflection response in opposite directions at each storey. This performance requirement is deemed to be satisfied if the following rule is met at every storey:

$$\frac{\left|A^{+}-A^{-}\right|}{A^{+}+A^{-}} \leq 0,05 \tag{2.16}$$

where A^{+} and A^{-} are the areas of the vertical projections of the cross-sections of the tension diagonals (See Fig. 2.7) when the horizontal seismic actions have a positive or negative direction, respectively.

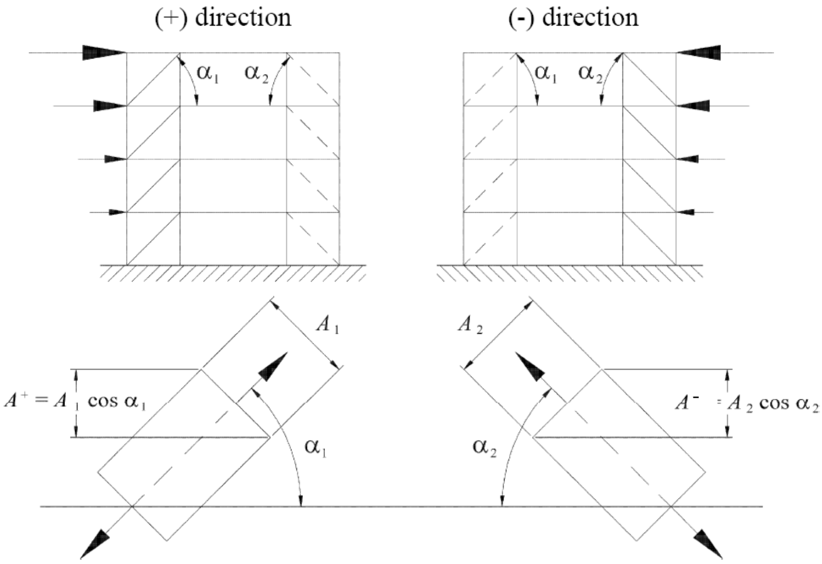

Figure 2.7 Requirement for assuring similar lateral load-deflection response in opposite directions at each storey

For X-CBFs, the diagonal braces have to be designed in such a way that the yield resistance $N_{pl,br,Rd}$ of their gross cross-section is such that $N_{pl,br,Rd} \geq N_{Ed,br}$, where $N_{Ed,br}$ is calculated from the elastic model ideally composed by a single brace (i.e. the diagonal in tension). In addition, the brace slenderness must fall in the range $1.3 \leq \overline{\lambda} \leq 2.0$ (EN 1998-1 6.7.3(1)). The lower bound value is imposed in order to limit the maximum compression axial forces transmitted to column. The upper bound value is given in order to limit excessive vibrations and undesired buckling under service loads.

Differently from X-CBFs, in frame with inverted-V bracing compression diagonals should be designed for the compression resistance, such that $\chi N_{pl,br,Rd} \geq N_{Ed,br}$, where χ is the buckling reduction factor calculated according to EN 1993:1-1 6.3.1.2 (1), and $N_{Ed,br}$ is the required strength. Differently from the case of X-CBFs, the code does not impose a lower bound limit for the non-dimensional slenderness $\bar{\lambda}$, while the upper bound limit ($\bar{\lambda} \leq 2$) is retained.

For all types of bracing configurations, in order to guarantee the formation of a global mechanism, beams and columns are designed to behave elastically. In order to meet capacity design objectives the required strength of beam-column members is evaluated in according to the following expression:

$$N_{pl,Rd}(M_{Ed}) \geq N_{Ed,G} + 1.1 \cdot \gamma_{ov} \cdot \Omega \cdot N_{Ed,E} \tag{2.17}$$

where:

$N_{pl,Rd}(M_{Ed})$ is the design resistance to axial force of the beam or the column calculated in accordance with EN 1993:1-1, taking into account the interaction with the design value of bending moment, M_{Ed}, in the seismic design situation;

$N_{Ed,G}$ is the axial force in the beam or in the column due to the non-seismic actions included in the combination of actions for the seismic design situation;

$N_{Ed,E}$ is the axial force in the beam or in the column due to the design seismic action;

γ_{ov} is the material overstrength factor;

Ω is the minimum overstrength ratio $\Omega_i = N_{pl,br,Rd,i}/N_{Ed,br,i}$, which may vary within the range Ω to 1.25Ω.

For beams belonging to braced spans V and inverted-V configurations, the code provides further requirements in order to account for the behaviour of the system in the post-buckling range.

Indeed, in such configuration, after the buckling of the brace under compression, a vertical resulting from axial forces transmitted by both braces is applied at the beam mid-length, inducing significant bending demand. Thereby, in order to avoid flexural yielding phenomena at the brace-intercepted section, the beam is designed to withstand the following loading conditions: (i) all non-seismic actions without considering the intermediate support given by the diagonals; (ii) the vertical component of the force transmitted by the tension and compression braces. This vertical component is calculated assuming that the tension brace transfers a force equal to its yield resistance ($N_{pl,br,Rd}$) and the compression brace transfers a force equal to a percentage of its original buckling strength ($N_{b,br,Rd}$) to take into account the strength degradation under cyclic loading. The reduced compression strength is estimated as equal to $\gamma_{pb}N_{pl,br,Rd}$ with a value of the factor γ_{pb} to be found in the National Annexes. The value recommended by EN 1998 is 0.30.

The seismic behaviour of concentrically braced frames is specifically and detailed deepened in Chapter III, where also the framework of codified seismic provision is accurately discussed.

2.3.4 *Design criteria and detailing rules for EBFs.*

Eccentrically braced frames (EBFs) are characterized by diagonal members arranged as to define a segment of beam called “link” (bold line in Fig. 2.8), thus subjected to shear and bending.

Figure 2.8 shows common eccentric bracing configuration: split-K-braced frame (a), D-braced frame (b), V-braced (c) and finally inverted-Y-braced frame (d).

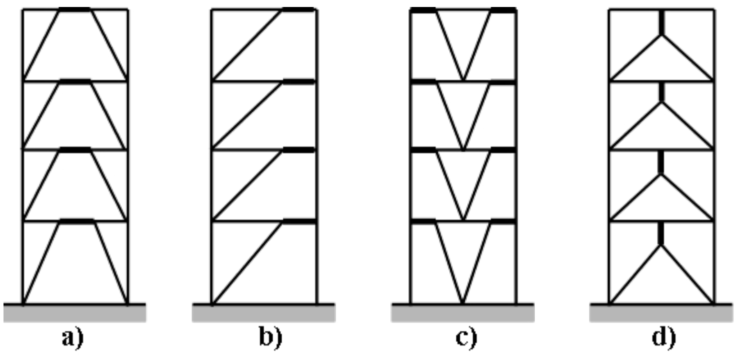

Figure 2.8 Eccentric bracing configuration: split -K-braced frame (a), D-braced frame (b), V-braced (c) inverted-Y-braced frame (d).

Differently from concentrically braced frames, the diagonal members should be designed to remain in the elastic range, while the link is the element responsible of the energy dissipation. In Eurocode 8, links are classified on the basis of the type of plastic mechanism as follow:

(i) Short links, which dissipate energy by yielding essentially in shear;

(ii) Intermediate links, in which the plastic mechanism involves bending and shear;

(iii) Long links, which dissipate energy by yielding essentially in bending.

The mechanical parameter influencing the plastic mechanism is the link length "*e*", related to the ratio plastic bending moment ($M_{p,link}$) over plastic shear ($V_{p,link}$) of the link cross section, evaluated according to the following expression:

$$M_{p,link} = f_y b t_f \left(d - t_f\right) \tag{2.18}$$

$$V_{p,link} = \left(f_y \big/ \sqrt{3}\right) \cdot t_w \cdot \left(d - t_f\right) \tag{2.19}$$

where f_y is the value of steel yielding stress, d is the depth of the cross section, t_f is the flange thickness and t_w is the web thickness.

In the cases where equal moments could form simultaneously at both ends of the link (e.g. the split-K configuration) the link can be classified as follows:

Shor links: $e \le e_s = 1.6 \dfrac{M_{p,link}}{V_{p,link}}$ (2.20)

Long links: $e \ge e_L = 3 \dfrac{M_{p,link}}{V_{p,link}}$ (2.21)

Intermediate links: $e_s < e < e_L$ (2.22)

It should be noted that Eqs. from (2.20) to (2.22) can be generalized to other eccentrically braced configurations, where only one plastic hinge would form at one end of the link (e.g. inverted-Y configuration, see Fig. 2.28d):

Shor links: $e \leq e_s = 0.8 \cdot (1 + a)\dfrac{M_{p,link}}{V_{p,link}}$ (2.23)

Long links: $e \geq e_L = 1.5 \cdot (1 + a)\dfrac{M_{p,link}}{V_{p,link}}$ (2.24)

Intermediate links: $e_s < e < e_L$ (2.25)

being α is the ratio of the smaller bending moments $M_{\mathrm{Ed,A}}$ at one end of the link in the seismic design situation, to the greater bending moments $M_{\mathrm{Ed,B}}$ at the end where the plastic hinge would form, both in absolute values.

Although short links suffer high ductility demands, they yield primarily in shear, while flexural demand became dominant in long links. Several experimental studies (Hjelmstad and Popov, 1983; Kasai and Popov, 1986; Engelhardt and Popov, 1989) demonstrated that the shear link behaviour is able to provide larger energy dissipation capacity respect to the flexural plastic hinges of long links. However, other considerations such as architectural requirements may necessitate the use of long links, for instance to allow the placement of doors, windows, etc.

However, in order to assure stable behaviour of the system, EN 1998 states that the link rotation should not exceed specific limitations dependant on the expected type of plastic mechanism:

- Short links: $\theta_{\mathrm{p}} \leq \theta_{\mathrm{pR}} = 0.08$ radians
- Long links: $\theta_{\mathrm{p}} \leq \theta_{\mathrm{pR}} = 0.02$ radians
- Intermediate links: $\theta_{\mathrm{p}} \leq \theta_{\mathrm{pR}}$ = the value determined by linear interpolation between the above values

The link rotation θ_{p} is defined as the rotation angle between the link and the element outside of the link (see Fig. 2.9) As it can be observed, the shorter is the link length and the greater is the ductility demand.

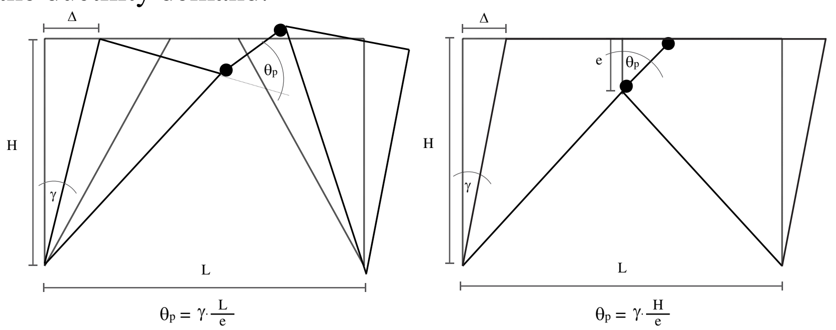

Figure 2.**9** Link rotation angle

In order to guarantee the formation of a ductile collapse mechanism, the seismic-induced effects on connections, beams and columns are evaluated according to the following equation:

$$N_{pl,Rd}(M_{Ed},V_{Ed}) \geq N_{Ed,G} + 1.1 \cdot \gamma_{ov} \cdot \Omega \cdot N_{Ed,E} \tag{2.26}$$

Where:

- $N_{pl,Rd}(M_{Ed},V_{Ed})$ is the design resistance to axial force the column or diagonal member calculated in accordance with EN 1993:1-1, taking into account the interaction with the design value of bending moment, M_{Ed}, and the shear force, V_{Ed}, in the seismic design situation;
- $N_{Ed,G}$ is the compression force in the column or diagonal member due to the non-seismic actions included in the combination of actions for the seismic design situation;

- $N_{Ed,E}$ is the compression force in the column or diagonal member due to the design seismic action;
- γ_{ov} is the material overstrength factor.

The magnification coefficient Ω is evaluated as the minimum of the following values: (i) the minimum value of $\Omega_i = 1.5V_{p,link,i}/V_{Ed,i}$ among all short links; (ii) the minimum value of $\Omega_i = 1.5M_{p,link,i}/M_{Ed,i}$ among all intermediate and long links, where:
- $V_{Ed,i}$ and $M_{Ed,i}$ are the design values of the shear force and of the bending moment respectively in the link at the *i*-th storey;
- $V_{p,link,i}$ and $M_{p,link,i}$ are the corresponding shear and bending plastic design resistances.

2.3.5 *Design of connections*

In order to achieve stable overall behaviour EN 1998-1 6.5.5 provides a general rule devoted to avoid plastic deformation localized in the joint assemblies connected to the dissipative zones. With this aim, the connections are designed to withstand the following action:

$$R_d \geq 1.1 \cdot \gamma_{ov} \cdot R_{fy} \tag{2.27}$$

Where R_d is the resistance of the connection, R_{fy} is the plastic resistance of the connected dissipative member based on the design yield stress of the material, γ_{ov} is the material overstrength factor.

This general rules identically apply for non-dissipative connection in all the structural typologies above described; however, EN 1998-1 6.6.4 allows locating dissipative zones in the connection in case of MRFs.

In detail, semi-rigid and/or partial strength joints can be used, provided the following conditions:

- the joints have a rotation capacity consistent with the global deformations;
- members framing into the joints are stable at the ultimate limit state (ULS);
- the effect of joints deformation on global drift is taken into account using nonlinear static (pushover) global analysis or non-linear time history analysis;
- the rotation capacity of the dissipative joints θ_p is not less than 35 mrad for structures of ductility class DCH and 25 mrad for structures of ductility class DCM with q > 2.

The rotation capacity of the joint has to be verified by performing qualification tests on joint sub-assemblages. The joint ductility is specified by the joint chord rotation $\theta_p = \delta/0{,}5L$, where δ is the beam deflection at mid-span and L is the beam span.

Stiffness and strength degradation smaller than 20% should be assured in the plastic hinge zone; moreover the column web panel shear deformation should not exceed the 30% of the total plastic rotation capacity of the joint.

2.4 REFERENCES

Elghazouli A.Y., editor (2009) Seismic Design of Buildings to Eurocode 8, Spon Press, 2 Park Square, Milton Park, Abingdon, Oxon OX14 4RN, ISBN13: 978-0-415-44762-1

EN 1993:1-1, Eurocode 3: Design of Steel Structures — Part 1–1: General Rules and Rules for Buildings, CEN, 2005

EN 1998-1-1, Eurocode 8: Design of Structures for Earthquake Resistance — Part 1:General Rules, Seismic Actions and Rules for Buildings, CEN, 2005.

Engelhardt, M. D. and Popov, E. P., (1989), On the design of eccentrically braced frames, *Earthquake Spectra*, 5: 495–511.

Hjelmstadt, K. D., and Popov, E. P., (1983), Seismic Behavior of Active Beam Links in Eccentrically Braced Frames, *Report No. UCB/EERC–83/15, Earthquake Engineering Research Center,* University of California, Berkeley, CA

Kasai, K. and Popov, E. P. (1986): General behavior of wf steel shear link beams. *Journal of Structural Engineering*, ASCE, 112(2), 362-382.

Chapter III

Seismic behaviour of concentrically braced frames

3.1 INTRODUCTION

The seismic behaviour of concentrically braced frames is deeply described and discussed in this Chapter.

In detail, the framework of existing seismic design provisions concerning concentrically braced frames (CBFs) is outlined hereinafter, with reference to design criteria and rules provided by most used and well-established seismic codes.

Moreover, since the seismic performance of concentrically braced frames is primarily affected by the behaviour of the diagonal members, the hysteretic response of bracing members under axial loading is widely discussed.

In addition, a critical review of existing literature on seismic design criteria conceived to improve seismic performance of concentrically braced frames is outlined.

Finally, the main technological aspects to be accounted for in the design of ductile concentrically braced frames are briefly addressed, with special focus on the detailing of brace-to-brace, brace-to-beam/column, brace-to-beam mid-span and brace-to-column base connections.

3.2 FRAMEWORK OF STANDARDS AND SEISMIC DESIGN PROVISIONS

Both European and North-American (US and Canadian) codes adopt capacity design principles for CBFs, aimed at guaranteeing a similar seismic performance, namely restraining the dissipative behaviour into diagonal members and preventing the damage in the remaining structural members. However, in order to achieve this purpose European and North-American codes recommend some different requirements and design provisions.

Since the overall performance and energy dissipation capacity are strongly related to these detailing rules, in this Section the provisions by EN-1998 (i.e. hereinafter referred as either Eurocode 8 or EC8), AISC 341and CSA S16-09 are critically revised and compared for concentrically braced frames in both cross (X-CBFs) and chevron (Inverted V-CBFs) configurations.

In order to avoid deceiving conclusion, the comparison has been done considering the same hazard level, whose definition would differ in the three examined codes. Indeed, if one code stipulates design force larger than those given by the others, it could appear that stronger structures are designed using the former code. However, if this code allows assuming larger strength reduction factors, that conclusion cannot be valid.

In order to highlight the criticisms of the codes under consideration, hereinafter the comparative discussion has been developed focusing on the following issues:

(i) the ductility classes and the relevant levels of expected plastic engagement with the associated force reduction factors;

(ii) the recommended methodologies for structural analysis and the corresponding modelling assumptions;

(iii) the detailing rules to assure the achievement of the hierarchy of resistances for both dissipative (i.e. bracings) and non-dissipative members (i.e. beams and columns).

3.2.1 *Ductility classes and force reduction factors*

Seismic codes generally provide different ductility classes depending on the level of plastic engagement ensured in the dissipative zones. Therefore, a force reduction factor is assigned per ductility class, directly related to the expected dissipative capacity. Some requirements are generally relaxed in lower ductility classes expected to provide smaller energy dissipation.

As previously described in Chapter II, the ductility classes considered by EN-1998 are the following: (i) low ductility class (DCL); (ii) medium ductility class (DCM); (iii) and high ductility class (DCH). In case of DCL poor plastic deformations are expected and the Code allows performing global elastic analysis using a behaviour factor q factor within [1.5, 2.0]; the strength of elements (both members and connections) is verified according to EN-1993 (Eurocode 3: Design of Steel Structures) without accounting for capacity design rules (recommended just for low seismic areas). On the contrary, systems designed for DCM or DCH are expected to have moderate or large plastic engagement in dissipative parts, respectively. A specific force reduction factor is correlated at each class and the Eurocode 8 prescribes specific rules at both global and local level to assure the achievement of the expected level of ductility. With this regard, EC8 adopts the EC3 classification for cross sections relating it to the restrictions to the value of the behaviour factor q: cross-sectional class 1, 2 or 3 is required corresponding to behaviour factors in the range [1.5, 2.0], while class 1 or 2 is required for q in a range [2.0, 4.0]; Only class 1 is allowed for DCH ($q > 4.0$).

The q factor according to EN 1998-1 for regular structural systems is given according to Eq. (2.4) (see Section 2.2.3). For concentrically braced frames, EC8 recommends $\alpha_u/\alpha_1 = 1$ for CBFs.

It's worth to note that EN 1998, directly relates the classification of cross section to the energy dissipation capacity of the whole system, specified through the behaviour factor q. However, differently from other codes, EN 1998 does not address width-to-thickness limitation specific for members in seismic resistant systems and the classification provided for non-seismic code (namely, EN 1993) are adopted. Moreover, several studies and researches carried out in the recent past (Mazzolani and Piluso, 1992 and 1996; Gioncu and Mazzolani, 1995;

Gioncu, 2000, Plumier, 2000; Gioncu and Mazzolani, 2002, D'Aniello *et al*, 2012 and 2013, Güneyisi *et a*l 2013 and 2014) have highlighted some criticisms in the Eurocode 3 classification mainly due to the small number of parameters considered to characterize the beam performance (Landolfo, 2013). In fact, Eurocode relates rotation capacity to material and cross section factors only, neglecting several parameters significantly affecting the cross section ductility, such as the flange-web interaction, the overall member slenderness, the moment gradient, the lateral restraints, the loading conditions (Landolfo, 2013).

In EN-1998 a q factor equal to 4.0 in both DCM and DCH is allowed for X-CBFs, while q = 2 and q = 2.5 are used for chevron concentrically braced frames in DCM and DCH, respectively. Indeed, in the framework of Eurocode 8 the bracings in chevron configuration are expected to provide smaller energy dissipation, while it is unclear the reason why the behaviour factor for cross bracings coincides in both medium and high ductility classes. In addition, a further inconsistency can be recognized considering that EN-1998 states to assume q = 2.5 for braced frames in chevron configuration for high ductility class; indeed, according to the ductility classification given in the Section 6.1.2 of the Code, such value of the behaviour factor belongs to the range [2.0, 4.0] corresponding to the DCM.

AISC 341 provides two different categories based on their expected energy-dissipation capacity (i) special concentrically braced frames (SCBFs), which are expected to provide significant ductility, and (ii) ordinary concentrically braced frames (OCBFs), characterized by smaller energy dissipation capacity. OCBFs have minimal requirements compared to the other braced-frame systems; however, AISC 341 significantly restricts the permitted use of OCBFs and larger seismic force must be considered to compensate for their smaller ductility. Indeed, in US codes (FEMA P-750, 2009; ASCE/SEI 7-10, 2010) the shear force reduction factor R is independent from the bracing configuration, while it depends only on the ductility class: a lower value of R factor is prescribed for OCBFs (namely equal to 3.25), while a larger value (namely equal to 6.0) is specified for SCBFs.

Also in the Canadian seismic codes (CSA S16-09, 2009), two ductility categories are accounted for as follows: (i) moderately ductile CBFs (MD), and (ii) limited-ductility CBFs (LD). In both cases, energy dissipation is obtained by means of the yielding of the brace in tension and in case of chevron bracings also of the flexural yielding at the mid-length of brace in compression after buckling. A capacity design procedure and the same design requirements apply to both classes, but some relaxations are permitted in LD Type. Similarly to US codes, the force reduction factor is independent on the brace configuration and specified as $R = R_\mathrm{d} \times R_\mathrm{o}$. The factor R_o accounts for the overstrength of the structure and it is taken equal to 1.3 for CBFs, while R_d accounts for the expected ductility and it is equal to 3.0 for MD class and equal to 2.0 for LD class.

In the following Sections, the design criteria and code requirements are compared especially focusing on the ductility category expected to experience the largest plastic engagement, namely: (i) EC8-compliant CBFs in DCH; (ii) AISC-compliant SCBFs; (iii) CSA-compliant CBFs in MD class.

3.2.2 *Structural analysis and modelling aspects*

Seismic codes allow performing simplified design procedures to calculate the internal seismic forces acting on CBFs. For what concerns the design of braces, all codes allow performing a linear elastic analysis of the structure to evaluate the required strengths of diagonal members. However, the response of concentrically braced frames is basically ruled by the behaviour of bracing members, which exhibit large plastic engagement after the buckling of braces; thereby the nonlinear response of the system significantly differs from the elastic behaviour. In the light of these considerations, codes provide different approaches to calculate the inner forces acting into non-dissipative members in post-buckling regime and two main methods can be recognized:

(i) the earthquake-induced effects in non-dissipative components (namely beams, columns and connections) are estimated magnifying by an overstrength factor Ω the internal forces calculated by means the former elastic analysis;

(ii) a plastic mechanism analysis is used by calculating the internal forces on the basis of a free-body distribution of plastic forces transmitted by the braces yielded under tension and those under compression behaving in the post-buckling range.

In USA, the provisions of AISC 341 and the applicable building code, typically ASCE 7, govern the global analysis of structures equipped with both ordinary and special concentrically braced frames. Only for SCBFs - which are expected to provide significant energy dissipation capacity- AISC 341 requires, in addition to the elastic global analyses, a plastic mechanism analyses to determine the required strengths of columns, beams and connections which are thus given by considering the most unfavourable condition obtained from the following analyses:

i) an elastic analysis with both braces in tension and compression resisting the design forces due to the seismic event. The obtained forces are magnified by using the system overstrength factor Ω_o.

ii) an analysis in which all braces in tension are assumed to attain forces corresponding to their expected tensile strength, and all braces in compression are assumed to exhibit their expected post-buckling strength, representing the frame behaviour in the nonlinear range, when significant loss of compression strength and stiffness occurs.

The Canadian code also evaluates the required strength of braces by performing elastic analysis. However, differently from US codes, only plastic mechanism analysis is permitted to evaluate required strengths of beams and columns and the concept of overstrength factor to magnify the earthquake-induced forces on non-dissipative elements is absent. In order to assure the fulfilment of capacity design requirements, two different scenarios should be considered: (i) the first in which all the tension braces are assumed yielded in tension and the compression braces attain their buckling resistance (ii) the second in which all the tension braces are assumed yielded in tension and the post-buckling strength occurs in the compression ones.

Differently from the North-American codes, EN-1998 (except for the beams in V-CBFs) allows performing a simplified design procedure starting from a linear analysis of the system devoted to evaluate the required strengths of bracing members and the strength hierarchy is intended guaranteed by magnifying the seismic forces given by elastic analysis acting in the non-dissipative elements by using an overstrength factor. In addition, significant difference between EC8 and other codes is related to the modelling assumptions for bracing members in X-CBF configuration. Indeed, for this type of structural scheme, EC8 allows performing the linear analysis on a tension-only diagonals scheme (Figs. 3.1 and 3.2a), where the contribution given by the compression diagonals is neglected. This simplified assumptions needs to develop two separate models, one with the braces tilted in one direction and another with the braces tilted in the opposite direction, in order to make tension alternatively developing in all the braces at any storey (see Fig. 3.1).

Contrarily to Eurocode 8, both US and Canadian codes mandate tension-compression bracings model (see Fig. 3.2b) for special X-CBFs. Simplified tension-only model is allowed only for ordinary concentrically braced frames

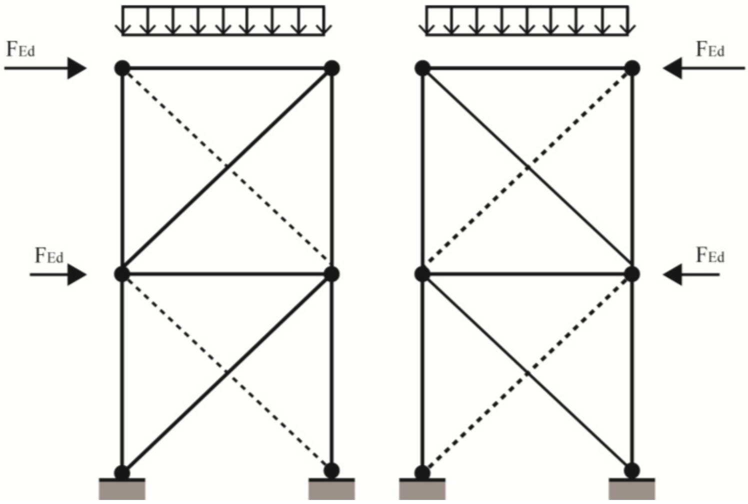

Figure 3.1 Calculation models of X and Diagonal CBFs.

Figure 3.2 depicts the force transfer mechanism obtained by using either tension only (a) or tension-compression (b) model for X-CBFs. As it can be observed, these methods lead calculating different distributions of internal forces with significant differences in terms of seismic demand on the non-dissipative members (Faggiano *et al.*, 2014) Indeed, neglecting the diagonals under compression leads to disregard force contributions in both columns and beams that could be significant (see Fig. 3.2b).

Eurocode 8 mandates plastic mechanism analyses solely to determine the design force acting on the braced-intercepted beam in chevron configuration. Indeed in this case, following the buckling of the brace in compression, an unbalanced vertical force (absent in the elastic range) resulting from the axial forces transmitted by both braces is applied on the beam, inducing a significant bending moment at the brace-intercepted section. For columns, EC8 stipulates to magnify elastic forces calculated as shown in Fig. 3.3a. However, by comparing Fig. 3.3a to 3.3b it is clear that performing elastic analyses could lead to underestimate the force acting into the columns.

Concerning the use of overstrength factors, it is worth to note that the main philosophy is practically similar in both European and US codes; however, significant differences can be recognized in the factors definition. Indeed in US codes the overstrength factor (named Ω_o) is fixed *a-priori* depending only on the structural typology (it is equal to 2 in SCBFs). Conversely, in EN-1998 the magnification factor Ω is assumed as the minimum ratio ($N_{pl,br,Rd,i}/N_{Ed,br,i}$), being $N_{pl,br,Rd,i}$ the plastic design strength of *i*-th brace and $N_{Ed,br,i}$ its relevant required strength. As it can be easily observed the European magnification factor could be larger than 2 because it depends on the actual design overstrength of the bracing members. The main issues related to the influence of magnification factors are widely discussed in the following Sections, where the design provisions for non-dissipative members are described.

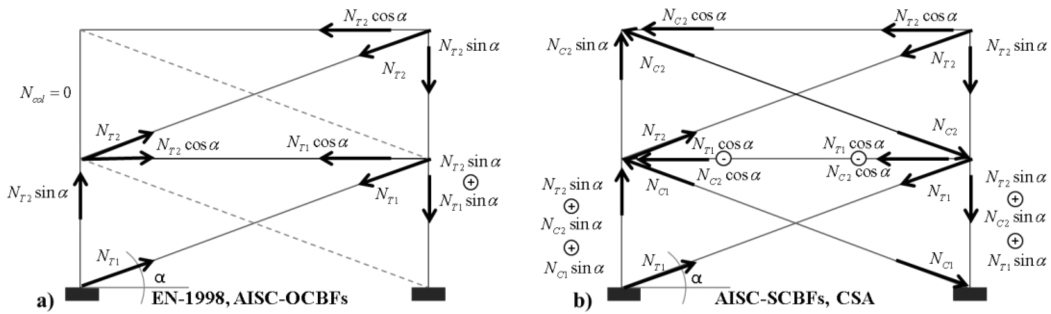

Figure 3.2 Tension-only bracing model (a) and tension-compression bracings model (b) for X-CBFs in different codes.

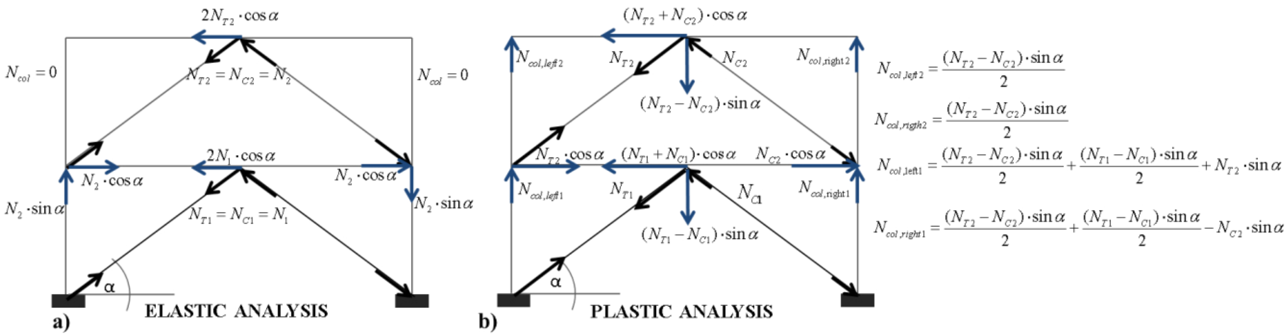

Figure 3.3 Force transfer mechanisms in chevron CBFs given by a) elastic analysis and b) plastic analysis.

3.2.3 *Design of bracing members.*

In EN-1998 the diagonal members in X configuration should be designed in order to guarantee that $N_{pl,br,Rd} \geq N_{Ed,br}$, where $N_{pl,br,Rd}$ is the design plastic strength of brace cross-section and $N_{Ed,br}$ is calculated as shown in Fig. 3.2a. On the contrary, for inverted-V CBFs, EC8 stipulates to design the braces to resist the forces calculated as shown in Fig. 3.3a. Thereby, compression diagonals should be designed for the compression resistance, such that $\chi N_{pl,br,Rd} \geq N_{Ed,br}$, where χ is the buckling reduction factor calculated according to EN 1993:1-1 6.3.1.2 (1), and $N_{Ed,br}$ is the required strength.

In addition, for both inverted V and X configurations, in order to assure an uniform distribution of damage along the building height and to avoid detrimental soft-storey mechanisms, EC8 imposes that the overstrength ratio $\Omega_i = N_{pl,br,Rd,i}/N_{Ed,br,i}$ should vary within the range Ω to 1.25Ω. It is worth to note that this requirement forces to use different cross-sections of the braces along the building height. Moreover, since the top storey is generally characterized by higher values of the overstrength ratio, the designers are forced to oversize the diagonal members at lower storeys in order to satisfy the requirement on the variation of Ω. With this regard, it may be more effective to define the *i*-th overstrength ratio by considering the compression axial strength of the brace at the *i*-th storey (rather than the plastic strength) being the buckling of the brace under compression the actual first nonlinear event occurring at each storey.

AISC 341 allows tension-only bracing model just for X ordinary concentrically braced frames. Therefore, braces of special V- and X-CBFs are designed to resist both tension and compression forces evaluated by using linear analysis (see Fig. 3.2b and 3.3a). Differently from European code, in US standards, “expected” strengths are considered as design resistances for ductile elements (i.e. the capacity in tension corresponds to $\gamma_{ov}N_{pl,br}$ and that in compression corresponds to $\gamma_{ov}\chi N_{pl,br}$), while the factored resistances are assumed in the European code.

In CSA S16-9 the design of diagonal members is addressed similarly to US codes. For cross and chevron configurations both tension and compression braces are designed to withstand the earthquake-induced forces. The strength capacity of the brace in tension is calculated by using the “probable” resistance (corresponding to $\gamma_{ov}N_{pl,br}$). The compressive resistance is taken as the lesser of $\gamma_{ov}N_{pl,br}$ and the brace buckling resistance (corresponding to $\gamma_{ov}\chi N_{pl,br}$) also evaluated using the average yield stress of the material.

It should be noted that the resistances of braces have been above defined by using the European notation also for both the US and Canadian codes, in order to allow easier comparison between the different codified rules. In particular, the European definition for the buckling capacity (namely by using the plastic strength reduced by the factor χ as defined in EN 1993:1-1 6.3.1.2 (1)) has been extended to the other standards. However, slight differences in the evaluation of compression strength of braces between the examined codes can be recognized due to the different definitions of the mean buckling curve. Indeed, in the US code, the “expected” buckling strength is given as $1.14F_{cre}A_g$, where A_g is the cross section area of the diagonal member and F_{cre} is the Eulerian critic load that is determined by using the expected yield stress R_yF_y (being R_y the material randomness coefficient, which corresponds to γ_{ov} in Eurocode 8, and F_y is the specified minimum yield stress of the steel, which corresponds to the European characteristic yield stress f_y). On the other hand, in the Canadian code, the "probable" buckling resistance of bracing members is given as $1.2 \cdot \frac{C_r}{\phi}$ where C_r is the Eulerian critic load computed using R_yF_y, whose meanings are the same of the corresponding parameters given by AISC 341-10.

Since the braces provide poor energy dissipation in post-buckling range, the codes state further requirements devoted to limit the global and local slenderness of the bracing members. EN-1998 refers to the normalized slenderness:

$$\bar{\lambda} = \sqrt{\frac{N_{pl,\mathrm{br},Rd}}{N_{cr,br}}} \tag{3.1}$$

(being $N_{cr,br}$ the Eulerian critical load) of bracing members. Within European code, slenderness ratio limitation differs between X and chevron configuration: in the former case, the brace normalized slenderness $\bar{\lambda}$ must fall in the range [1.3, 2] (EN 1998-1 6.7.3(1)). This requirement is due to the simplified tension-only diagonal model assumed for structural analysis (see Fig. 3.2a). Indeed, since the presence of the compression diagonal is neglected, the lower bound slenderness limit is imposed in order to control the maximum compression axial force transmitted to the column. On the other hand, the upper bound value is stipulated in order to avoid significant vibration and undesired buckling under service loads.

For chevron CBFs, the Eurocode 8 does not impose a lower bound limit for the non-dimensional slenderness $\bar{\lambda}$, while the upper bound limit ($\bar{\lambda} \leq 2$) is retained. As previously discussed in Chapter II, EN1998-1 stipulates also local slenderness limits for cross section of braces, directly related to ductility classes; however no specific limitation are provided for members in seismic-resistant structures and the classification given by EN 1993 is extended also to dissipative members. (see Section 2.2.3.1).

Differently from Eurocode 8, both US and Canadian codes refers to the geometrical slenderness *KL*/*r* (where *K* is the effective length factor; *L* is the unsupported length; *r* is the radius of gyration). The upper bound limit is fixed as 200 for braces in both X and inverted V configurations, thus resulting slightly less stringent than EN-1998 ($\bar{\lambda} \leq 2$). Several studies (Tang and Goel, 1989; Goel and Lee, 1992, Tremblay, 2000) confirmed that frames with slender braces designed for compression strength behave well, showing also that the post-buckling cyclic fracture life increases with the slenderness ratio. However, limiting the geometrical slenderness $KL / r \leq 200$ avoids dynamic effects in very slender braces (Elghazouli, 2008). This requirement is relaxed in AISC 341 for OCBFs in V or inverted V configurations, for which $KL / r \leq 4\sqrt{E/F_y}$ is provided, being E is Young's modulus and F_y is the yield strength, broadly equivalent to $\bar{\lambda} \leq 1.3$ for typical material properties.

Even North-American codes provide width-to-thickness ratio limitations to minimize the detrimental effects of local buckling; AISC 341 for SCBFs imposes to apply specific width-to-thickness limit ratios λ_{hd} provided for members designated as highly ductile members. The requirements for OCBFs are relaxed; indeed the braces should not exceed width-to-thickness limit ratios λ_{md} provided for moderately ductile members. With reference to local buckling phenomena, the Canadian code provides with-to-thickness ratios varying on the member slenderness: they are more strict if $KL/r \leq 100$, while linearly increase for 100 < KL/r < 200, in the light of the above mentioned results (Tang and Goel, 1989; Goel and Lee, 1992, Tremblay, 2000).

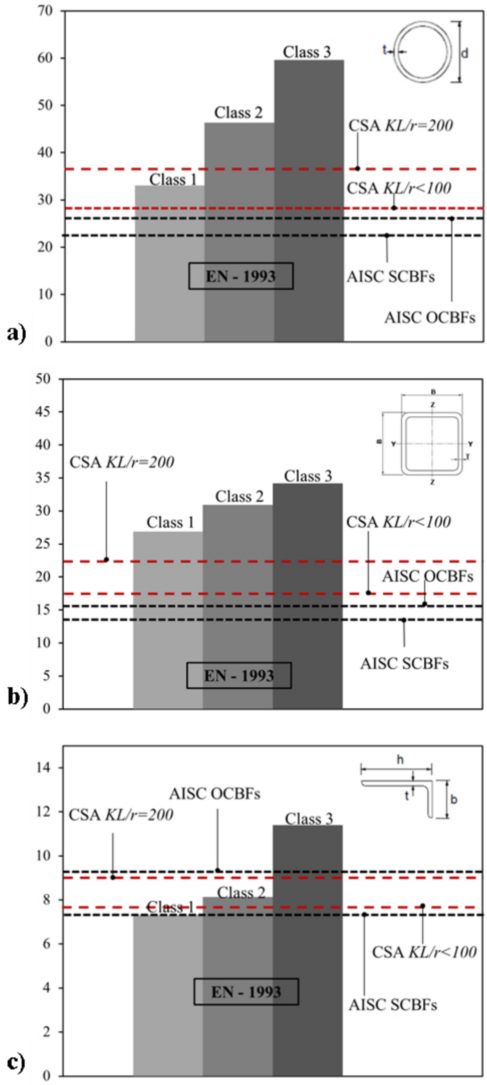

Figure 3.4 Width-to-thickness ratio limitations to avoid local buckling phenomena: comparison between different codes.

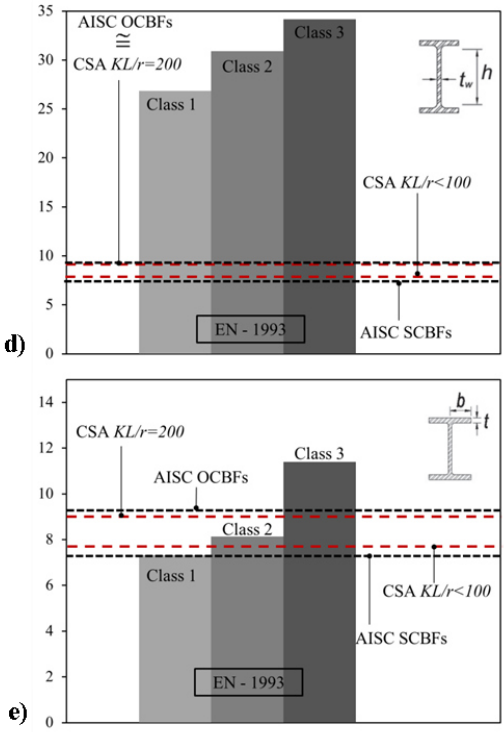

Figure 3.4 Width-to-thickness ratio limitations to avoid local buckling phenomena: comparison between different codes.

In Fig. 3.4 the width-to-thickness ratio limitations provided by different codes are quantitatively compared for circular hollow sections (see Fig. 3.4a), square hollow section (see Fig. 3.4b), angle members (see Fig. 3.4 c) and for both flange and web of hot rolled I section (see Fig. 3.4 d and e, respectively) considering the same steel grade (e.g. S355); as shown in the picture, the EC8 requirements for hollow structural sections (see Fig. 3.4 a and b) are the least severe also if compared to OCBFs, which are expected to provide very limited ductility. The most severe requirement is provided by AISC 341, for SCBFs. Conversely, the width-to-thickness limitation provided for by EN 1993 for angle section belonging to Class 1 are close to both AISC limitations for SCBFs and CSA limitation for relatively stocky members (KL/r<100). For what concern hot rolled I-shape profiles, (see Fig. 3.4 d and e) similar requirements can be recognized for flanges belonging to EN 1993-compliant Class 1, AISC-compliant limit for SCBFs and for CSA-compliant limit for members having KL/r<100. Conversely, the European code provides significantly less severe local slenderness limitations for webs of hot rolled I-shape sections respect to both the North-American codes (see Fig. 3.4d).

Thereby, the above considerations confirm the need for European standards to develop local slenderness requirements specifically conceived for dissipative members and seismic applications.

In Table 3.1 the design requirements ruling the design of diagonal members are summarized and compared for the examined seismic codes; in order to get easy the comparative reading, the nomenclature adopted by European codes was extended to all the standards under consideration

Table 3.1. Design of diagonal members: comparison between EN-1998, AISC 341-10 and CSA S16-9

Requirement	EN-1998 (DCM, DCH)	AISC 341 - SCBF	CSA S16-9– MD CLASS
Required strength	in X-CBF: tension brace is verified for $N_{pl,br,Rd} \geq N_{Ed,br}$ (tension-only bracing model is used) in V-CBF: tension brace is verified for $N_{pl,br,Rd} \geq N_{Ed,br}$; compression brace is verified $\chi N_{pl,br,Rd} \geq N_{Ed,br}$	tension brace is verified for $\gamma_{ov} N_{pl,br} \geq N_{Ed,br}$ compression brace is verified for $\min(\gamma_{ov} N_{pl,br} ; \gamma_{ov} \chi N_{pl,br}) \geq N_{Ed,br}$	tension brace is verified for $\gamma_{ov} N_{pl,br} \geq N_{Ed,br}$ compression brace is verified for $\min(\gamma_{ov} N_{pl,br} ; \gamma_{ov} \chi N_{pl,br}) \geq N_{Ed,br}$
Check for dissipative behaviour	Ω should vary in a range: $(\Omega, 1{,}25\Omega)$	No requirement on variation of brace overstrength is imposed	
Limitation on slenderness	in X-CBF: $1.3 \leq \bar{\lambda} \leq 2$ in V-CBF: $\bar{\lambda} \leq 2$	Bracing members should have: $KL / r \leq 200$	
Cross-sections limitations	DCM (q>4): Class 1 or 2* DCH ($2 < q \leq 4$): Class 1*	specific width-to-thickness limit ratios λ_{hd} provided for members designated as highly ductile members are applied	with-to-thickness ratios are provided varying on the member slenderness: more strict if $KL / r \leq 100$, while linearly increase for $100 < KL/r < 200$

*according to EN1993:1-1

3.2.4 *Design of beams*

EN-1998 imposes to design non-dissipative members to withstand the following force:

$$N_{pl,Rd}(M_{Ed}) \geq N_{Ed,G} + 1.1 \cdot \gamma_{ov} \cdot \Omega \cdot N_{Ed,E} \tag{3.2}$$

where:

$N_{pl,Rd}(M_{Ed})$ is the design resistance to axial force of the beam or column calculated in accordance with EN 1993:1-1, taking into account the interaction with the design value of bending moment, M_{Ed}, in the seismic design situation;

$N_{Ed,G}$ is the axial force in the beam or in the column due to the non-seismic actions included in the combination of actions for the seismic design situation;

$N_{Ed,E}$ is the axial force in the beam or in the column due to the design seismic action;

γ_{ov} is the material overstrength factor;

Ω is the minimum overstrength ratio $\Omega_i = N_{pl,br,Rd,i}/N_{Ed,br,i}$;

It is interesting to observe that in most of cases the brace overstrength factors Ω for X-CBFs ranges within [1.0, 2.0], while [2.0, 3.0] for chevron CBFs, owing to the necessity to satisfy both the limits on variability of Ω and the slenderness limits for braces imposed by EC8.

In EC8, plastic mechanism analysis is required only for the braced-intercepted beams belonging to both V and inverted-V CBFs. Indeed, for those types of structural schemes, the beam behaviour significantly affects the seismic response. After brace under compression buckles, an unbalanced vertical force due to the different forces transferred by tension and compression braces is applied on the brace-intercepted beam, which is subjected to large bending moment. In such condition, the formation of a plastic hinge at mid-span of the beams should be avoided; otherwise it would result in a drop of storey lateral resistance with consequent inelastic drift concentration at the storey with yielded beam and significant deterioration of the overall response. In order to prevent this detrimental behaviour, the brace-intercepted beam should be designed to withstand: (i) all non-seismic actions without considering the intermediate support given by the diagonal members; (ii) the vertical component of the resultant force transmitted by the tension and compression braces. EN-1998, calculates the vertical component acting on the brace-intercepted beam in chevron bracings assuming that the tension brace transfers a force equal to its design plastic resistance ($N_{\mathrm{pl,br,Rd}}$) and the compression brace transfers a force corresponding to reduced compression strength due to degradation under cyclic loading. The post-buckling compression strength is estimated as $\gamma_{\mathrm{pb}}N_{\mathrm{pl,br,Rd}}$ with a value of the factor γ_{pb} to be found in the National Annexes; the value recommended by EN 1998 is equal to 0.30.

According to the AISC341, the required strength for beams in SCBFs (whatever bracing configuration is selected) should be defined by considering the most detrimental condition derived from (i) performing plastic mechanism analyses or (ii) by using the system overstrength factor Ω_o (fixed equal to 2) to magnify the earthquake-induced effects evaluated by mean of elastic analysis.

No overstrength factor is recommended by Canadian code and only plastic mechanism analysis is permitted.

With reference to plastic mechanism analysis approach, it is interesting to note that the calculation of tension and compression post-buckling strengths of braces varies between the different codes. These differences can significantly affect the design of non-dissipative elements modifying mutual strength and stiffness ratios between the elements and thus the global performance (Longo *et al.*, 2008; Longo *et al.*, 2009; D'Aniello *et al.*, 2010; Marino, 2014; D'Aniello *et al.*, 2015). According to AISC 341, non-dissipative members should be designed to resist design forces derived by assuming full expected yield strength (namely $\gamma_{ov}N_{pl,br}$) for the braces in tension and the 30% of the average buckling strength for the braces in compression (namely $0.3\gamma_{ov}\chi N_{pl,br}$). In CSA S16-09, full probable yield strength ($\gamma_{ov}N_{pl,br}$) is assumed for tension brace, while the compression post-buckling strength is taken as the lesser between the 20% of the relevant probable tension strength ($0.2\gamma_{ov}N_{pl,br}$) and the buckling strength also computed using probable yield stress of the steel ($\gamma_{ov}\chi N_{pl,br}$).

In the light of these considerations, EC8 potentially leads to weaker beams, because it assumes the larger post-buckling strength for braces; more details about the evaluation of post-buckling capacity of bracing members under repeated cyclic loadings can be found in Section 3.3. However, it is necessary to underline that all codified design rules and requirements for beams belonging to spans equipped with bracings in V and inverted-V configurations focus the attention only on the strength of the beam intercepting the bracing members, disregarding the role played by its flexural stiffness. Conversely, several studies (Khatib *et al.*, 1998; Tremblay and Robert, 2001; D'Aniello *et al.*, 2015) already showed the influence of the beam flexural stiffness on the seismic performance of chevron bracings, being the beam displacement and the brace axial deformation correlated phenomena (See Fig. 5.1 in Chapter V). This issue is specifically addressed and widely discussed in Chapter V, where the reader can found more details.

All codes requirements related to the beams belonging to the braced spans are compared and summarized in Table 3.2, where the nomenclature adopted by EN-1998 is extended also to other standards.

Another key aspect is related to the beam-to-column connections in the braced bays. Indeed, AISC 341 requires moment-resisting beam-to-column connections in the braced bays in order to improve the degree of redundancy and thus favouring redistribution of damage. In addition, this requirement also allows increasing the beams flexural stiffness, thus resulting in better performance (Khatib *et al.*, 1998; Tremblay and Robert, 2001; D'Aniello *et al.*, 2015). No similar requirement can be recognized in European and Canadian codes.

3.2.5 *Design of columns.*

EN-1998 imposes to design the columns of the braced bays, independently from bracing configuration, to withstand the force given from Eq. (3.2); no plastic mechanism analysis is requested to evaluate the required strength of columns. According to the US approach, similarly to the requirements for beams, the required strength of columns in SCBFs is defined by considering the most severe condition among the forces obtained magnifying by the system overstrength factor $\Omega_o = 2$ or those obtained by plastic mechanism analysis (as described in Sections 3.2.2 and 3.2.4).

Similarly to the design of beams, CSA S16 does not provide any overstrength factor and the strength hierarchy is assured only by means of plastic mechanism analysis. With this purpose, two loading conditions occurring in the compression braces should be considered in conjunction with tension braces developing their probable yielding strength: (i) the compression acting braces attaining their probable compressive strength (ii) the compression acting braces attaining their probable buckled resistance.

Moreover, the Canadian code includes additional provisions to account for the flexural demand imposed on continuous columns of multi-storey structures deriving from the variation in storey drifts between adjacent storeys in seismic event. Since this bending moment is usually disregarded by performing linear elastic analysis, CSA S16 states that columns of braced bays should be designed considering an additional bending moment equal to the 20% of their plastic flexural strength. No similar requirement is given by other codes.

Table 3.2. Required strength of non-dissipative elements

If plastic mechanism analysis is used			
Assumption	*EN-1998 (DCM, DCH)	AISC 341 (SCBF)	CSA S16-09 (MD CLASS)
Force in tension braces	$N_{\mathrm{pl,br,Rd}}$	$\gamma_{\mathrm{ov}} N_{\mathrm{pl,br}}$	$\gamma_{\mathrm{ov}} N_{\mathrm{pl,br}}$
Force in compression braces	$0.3N_{\mathrm{pl,br,Rd}}$	$0.3\chi\gamma_{\mathrm{ov}} N_{\mathrm{pl,br}}$	$min(0.2\gamma_{\mathrm{ov}} N_{\mathrm{pl,br}};\ \gamma_{\mathrm{ov}}\chi N_{\mathrm{pl,br}})$
If overstrength factor is used			
Assumption	EN-1998 (DCM, DCH)	AISC 341 - SCBF	CSA S16-09 MD CLASS
Overstrength factor	$1.1\ \gamma_{\mathrm{ov}}\ \Omega_{\mathrm{i\ i}}$	Ω=2	-

*required only for beams in V and inverted-V configurations

3.3 DISSIPATIVE BEHAVIOUR OF DIAGONAL MEMBERS

3.3.1 *Inelastic behaviour of bracing members subjected to cyclic axial loading*

3.3.1.1 Hysteretic response

As widely discussed in previous Sections, the seismic performance of concentrically braced frames is primarily affected by the behaviour of the diagonal members, which are selected as structural fuses responsible of dissipating the input seismic energy. Thereby, the energy dissipation capacity of the system strongly depends on the capability of its bracing members to sustain several cycles of inelastic deformation including both yielding in tension and buckling phenomena under compression.

In light of the above consideration, the knowledge of the inelastic behaviour of bracing members subjected to cyclic axial loading represents a fundamental support to satisfactory seismic design of concentrically braced frames. Moreover, in accordance with capacity design philosophy, a reliably evaluation of the actual axial forces developing into diagonal members during the earthquake is also necessary to assure adequate overstrength in non-dissipative elements.

The cyclic response of steel bracing members has been widely discussed, and numerous theoretical studies and experimental investigations are available in literature. A typical hysteretic response for a rectangular hollow section (RHS) subjected to quasi-static test (performed by Archambault *et al.*, 1995) is shown in Fig. 3.5 (picture taken from Tremblay, 2002).

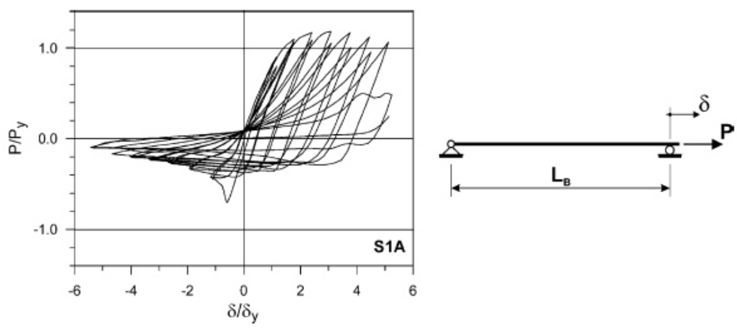

Figure 3.5 Typical hysteretic response of RHS (from Tremblay, 2002)

As described by Bruneau *et al.* (1998), the consecutive stages composing the hysteretic cycle of a brace under cyclic loading are depicted in Fig. 3.6, where the axial force is indicated with the capital letter *P*, while *d* is the axial elongation and *w* is the out-of-plane displacement at the mid-length of the brace.

A complete hysteretic cycle can be schematically described as follow:

- OA branch: at first stage the brace is subjected to compression axial load and behaves elastically; the elastic range ends when the diagonal member attains its compression strength and buckling occurs at point A.

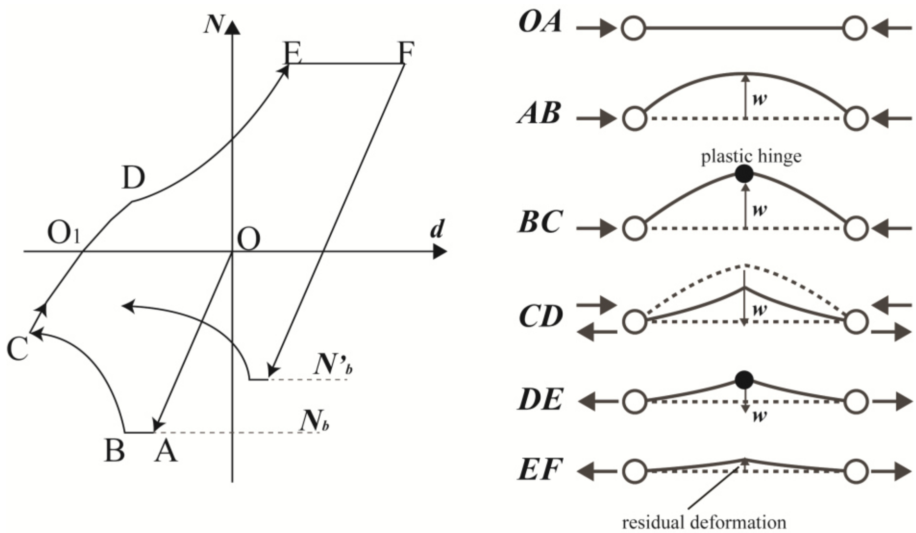

Figure 3.6 Hysteretic response of a bracing member under axial cyclic loading

- AB branch represents the elastic buckling: the bracing can sustain the applied axial load while the member deflects laterally. Up to point B, the brace experiences reversible (elastic) deformation and eventual unloading would proceed along BAO path.

  During the buckling, flexural bending moment develops along the member, equal to the axial force multiplied by the out-of-plane deflection *w*. If the flexural strength of brace (accounting for the interaction with the axial force) is attained, plastic hinge starts forming at the brace mid-length (see point B).

- Branch BC is characterized by nonlinear interaction between axial force N and axial elongation d with increasing plastic hinge rotation at the mid-length. The "shape" of branch BC mainly depends on the brace slenderness ratio.
- When the load direction is inverted, the member is subjected to unloading from point C; residual deformation is retained (see point O_1) as well as large lateral deflection.
- Tension loading is applied; the brace experiences elastic elongation from point O_1 to point D. At this stage the bending moment given by $N \cdot w$ reaches the plastic strength (reduced due to the interaction with axial force and to the plastic deformation occurred in the first part of the cycle) and a plastic hinge occurs at the brace mid-span, experiencing rotations with opposite sign respect to those occurred in branch BC; thereby, the out-of-plane deflection is reduced and progressively larger axial force can be applied.

However, before the brace can experience yielding under tension, perfectly straight configuration cannot be achieved; therefore when the brace is unloaded and reloaded in compression, it is subjected to an initial deformation and its buckling capacity N'_b is decreased respect to the initial buckling capacity N_b. Moreover, if out-of-plane deflection becomes dominant, catenary effect is activated and the brace suffers tensile-elongation; this implies that the effective length of the brace becomes larger respect to its nominal value, thus resulting in increased slenderness ratio and smaller compression capacity.

After further loading cycles, the buckling capacity progressively decreases and stabilizes to a relatively constant value (Bruneau *et al.*, 1998).

The evaluation of post-buckling compression brace resistance (N_{pb}) under cyclic loading represents a key aspect of seismic design of concentric bracings, because it directly affects the design of other frame members. Seismic code generally provide recommended values to account for the compression strength degradation, simply expressed as a percentage of the relevant buckling capacity; with this regard, it is worth noting that the requirement given by EN1998-1 (see Section 3.2) leads to assume a distribution of forces that is inconsistent when slender braces are used. Indeed, for normalized slenderness close to the Eurocode 8 upper bound limit (namely equal to 2), the brace buckling resistance tends to the 20% of the plastic strength (χ factor is about 0.2), thus resulting lower than the value (i.e. 30%) suggested by the code to evaluate the brace post-buckling strength. Moreover, several researches showed that the threshold of brace post-buckling strength is highly dependent on the brace ductility demand (D'Aniello *et al.*, 2010; 2013, 2015). Nakashima *et al*. (1992) showed that for braces with intermediate slenderness ratios the post-buckling resistance drops at the 20% of axial plastic strength; according to Hassan ad Goel (1991) the residual post-buckling strength of braces in compression has to be assumed varying from 30% to 50% of the initial compressive strength. Moreover, Lee and Buneau (2005) recognized that the compression strength for brace with intermediate slenderness might considerably drop to approximately 20% of its original buckling strength for H-shaped bracing and 40% for square hollow section (SHS) bracing.

Thereby, from all the mentioned researches, it is clear that the post-buckling strength of braces under cyclic loading cannot univocally fixed, because it is affected by the slenderness of the member, the level of ductility demand and by the shape of the cross section.

Several authors suggest alternative formulations to assess the post-buckling compressive strength: Remeninikov and Walpole (2014) suggest using $0.3N_b/\bar{\lambda}$ for members with $\bar{\lambda} \geq 0.3$. Elghazouli (2010) proposes to use $0.6N_{pb}/q\bar{\lambda}^{1.5}$ involving as main parameters the normalized slenderness and the level of inelastic engagement given by the value of the behaviour factor *q*.

Moreover, for bracings in V and inverted-V configuration, the braced-intercepted beams are characterized by large displacement demand at brace intersection (Shen *et al.*, 2014, 2015; D'Aniello *et al.*, 2015) and in the most of cases, it is not possible to achieve the yielding of the braces in tension, while severe ductility demand is imposed to braces under compression. As already mentioned, several studies (Khatib *et al.*, 1998; Tremblay and Robert, 2001; D'Aniello *et al.*, 2015) already showed that the flexural stiffness of the brace-intercepted beam deeply affects the response of bracings in V and inverted-V configurations under reversal cyclic loads. Indeed, the brace ductility demand in compression significantly increases with the beam vertical deflection. Therefore, structures with strong and deformable beams are characterized by poor seismic performance, showing severe damage concentration in the braces under compression, while those in tension behave elastically. In particular, D'Aniello *et al* (2015), based on a comprehensive parametric numerical study, provide an analytical relationship correlating the brace post-buckling compression strength to the mutual beam-to-brace vertical stiffness ratio K_F; more detail about this issue can be found in Chapter V.

The brace post-buckling prediction curves obtained by both Remennikov and Walpole (2014) and Elghazouli (2010) (a) and D'Aniello *et al.*, (2015) (b) are shown in Fig. 3.7.

By comparing the different formulations, it can be noted that the post-buckling strength recommended by EN 1998-1 is larger respect to the values resulting from the analyses and proposed by the above mentioned researchers, thus resulting in non-conservative evaluation of required strength for the brace-intercepted beam.

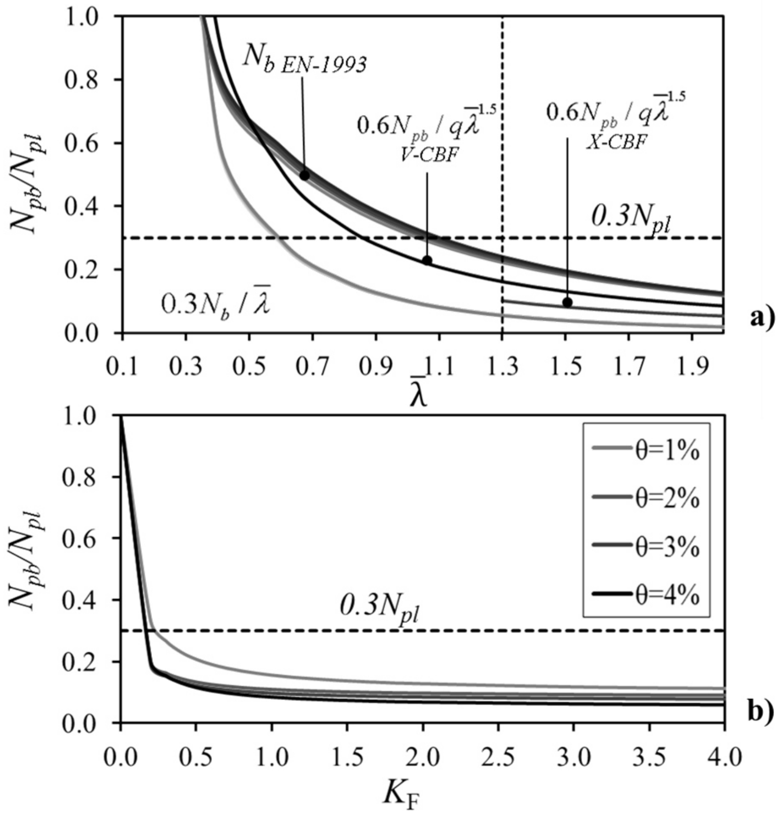

Figure 3.7 Post-buckling strength evaluation: comparison between different formulations.

Beside the compression strength degradation, another key aspect for the seismic design of concentrically braced frames deals with the need to quantify both the actual energy dissipation and the ductility capacity of the diagonal members, subjected to repeated cyclic loads.

Previous researchers (Jain *et al.*, 1980; Remennikov and Walpole, 1998; Tremblay, 2002, Elchalakani *et al.*, 2003) identified several key parameters affecting the hysteretic response of bracing members, among them both global and local slenderness. As described in the previous Sections, both US and European seismic codes provide design requirements and detailing rules based on the assumption that diagonal members with low normalized slenderness offer advantages in terms of large compression strength and energy dissipation capacity; however, several study (Tang and Goel, 1989; Goel and Lee, 1992, Tremblay, 2000) highlighted that stocky members are more sensitive to local buckling phenomena leading to lower ductility capacity and brittle failure, having found that the post-buckling cyclic fracture life of bracing members generally increases with an increase in slenderness ratio, mainly due to the severe strain demand experienced at plastic hinges location. Such results were implemented in the Canadian seismic code (CSA 16-09) in which the width-to-thickness ratios are provided depending on the member slenderness ratio (See Section 3.2.3).

Kumar *et al.* (2015) carried out a comprehensive FEM campaign to investigate the optimal width-to-thickness limitations for bracings made of circular hollow sections; the analyses results confirmed the relationship between local and global slenderness and a simple exponential equation based on regression analysis of data has been proposed relating the limiting values of slenderness ratio and the diameter-to-thickness ratio. Moreover, results from simulations suggest that the local slenderness limitation provided by seismic codes (See Section 3.2.3) generally exceed the optimal values of width-to-thickness ratios suitable to prevent premature brace fracture and degradation of energy dissipation capacity.

The co-existing influence of both global and local slenderness was also observed by Goggins et al. (2006): the hysteretic behaviour of tubular steel bracings was experimentally investigated and examined in terms of buckling and post-buckling strength, ductility capacity and energy dissipation capacity. The test results showed that stockier members exhibits the largest initial compressive capacity and energy dissipation capacity; nevertheless, slender braces showed the largest ductility capacity. This feature can be explained considering that for stocky bracings local buckling was early observed, causing progressive strain localization more accentuated at each cycle. Conversely, no sign of fracture was recognized during the tests (namely until applied displacement value of 40mm) for slender bracings. In addition, tests carried out by Goggins *et al.* (2006) showed that, even though stockier members exhibited the larger compressive resistance, they were also prone to severe strength degradation in the post-buckling range. This behaviour have been also noted in both numerical results carried out and experimental data collected by Lee and Bruneau (2002, 2005), showing that, in the most of cases, slender bracing members have higher ductility demand, but less cumulative energy dissipation. Moreover, they observed that too strict slenderness ratio requirements, often lead to select large brace cross sections, behaving elastically during the entire duration of the earthquake and thus making paradoxal a detailing rules devoted to ductile design.

Numerous authors proposed analytical and semi-empirical formulation based on experimental results for predicting the ductility capacity of bracing members, as well as the fracture life and the rotation of fracture.

Relationships between the the ductility capacity (defined as the peak displacement divided by the yield displacement) and global slenderness have been established by several researchers (Trembaly, 2002; Goggins *et al*. (2006), based on regression analyses of experimental data, which satisfactorily match the test results. Other predictive equations available in literature address the co-existing influence of both global and local slenderness (e.g. Goggins *et al*., 2006, Nip *et al*., 2010). It is worth noting that all the above mentioned formulations predict values of ductility demand for bracing members that far exceed the limitation for brace axial deformation provided for by EN1998-3, showing that the requirement recommended by the European standards is too restrictive. Such results was also confirmed by D'Aniello *et al.*(2015); more detail about this issue can be found in Chaper V.

Empirical formulae are also available in literature to predict the fracture life, invoving both global and local slenderness parameters (Shaback and Brown, 2003; Tremblay *et al.*, 2003).

3.3.1.2 Out-of-plane deflection

In the post-buckling range of the hysteretic response, significant out-of-plane deflection should be expected at large ductility demand. Thereby, in order to avoid extent damage to the cladding walls, such parameter should be evaluated and controlled. Tremblay (2002) developed a simple formulation to reliably predict the lateral deflection at the brace-mid length, given as a function on the axial compression displacement and the length of the element between plastic hinghes at both ends (a plastic hinge model for a buckled fixed-ended strut is considered). The accuracy of the prediction given according to Tremblay equation has also been verified by Goggins *et al.* (2006), showing a good matching with experimental results except for very large displacements (see Fig. 3.8).

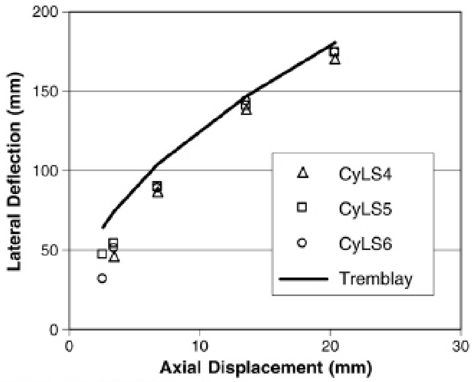

(b) 20 × 20 × 2.0 SHS specimens.

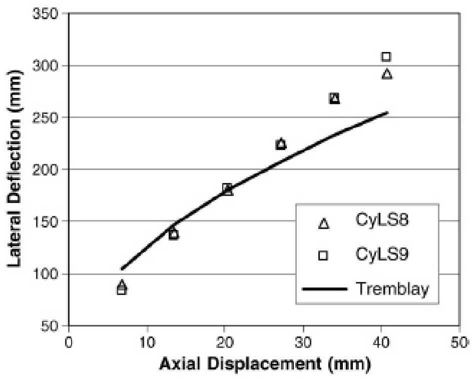

(c) 50 × 25 × 2.5 RHS specimens.

Figure 3.8: comparison between predictive formulation by Tremblay (2002) and experimental results carried out by Goggins *et al.* (2006). (Picture taken by Goggins *et al.,* 2006)

3.3.1.3 Tensile strength

Beside the compressive capacity, realistic predicion of axial force developing in tension braces plays also a key role in assuring adequate protection of beams and columns. Monotonic tensile tests (Goggins *et al.*, 2006) on HSS showed that the yield strength of bracing members can be up 30% greater respect to the properties measured during copuon tests. In the framework of capacity design philosophy, appropriate attention should be put on this issue. Indeed, if the braces is selected as dissipative zone, its expected yield strength directly affects the design of non-dissipative members, potentially leading to non-conservative estimation of relevant required strengths.

Although seismic codes generally account for this effect by using the overstrength factors and/or material randomness coefficients, the actual increase in terms of tensile strength often exceed the value recommended by seismic standards. (Goggins *et al.*, 2006; Landolfo, 2013).

3.4 DESIGN CRITERIA: REVIEW OF EXISTING LITERARURE

Concentrically braced frames are widely used in seismic areas, owing their structural efficiency against lateral loads. Indeed, the large lateral stiffness provided by the diagonal members allows easily fulfilling serviceability limit state requirements; conversely, the seismic response under strong seismic action is strongly affected by several uncertainties, mainly due to the complexity of the hysteretic behavior of bracing members under

cyclic axial loading, which is not easy to be accurately predicted (see Section 3.3).
To account for these features, seismic codes generally provide relatively low response modification factors if compared to other steel seismic resistant systems (e.g. Moment resisting frames and eccentrically braced frames). AISC 341 provides a response modification factor R =6 for Special CBFs, while R=7 and R=8 are stipulated for eccentrically braced frames and special moment resisting frames, respectively; Japanese Seismic Code recommends a force reduction factor $1/D_s$ ranging from 2 to 4 for braced frames, while set equal to 4 for MRFs; in the Canadian code the response factor is specified as $R = R_d \times R_o$. The factor R_o accounts for the overstrength of the structure; R_d factor accounts for the expected ductility and it is equal to 3.0 for both EBFs and CBFs, and 3.5 for MRFs in MD class (moderate ductile class).
Moreover, it is interesting to note that all the above mentioned seismic codes assign the response modification factor regardless the bracings configuration. Conversely, Eurocode 8 considers two sub-categories of concentrically braced frames, relating the value of the behaviour factor q to the configuration of diagonal members, namely q=2.5 for bracings in chevron configuration, and q=4 for both X-CBFs and diagonal bracings.
Bracings in chevron configurations represent one of the most cost-effective solutions for seismic resistant systems in steel buildings (see Chapter VI for more details); moreover, inverted-V configuration is often preferred owing to its inherent architectural functionality, allowing openings to be included in bracing bents. However, under strong seismic action chevron

concentrically braced frames would exhibit rather poor inelastic response, mainly due to the early buckling of the diagonal under compression and severe vertical deflection of the beams connected to the bracing systems. Indeed, only relatively recently US code provisions (AISC in 1997 and ICBO in 1997) permit the use of bracings in chevron configuration in the Special Concentrically Braced Frames category (see Section 3.2.1), provided that additional requirements for the brace-intercepted beams are satisfied.

Several Authors (Longo *et al.*, 2008 and 2009; Marino, 2014) proposed new design criteria devoted to improve the seismic performance of concentrically braced frames, accurately accounting for the nonlinear behaviour of diagonal members under cyclic axial load. In this Section, a critical review of design criteria from existing literature is provided, with special reference of steel braced systems equipped with bracing in chevron configuration, being the design of X-CBFs out of the scope of this thesis.

Marino (2014) proposed a unified approach for the seismic design of high ductility steel frames equipped with concentric bracings (whatever configuration is considered) in the framework of EN 1998; the method includes design criteria previously proposed by the author (Marino and Nakashima, 2006) for chevron bracings and then extended to diagonal configuration. According to this procedure, a behaviour factor q=3.5 is assumed and the lateral resistance of a pair of diagonal members is evaluated assuming that the tension and compression bracings provide their yielding and buckling forces respectively; this procedure allows ensuring identical elastic stiffness and

similar strength regardless of the brace slenderness. The unified approach proposed by Marino (2014) assures an equivalent level of structural safety as the EC8 procedure, and it leads to similar seismic performances in terms of demand on both dissipative and non-dissipative elements, whatever configuration is considered.
Longo *et al.* (2008, 2009) suggested that the design recommendation provided by modern seismic codes (based on hierarchy of strength criteria at local level), are not sufficient to assure ductile global failure mode forms and to avoid the development of soft-storey mechanisms. In order to overcome the critical issues affecting the seismic response of chevron concentrically braced frames, Longo *et al.* (2008, 2009) proposed a new design methodology aimed at assuring the development of a global collapse mechanism characterized by the full yielding of braces under tension; with this aim, the axial forces acting in non-dissipative members are evaluated considering a distribution of internal action based on a deformed configuration in which the braces are yielded at all storeys. The proposed procedure basically overcomes some criticism of the EC8-compliant method mainly due to the underestimation of axial force acting in the columns; on the other hand, an increase in structural weight (and as a consequence of the cost of construction) is recognized, without reaching significant benefits in terms of yielding in tension and energy dissipation capacity.
Such result can be explained considering that the assumed deformed configuration corresponding to the global failure mode, do not account for the beams vertical deflection. Conversely D'Aniello *et al.* (2015), underlined that, for bracing in chevron configuration, the axial demand in the diagonal

members strongly depends on the beam vertical deflection at the brace intercepted section and thus on the beam flexural stiffness; more details about this issue can be found in Chapter V, where the influence of the beam flexural stiffness on the seismic performance of chevron bracings is widely discussed.

3.5 TECHNOLOGICAL ASPECTS

Beside the capacity design requirements, accurate design of ductile detailing is even necessary to guarantee satisfactorily seismic performance of concentrically braced steel structures.

Unfortunately, in the frame of EN 1998-1 several issues related to conceptual design, technological aspects, ductile design of components and connections are missing or scarcely addressed. On the contrary US codes provide more comprehensive design information about the rational and effective design of ductile details.

In this Section, the main technological aspects to be accounted for in the design of ductile concentrically braced frames are briefly addressed, with special focus on the detailing of brace-to-brace, brace-to-beam/column, brace-to-beam mid-span and brace-to-column base connections.

3.5.1 *Detailing for brace-to-beam/column connections*

As discussed in Section 3.3 the seismic performance of bracing members of CBFs is characterized alternate buckling under compression and yielding under tension of diagonal members.

The buckling mode of the compression brace leads to the formation of plastic hinge(s) at both the mind-length of the member and its ends, depending on the restraint-degree (namely pinned or fixed restraints) provided for by the connections between the bracings and the beams and columns.

If the braces are designed to be fully fixed at both ends, the connections should be detailed to restrain the plastic rotation of the diagonal members; conversely, if the braces are designed as pinned-restrained, the connections should allow the plastic out-of-plane rotation and they should be able to sustain large plastic deformation in order to provide adequate flexural ductility.

According to capacity design objectives, the gusset plates connecting braces to the beams and columns should be designed to withstand the inelastic capacity of brace in tension and compression. EN1998-1 states that the required strength of the brace end-connections should satisfy the following inequality:

$$N_{j,Rd} \geq 1.1 \cdot \gamma_{ov} \cdot N_{pl,\mathrm{br},Rd} \tag{3.3}$$

Where $N_{\mathrm{j,Rd}}$ is the joint required axial strength; $N_{pl,br,Rd}$ is the plastic axial strength of the brace; γ_{ov} is the material overstrength factor.

It is worth to note that such requirement only addresses the axial required strength, while the flexural capacity of the connection is disregarded. As a consequence, in case fixed restrained are provided at both ends, the Eq. (3.3) does not guarantee to confine inelastic rotation to the bracing member only. In addition, no ductility requirement is provided to assure adequate rotation capacity in case of pinned restraints.

Larger attention is given to proper detailing of connections in the US code. AISC 341-10 states that if the end connections are conceived as fixed, they should be design to withstand the brace yield strength in tension and the bending-axial interaction effect due to the buckling of the brace in compression. In detail, the axial force is assumed equal to the buckling strength of the brace, while the bending moment is assumed equal to the plastic flexural strength of the brace amplified to account for both material randomness and strain-hardening coefficients. However, this type of bracing end connections are not widely employed in building frames because double gusset-plates (i.e. one for each side of the brace cross section) are necessary to provide adequate flexural strength.

Most commonly, pinned end-restrained are realized by using single gusset plates to connect bracings to the main frame; in this case the out-of-plane buckling is accepted, and the brace end rotations induce weak-axis bending in the gusset plate, as shown in Fig. 3.9.

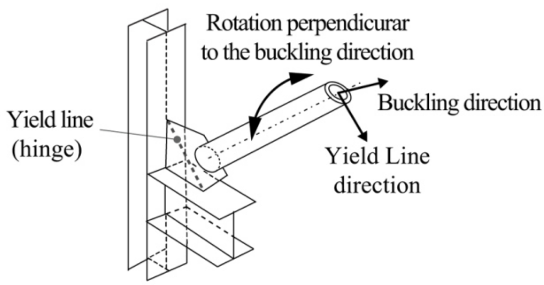

Figure 3.9 Weak-axis bending in the gusset plate due to out-of-plane buckling of braces.

Under this condition, the buckling of gusset plates should be avoided, enforcing restraint-free plastic rotations into a hinge line (i.e. yield line) in the gusset plate, which acts as an equivalent pin connection, allowing the brace rotation (see Fig. 3.10).

The yield lines at each end of the brace must be perpendicular to the brace axis (see Figs. 3.11). AISC 341-10 recommends to assure for the gusset-plate hinge-zone (namely the zone where yield line can form) a minimum free length short enough to avoid the plate buckling prior to the member buckling and long enough to permit plastic end rotations: on the basis of tests and recommendations by Astaneh-Asl et al. (1982, 1983, and 1985), the free length is assumed equal to 2*t* (where *t* is the thickness of the gusset plate) between the end of the brace and the assumed geometric line of gusset restraints that is drawn from the point on the gusset plate nearest to the brace end that is constrained from out-of-plane rotation (see Fig. 3.12 where gusset-plate hinge-zone is indicated as "*a*" segment).

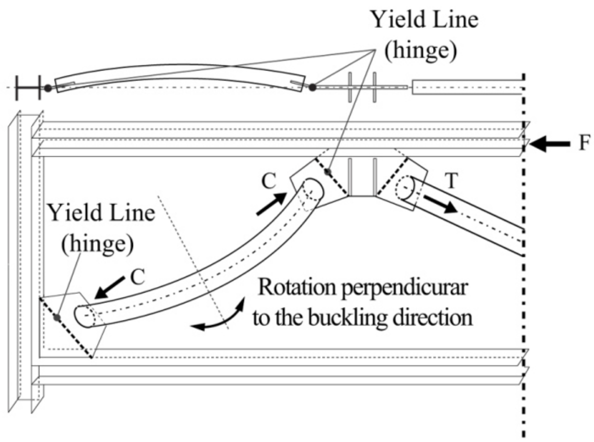

Figure 3.10 Out-of-plane buckling mode of braces and formation of yield line in the gusset plate.

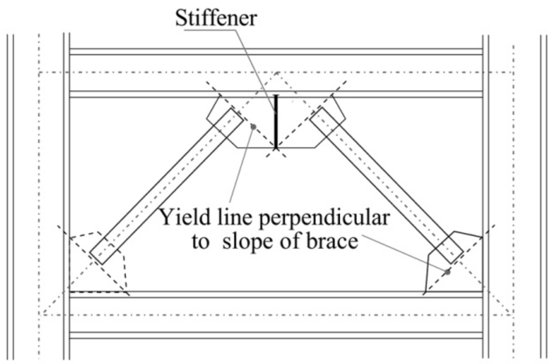

Figure 3.11: Bracing centrelines and gusset plate yield lines.

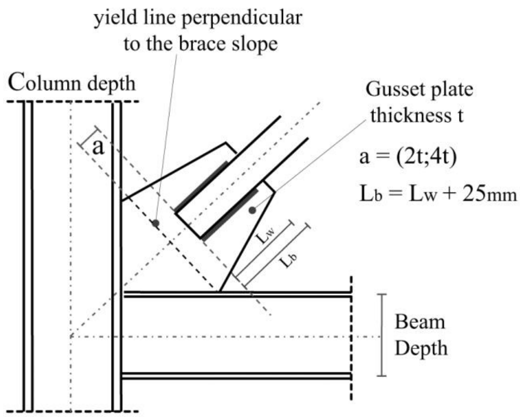

Figure 3.12: Gusset plate yield line and off-set requirements.

It should be noted that $2t$ is the minimum offset for the yield line. As shown by Cochran (2003), due to erection tolerances larger offset are recommendable (e.g. $3t$). Anyway, according to Astaneh-Asl et al. (2006) actual hinge-zone length at either end of the brace should be no larger than 4*t* in order to guarantee that the detail works properly.

The yield line off-set (namely the *a* length) should properly extend across the width of the gusset plate to both free edges of the gusset plate. Typically, the yield line intersects the beam or column flange with one end of the gusset plate (as shown in Fig. 3.12).

At the contrary, if the yield line intersects the zone of gusset plate welded to the beam or to the column (see Fig. 3.13), the out-of-plane deformation of the plate is restrained and thus susceptible of tearing along the edges owing severe plastic strain concentration due to the brace rotation.

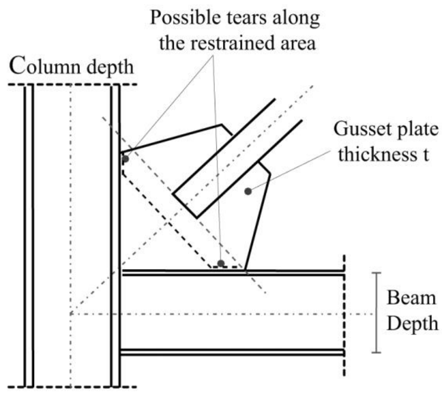

Figure 3.13 Not recommended gusset plate yield line: inadequate off-set and potential tears along gusset plate restraints.

Similar phenomenon may also occur owing the interaction between gusset plate and concrete slab (see Fig. 3.14). Indeed, the presence of concrete slab around the gusset plates implies flexural restraint inhibiting out-of-plane rotation and the formation of the yield line at the intersection with the beam flange. To avoid this detrimental effect, a interposed zone isolating the gusset plate from the concrete slab can be arranged and filled by using a compressible material as shown in Fig. 3.14a (e.g. polystyrene, fire caulking, etc.). Figure 3.14b shows a gusset plate restrained by the presence of the concrete slab. In this case no interposing zone is provided for and the yield line is expected at the top of the slab. In such condition, the free length a of the gusset plate is too large generally more than $4t$ beyond the theoretical yield line) and an edge stiffener can be arranged to stabilize the gusset plate and restrain the yield line. An offset of 2 times the thickness of the gusset plate should be provided between the end of the stiffener and the location of the yield line: in such a way no welds are located close to the yield line, thus preventing any possible fracture initiation in or near the gusset plate hinge-zone.

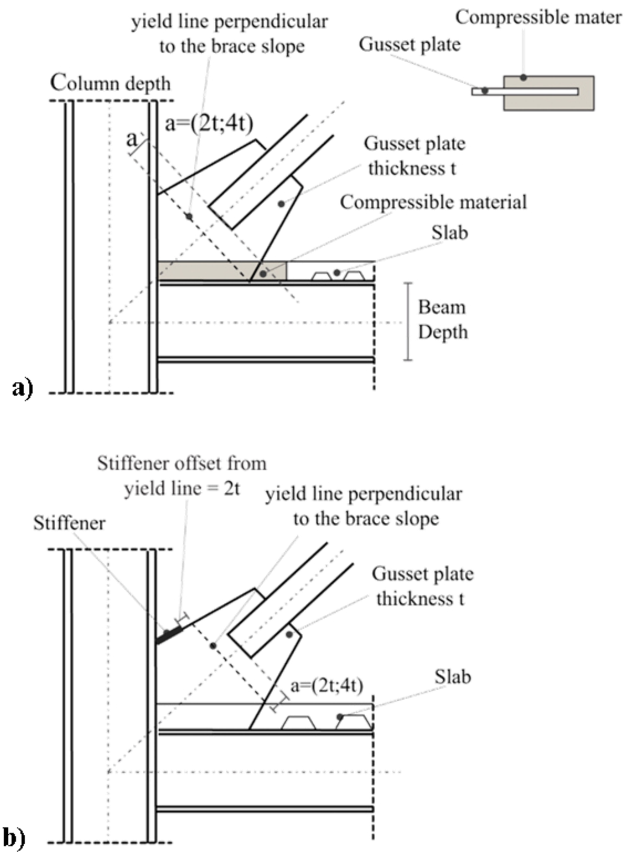

Figure 3.14 Interaction between slab and gusset plate: (a) gusset plate with yield line isolated from concrete slab (b) edge stiffener for gusset plate.

The design of gusset plate in terms of both shape and size is significantly influenced by the geometrical dimension of the braced bays. Indeed, the slope of diagonal members determines the dimension of the gusset plate in order to satisfy the geometric requirement of yield line offset between 2*t* and 4*t* from the end of the brace. Figure 3.15 shows the so-called “critical angle”. The critical angle is defined as the minimum between brace-to-beam and brace-to-column angles, which corresponds to the side of the brace yield line intersects either the column or beam flange at one end, while at the other end, it intersects the free edge of the gusset plate. Only in the rare case that both column and beam have the same depth, and the brace slope is 45°, each end of the yield line would intersect both column and beam flange simultaneously.

The concept of critical angle has been developed in the US constructional practice, while it is absent in the European framework. The US designer usually provides solely this geometrical datum to the steelwork company which provides the gusset plate geometry on the bases of the actual building dimensions. Figure 3.15a depicts a critical angle on the beam side, since the first restraint of the yield line occurs at the beam flange and the opposite end occurs at the free edge of the gusset plate. On the contrary, Figure 3.15b shows an example of critical angle on column side.

In addition, Cochran (2003) and Astaneh-Asl et al. (2006) provide some useful prescriptions to detail properly the gusset plate, which are summarized as follows:

1. A minimum offset equal to 25 mm from each side of brace to the free edge of gusset plate should be considered, thus improving the gusset plate strength against block shear check;

2. A slope γ of 30 degrees at the edge of the gusset plate as respect to the brace axis is advisable (see Fig. 3.15);

3. The brace lap length L_b onto the gusset plate when welding is used should be detailed 25mm longer than the specified weld length L_w as shown in Fig. 3.12 This allows for beginning and termination of the weld slightly away from the end of the brace member and end of the gusset plate.

4. Assuming a gusset plate thickness between 15 mm to 40 mm to determine the 3*t* offset distance to avoid huge dimensions of connections.

As already mentioned, the gusset plate should be verify against the axial forces transferred by the yielded tension brace and the buckled compression brace; with this regard it is necessary to define the effective width W_d of the plate at the hinge zone, in order to determine the relevant resisting zone. Whitmore (1952) proposes to assume the effective width of the gusset plate as shown in Fig. 3.16.

The width of the gusset plate to resist the applied axial force for bolted connections is defined by two lines 30° tilted respect the centreline axis of the brace, starting from the first bolts on the gusset plate. The portion of gusset plate outside the "Whitmore's width" should not be considered as able to resist design loads. In case of welded connection, Astaneh-Asl *et al*. (1982) recommended to consider the 30° lines from the starting point of the weld to the line passing through the end points of the weld itself.

The Whitmore's width W_d can be calculated as follows:

$$W_d = b + L_w \cdot 2\sqrt{3} \quad \text{for welded connections} \tag{3.4}$$

$$W_d = b + L_{bc} \cdot 2\sqrt{3} \quad \text{for bolted connections} \tag{3.5}$$

where L_w is the length of the weld connecting the bracing member to the gusset plate; L_{bc} is the length of the bolted connection of the bracing member to the gusset plate; b is the distance between the weld lines or bolt lines.

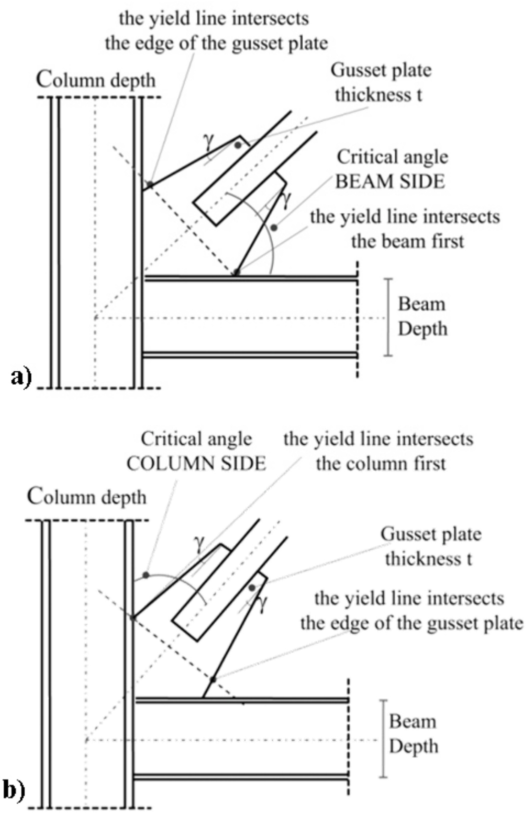

Figure 3.15: Critical angle concept: a) on beam side; b) on column side.

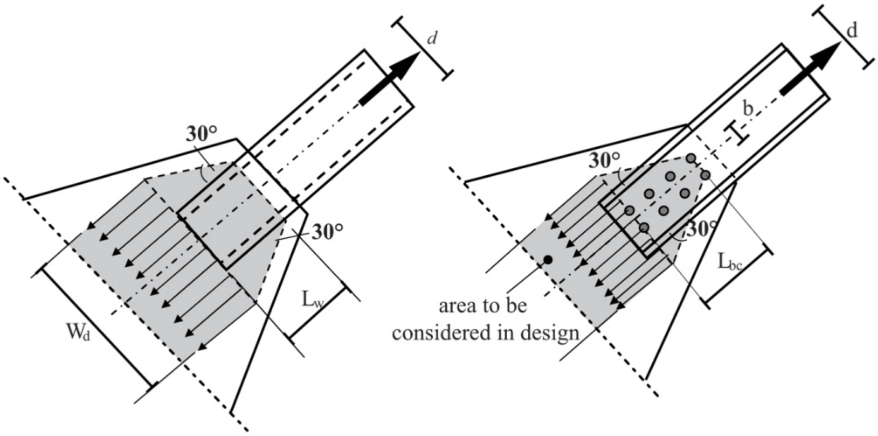

Figure 3.16: The effective width W_d calculated with Whitmore's method.

To accommodate the brace end rotation, by using a linear offset rule, often leads to design quite large gusset plates, resulting in uneconomical and unpractical solutions; with this regard Lehman *et al.* (2008), carried out a comprehensive experimental study devoted to investigate alternative details for gusset plates splices, in order to improve both the performance of the connection and its constructability. In order to obtain more effective and more compact shape of gusset plates, Lehman *et al.* (2008), proposed an elliptical clearance requirement in place of the linear yield line concept.

Figure 3.17 shows this type of detail, where the plastic hinge zone is shape as elliptical band with a clear 8*t* width, where *t* is the thickness of the gusset plate. The experimental evidence confirmed that, if the gusset plate is designed according to conform to this elliptical clearance, the connection provides large system ductility and deformation capacity, limiting fracture of the welds or brace.

The actual dimensions of the elliptical band can be easily determined graphically from the gusset plate dimensions.

Regarding the weld size requirements for gusset plates, several experimental and analytical studies are available (Johnson 2005, Yoo 2006), showing that, if fillet welds are used, their side should be equal to or greater than the thickness of the gusset plate.

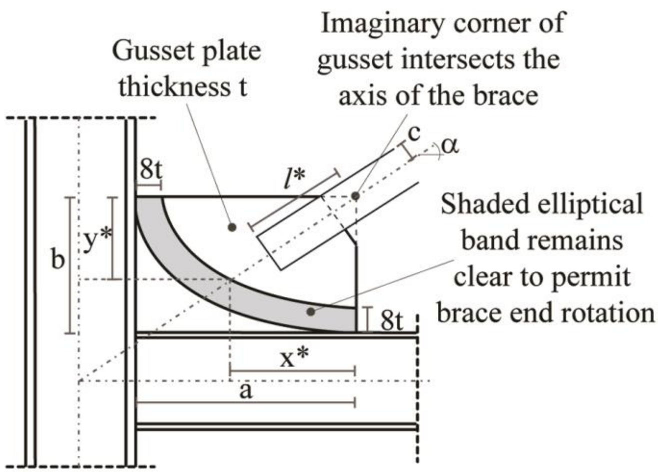

Figure 3.17 Elliptical clearance with 8t band width (Lehman *et al*. 2008).

3.5.2 *Detailing for braces-to-beam mid-span connections (V and inverted-V configuration)*

The mid-span braces-to-beam connection is typical of steel frames equipped with bracing in V or inverted-V configuration. The mid-span connection exhibit similar behaviour to the brace-to-beam/column connection; thereby its geometrical properties and design rules do not significantly differ (Astaneh-Asl *et al.* 2006). As a consequence, the concept of yield line (both linear and elliptical) described in Section 3.5.1) can be also extended to the braces-to-beam mid-span connection.

In addition, special attention should be reserved to the bottom edge of gusset plate, traditionally designed as straight free edge (see dashed line in Fig. 3.18). However, a recent research (Astaneh-Asl *et al.*, 2006) suggests tapering this portion of the gusset plate in order to reduce the length of the free-edge and avoid premature buckling of the plate (see Fig. 3.18)

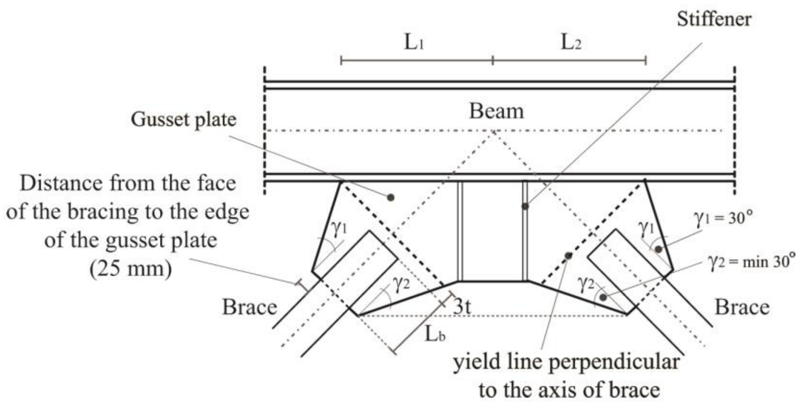

Figure 3.18 Details of brace-to-beam mid-span connection.

Moreover, the gusset plates should be trimmed back in order to avoid the overlapping of the two yield lines

Brace-to-beam mid-span gusset plates are generally quite large and slender. Therefore, transverse stiffeners (see Fig. 3.18) are necessary to prevent out-of-plane buckling and they should also be held at least $2t$ offset back from the plastic zone to prevent welding near this hinging area.

3.5.3 *Detailing for brace-to-brace connections (X configuration)*

The efficiency of bracing systems in cross-configuration strongly depends on detailing of both brace-end connections and brace-to-brace connection. Indeed, the slenderness is highly affected by the brace boundary conditions, which can vary from pinned to fixed, affecting the effective length of the elements.

The main issue relating to the design of the brace-to-brace mutual connection are discussed hereinafter. Intersected bracings can be conceived as either continuous (see Fig. 3.19) or discontinuous. In the former case, the braces are directly welded to each other and continuity plates are used as internal rigid restraint. The actual degree of the flexural restraint at the brace intersection depends on both flexural and torsional stiffness of the transverse diagonal member.

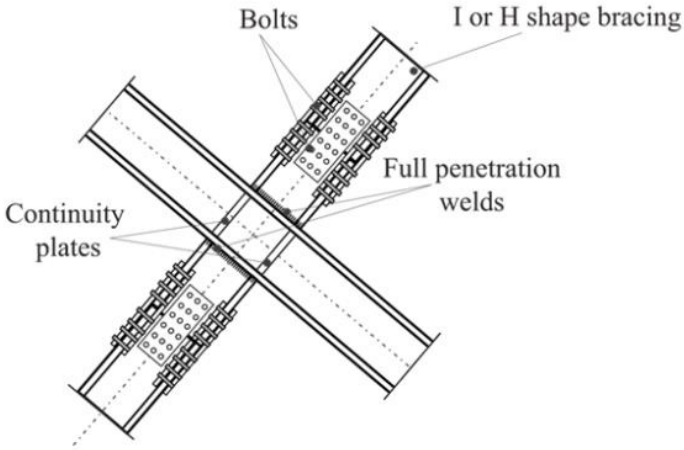

Figure 3.19 Example of continuous brace-to-brace connection.

Conversely, discontinuous X-bracings are constituted by two segments of bracing connected to one continuous brace. The connection at the braces intersection can be realized according to several types of details, namely by using welded or hybrid welded-bolted splices (see Fig. 3.20). Whatever type of splice is considered, in the structural model, the brace segments should be assumed to be pinned restrained, being the out-of-plane flexural stiffness of the gusset plate negligible compared to the braces one.

Finally, the connection at braces intersection can be also realized by using two discontinuous bracings, namely four brace segments connected to the gusset plate (see Fig. 3.21). In this case, the ends of each brace should be properly detailed (as discussed in previous Sections) in order to develop the yield line mechanism. In addition, this type of splice requires a very heavy central core (Ebadi and Sabouri-Ghomi, 2012) in order to restrain effectively the braces and to impose the buckling mode in the free portion of the brace between the yield lines of the gusset plates at both ends of each brace segment. This arrangement guarantees out-of-plane buckling with a buckling length clearly identified (i.e. roughly effective length equal to half length of the entire diagonal). In addition, the ductility and the fracture life of the bracing system is large because the gusset plates are mainly engaged in bending with poor torsion interaction.

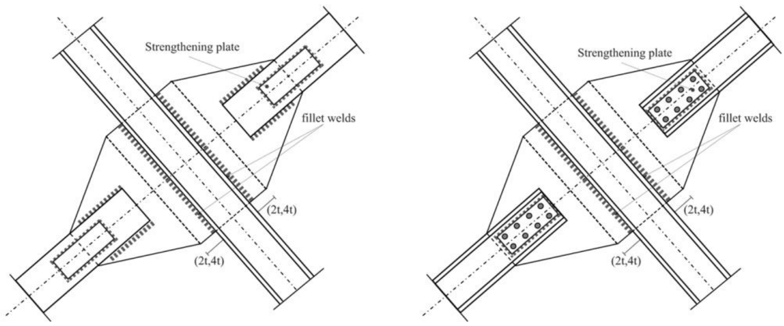

Figure 3.20 Example of discontinuous X-CBFs using different types of mid-length splices: a) welded and b) hybrid welded/bolted connection.

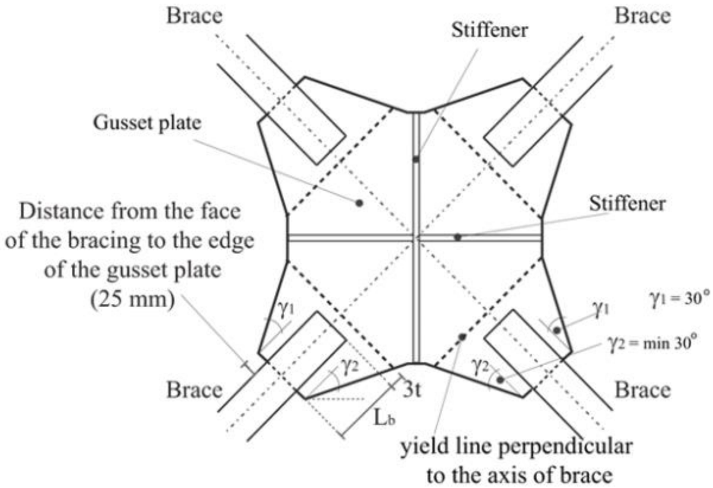

Figure 3.21 Example of brace-to-brace connection using two discontinuous bracing members and a stiffened central core.

3.5.4 *Detailing for brace-to-column base connections*

Geometrical requirements for gusset plates in brace-to-column base connection are basically similar to those described in Section 3.5.1. In addition, it is necessary to define the point of intersection of the re-entrant corner of the gusset plate, which can intersect the base plate (see Fig. 3.22a) or the column (see Fig. 3.23b).

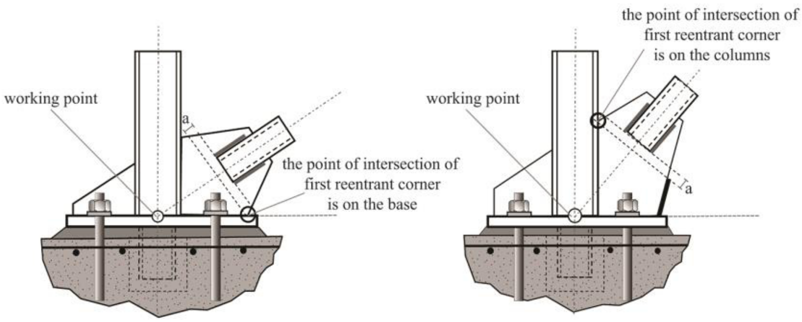

Figure 3.22 Examples of brace-to-column base connections.

3.5.5 *Optimal slope of bracings members and constructional tolerances and local details for braces*

The seismic response of concentrically braced frames significantly depends on the geometrical features of the bracing members; indeed the slope of diagonals directly affects the lateral stiffness of the system. Moreover, the slope of the bracings is important also for technological and constructional reasons. Indeed, if the relative brace-to-beam angle is either too small or too large, the gusset plate becomes too large. Astaneh-Asl *et al.* (2006) suggest the range [30°-60°] as optimal value for the brace-to-beam angle. Conversely, is advisable to change the arrangement of bracings, by shifting the diagonal into another span such that the brace slope is within the range of 30° to 60°.

It is worth to note that in theoretical models of CBFs the braces, the column and beam centrelines intersect together in the same node. However, this assumption may often impose quite large gusset plate leading to impractical and expensive solutions. Therefore, in actual structures, the end connections of bracings can be detailed with some eccentricities as respect to the ideal concentric model (see Fig. 3.23).

However, this detail can entail potential change of predominate inelastic deformation away from the bracing; thereby secondary moment developing into the connection due to the eccentricity between axial force transferred by brace and the frame centrelines should be accounted for. However, this design choice may arise some weaknesses and fallacies in the prediction of the actual structural behaviour. Indeed, if the brace-to-frame eccentricity is too large the structural scheme shifts from CBF to EBF. The most of seismic codes do not provide restrictions on the amount of eccentricity allowed in the brace-to-frame connections. Solely Uniform Building Code (1997), limits the maximum connection eccentricity to the smaller of half of the beam depth or half of the column depth intersected by the brace.

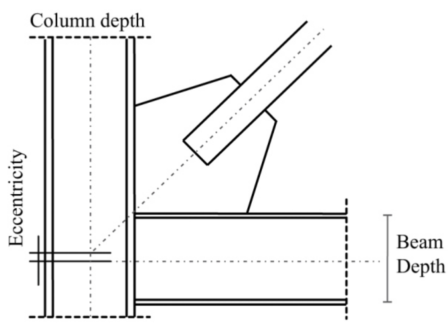

Figure 3.23 Examples of eccentricity between brace and frame centerlines.

3.6 CONCLUSIVE REMARKS

In the current Chapter the seismic behaviour of concentrically braced frames has been widely described and discussed.

The framework of existing standard provisions has been provided, by analysing the seismic design rules given by European and North-American standards. With this regard, the following remarks can be drawn:

- The behaviour factor given by US and Canadian codes does not depend on the bracing configuration. This implies that both X-CBFs and Chevron CBFs can be designed with the same design base shear force. On the contrary, Eurocode 8 recommends different behaviour factors for different bracing configurations, namely larger for cross CBFs (e.g. q = 4) than those for chevron CBFs (e.g. q = 2.5), because the former are expected to provide the largest ductility.
- AISC 341 allows using the largest behaviour factor (i.e q = 6), thus leading to braces more slender than those obtained according to EC8.
- EC8 generally allows using simplified design procedures; indeed, in the most of cases is sufficient to perform only a linear elastic analysis without calculating the plastic distribution of forces occurring after the brace buckling. On the contrary, both US and Canadian codes stipulate to perform further plastic mechanism analyses in order to assure the fulfilment of capacity design criteria. Even

though the European approach involves a significant simplification of design process, it often leads to underestimate the earthquake-induced effects in the non-dissipative members, leading to non-conservative design in the most of cases. This aspect is more evident for the columns in X-CBF configuration and for the beams in chevron configuration.

- With reference to the design of dissipative bracings, the requirements devoted to limit both global and local slenderness mighty differ between the examined codes. The requirements on global slenderness of the members are more relaxed in North-American codes respect to EN-1998, being based on the evidence that the post-buckling cyclic fracture life increases with an increase in geometrical slenderness. Moreover, by quantitatively comparing the width-to-thickness ratio (namely local slenderness) limitations, it emerged that US code provides the most severe limits. Conversely, EC8 limitations also for higher ductility classes are less severe even than US requirements for OCBFs, which are expected to provide the smallest ductility.
- With reference to the evaluation of post-buckling force acting in the diagonal members after the buckling of the compression bracings, it is not possible to recognize a unified approach between different codes. All examined codes do not relate the brace post-buckling strength either the brace slenderness or the level of plastic engagement, which instead significantly affect the degradation of brace compressive strength under repeated cyclic loading.

- Design provisions for chevron concentrically braced frames need to focus also on the stiffness of the brace-intercepted beam, being the beam deflection and the braces ductility demand correlated phenomena.
- Only US code provides further requirement relating to the beam-to-column connections in the braced bays, which should be moment-resisting type, in order to improve the redundancy of the system and thus favouring redistribution of damage. No similar requirement can be recognized in European and Canadian codes.

Since the energy dissipation capacity of the concentrically braced
frames strongly depends on the capability of its bracing members to sustain several cycles of inelastic deformation including both yielding in tension and buckling phenomena under compression, the inelastic behaviour of diagonal members under axial cyclic loads has been described, discussing on the hysteretic response, the brace out-of-plane deflection, and the brace tensile strength. With this regard, the following remarks can be drawn:

- The knowledge of the inelastic behaviour of bracing members subjected to cyclic axial loading has a key role in satisfactory seismic design of concentrically braced frames. Indeed, in accordance with capacity design philosophy, a reliably evaluation of the actual axial forces developing into diagonal members during the earthquake is necessary to assure adequate overstrength in non-dissipative elements.

- Even the energy dissipation capacity and the ductility capacity of diagonal members, subjected to repeated cyclic loads are significantly affected by both global and local slenderness. With this regard, test results (Goggins *et al.*, 2006) show that stockier members exhibits the largest initial compressive capacity and energy dissipation capacity; nevertheless, slender braces showed the largest ductility capacity. Indeed brace fracture life increase with increasing of slenderness ratio.
- Several researches (Elghazouli, 2010; Remennikov and Walpole, 2014; D'Aniello *et al.*, 2015) confirm that the post-buckling strength of braces under cyclic loading cannot univocally fixed, because it is affected by the slenderness of the member, the level of ductility demand and by the shape of the cross section. Different formulations are available in literature, involving the above mentioned parameter; in addition recent results show that the value of post-buckling capacity recommended by seismic code are not conservative in the most of cases.
- Monotonic tensile tests (Goggins *et al.*, 2006) on HSS showed that the yield strength of bracing members can be up 30% greater respect to the properties measured during copuon tests.
- In the post-buckling range of the hysteretic response, significant out-of-plane deflection should be expected at large ductility demand. Tremblay (2002) developed a simple formulation to reliably predict the lateral deflection

at the brace-mid length, given as a function on the axial compression displacement and the length of the element.

A critical review of design criteria from existing literature has been provided.

Beside the capacity design requirements, accurate design of ductile detailing is even necessary to guarantee satisfactorily seismic performance of steel systems. The main technological aspects to be accounted for in the design of ductile concentrically braced frames have been briefly addressed, with special focus on the detailing of brace-to-brace, brace-to-beam/column, brace-to-beam mid-span and brace-to-column base connections

3.7 REFERENCES

American Institute of Steel Construction, Inc. (AISC). (2010). Seismic Provisions for Structural Steel Buildings. ANSI/AISC Standard 341-10. AISC, Chicago, Illinois

Archambault M.H., Tremblay R., Filiatrault A. (1995) E´ tude du comportement se´ismique des contreventements ductiles en X avec profile´s tubulaires en acier. *Rapport no. EPM/GCS-1995-09*. In: Montreal,Canada: De´partement de ge´nie civil, E´ cole Polytechnique.

ASCE (2010). Minimum design loads for buildings and other structures (ASCE/SEI 7-10), American Society of Civil Engineers, Reston, VA.

Astaneh-Asl A., Cochran M.L., Sabelli R. (2006). Seismic

Detailing of Gusset Plates for Special Concentrically Braced Frames. *Structural Steel Educational Council- Steel TIPS.*

Astaneh-Asl A., Goel S. C. (1984). Cyclic In-Plane Buckling of Double Angle Bracing. *Journal of Structural Engineering, American Society of Civil Engineers (ASCE),* Vol. 110, No. 9, pp. 2036–2055 (www.asce.org).

Astaneh-Asl A., Goel S. C., Hanson R. D. (1982) Cyclic Behavior of Double Angle Bracing Members with End Gusset Plates. *Report No. UMEE 82R7*. Ann Arbor: University of Michigan.

Astaneh-Asl A., Goel S. C., Hanson R. D. (1983). Cyclic Behavior of Double Angle Bracing Members with Bolted Connections. *Engineering Journal, AISC*, Chicago (www.aisc.org).

Astaneh-Asl A., Goel S. C., Hanson, R. D. (1985). Cyclic Out-of-Plane Buckling of Double Angle Bracing. *Journal of Structural Engineering*, ASCE, Vol. 111, No. 5, pp. 1135–1153 (www.asce.org).

Bruneau, M., Uang, C.M., Whittaker, A. (1998) Ductile design of steel structures, McGraw-Hill, Network..

Cochran M.L. (2003) Seismic design and steel connection detailing. *Proceedings of NASCC*, Baltimore, MD – April 2-5.

CSA. 2009. Design of Steel Structures, CSA-S16-09, Canadian Standards Association, Toronto, ON

M. D'Aniello, S. Costanzo S., Landolfo R. (2015) The influence of beam stiffness on seismic response of chevron concentric bracings. *Journal of Constructional Steel Research,* Vol. 112, pp 305–324.

D'Aniello M., La Manna Ambrosino G., Portioli F., Landolfo R. (2013) Modelling aspects of the seismic response of steel concentric braced frames *Steel and Composite Structures, An International Journal*, Vol. 15, No. 5, pp 539-566.

D'Aniello M., La Manna Ambrosino G., Portioli F., Landolfo R. (2015) The influence of out-of-straightness imperfection in Physical-Theory models of bracing members on seismic performance assessment of concentric braced structures. *The Structural Design of Tall and Special Buildings*, 24(3), pp. 176-197 . 2015. DOI: 10.1002/tal.1160.

D'Aniello M., Portioli F., Landolfo R. (2010) Modelling issues of steel braces under extreme cyclic actions. *In Proceedings of COST-C26 Final Conference* — Naples 16-18 September; pp. 335-341, 2010.

D'Aniello, M., Landolfo, R., Piluso, V., and Rizzano, G. (2012). Ultimate Behaviour of Steel Beams under Non-Uniform Bending. *Journal of Constructional Steel Research* 78: 144–158.

D'Aniello, M., Güneyisi, E.M., Landolfo, R., and Mermerdaş, K. (2013). Analytical prediction of available rotation capacity of cold-formed rectangular and square hollow section beams. *Thin-Walled Structures*. 10.1016/j.tws.2013.09.015

Ebadi P., Sabouri-Ghomi S. (2012). Conceptual study of X-braced frames with different steel grades using cyclic half-scale tests. *Earthquake Engineering & Engineering Vibration* 11: 313-329.

Elchalakani M, Zhao XL and Grzebieta R (2003) Tests of coldformed circular tubular braces under cyclic axial loading. *Journal of Structural Engineering,* ASCE 129(4): 507–514.

Elghazouli A.Y.(2008) Seismic design of steel framed structures to Eurocode 8, , in *Proceedings of the 14th World Conference on Earthquake Engineering*, Beijing, China, 12-17 October. 2008.

Elghazouli A.Y. (2010) Assessment of European seismic design procedures for steel framed structures. *Bulletin of Earthquake Engineering,* 8, pp. 65-89, 2010..

EN 1993, Eurocode 3: Design of steel structures – Part 1-1: General rules and rules for buildings. CEN; 2005.

EN 1998-1-1. Eurocode 8: Design of structures for earthquake resistance – Part 1: General rules, seismic actions and rules for buildings. CEN; 2005.

Faggiano B., Fiorino L., Formisano A., Macillo V., Castaldo C., Mazzolani F.M. (2014) Assessment of the design provisions for steel concentric X bracing frames with reference to Italian and European codes.*The Open Construction and Building Technology Journal*, 11/2014; 8((Suppl 1: M3)), pp 208-215.

FEMA P-750. (2009). Recommended Seismic Provisions for New Buildings and Other Structures. Federal Emergency Management Agency - U.S. Department of Homeland Security - Building Seismic Safety Council of the National Institute of Building Sciences

Gioncu, V. (2000). Framed structures, Ductility and seismic response: General Report, *Journal of Constructional Steel Research*, 55: 125–154.

Gioncu, V., and Mazzolani, F.M. (2002). Ductility of seismic resistant steel structures, London, Spon Press.

Goel S.C., S. Lee S. (1992) A Fracture Criterion for Concrete-Filled Tubular Bracing Members Under Cyclic Loading", *in Proceedings of the 1992 ASCE Structures Congress,* ASCE, pp. 922–925, Reston, VA.

Goggins J.M., Broderick B.M., Elghazouli A.Y., Lucas A.S. (2006) Behaviour of tubular steel members under cyclic axial loading. *Journal of Constructional Steel Research* 62 121-131.

Güneyisi, E.M., D'Aniello, M., Landolfo, R., and Mermerdaş K. (2014). Prediction of the flexural overstrength factor for steel beams using artificial neural network. *Steel and Composite Structures, An International Journal*, 17(3): 215-236.

Güneyisi, E.M., D'Aniello, M., Landolfo, R., and Mermerdaş, K. (2013) . A novel formulation of the flexural overstrength factor for steel beams. *Journal of Constructional Steel Research* 90: 60-71.

O. Hassan O., S.C. Goel S.C. (1991) , “Modelling of Bracing Members and Seismic Behavior of Concentrically Braced Steel Structures, *Report No. UMCE91-1*, University of Michigan, Ann Arbor, MI, 1991..

Jain A.K., Goel S.C., Hanson R.D. (1980) Hysteretic cycles of axially loaded steel members. *Journal of the Structural Division*;106(ST8): 1777–95.

Johnson S. (2005). Improved seismic performance of special concentrically braced frames. *Master thesis, University of Washington, Seattle.*

Khatib I.F., Mahin S.A, Pister K.S (1998) Seismic behavior of concentrically braced steel frames. *Report UCB/EERC-88/01, Earthquake Engineering Research Center*, University of California, Berkeley, CA, 1998.

Landolfo, R. Editor (2013). Assessment of EC8 provisions for seismic design of steel structures. Technical Committee 13—Seismic Design, No 131/2013. ECCS—European Convention for Constructional Steelwork.

Lee K., Bruneau M. (2005) Energy Dissipation of Compression Members in Concentrically Braced Frames: Review of Experimental Data.. *Journal of Structural Engineering*, ASCE, 131(4), 2005..

Lehman D.E., Roeder C.W., Herman D., Johnson S., Kotulka B. (2008) Improved Seismic Performance of Gusset Plate Connections. *Journal of Structural Engineering,* Vol. 134, No. 6, June 1.

Longo A., Montuori R., Piluso V. (2008) Plastic design of seismic Resistant V-Braced frames. *Journal of Earthquake Engineering* 12:8, 1246-1266

Longo A., Montuori R., Piluso V. (2009) Seismic reliability of V-braced frames: Influence of design methodologies. *Earthquake Engineering and Structural Dynamics* 38, 1587-1608

Marino E. (2014) A unified approach for the design of high ductility steel frames with concentric braces in the framework of Eurocode 8. *Earthquake Engineering & Structural dynamics* 43:97-118

Marino E. M., Nakashima M. (2006) Seismic performance and new procedure for chevron braced frames. *Earthquake Engineering and Structural Dynamics* 35, 422-452

Mazzolani, F.M., and Piluso, V. (1992.) Member behavioural classes of steel beams and beam-columns, *In: Proc. of First State of the Art Workshop*, COST I, Strasbourg. p. 517–29.

Mazzolani, F.M., and Piluso, V. (1996.) Theory and Design of Seismic Resistant Steel Frames, E & FN Spon, an imprint of Chapman & Hall, London.

Nakashima M., Nishiro T., Tsuji B., Iwasa K. (1992) Effect of Strain Hardening on Post-Buckling Resistance of Steel Braces. *Proceeding of the 3rd Pacific Structural Steel Conference*, Tokyo, Japan: 561-568.

Nip A.K.H., Gardner L., Davies C.M., Elghazouli A.Y. (2010) Cyclic testing and numerical modelling of carbon steel and stainless steel tubular bracing members. *Engineering Structures* 32(2) 424-441

Plumier, A. (2000). General report on local ductility, *Journal of Constructional Steel Research*, No. 55: 91–107.

Tremblay R. (2000) Influence of Brace Slenderness on the Seismic Response of Concentrically Braced Steel Frames in *Behaviour of Steel Structures in Seismic Areas Stessa 2000: Proceedings of the Third International Conference*, August 21-24, 2000, F.M. Mazzolani and, R. Tremblay, eds., pp. 527–534, Montreal, QU, 2000.

Remennikov AM, Walpole WR. (1998) A note on compression strength reduction factor for a buckled strut in seismic-resisting braced system. *Engineering Structures* 20(8):779–82.

Shaback B., Brown T (2003). Behaviour of square hollow structural steel braces with end connections under reversed cyclic axial loading. *Canadian Journal of Civil Engineering* ;30(4):745_53

Shen J., Wen R., Akbas B., (2015) Mechanisms in Two-story X-braced Frames. *Journal of Constructional Steel Research*, vol. 106, pp 258-277, 2015..

]Shen J., Wen R., Akbas B., J.Shen, Doran B., Uckan E. (2014), Seismic demand on brace-intersected beams in two-story X-braced frames. *Engineering Structures*, vol.76, pp 295-312.

Tang X., Goel S.C. (1989) Brace Fractures and Analysis of Phase I Structure. *Journal of Structural Engineering*, ASCE, Vol. 115, No. 8, August, pp. 1960–1976,Reston, VA.

Tremblay R. (2002) Inelastic seismic response of steel bracing members. *Journal of Constructional Steel Research* 58:665–701.

Tremblay R., Archambault M.H., Filiatrault A (2003) Seismic response of concentrically braced steel frames made with rectangular hollow bracing members. *Journal of Structural Engineering*, ASCE;129(12):1626_36.

Tremblay R., Robert N. (2001) Seismic performance of low- and medium-rise chevron braced steel frames. Canadian *Journal of Civil Engineering*, 28, pp. 699-714.

Tremblay, R., Lacerte, M. (2002) Influence of the properties of bracing members on the seismic response of concentrically braced steel frames. *Proc., 12th European Conference on Earthquake Engineering*,Society for Earthquake and Civil Engineering Dynamics,London.

Uniform Building Code (1997). International Council of Building Officials, Whittier, California.

Whitmore R. E. (1952). Experimental Investigation of Stresses in Gusset Plates. *Bulletin No. 16, Engineering Experiment Station*, Univ. of Tennessee, Knoxville, May.

Yoo J. H. (2006). Analytical investigation on the seismic performance of special concentrically braced frames. *Ph.D. dissertation*, University of Washington, Seattle.

American Institute of Steel Construction, Inc. (AISC). (2010). Seismic Provisions for Structural Steel Buildings. ANSI/AISC Standard 341-10. AISC, Chicago, Illinois

Archambault M.H., Tremblay R., Filiatrault A. (1995) E´ tude du comportement se´ismique des contreventements ductiles en X avec profile´s tubulaires en acier. *Rapport no. EPM/GCS-1995-09*. In: Montreal,Canada: De´partement de ge´nie civil, E´ cole Polytechnique.

ASCE (2010). Minimum design loads for buildings and other structures (ASCE/SEI 7-10), American Society of Civil Engineers, Reston, VA.

Astaneh-Asl A., Cochran M.L., Sabelli R. (2006). Seismic Detailing of Gusset Plates for Special Concentrically Braced Frames. *Structural Steel Educational Council- Steel TIPS.*

Astaneh-Asl A., Goel S. C. (1984). Cyclic In-Plane Buckling of Double Angle Bracing. *Journal of Structural Engineering, American Society of Civil Engineers (ASCE),* Vol. 110, No. 9, pp. 2036–2055 (www.asce.org).

Astaneh-Asl A., Goel S. C., Hanson R. D. (1982) Cyclic Behavior of Double Angle Bracing Members with End Gusset Plates. *Report No. UMEE 82R7*. Ann Arbor: University of Michigan.

Astaneh-Asl A., Goel S. C., Hanson R. D. (1983). Cyclic Behavior of Double Angle Bracing Members with Bolted Connections. *Engineering Journal, AISC*, Chicago (www.aisc.org).

Astaneh-Asl A., Goel S. C., Hanson, R. D. (1985). Cyclic Out-of-Plane Buckling of Double Angle Bracing. *Journal of Structural Engineering*, ASCE, Vol. 111, No. 5, pp. 1135–1153 (www.asce.org).

Bruneau, M., Uang, C.M., Whittaker, A. (1998) Ductile design of steel structures, McGraw-Hill, Network..

Cochran M.L. (2003) Seismic design and steel connection detailing. *Proceedings of NASCC*, Baltimore, MD – April 2-5.

CSA. 2009. Design of Steel Structures, CSA-S16-09, Canadian Standards Association, Toronto, ON

D'Aniello M., La Manna Ambrosino G., Portioli F., Landolfo R. (2013) Modelling aspects of the seismic response of steel concentric braced frames *Steel and Composite Structures, An International Journal*, Vol. 15, No. 5, pp 539-566.

D'Aniello M., La Manna Ambrosino G., Portioli F., Landolfo R. (2015) The influence of out-of-straightness imperfection in Physical-Theory models of bracing members on seismic performance assessment of concentric braced structures. *The Structural Design of Tall and Special Buildings*, 24(3), pp. 176-197 . 2015. DOI: 10.1002/tal.1160.

D'Aniello M., Portioli F., Landolfo R. (2010) Modelling issues of steel braces under extreme cyclic actions. *In Proceedings of COST-C26 Final Conference* — Naples 16-18 September; pp. 335-341, 2010.

D'Aniello, M., Landolfo, R., Piluso, V., and Rizzano, G. (2012). Ultimate Behaviour of Steel Beams under Non-Uniform Bending. *Journal of Constructional Steel Research* 78: 144–158.

D'Aniello, M., Güneyisi, E.M., Landolfo, R., and Mermerdaş, K. (2013). Analytical prediction of available rotation capacity of cold-formed rectangular and square hollow section beams. *Thin-Walled Structures*. 10.1016/j.tws.2013.09.015

Ebadi P., Sabouri-Ghomi S. (2012). Conceptual study of X-braced frames with different steel grades using cyclic half-scale tests. *Earthquake Engineering & Engineering Vibration* 11: 313-329.

Elchalakani M, Zhao XL and Grzebieta R (2003) Tests of coldformed circular tubular braces under cyclic axial loading. *Journal of Structural Engineering,* ASCE 129(4): 507–514.

Elghazouli A.Y. (2010) Assessment of European seismic design procedures for steel framed structures. *Bulletin of Earthquake Engineering,* 8, pp. 65-89, 2010..

Elghazouli A.Y.(2008) Seismic design of steel framed structures to Eurocode 8, , in *Proceedings of the 14th World Conference on Earthquake Engineering*, Beijing, China, 12-17 October. 2008.

EN 1993, Eurocode 3: Design of steel structures – Part 1-1: General rules and rules for buildings. CEN; 2005.

EN 1998-1-1. Eurocode 8: Design of structures for earthquake resistance – Part 1: General rules, seismic actions and rules for buildings. CEN; 2005.

Faggiano B., Fiorino L., Formisano A., Macillo V., Castaldo C., Mazzolani F.M. (2014) Assessment of the design provisions for steel concentric X bracing frames with reference to Italian and European codes. *The Open Construction and Building Technology Journal*, 11/2014; 8((Suppl 1: M3)), pp 208-215.

FEMA P-750. (2009). Recommended Seismic Provisions for New Buildings and Other Structures. Federal Emergency Management Agency - U.S. Department of Homeland Security - Building Seismic Safety Council of the National Institute of Building Sciences

Gioncu, V. (2000). Framed structures, Ductility and seismic response: General Report, *Journal of Constructional Steel Research*, 55: 125–154.

Gioncu, V., and Mazzolani, F.M. (2002). Ductility of seismic resistant steel structures, London, Spon Press.

Goel S.C., S. Lee S. (1992) A Fracture Criterion for Concrete-Filled Tubular Bracing Members Under Cyclic Loading”, *in Proceedings of the 1992 ASCE Structures Congress,* ASCE, pp. 922–925, Reston, VA.

Goggins J.M., Broderick B.M., Elghazouli A.Y., Lucas A.S. (2006) Behaviour of tubular steel members under cyclic axial loading. *Journal of Constructional Steel Research* 62 121-131.

Güneyisi, E.M., D'Aniello, M., Landolfo, R., and Mermerdaş K. (2014). Prediction of the flexural overstrength factor for steel beams using artificial neural network. *Steel and Composite Structures, An International Journal*, 17(3): 215-236.

Güneyisi, E.M., D'Aniello, M., Landolfo, R., and Mermerdaş, K. (2013) . A novel formulation of the flexural overstrength factor for steel beams. *Journal of Constructional Steel Research* 90: 60-71.

Jain A.K., Goel S.C., Hanson R.D. (1980) Hysteretic cycles of axially loaded steel members. *Journal of the Structural Division*;106(ST8): 1777–95.

Johnson S. (2005). Improved seismic performance of special concentrically braced frames. *Master thesis, University of Washington, Seattle.*

Khatib I.F., Mahin S.A, Pister K.S (1998) Seismic behavior of concentrically braced steel frames. *Report UCB/EERC-88/01, Earthquake Engineering Research Center*, University of California, Berkeley, CA, 1998..

Landolfo, R. (2013). Assessment of EC8 provisions for seismic design of steel structures. Technical Committee 13—Seismic Design, No 131/2013. ECCS—European Convention for Constructional Steelwork.

Lee K., Bruneau M. (2005) Energy Dissipation of Compression Members in Concentrically Braced Frames: Review of Experimental Data.. *Journal of Structural Engineering*, ASCE, 131(4), 2005..

Lehman D.E., Roeder C.W., Herman D., Johnson S., Kotulka B. (2008) Improved Seismic Performance of Gusset Plate Connections. *Journal of Structural Engineering,* Vol. 134, No. 6, June 1.

Longo A., Montuori R., Piluso V. (2008) Plastic design of seismic Resistant V-Braced frames. *Journal of Earthquake Engineering* 12:8, 1246-1266

Longo A., Montuori R., Piluso V. (2009) Seismic reliability of V-braced frames: Influence of design methodologies. *Earthquake Engineering and Structural Dynamics* 38, 1587-1608

M. D'Aniello, S. Costanzo S., Landolfo R. (2015) The influence of beam stiffness on seismic response of chevron concentric bracings. *Journal of Constructional Steel Research,* Vol. 112, pp 305–324.

Marino E. (2014) A unified approach for the design of high ductility steel frames with concentric braces in the framework of Eurocode 8. *Earthquake Engineering & Structural dynamics* 43:97-118

Marino E. M., Nakashima M. (2006) Seismic performance and new procedure for chevron braced frames. *Earthquake Engineering and Structural Dynamics* 35, 422-452

Mazzolani, F.M., and Piluso, V. (1992.) Member behavioural classes of steel beams and beam-columns, *In: Proc. of First State of the Art Workshop*, COST I, Strasbourg. p. 517–29.

Mazzolani, F.M., and Piluso, V. (1996.) Theory and Design of Seismic Resistant Steel Frames, E & FN Spon, an imprint of Chapman & Hall, London.

Nakashima M., Nishiro T., Tsuji B., Iwasa K. (1992) Effect of Strain Hardening on Post-Buckling Resistance of Steel Braces. *Proceeding of the 3rd Pacific Structural Steel Conference*, Tokyo, Japan: 561-568.

Nip A.K.H., Gardner L., Davies C.M., Elghazouli A.Y. (2010) Cyclic testing and numerical modelling of carbon steel and stainless steel tubular bracing members. *Engineering Structures* 32(2) 424-441

O. Hassan O., S.C. Goel S.C. (1991) , "Modelling of Bracing Members and Seismic Behavior of Concentrically Braced Steel Structures, *Report No. UMCE91-1*, University of Michigan, Ann Arbor, MI, 1991..

Plumier, A. (2000). General report on local ductility, *Journal of Constructional Steel Research*, No. 55: 91–107.

Remennikov AM, Walpole WR. (1998) A note on compression strength reduction factor for a buckled strut in seismic-resisting braced system. *Engineering Structures* 20(8):779–82.

Shaback B., Brown T (2003). Behaviour of square hollow structural steel braces with end connections under reversed cyclic axial loading. Canadian Journal of Civil Engineering ;30(4):745_53

Shen J., Wen R., Akbas B., J.Shen, Doran B., Uckan E. (2014), Seismic demand on brace-intersected beams in two-story X-braced frames. *Engineering Structures*, vol.76, pp 295-312.

Shen J., Wen R., Akbas B., (2015) Mechanisms in Two-story X-braced Frames. *Journal of Constructional Steel Research*, vol. 106, pp 258-277, 2015..

Tang X., Goel S.C. (1989) Brace Fractures and Analysis of Phase I Structure. *Journal of Structural Engineering*, ASCE, Vol. 115, No. 8, August, pp. 1960–1976,Reston, VA.

Tremblay R. (2000) Influence of Brace Slenderness on the Seismic Response of Concentrically Braced Steel Frames in *Behaviour of Steel Structures in Seismic Areas Stessa 2000: Proceedings of the Third International Conference*, August 21-24, 2000, F.M. Mazzolani and, R. Tremblay, eds., pp. 527–534, Montreal, QU, 2000.

Tremblay R. (2002) Inelastic seismic response of steel bracing members. *Journal of Constructional Steel Research* 58:665–701.

Tremblay R., Archambault M.H., Filiatrault A (2003) Seismic response of concentrically braced steel frames made with rectangular hollow bracing members. *Journal of Structural Engineering*, ASCE;129(12):1626_36.

Tremblay R., Robert N. (2001) Seismic performance of low- and medium-rise chevron braced steel frames. Canadian *Journal of Civil Engineering*, 28, pp. 699-714.

Tremblay, R., Lacerte, M. (2002) Influence of the properties of bracing members on the seismic response of concentrically braced

Uniform Building Code (1997). International Council of Building Officials, Whittier, California.

Whitmore R. E. (1952). Experimental Investigation of Stresses in Gusset Plates. *Bulletin No. 16, Engineering Experiment Station*, Univ. of Tennessee, Knoxville, May.

Yoo J. H. (2006). Analytical investigation on the seismic performance of special concentrically braced frames. *Ph.D. dissertation*, University of Washington, Seattle.

Chapter IV
Brace Modelling

4.1 INTRODUCTION

As already discussed in previous Sections, the seismic performance of concentrically braced frames is primarily affected by the behaviour of the bracing elements, which are the members devoted to dissipate the input energy according to the capacity design philosophy.

The hysteretic behaviour of steel concentric braces is characterized by the buckling in compression, the yielding in tension, moderate hardening and significant pinching when the deformation reverses. As a matter of fact, this nonlinear performance is very complex to be simulated. On the other hand, an accurate model for braces is essential for an effective estimation of both interstorey drift ratios and ductility demand of concentrically braced frames under seismic conditions.

In general, the hysteretic models used to simulate the brace nonlinear response introduce significant simplifications if compared to the experimental behaviour. These simplifications could lead to inaccurate prediction of the peak responses or even behaviour modes. The hysteretic behaviour of steel concentric braces has been experimentally and theoretically investigated by a large number of authors in the last thirty years (Jain and Goel, 1978; Black *et al.*, 1980; Shibata, 1982; Ikeda and Mahin, 1986; Tremblay, 2002; Uriz, 2005; Goggins *et al.*, 2006; Dicleli and Mehta, 2007; Dicleli and Calik, 2008; Goggins *et al*., 2008; Lee and Noh, 2010). In particular, three different modelling approaches may be recognized (Uriz *et al.* 2008): (i) phenomenological models (PM); (ii) continuum finite element models (FEM); (iii) physical-theory models (PTM).

PMs are based on equivalent one-dimensional truss elements with hysteretic behaviour simulating the experimental response (Jain and Goel. 1978; Ikeda and Mahin. 1986). The hysteretic properties are defined using a set of empirical rules for the shape of hysteretic loops without representing the physical phenomena (e.g. the out-of-plane displacement induced by buckling) that characterize the brace response. Although this approach allows simulating the overall behaviour of such braces, there are some disadvantages limiting their effective use.

Indeed, the reliability and accuracy of these models depend on the availability of experimental data, which are necessary to determine the appropriate modelling parameters. Moreover, these models do not provide any information on damage produced by the lateral buckling of braces. Hence, in performance-based assessment it is not possible to evaluate the lateral displacements which can damage non-structural elements and interfere with the operation of adjacent mechanical components, such as elevators.

Contrary to PMs, FEM is the most accurate approach to simulate the brace behaviour. Indeed, general purpose finite element programs capable of large displacement analysis allow overcoming the modelling limitations previously illustrated. In FEM approach braces and their connections can be simulated using shell or solid elements characterized by appropriate material models. Several studies of this type have been carried out recently (Fell *et al*. 2009; Takeuchi and Matsui 2011; Serra *et al.*, 2012). However, because of the huge time amount requested for the preparation of input files and for calculations, such detailed finite element models can be mainly used to simulate local details. Being the application to seismic analysis of whole building frame very difficult, FE models are not convenient for structural engineering practice and even research in seismic assessment of whole structures.

In PTM approach the brace hysteretic behaviour is usually modelled with two elements connected by a generalized plastic hinge for braces simply pinned. Inelastic hinges concentrated at the element ends and mid-span are used in the case of fixed-end braces (Jin and El-Tawil 2003; Uriz et al. 2008). In this type of models geometric nonlinearities (namely an initial camber) are usually introduced to account for buckling of braces.

PTMs can generally overcome the disadvantages and the application limits of PMs and FEMs. The main advantage of

PTMs consists in the number of experimental parameters to be specified, which is less than the case of PMs. The basic input data to be implemented are the material properties, the brace geometry and the distribution of fibres at critical sections. Moreover, although PTMs need a computational effort increased respect to PMs, the complexity in preparing input files and the computational time expense typically necessary in FEMs are overcome. Only few factors are not taken into account as initial stresses and variations of the shape of the cross section due to local/distortional buckling.

A large number of research studies on the application of PTMs for pushover and time history analyses of various bracing shapes and configurations can be found in the literature (e.g. Dicleli and Mehta, 2007; Dicleli and Calik, 2008; Uriz, 2005; Wijesundara, 2009; Goggins and Salawdeh, 2012, Salawdeh and Goggins, 2013).

In these studies different modelling assumptions are used, including the initial camber (e.g. camber amplitude obtained by means of analytical formulations or simply assumed as a fixed percentage of the brace total length), the material model (e.g. monotonic and hysteretic) and the type of inelasticity element (e.g. distributed and concentrated plasticity).

It is known that the modelling of buckling, post-buckling and cyclic behaviour of braces is sensitive to these parameters, which have been set differently among the literature studies.

As a consequence, it is interesting to verify the accuracy and the suitability of the existing formulations in predicting the monotonic and cyclic response of braced structures under static and dynamic loading conditions. D'Aniello *et al.*, 2013 provided a comprehensive study in which the response obtained for the formulations available in the literature are examined and compared, extending the analysis to structural configurations and loading conditions different from those used for validation in the relevant original studies.

In this Section, such comparison is furtherly discussed, being a key issue for the numerical simulation with PTMs, considering that this type of models have been used to perform numerical analyses devoted to determine the ductility demand and design parameters, such as the behaviour factors, the post-buckling strength of brace in compression for capacity design and overall over-strength. On the other hand, being nonlinear analyses introduced in modern seismic codes, nowadays apart from researchers it is fundamental to provide adequate numerical modelling instructions also to FE analysts (D'Aniello *et al.*, 2010), because the accuracy and effectiveness of numerical models strongly influence the assessment of demands imposed on structural elements and the global ductility demands, as well.

These concerns motivated the study presented in this Section, which is also addressed at providing recommendations for modelling of conventional concentric braced frames within the context of a specific computational platform, by examining the capability of handling different geometries as well as material and geometric nonlinearities. However, it should be noted that some phenomena such as the plastic local buckling and the low-cycle fatigue effects were not considered in this study. Indeed, fibre PTMs do not allow accounting for local buckling and computing the actual local distribution and the amplitude of strains in the plastified zones due to local nonlinear geometric effects. Although the former aspect cannot be accounted for in PTMs, as early demonstrated by Uriz et al. (2008) the plastic local buckling is poorly significant on the overall hysteretic force-displacement response of braces made of compact sections, as those examined herein and generally adopted in seismic design according to modern codes (e.g. EN1998-1). For what concerns the evaluation of low-cycle fatigue capacity of braces, it is known that this aspect is physically dependent on the accumulation of damage, namely the strains. This implies that, using such a kind of modelling strategy, it could be convenient to verify a-posteriori the fracture life of braces by means of refined analytical equations proposed by a number of researchers (Lee and Goel, 1987; Tang and Goel, 1989; Archambault *et al.,* 1995; Tremblay, 2002; Shaback and Brown, 2003, Tremblay *et al.*, 2003) and recently updated on a large database of experimental results, thus proposing predictive expressions as function of both the global and the local slenderness of braces (Nip *et al.*, 2010).

It is worth of mentioning that recent studies have proposed novel fibre elements accounting for low-cycle fatigue (Uriz, 2005; Wijesundara, 2009; Salawdeh and Goggins, 2013), but as noted by the proposers all parameters used in the model should be calibrated to compensate the fact that PTMs do not allow computing the actual strains.

On the basis of the motivations previously discussed, a wide systematic study was carried out by varying the fundamental numerical parameters at the same set of case studies, which were selected to be representative of a wide range of structural configurations, in order to evaluate the accuracy and the suitability of the existing formulations to predict the monotonic and cyclic response of braced structures under static and dynamic loading conditions.

After a brief introduction on the basic features of the generated models, the results of the parametric analysis on single braces are presented and discussed. The effectiveness of modelling assumptions is validated against experimental results available from tests by Black et al. (1980). Moreover, the modelling aspects of braced frames are investigated and the accuracy verified against experimental results on different building prototypes under pseudo-static (Wakawayashi *et al.*, 1970; Yang *et al.*, 2008) and dynamic (Uang and Bertero, 1986) conditions.

4.2 NUMERICAL MODEL FOR CONVENTIONAL CONCENTRIC BRACING

The numerical models implemented in this study were generated using the nonlinear finite element based software "Seismostruct". The models were developed using the distributed inelasticity elements (e.g. Filippou and Fenves, 2004; Scott and Fenves 2006;Fragiadakis and Papadrakakis 2008). These elements account for distributed inelasticity through integration of material response over the cross section and integration of the section response along the length of the element. The cross-section behaviour is reproduced by means of the fibre approach, assigning a uniaxial stress-strain relationship at each fibre.

For the use of distributed inelasticity elements it is not necessary to carry out a specific calibration of the response curve parameters, thus resulting more advantageous respect to the more common lumped-plasticity models.

Distributed inelasticity frame elements can be formulated with either displacement-based (DB) approach or the more recent force-based (FB) approach (Spacone *et al*., 1996, Calabrese *et al*., 2010). In the former case displacement shape functions are used, instead in the second approach, equilibrium is strictly imposed, namely it is perfectly dual of previous approach. In this study FB formulated elements are used. This selection is due to the fact that FB formulation can be considered as "exact" as respect to DB formulation (Calabrese *et al*., 2010), because satisfying equilibrium the force field is always exact for any level of inelastic deformation, even in the presence of strength softening (which is typically the case of buckling in steel braces).

The numerical integration method used is based on the Gauss-Lobatto distribution (Abramowitz and Stegun, 1964; Szabó and Babuška, 1991), which includes, at a minimum, monitoring points at each end of the element. Such feature allows each structural member to be modelled with a single FE element, thus requiring no meshing for each element. In the Gauss-Lobatto integration scheme the first and last integration points always coincide with the end sections. This is very advantageous for the case of braces because the maximum internal forces (N, M) develop at the end of the element.

Second order effects have been accounted in all analyses presented in this paper, by assuming large displacements/rotations and large independent deformations relative to the chord of the frame element through the employment of the co-rotational formulation given by Correia and Virtuoso (2006).

In the present study, the braces were modelled with frame elements arranged to have a lateral (either bilinear or sinusoidal) shape with an initial camber (Δ_o). Indeed, the presence of this initial out-of-plane imperfection allows reproducing the transverse deformation of the brace.

Uriz *et al.* (2008) proposed to use an initial camber equal to 0.05-0.1% of the brace length applied at brace mid-span. The problem of the calculation of initial camber was differently addressed herein. Indeed, in order to reproduce the buckling response as close as possible to the experimental behaviour, the accuracy of some theoretical models was investigated, as described in the following Sections, in more detail.

For monotonic and cyclic static analysis, it was applied an incremental horizontal displacement history equal to that experimentally applied during each test. In particular, the geometric nonlinearity formulation (i.e., “large displacements and small strains”) was adopted and the Skyline solver was used for each displacement-step to ensure the equilibrium of the internal member forces and overall frame base shear at each iteration.

For dynamic time history analysis the numerical response was calculated using the Newmark numerical integration scheme.

Figure 4.1 schematically shows the type of model investigated in this study, where integration points (IP) per element and the end joints (J) are clearly highlighted.

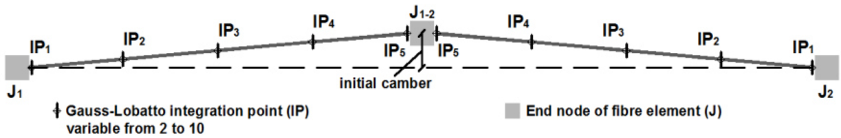

Figure 4.1 The implemented model to mimic the brace behaviour.

4.3 CHARACTERIZATION OF SINGLE BRACE MODEL: PARAMETRIC STUDY

4.3.1 *Generality*

In order to characterize the response of the single brace model, the following parameters were investigated: the type of material model, the initial camber (Δ_o), the type of FB inelasticity (distributed or concentrated) elements, the number of IPs used along each of these line elements, the number of elements and shape of the initial camber, the number of fibres.

To investigate the influence of different parameters, the numerical curves were compared to the experimental tests on strut specimens indicated as No. 1, 15 and 17 in Black *et al.* (1980). For each brace specimen, Figure 4.2 depicts the configuration of the specimens, while Table 4.1 reports the reference of the test ID, the member size, the average yield stress of the steel (f_{ym}), the total length (L), the specimen length (L_s) and the brace effective slenderness ratio ($\lambda = kL/r$).

Table 4.1 Characteristics of the brace specimens (from Black *et al.* 1980).

Test ID	Type of Section	Size	f_{ym}	L	L_s	$\lambda = kL/r$
(-)	(-)	(-)	(MPa)	(mm)	(mm)	(-)
1	W	203× 508 ×6.4×10.2	278	3810	3188	120
15	CHS	113.64×6.02	327	3070	2448	80
17	SHS	101.60×6.35	407	3050	2428	80

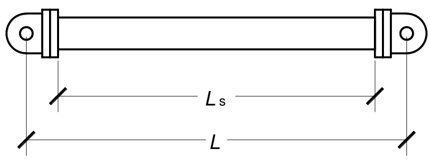

Figure 4.2 geometry of the brace specimens

4.3.2 *Investigated parameters*

4.3.2.1 Material models

The influence of two different types of steel models was investigated, namely:

(i) Menegotto-Pinto (MP) hysteretic model;

(ii) Bi-linear kinematic (BLK) model.

Except for the elastic modulus (E) and the yield stress (f_y), the parameters used for the monotonic and cyclic response were calibrated on the basis of the average stress-strain relationship derived from cyclic coupon tests performed by Black *et al.* (1980).

It is worth noting that the material library of the software used for the analysis (namely Seismostruct) implements the Menegotto and Pinto (1973) modified by Filippou et al (1983) to include isotropic strain hardening. In the examined cases the parameters accounting for isotropic strain hardening were set equal to zero, thus practically obtaining the same results of those given by the original MP formulation. This choice was taken in order to simulate faithfully the overall force-displacement response of braces. Indeed, the experimental evidence showed that the cyclic behaviour of bracings do not appreciably experience isotropic hardening at overall level, because this material effect is counterbalanced by the deterioration due to the buckling and corresponding plastic hinging in the brace. Since PTMs cannot simulate the plastic local buckling, neglecting the isotropic component of material model allowed to fictitiously compensating this effect at global level.

In order to clarify the role of each parameter in case of MP model, the material parameters are described hereinafter as follows:

- The kinematic hardening E_h;
- The curvature parameters R_0, which characterizes the shape of the transition curve between initial and post-yield stiffness allowing a representation of the Bauschinger effect;

- A_1 and A_2, which affect the shape of the hysteretic curve and hence the representation of the transition from the elastic and hardening branch and also the pinching of the hysteretic loops.
- A_3 and A_4, which quantify isotropic hardening.
- For the BLK model the post-yield stiffness (E_h) is the only parameter to be fixed.
- The calibrated material parameters are reported in Table 4.2, while the comparison of the numerical response and the experimental average envelope is plot in Fig. 4.3.

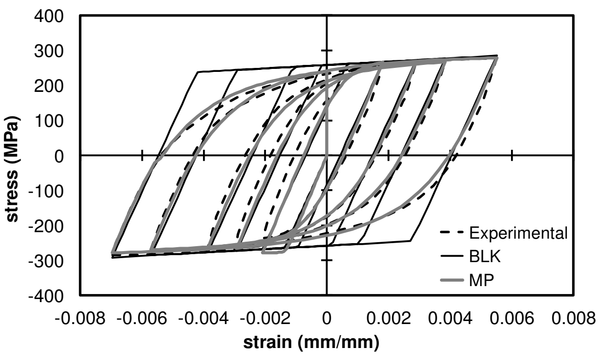

Figure 4.3 Calibrated vs. Experimental steel response.

Table 4.2 Calibrated parameters of steel hysteretic models.

Steel model	E_h	R_0	A_1	A_2	A_3	A_4
MP	0.025	20.00	18.50	0.15	0.00	1.00
BLK	0.025	-	-	-	-	-

4.3.2.2 Initial camber

It is well known that the sensitivity of the buckling strength to initial camber has practical implications for design and modelling. It was observed that using camber amplitude arbitrarily selected in the range of 0.05% - 0.1% of brace length may lead to different results. Analysing the existing literature a large number of existing studies differently addressed this issue. Jin and El-Tawil (2003) utilized an initial imperfection empirically calibrated and equal to 0.2% to simulate the experimental response from shake table test of 0.6 scale three-story X-braced steel frame. In the NIST GCR 10-917-5 guidelines, Deierlein *et al.* (2010) indicated initial geometric imperfection amplitude of 0.05 % to 0.1 % of the brace length according to the study provided by Uriz *et al.* (2008). Cho *et al.* (2011) proposed to adjust the width of the initial imperfection on the basis of a trial-and-error procedure in order to match the target buckling strength of the brace. More recently Wijesundara *et al.* (2011) proposed to use an initial camber equal to $L/350$, while Goggins and Salawdeh (2012) proposed to use an initial camber of 1% of the length of the brace. The differences seem to be due to the fact that different types of bracing configurations were examined in each study. On the other hand theoretical formulations (Maquoi and Rondal, 1978; Georgescu, 1996; Dicleli and Mehta, 2007; Dicleli and Calik, 2008) were also developed to solve this matter.

With the aim to clarify this issue, the influence of the amplitude of Δ_0 on the brace response was investigated and the main results are shown in Section 4.3.3.2.

The out-of-plane imperfections were calculated using the following formulations:

i. ECCS-78. On the basis of Ayrton-Perry theory, the initial deflection is obtained from the condition corresponding to the achievement of the yield stress in the outermost fibre under the combined presence of the buckling load N_b and the related bending moment $M(N_b)$, obtained having assumed an initial sinusoidal shape, thus leading to the following Equation:

$$\Delta_0 = \frac{W}{A} \cdot \alpha \cdot \sqrt{\bar{\lambda}^2 - 0.04} \tag{4.1}$$

being W the section modulus in the buckling plane, A the cross section area, $\bar{\lambda}$ the dimensionless slenderness and α takes into account the element imperfections and characterized the buckling curves adopted in ECCS 1978.

ii. Georgescu (1996). Starting from the same hypotheses, the camber is given by the following:

$$\Delta_0 = \left(\frac{1}{\chi} - 1 \right) \cdot \left(1 - \frac{\chi f_y}{\sigma_E} \right) \cdot \frac{W}{A} \tag{4.2}$$

where χ is the buckling reduction factor and σ_E is the critical Eulerian stress. The buckling reduction factor can be obtained according to EN 1993:1-1(2005) as function of $\bar{\lambda}$ and α.

iii. EN 1993:1-1 (2005). For structural analysis EN 1993:1-1(2005) recommends to introduce initial local bow imperfections of members in frames sensitive to buckling in a sway mode. The code provides the values of such imperfections in terms of Δ_o/L, where L is the member length.

iv. Dicleli and Mehta (2007). The initial camber Δ_o is derived assuming along the length of the brace a linear variation of the second-order bending moment generated by the axial force in the deflected bi-linear configuration of the strut, by imposing the equilibrium state at the mid-brace the second-order transverse displacement Δ_b of the brace at buckling load N_b. Hence, Δ_o is obtained as follows:

$$\Delta_0 = \frac{M_{pb}}{N_b} \cdot \left(1 - \frac{N_b L^2}{12 EI} \right) \tag{4.3}$$

v. Dicleli and Calik (2008). The initial camber Δ_o is derived assuming that the sinusoidal deformed shape of the brace prior to buckling and the imposing the second order flexural equilibrium in the section located at the mid-length of the buckling semi-wave, Δ_o is obtained as follows:

vi.

$$\Delta_0 = \frac{M_{pb}}{N_b \left(1 + \dfrac{N_b L^2}{8EI \left(1 - \dfrac{N_b L^2}{\pi^2 EI} \right)} \right)} \tag{4.4}$$

4.3.2.3 FB inelasticity element types

Two types of FB inelasticity elements were used, namely the “infrmFB” and “infrmFBPH”. The former are formulated to take into account the plasticity along the element, while in the second the inelasticity is concentrating within a fixed length of the element (Scott and Fenves, 2006).

Both types of FB elements were examined to highlight the differences in terms of accuracy and computational time.

4.3.2.4 Number of integration points

This parameter has a key role owing to the fact that the element response is reproduced by integrating the nonlinear uniaxial material response of the individual fibres in which each section was subdivided, fully accounting for the spread of inelasticity along the member length. In general, the numerical integration of the element integrals may lead to deformation localization at the end integration points (Coleman and Spacone, 2001). In case of material strain hardening negligible localization problems should be expected being necessary a certain number of IPs (Coleman and Spacone, 2001). Hence, in order to evaluate the sufficient number of IPs to guarantee accurate integration and to avoid immediate stiffness changes in the response it was examined their effects varying the number from 3 to 10 per element.

4.3.2.5 Number of elements and shape of the initial camber

In case of FB elements with distributed plasticity, the numerical response of straight structural members is not dependant on the number of elements. This is not the case of concentrated plasticity elements, which need calibration of the hinge length changing the length of element. In case of structural elements having curved shape or not-straight axis it is necessary to mesh the model by subdividing the member in a number of FB elements. This is the case of braces simulated imposing a sinusoidal axis as those assumed in some theoretical models (ECCS-78; Georgescu, 1996; Dicleli and Calik, 2008). In order to examine the role of both the mesh sizing and the shape of the brace axis, this parameter has been varied from 2 to 32 sub-elements as illustrated in Fig. 4.4. In addition, this aspect has been investigated for both distributed and concentrated FB elements.

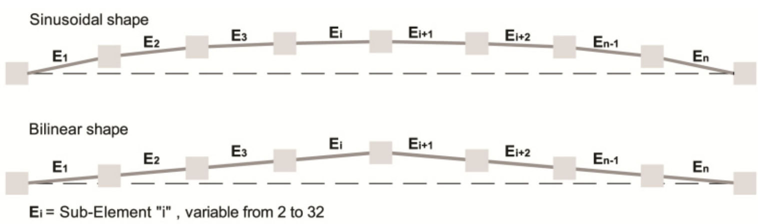

Figure 4.4 Discretization of bracing for both sinusoidal and bilinear shape of the initial camber.

4.3.2.6 *Number of integration fibres*

The number of fibres to be used to discretize the element sections is very important to simulate the stress-strain distribution across the element cross-section. The ideal number of section fibres depends on the shape and material characteristics of the latter and on the level of inelastic deformation imposed to the element. A sensitivity study was carried out to establish the optimum number of section fibres. The number of fibres was assigned in the range 10-400.

4.3.3 ***Outcomes of parametric analysis***

4.3.3.1 *Influence of material model*

The results of the analyses carried out to assess the influence of steel model are presented in Fig. 4.5 with axial force-axial deformation curves. These curves are obtained assuming the camber calculated by Eq. (4.4), 5 IPs and 100 fibres per element.

It can be observed that the model is capable to predict the typical phases of brace response, namely the buckling, the plastic mechanism with the loss of axial strength, the elastic unloading in compression and the reloading in tension up to the axial yielding.

The effect of steel model can be observed in the three different phase of brace response that are: i) the part in large tensile deformation, ii) the residual post-buckling strength and iii) the compressive strength and the transition zone beyond the first buckling when the axial compressive load gradually increased up to buckling initiates again.

In tension part the model with steel MP fits well the experimental response, while model with steel BLK slightly underestimates the experimental tensile strength. This result is due to the fact that in BLK the isotropic hardening is neglected. Anyway, for steel BLK the scatter is not significant, being roughly 2% lesser the peak experimental strength.

In residual post-buckling strength the analyses clearly show that the effect of steel model is negligible.

For the camber formulations in Section 4.3.2.2, both MP and BLK models are able to predict the degradation of the buckling load related to the number of loading cycles as well as the lateral deflection of the brace resulting from the plastic hinge rotations during the previous cycles. Anyway, in the transition zone the models with steel BLK overestimate the buckling strength after the first cycle. As it can be clearly recognized comparing Fig. 4.5a to 4.5b and 4.5c, in this phase of the brace response the influence of the material model differs with the type of cross section shape. Indeed, for truss 1 having wide flange section the model with steel BLK give the larger scatter (approximately the 55%) between numerical and experimental values of buckling strength after the first cycle than those given by models with MP (approximately the 32%). In case of braces made of hollow sections (as the case of truss 15 and 17) the models with steel BLK widely overestimated (approximately more than 100%) the compression strength beyond the first buckling, while models with steel MP give an excellent prediction (slightly larger than 5%). These results are due to different reasons. First, BLK model does not take into account the Bauschinger effect, which is characterized by a gradual transition in reloading part of hysteretic loops. In addition, since PTM approach cannot take into account any local buckling phenomena which typically affect the response of hollow sections, a smooth transition from the elastic to the hardening branch of the material stress-strain response allows compensating fictitiously this lack of the modelling.

At the light of the above considerations, it can be concluded that the numerical prediction of MP material models match better the experimental curves. Therefore, the parametric analyses shown hereinafter were carried out using this type of steel model.

a)
b)
c)
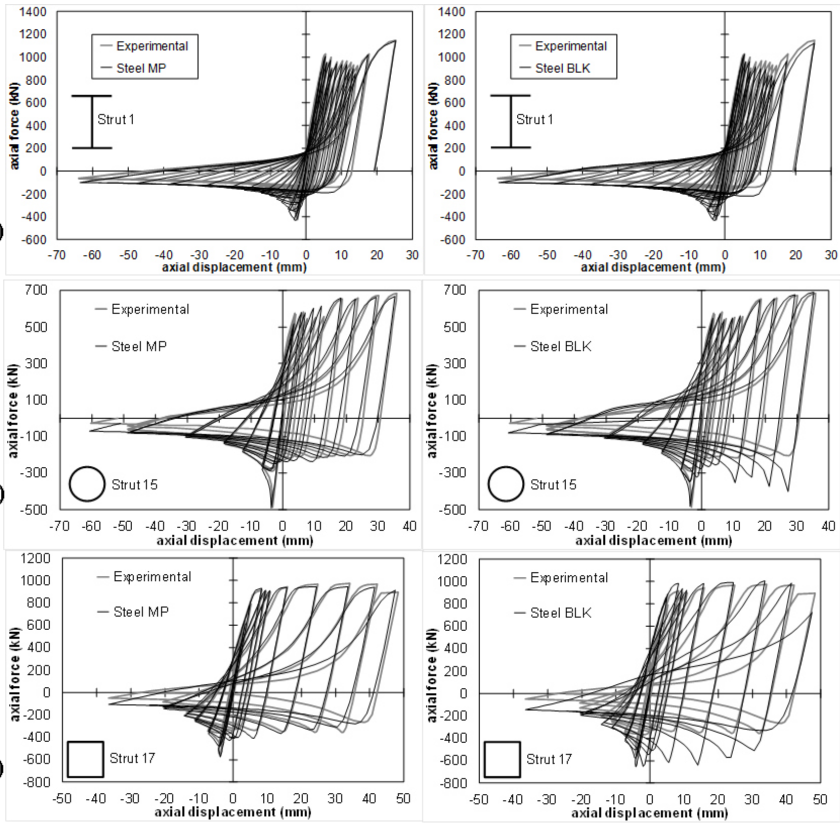

Figure 4.5 Influence of material model: braces having wide flange (a), circular hollow (b) and square hollow (c) cross section.

4.3.3.2 Influence of camber

According to the hypotheses of the examined formulations for the camber Δ_o, for these analyses the geometric imperfection was placed where the brace buckled shape experiences the peak transverse displacement. For example, in case of pinned braces the camber was located at $0.5L$.

The strut was initially analysed under monotonically increasing axial compression displacements. The monotonic response curves in terms of axial force−axial displacement and axial force-lateral deflections for strut 1 are shown in Fig. 4.6. This plot clearly illustrates the sensitivity of the initial buckling load to the assumed initial camber, where differences in load-carrying capacity diminish as axial displacements increase. As it can be observed, each theoretical formulation gives different amplitudes of initial camber and the value of initial camber varies if the brace section and the brace slenderness change. It should be also noted that the plots depicted in Fig. 4.6 were obtained assuming two beam-column elements with distributed plasticity and five IPs each. Increasing the number of sub-elements for each formulation of the camper amplitude leads to a small reduction of the buckling load, but negligible differences in the post-buckling response can be recognized. The influence of the number of sub-elements on the numerical prediction of braces has been deepened in Section 4.3.3.5.

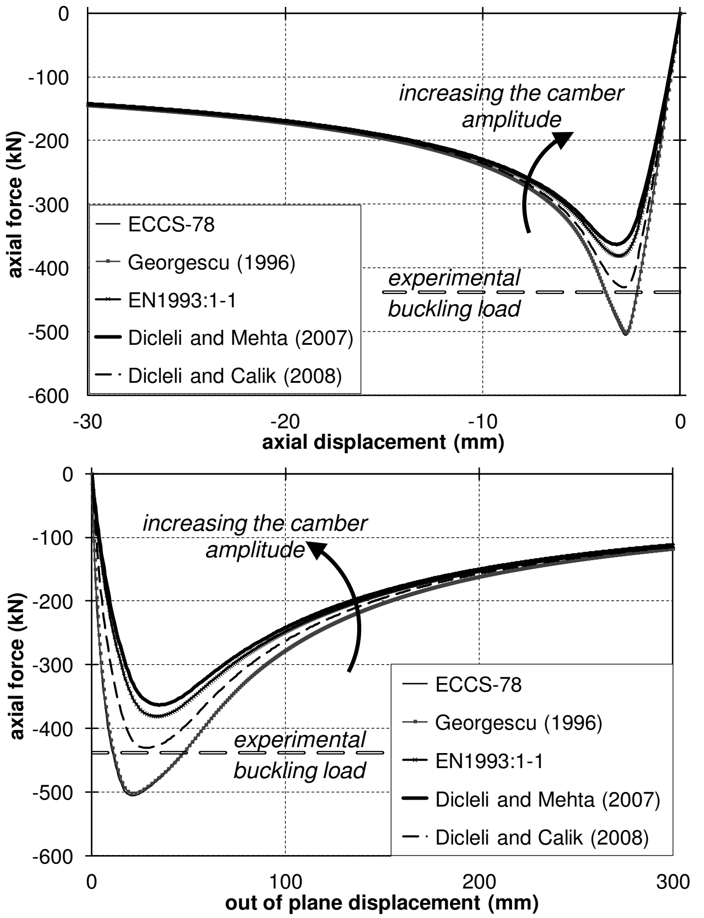

a)

b)

Figure 4.6 Influence of camber under monotonic loading

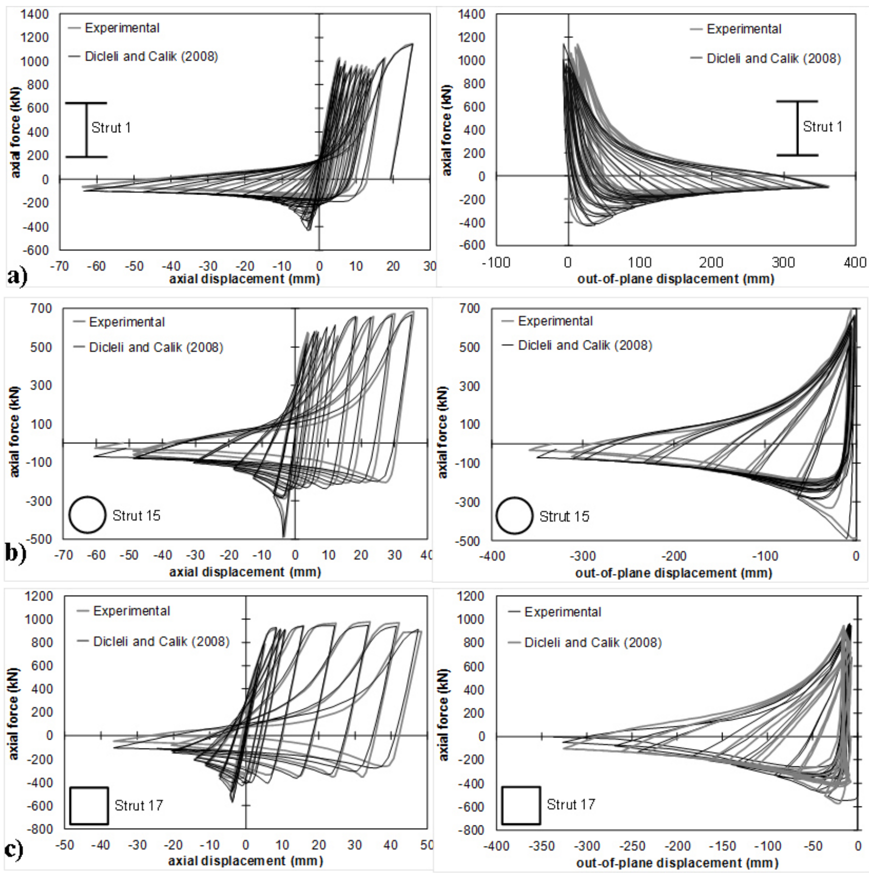

Figure 4.7 Accuracy of the models with Dicleli and Calik (2008) formulation under cyclic loading

The scatter between numerical and experimental buckling loads and the corresponding statistical parameters (namely mean value, standard deviation "Std.Dev" and coefficient of variation "CV") are reported in Table 4.3 for each model. As, it can be easily recognized that models with the camber calculated according to Dicleli and Calik (2008) provides the better accuracy to test results.

The influence of camber under cyclic conditions was also investigated. Also in cyclic conditions the model of Dicleli and Calik (2008) leads to the better resemblance between the test and analysis result (See Fig. 4.7). The results obtained using the other camber formulations show non-negligible misestimate of buckling strength. For all examined formulations the calculated residual post-buckling strength was larger than the experimental value. This outcome highlights one of the limits of PTMs, which is the impossibility to take into account the deterioration phenomena due to the accumulation of plastic deformation in locally buckled parts of plastic hinge zones.

Another important aspect to be highlighted is the influence on the shape and on the area variations of the hysteretic envelopes for each camber formulation and material model, considering the effects on energy absorption. In Table 4.4 the differences of hysteretic areas (namely dissipated energy) among the examined models is given considering also the influence of the type of steel model. As it can be observed the best approximation to experimental hysteretic areas is given using steel MP.

At the light of the considerations shown in this Section, it can be noted that the better agreements to experimental curves were obtained using the formulation by Dicleli and Calik (2008) and MP material model (Menegotto and Pinto, 1973).

Table 4.3 Differences between experimental and numerical buckling load.

Strut	Camber formulation				
	ECCS-78	Georgescu	EN1993	Dicleli and Mehta	Dicleli and Calik
1	18.56%	17.54%	-10.77%	-14.92%	0.94%
15	1.63%	1.24%	17.06%	10.55%	1.94%
17	14.39%	11.65%	-7.14%	-8.51%	1.03%
Mean	11.53%	10.14%	11.66%	11.33%	1.30%
Std.Dev	8.82%	8.25%	5.02%	3.27%	0.55%
CV	0.77	0.81	0.43	0.29	0.42

Table 4.4 Differences between experimental and numerical hysteretic envelope areas.

Strut	Steel model	Camber formulation				
		ECCS-78	Georgescu	EN1993	Dicleli and Mehta	Dicleli and Calik
1	MP	4.30%	3.86%	3.19%	3.13%	3.59%
	BLK	9.24%	8.71%	7.55%	7.46%	7.76%
15	MP	4.29%	3.88%	2.93%	1.74%	1.55%
	BLK	23.02%	21.91%	17.37%	10.35%	10.04%
17	MP	5.59%	5.30%	2.70%	1.48%	1.39%
	BLK	30.11%	29.74%	16.61%	15.90%	17.43%

4.3.3.3 Distributed vs. concentrated plasticity FB elements

In this Section a comparison of response obtained with distributed and concentrated FB plasticity elements is shown. For concentrated plasticity FB elements the examined plastic hinge lengths range as 10%, 15%, 20%, 25% and 30% of the element length. Referring the strut 1, the monotonic response curves for both concentrated and distributed plasticity elements are depicted in Fig. 4.8.

As it can be easily noted, the prediction of buckling load is strongly affected by the hinge length. Indeed, if concentrated plasticity elements are used, the reduction of the plastic length produces an increase of strength. For what concerns the transverse displacements, a good agreement for all cases was obtained for high deformation demand. For the case shown the model with plastic hinge equal to 30%L gives the better response as compared to that given by distributed FB elements. Anyway, this result cannot be generalized, since it depends on the length of plastic zone which should be noted *a-priori* and which varies case by case. Therefore, it is more reliable and effective to use distributed elements, because it is possible to overcome the need to define the plastic hinge length. It is interesting to note that the sensitivity analyses performed varying the type of plasticity element showed that the elapsed time for the analysis with concentrated plasticity elements is lower than in the analysis with distributed plasticity. This is due to the fact that numerical integration of fibres is carried out for the two end sections of the plastic length only.

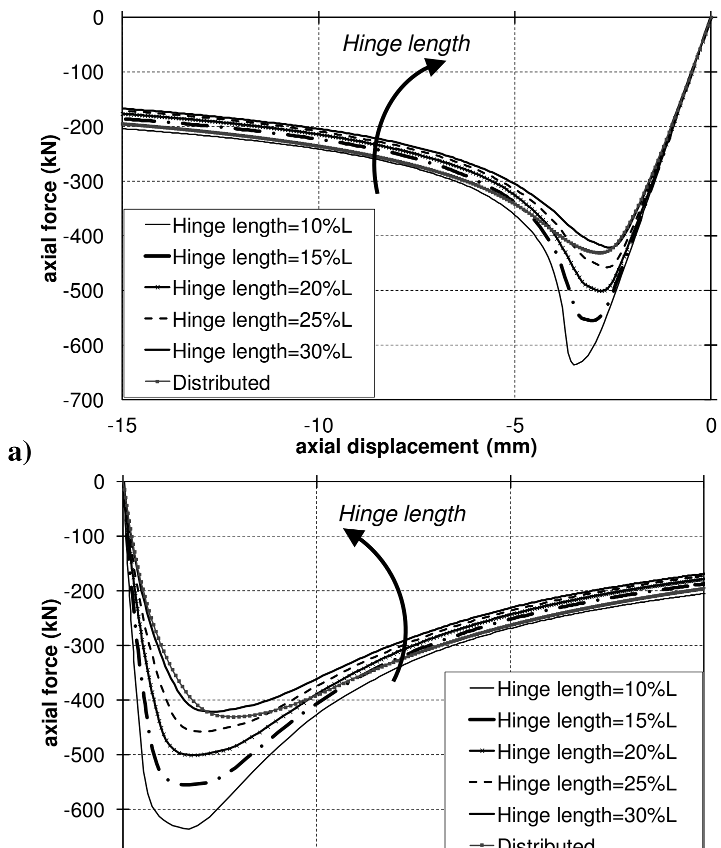

Figure 4.8 Distributed vs. Concentrated FB elements: a) axial force-axial displacement; b) axial force-lateral deflection

4.3.3.4 Influence of number of integration points

Figures 4.9a,b show the results for monotonic shortening of the brace varying the number of IPs per element. Owing to under-integration, the model with three IPs per element exhibits the more soften response in the post-buckling regime (about the 8% in the final stage was recognized). The models with four to ten IPs present similar results, thus highlighting that PTMs of bracing are less affected by localization problems. In addition, it was recognized that reducing the number of IPs leads to minimize the time analysis, but increasing the number of IPs leads to improve the accuracy of the predicted response in nonlinear range.

The analyses showed that increasing the number of distributed plasticity elements in both models with bilinear or sinusoidal shape of the initial camber leads slightly underestimating the brace buckling strength, even though no significant differences can be recognized in post-buckling range, as depicted in Fig. 4.10a,b.

In case of concentrated plasticity elements the computational results are strongly sensitive to the number of sub-elements. As it can be noted in Fig. 4.10c,d, increasing the number of sub-elements does not correspond to an improvement of the model predictive response capability. Indeed, a stiffening effect in the descending post-buckling branch can be recognized in both cases with bilinear and sinusoidal shape. As it can be easily foreseen, the computational time is also affected by the number of sub-elements, increasing more than linearly with the number of elements up to 11 times the period elapsed for models with two elements only.

On the basis of these results it can be recognized that the more suitable manner to implement PTMs for bracing is to use distributed plasticity elements with bilinear shape and two elements only, thus providing both sufficient adequate accuracy and reduced computational effort.

4.3.3.5 Influence of number of fibres

Figures 11a,b show the results obtained using a number of fibres in cross section varying in the range 10÷400.

As it can be observed the sensitivity to this parameter is small. Only in the case with 10 fibres the hysteretic behaviour and the lateral deflection are not accurately represented. This is due to the reduced flexural stiffness and increased sensitivity to the interaction between moment and axial loads. The case with 25 fibres slightly underestimates the buckling strength, being not enough to represent the interaction between moment and axial loads. This result is mainly related to the numerical integration which determines the second moment of area of brace cross section. Indeed, as also observed by Uriz (2005) and Salawdeh and Goggins (2013) using fewer fibres to discretize the brace area may lead having lower distance of the centroid for the fibres, thus resulting in a smaller equivalent moment of inertia than that calculated by assuming a larger number of fibres. In addition, the analyses for the examined set of braces showed that some convergence problems may be observed for such a small number of fibres, especially in cases of the presence of biaxial bending moment interaction with axial load.

From 50 to 400 fibres it is observed that the axial hysteretic and monotonic response become independent from the accuracy of the mesh. This result may be explained by the fact that increasing the number of fibres allows meshing better the section by subdividing the thickness of the plates constituting the cross section. For the examined cases, the analyses showed that it is sufficient to have at least 2 fibres across the thickness to improve the accuracy and the stability of the analysis. In general, increasing the number of fibres makes more stable the computational effort, although it leads increasing the computational time. Using 100 fibres with at least two of them across the thickness of the plate components (namely flange, web or walls) is a satisfactory compromise among computational stability and time effort.

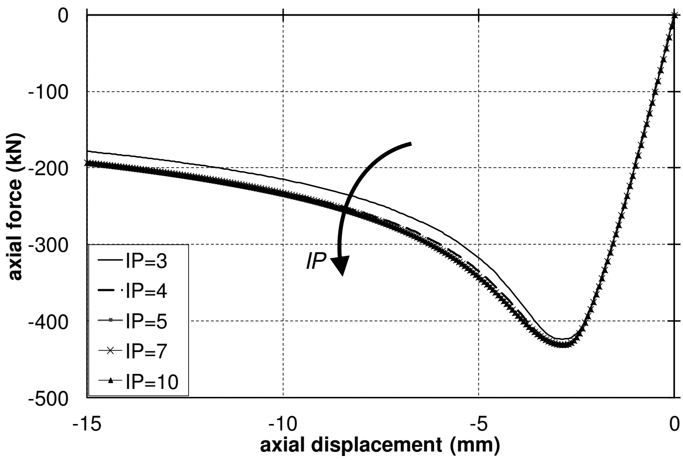

a)

Figure 4.9 Sensitivity to number of IPs: a) axial force-axial displacement; b) axial force-lateral deflection

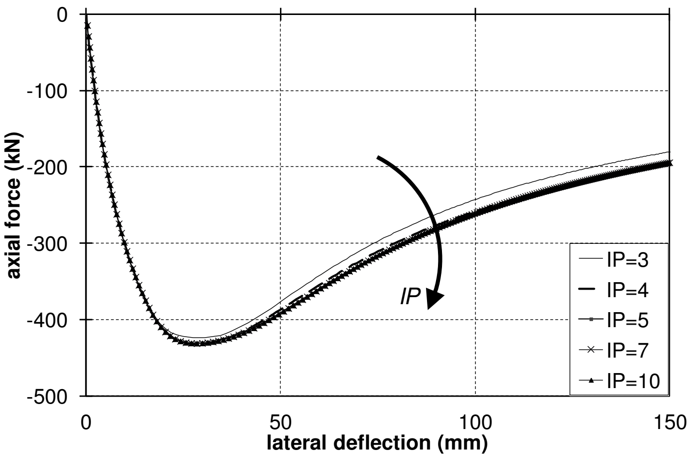

b)

Figure 4.9 Sensitivity to number of IPs: a) axial force-axial displacement; b) axial force-lateral deflection

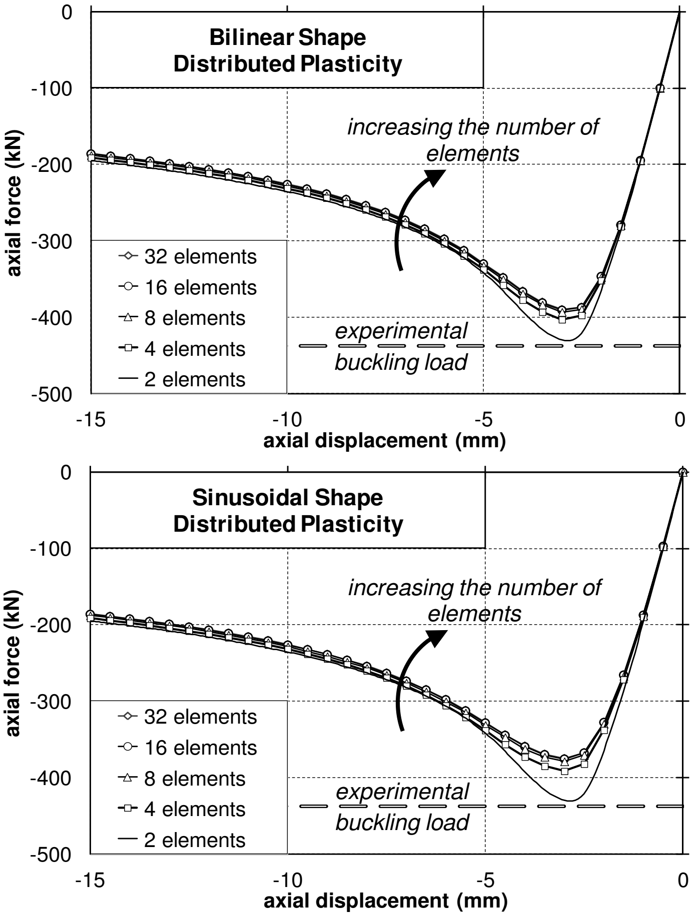

a)

b)

Figure 4.10 Sensitivity to number of elements for bilinear and sinusoidal shape of the initial camber.

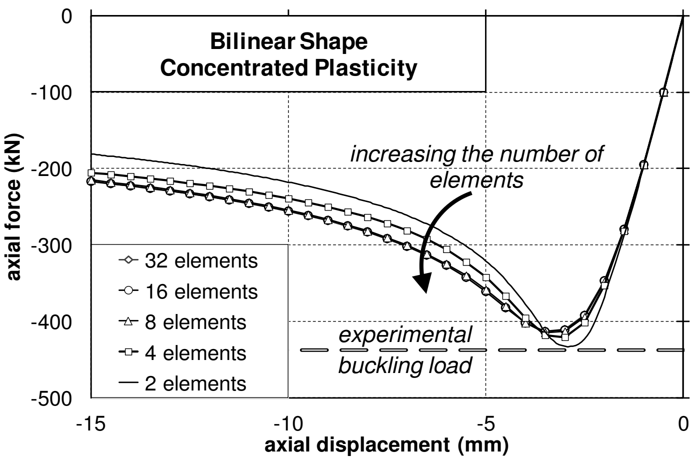

c)

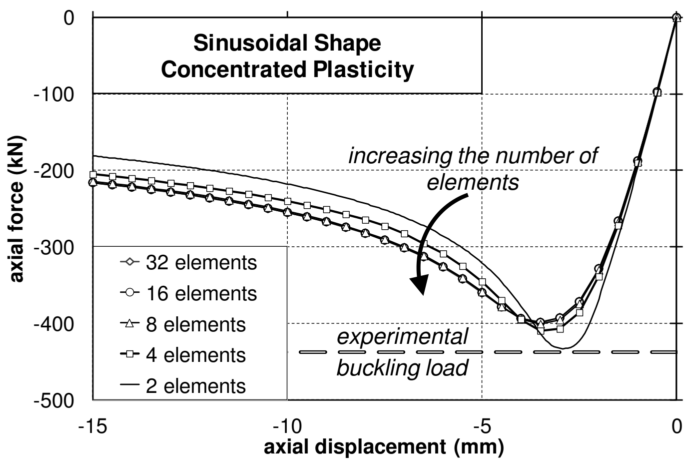

d)

Figure 4.10 Sensitivity to number of elements for bilinear and sinusoidal shape of the initial camber.

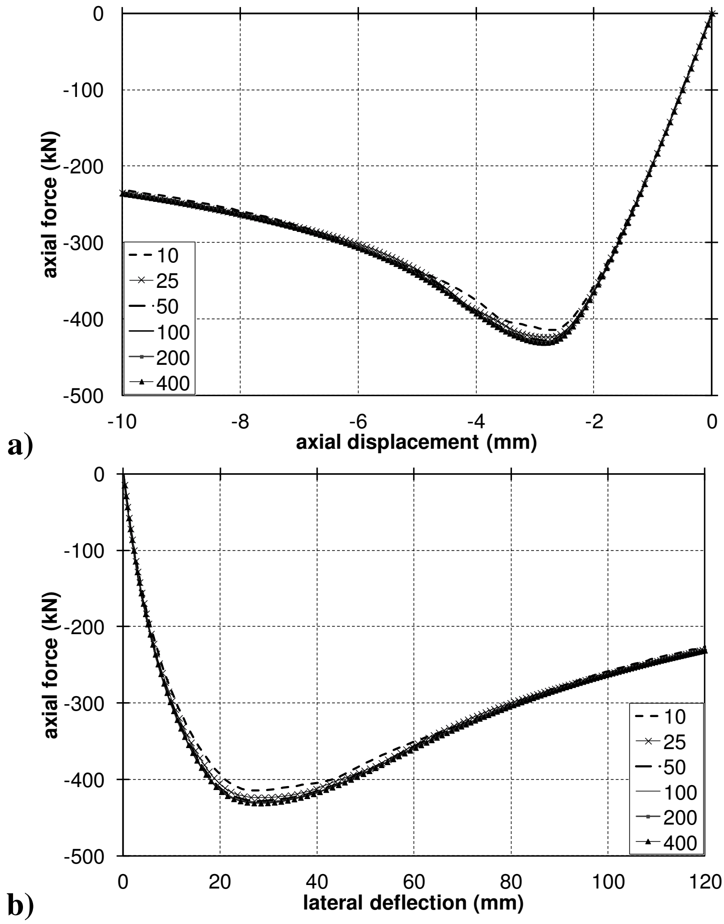

Figure 4.11 Sensitivity to number of fibers: a) axial force-axial displacement; b) axial force-lateral deflection.

4.4 CONCLUSIVE REMARKS

The main issues related to the numerical modelling for seismic analyses of steel concentric braced frames have been highlighted and discussed.

Physical-theory models (PTMs) of braces have been implemented using force-based (FB) elements with distributed or concentrated inelasticity and fibre discretization of the cross section. The features of the nonlinear finite element based software Seismostruct have been adopted.

The accuracy of numerical prediction obtained using different assumptions for modelling parameters proposed in the literature have been examined, extending the analysis to structural configurations and loading conditions different from those used for validation in the relevant original studies, considering the monotonic and cyclic response of braced structures under pseudo-static and dynamic loading conditions.

The examined parameters were the initial camber to trigger brace buckling, the type of material model, the type of force-based element, the number of integration points and the number of fibres to discretize the cross section.

On the basis of numerical investigation on a set of different struts experimentally tested by Black *et al.* (1980), the following considerations can be drawn:

1. the brace member should be subdivided into two FB distributed plasticity elements with a number of integrating section larger than 4.

2. the amplitude of initial camber calculated according to Dicleli and Calik (2008) gives the better accuracy.

3. the model of Menegotto and Pinto (1973) should be used to simulate the material model.

4. the cross section should be meshed with 100 fibres and at least two of them across the thickness of the plate components (namely flange, web or walls).

4.5 REFERENCES

Abramowitz, M.; Stegun, I.A., (1964), *Handbook of Mathematical Functions*. National Bureau of Standards, Applied Math. Series, vol. 55.

Archambault, M.H, Tremblay R, and Filiatrault A., (1995). *Etude du comportement seismique des contreventements ductiles en X avec profile´s tubulaires en acier*. Rapport no. EPM/GCS-1995-09. In: Montreal, Canada: Departement de genie civil, Ecole Polytechnique (in French).

Black, G. R., Wenger, B. A. and Popov, E. P., (1980). *Inelastic Buckling of Steel Struts Under Cyclic Load Reversals, UCB/EERC-80/40*, Earthquake Engineering Research Center, Berkeley, CA.

Calabrese, A., Almeida, J. P. and Pinho, R., (2010). "Numerical issues in distributed inelasticity modelling of RC frame elements for seismic analysis", *J. Earthquake Eng.*, 14, 38-68.

CEN (2005). "Eurocode 3: Design of steel structures-Part 1: General rules and rules for buildings, EN 1993-1 1" European Committee for Standardisation, Brussels.

CEN (2005). "Eurocode 8: Design of structures for earthquake resistance - Part 1: General rules, seismic actions and rules for buildings, EN 1998-1" European Committee for Standardisation, Brussels.

Cho, C.H., Lee C.H. and Kim, J.J., (2011). "Prediction of Column Axial Forces in Inverted V-braced Seismic Steel Frames Considering Brace Buckling", *J. Struct. Eng-Asce*, 137(12), 1440–1450.

Coleman, J. and Spacone, E., (2001). "Localization issues in force-based frame elements", *J. Struct. Eng-Asce*, 127(11), 1257-1265.

Correia, A.A., Virtuoso, F.B.E. (2006). "Nonlinear Analysis of Space Frames", *Proceedings of the Third European Conference on Computational Mechanics: Solids, Structures and Coupled Problems in Engineering, Mota Soares et al. (Eds.)*, Lisbon, Portugal.

D'Aniello, M., Della Corte, G. and Mazzolani, F.M., (2006a). "Seismic upgrading of RC buildings by buckling restrained braces: Experimental results vs numerical modeling", *Proceedings of the 5th International Conference on Behaviour of Steel Structures in Seismic Areas - Stessa 2006*, 815-820, Yokohama, August.

D'Aniello, M., Della Corte, G. and Mazzolani, F.M., (2006b). "Seismic upgrading of RC buildings by steel eccentric braces: Experimental results vs numerical modeling", *Proceedings of the 5th International Conference on Behaviour of Steel Structures in Seismic Areas - Stessa 2006* , 809-814, Yokohama, August.

D'Aniello, M., Della Corte, G. and Mazzolani, F.M., (2008). "Experimental tests of a real building seismically retrofitted by special Buckling-Restrained Braces". *AIP Conference Proceedings 1020 (PART 1)*, 1513-1520, Reggio Calabria, July.

D'Aniello, M., La Manna Ambrosino G., Portioli F., Landolfo R., (2013). “Modelling aspects of the seismic response of steel concentric braced frames” *Steel and Composite Structures,* Vol. 15, No. 5 (2013) 539-566

D’Aniello, M., Portioli, F. and Landolfo, R., (2010). "Modelling issues of steel braces under extreme cyclic actions", *COST ACTION C26: Urban Habitat Constructions under Catastrophic Events - Proceedings of the Final Conference,* Naples, September.

Deierlein, G. G., Reinhorn, A. M. and Willford, M. R., (2010). *Nonlinear Structural Analysis For Seismic Design: A Guide for Practicing Engineers*. NIST GCR 10-917-5, National Institute of Standards and Technology, California.

Dicleli, M. and Mehta, A., (2007). "Simulation of inelastic cyclic buckling behavior of steel box sections", *Comput. Struct.* 85, 446-457.

Dicleli, M. and Calik, E. E., (2008). "Physical Theory Hysteretic Model for Steel Braces", *J. Struct. Eng-Asce*, 134(7), 1215-1228.

ECCS (1978). "European Recommendations for Steel Construction", European Convention for Constructional Steelwork, Sfintesco, D., Brussels.

Fell, B. V., Kanvinde, A.M., Deierlein, G.G. and Myers, A.T., (2009). "Experimental Investigation of Inelastic Cyclic Buckling and Fracture of Steel Braces", *J. Struct. Eng-Asce*, 135(1), 19-32.

Filippou, F.C., Popov, E.P. and Bertero, V.V. (1983). *Effects of Bond Deterioration on Hysteretic Behavior of Reinforced Concrete Joints*. EERC Report 83-19, Earthquake Engineering, Research Center, Berkeley.

Filippou, F. C., and Fenves, G. L., (2004). "Methods of Analysis for Earthquake-Resistant", Chapter 6 from *Engineering Seismology to Performance-Based Engineering*. Bozorgnia, Y. and Bertero, V. V., eds., CRC Press, Florida, USA.

Fragiadakis, M. and Papadrakakis, M., (2008). "Modeling, analysis and reliability of seismically excited structures: computational issues", *Int. J. Comput. Methods*, 5(4), 483-511.

Georgescu, D., (1996). "Earthquake-Recent developments in theoretical and experimental results on steel structures. Seismic resistant braced frames", *Costruzioni metalliche*, 1, 39-52.

Goggins, J. M., Broderick, B. M., Elghazouli, A. Y. and Lucas, A. S., (2006). "Behavior of tubular steel members under cyclic axial loading", *J. Constr. Steel Res.*, 621(2), 121-131.

Goggins, J. M., Broderick, B. M. and Elghazouli A. Y., (2008). "Earthquake testing and response analysis of concentrically-braced sub-frames", *J. Constr. Steel Res*., 64, 997-1007.

Goggins, J. and Salawdeh, S., (2012). "Validation of nonlinear time history analysis models for single-storey concentrically braced frames using full-scale shake table tests". Earthquake Engng Struct. Dyn. In press. DOI: 10.1002/eqe.2264.

Ikeda, K., Mahin, S. A., (1986). "Cyclic response of steel braces", *J. Struct. Eng-Asce*, 112(2), 342-361.

Jain, A. K. and Goel, S., (1978). *Hysteresis Models For Steel Members Subjected to Cyclic Buckling or Cyclic End Moments and Buckling-Users Guide for DRAIN-2D*, University of Michigan, College of Engineering, Ann Arbor, MI.

Jin, J. and El-Tawil, S., (2003). "Inelastic Cyclic Model for Steel Braces", *J. Eng. Mech-Asce*, 129(5), 548-557.

Lee, S., and Goel, S.C., (1987). *Seismic behavior of hollow and concrete-filled square tubular bracing members*. Research Rep. No.UMCE 87-11, University of Michigan, Ann Arbor, MI.

Lee, P. S and Noh C. H. (2010). "Inelastic buckling behavior of steel members under reversed cyclic loading", *Eng. Struct.*, 32, 2579-2595.

Maquoi, R. and Rondal, J., (1978). "Mise en équation des nouvelles courbes européennes de flambement". *Construction Métallique*, 1, 17-30 (in French).

Mazzolani, F.M., Della Corte, G., D'Aniello, M., (2009). "Experimental analysis of steel dissipative bracing systems for seismic upgrading", *J. Civ. Eng. Manag* 15(1), 7-19.

Menegotto, M. and Pinto, P. E., (1973). "Method of Analysis for Cyclically Loaded Reinforced Concrete Plane Frames Including Changes in Geometry and Non-Elastic Behavior of Elements under Combined Normal Force and Bending", *Proceedings IABSE Symposium on Resistance and Ultimate Deformability of Structures Acted on by Well Defined Repeated Loads*, Lisbon.

Nip, K. H., Gardner, L., Elghazouli, A. Y. (2010). "Cyclic testing and numerical modelling of carbon steel and stainless steel tubular bracing members", *Eng. Struct*. 32, 424-441.

Salawdeh, S. and Goggins, J., (2013). "Numerical simulation for steel brace members incorporating a fatigue model", *Eng. Struct*. 46, 332-349.

Scott, M. H. and Fenves, G. L., (2006). "Plastic hinge integration methods for force-based beam–column elements", *J. Struct. Eng-Asce*, 132(2), 244-252.

Scott, M.H. and Fenves, G.L., (2006). "Plastic hinge integration methods for force-based beam–column elements", *J. Struct. Eng-Asce*, 132(2), 244-252.

Seismosoft (2011) "SeismoStruct - A computer program for static and dynamic nonlinear analysis of framed structures". Available from URL: www.seismosoft.com

Serra, M., Rebelo, C., Silva, L.S., Tenchini, A., D'Aniello, M. and Landolfo, R., (2012). "Study on concentrically V-braced frames under cyclic loading", *Proceedings of Stessa 2012 Conference*, Santiago, January.

Shaback, B. and Brown, T., (2003). "Behavior of square hollow structural steel braces with end connections under reversed cyclic axial loading", *Can. J. Civ. Eng.*, 30(4), 745-753.

Shibata, M., (1982). "Analysis of elastic-plastic behavior of a steel brace subjected to repeated axial force", *Int. J. Solids Struct.*, 18(3), 217-228.

Spacone, E., Ciampi, V. and Filippou, F. C., (1996). "Mixed formulation of nonlinear beam finite element", *Comput. Struct.*, 58 (I), 71-83.

Szabó, B.A., Babuška, I., (1991), *Finite Element Analysis*, John Wiley & Sons.

Takeuchi, T. and Matsui, R., (2011). "Cumulative Cyclic Deformation Capacity of Circular Tubular Braces under Local Buckling", *J. Struct. Eng-Asce*, 137(11), 1311-1318.

Tang, X. and Goel, S. C., (1989). "Brace fractures and analysis of phase I structures", *J. Struct. Eng-Asce*, 115(8), 1960-1976.

Tremblay, R., (2002). "Inelastic seismic response of steel bracing members", *J. Constr. Steel Res.*, 58, 665-701.

Tremblay, R., Archambault, M.,H., and Filiatrault, A., (2003). "Seismic Response of Concentrically Brace Steel Frames Made with Rectangular Hollow Bracing Members", *J. Struct. Eng-Asce*, 129(12), 1626-1636.

Uang, C. M. and Bertero V. V., (1986). *Earthquake simulation tests and associated studies of a 0.3-scale model of a six-story concentrically braced steel structure*, University of California, Berkeley.

Uriz, P., (2005). "Towards earthquake resistant design of concentrically braced steel buildings", PhD Dissertation. Department of Civil and Environmental Engineering, University of California, Berkeley.

Uriz, P., Filippou F. C. and Mahin, S. A., (2008). "Model for Cyclic Inelastic Buckling of Steel Braces". *J. Struct. Eng-Asce*, 134(4), 619-628.

Wakawayashi, M., Matsui, C., Minami, K. and Mitani, I., (1970). *Inelastic behaviour of full scale steel frames*, Kyoto University Research Information Repository, Disaster Prevention Research Institute annuals.

Wijesundara, K.K., (2009). "Design of concentrically braced steel frames with RHS shape braces", PhD Dissertation. Pavia: European Centre for Training and Research in Earthquake Engineering (EUCENTRE).

Wijesundara, K. K., Nascimbene, R. and Sullivan, T. J., (2011). "Equivalent viscous damping for steel concentrically braced frame structures", *B. Earthq. Eng*., 9(5),1535-1558.

Yang, C. S., Leon, R. T. and DesRoches, R., (2008). "Pushover Response of a Braced Frame with Suspended Zipper Struts", *J. Struct. Eng-Asce*, 134(10), 1619-1626.

Chapter V
The influence of beam flexural stiffness

5.1 INTRODUCTION

The response of chevron concentrically braced frames under seismic action involving large ductility demand is strongly dependent on the type of the developed plastic mechanism, which is deeply influenced by the behaviour of the beam of the braced span. Indeed, depending on the strength of the brace-intercepted beam, two different failure modes can be achieved:

(i) Weak beam mechanism: following the buckling of the brace in compression, an unbalanced vertical force resulting from the axial forces transmitted by both braces is applied on the beam. Subsequently, the beam yields in bending.

(i) Strong beam mechanism: the beam is sufficiently strong to resist elastically the unbalanced force due to the brace buckling and to allow the yielding of the brace in tension.

Flexural yielding of the beam may cause significant deterioration of overall force-displacement curve, while the strong beam mechanism is characterized by larger ductility and energy dissipation (Khatib *et al.*, 1998; tremblay and Robert 2000 and 2001). In light of these considerations, current seismic codes (e.g. EN1998-1, AISC341, CSA 16-09) provide capacity design criteria to achieve strong beam mechanism (see also Chapter III).

However, whatever design criterion is considered, analysing the results from literature, it can be observed that it is not possible to prevent negative post-buckling system stiffness and soft storey mechanisms for most building cases. Moreover, in most cases the brace members behave elastically in tension and suffer severe ductility demand in compression. This result can be explained as a consequence of the design rules and assumptions which are commonly focused on the strength of the beam connected to the bracing members, without accounting for its flexural stiffness. Indeed, it should be noted that differently from X bracings, in CCBs the brace ductility demand depends on both interstorey drift ratio and the mutual interaction between the beam and the connected braces. Several studies (Khatib *et al.*, 1998; tremblay and Robert 2000 and 2001) have early underlined the key role played by beam flexural stiffness in the performance of CCBs, being the flexural response of the beam and the brace deformation in compression correlated phenomena. As depicted in Fig. 5.1, the elastic deflection caused by the unbalanced force can be large enough to prevent yielding of the brace in tension and to concentrate the damage in the compression diagonal, thus leading to a very poor overall performance due to the brace deterioration. Therefore, even though there is a correlation between strength and stiffness of the beam, in most practical applications it is not enough to guarantee an effective performance of CCBs. Large-scale tests by Uriz (2005) and shaking table tests by Okazaki *et al.* (2013) (carried out on mock-ups designed for the unbalance force given by AISC341) showed that the beam vertical deflection induced by the unbalanced force increases the axial compressive deformation of the brace impairing the inelastic deformation capacity and anticipating the brace fracture.

As it can be easily recognized, such a type of behaviour should be avoided because the energy dissipation provided by the brace buckling (even though it is characterized by the formation of plastic hinge at the mid-length of the brace) is noticeably less than that provided by tensile yielding (Jain *et al.*, 1978; Black *et al.*, 1980; Ikeda and Mahin, 1986)

This result has been confirmed in the framework of a recent European project, i.e. HSS-SERF RFSR-CT-2009-00024 (Vulcu *et al.*, 2014), aimed at investigating the effectiveness of the combined use of high strength steel for non-dissipative elements and mild carbon steel for dissipative members. Indeed, the possibility to use high strength steel for beams and/or the need to design slim floor solutions may lead to very flexible and over-strong beams. In such cases, the ductility demand in compression overcomes the shortening capacity of the braces and the bracing in tension cannot yield, as well (D'Aniello *et al.*, 2012; Vulcu *et al.*, 2014).

More recently, the numerical studies carried out by Shen *et al.* (Shen *et al.*, 2014 and 2015) concluded that brace-intercepted beams designed with the minimum possible required strength permitted by the current US design provisions could undergo significant vertical inelastic deformations for interstorey drift ratios ranging within 0.02–0.04. Similarly to the results obtained in (Vulcu *et al.*, 2014), Shen *et al.* (2014 and 2015) also observed that the inelastic deformations in the middle spans of brace-intercepted beams considerably increase ductility demands on both braces and beam-to-column connections. On the basis of these outcomes, they suggested to consider the vertical displacements of brace-intercepted beams, together with interstorey drift ratios, as deformation response indexes to reveal the actual seismic response of critical components in CCBs.

In light of the above considerations, in this Section a numerical parametric study is described and discussed in order to investigate the influence of the flexural stiffness of the braced-intercepted beams on the overall seismic response of chevron concentrically braced frames. The numerical results are processed in order to highlight the relationship between the mutual stiffness ratio beam-to-bracing system and the global and local performance parameters affecting the seismic response of CCBs. On the basis of the regression of data, empirical formulations are provided as design aid to control the local brace ductility demand and the plastic mechanism at different performance levels. In addition, on the basis of the obtained results, some criteria are proposed to improve the design procedure of CCBs using EN 1998-1. The effectiveness of the proposed procedure has been evaluated by performing pushover and time history analyses on a case study building.

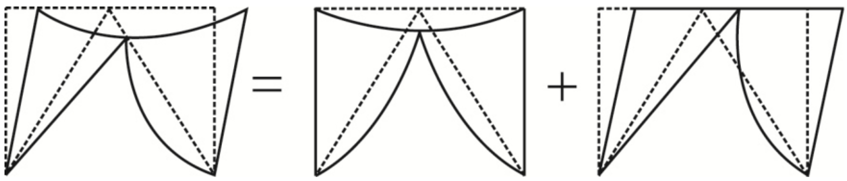

Figure 5.1 Lateral displacement shape of CCBs: a) contribution of the vertical displacements; b) contribution of the horizontal displacements

5.2 FRAMEWORK OF THE STUDY

5.2.1 *Investigated parameters*

A comprehensive set of single storey CCBs was designed to investigate the mutual interaction between the beam and connected bracing members. With this regard, the examined key parameter is the beam-to-brace stiffness ratio (in the following referred K_F) ranging from zero to infinitive by varying both geometrical and mechanical properties. K_F is defined as the ratio:

$$K_F = \frac{k_b}{k_{br}} \tag{5.1}$$

where k_b is the beam flexural stiffness at the intersection with braces and k_{br} is the vertical stiffness of the bracing members. In particular, the former is given by:

$$k_b = 48\zeta \frac{EI_b}{L_b^3} \tag{5.2}$$

where E is the elastic modulus of steel, I_b is the second moment of area of the beam section, L_b is the beam length and ζ is a factor depending on the beam boundary condition, namely $\zeta = 4$ for fixed ends and $\zeta = 1$ for pinned ends.
The vertical stiffness of the bracings is given by:

$$k_{br} = 2\frac{A_{br}E}{L_{br}} sen^2\alpha \tag{5.3}$$

where A_{br} is the area of the brace section, L_{br} is the brace length and α is the tilt angle of the brace (see Fig. 5.2)

In Table 5.1 all parameters and their relevant variations are summarized and described as follows:

- the beam cross section: the commercial standard European profiles IPE and HE have been used, thus covering the intermediate values of beam rigidity. In

addition, IPE and HE profiles have a different cross area at the same flexural stiffness, thus experiencing different behaviours under the combined action of axial force and bending moment occurring under large displacements, when catenary effects are activated;
- the aspect ratio $tg\alpha$, given by the ratio between the span length (L) and the interstorey height (h);
- the brace normalized slenderness $\bar{\lambda}$ has also been varied considering stocky, intermediate and slender braces;
- realistic dimensions have been assumed for both span lengths and column heights.

Table 5.1 Parameters of variation.

Parameter	Units	Variations
K_F	[-]	upper bound = ∞ – lower bound = 0
Beam	[-]	IPE (*) – HEA (**) – HEB (**) – HEM (**) upper bound (k_b = ∞) – lower bound (k_b = 0)
$tg\alpha$	[-]	0.6 – 0.7 – 0.75 – 0.8 – 0.875 – 1 – 1.167 – 1.333
Braces Slenderness ($\bar{\lambda}$)	[-]	0.6 – 0.8 – 1 – 1.2 – 1.4 – 1.6 – 1.8 – 2
Interstorey height (h)	[m]	3 – 3.5 – 4
Span length (L)	[m]	6 – 8 – 10

(*) beam depth from 240 mm to 600 mm (i.e. n. 10 profiles)
(**) beam depth from 240 mm to 1000 mm (i.e. n. 18×3 profiles)

5.2.2 *Monitored mechanical parameters*

Both local and global response parameters were selected to characterize the behaviour of CCBs and monitored during each analysis; they are described in the following:

- The normalized unbalanced force (β) applied to the beam when the buckling of the brace in compression occurs. This parameter is defined as:
-

$$\beta = \frac{N_{T,br} - N_{C,br}}{N_{pl,br}} \tag{5.4}$$

  Where $N_{T,br}$ is the brace axial force in tension; $N_{C,br}$ is the brace axial force in compression; $N_{pl,br}$ is the brace plastic axial strength.
- The brace ductility (μ) both in tension and in compression, given by the ratio d/d_y being d the brace axial displacement and d_y the displacement of the brace at yielding.
- The storey drift ratio (θ_y) corresponding to the brace yielding.
- The beam flexural yielding.

5.2.3 *Numerical Modelling*

Nonlinear monotonic and pseudo-static cyclic analyses were performed using SeismoStruct computational platform. The analysed structural scheme is depicted in Fig. 5.2, where the external boundary conditions are also shown. In addition, a rigid diaphragm constraining the both ends of the beam was used in order to have equal horizontal displacements, while the beam section at the brace intersection can deform axially. In such a way, the catenary effect can develop when the beam bends under large deformations.

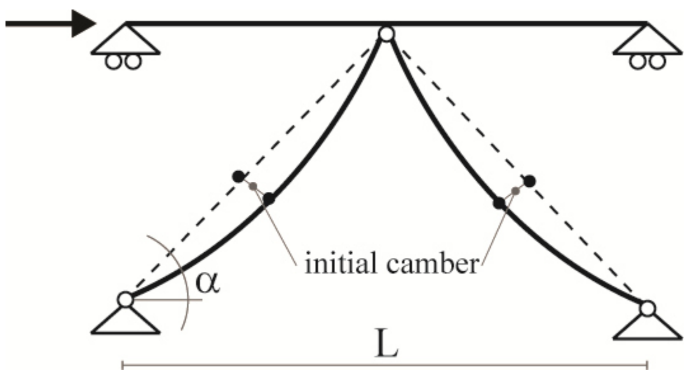

Figure 5.2 Numerical model of the analysed structures.

It is worth to note that in order to focus the attention on the mutual interaction between the beam and the brace system, the contribution to overall deformation due to the columns has been neglected. With this regard, it should be noted that the axial deformability of columns solely reduces the beam flexural stiffness, because columns act as a sort of mechanical spring. Therefore, the results of the presented parametric study can be easily extended to cases with the columns accounted for by calculating properly the beam stiffness with the presence of deformable bearings ($k^*_{b,i}$) according to the following equation:

$$k^*_{b,i} = K_{F,i} \big/ k_{br,i} = \frac{1}{\dfrac{1}{k_{b,i}} + \dfrac{1}{k_{col,1,i}} + \dfrac{1}{k_{col,2,i}}} \tag{5.5}$$

Where $k^*_{b,i}$ is the flexural stiffness of the beam neglecting the deformability of supports (namely, the deformability of the columns) and $k_{col,j,I}$ is the axial stiffness of the columns, evaluated as:

$$k_{col,ji} = \frac{1}{\sum_{1}^{i} \dfrac{1}{\dfrac{EA_{col,j,i}}{h_i}}} \tag{5.6}$$

Where E is the Young modulus of the material; $A_{col,j,i}$ is the area of the column cross section of the vertical alignment "*j*" at the generic level "*i*" and h_i is the interstorey height.

Physical-theory models (PTM) were used to simulate the braces response, using the out-of-plane imperfection Δ_0 calculated according to Dicleli and Calik (2008). Indeed, as already discussed in Chapter 4, recent studies showed that this approach is the most appropriate to simulate both the buckling and the hysteretic behaviour of bracing elements (D'Aniello *et al*. 2013, 2014).

The structural members were modelled using the force-based (FB) distributed inelasticity elements (Spacone *et al.* 1996). These elements account for distributed inelasticity through integration of material response over the cross section and integration of the section response along the length of the element. The cross-section behaviour is reproduced by means of the fibre approach, by assigning a uniaxial stress-strain relationship at each fibre. The Menegotto-Pinto (1973) hysteretic model was chosen to simulate the steel behaviour. The average value of yield steel stress was assumed for all members, which was obtained by multiplying the nominal value of the yield stress of the material by the randomness coefficient γ_{ov} set equal to 1.25 as recommended by EN1998-1. On the basis of the numerical calibration described by D'Aniello *et al.* (2010, 2013, 2014), in the present study the parameters accounting for isotropic strain hardening were set equal to zero (more details about this issue can be found in Chapter IV).

The numerical integration method used is based on the Gauss-Lobatto distribution, which includes, at a minimum, monitoring points at each end of the element (Abramowitz and Stegun, 1964). Such feature allows each structural member to be modelled with a single FB element, thus requiring no meshing for each element. In the present study, 5 Gauss-Lobatto integration points (IP) were used.

Second order effects were accounted in all analyses presented herein, by assuming large displacements/rotations and large independent deformations relative to the chord of the frame element through the employment of the co-rotational formulation given by Correia and Virtuoso (2006).

For what concerns the loading conditions, both monotonic and cyclic incremental horizontal displacements were applied at both beam ends. In the pseudo-static cyclic analyses the ECCS protocol was used (ECCS-45, 1986).

5.3 VALIDATION OF NUMERICAL ASSUMPTIONS

In order to verify the consistency and the effectiveness of the adopted modelling approach in predicting the nonlinear response of CCBs, the accuracy of numerical simulations has been validated against cyclic pseudo-static experimental results on a two-story full-scale CCB carried out by Uriz and Mahin (2008) at University of California, Berkeley (UCB). Figure 5.3 shows the geometry of the specimen, the details of members and the test setup.

Both beams and columns were modelled as distributed plasticity elements with 5 IPs per element and 200 fibers per section. Columns were assumed fixed at the base and continuous along the building height. Beam-to-column connections were modelled as elastic springs having flexural stiffness calculated according to EN1993:1-8. As discussed in the previous section, the braces were modelled as described by D'Aniello *et al.* (2013, 2014). The stiffness of end restraint provided by the gusset plate was calculated according to Helleslan (2007), considering its second moment of area evaluated around the axis of rotation where the brace buckles. Finally, the material properties derived from coupon tests were implemented in Menegotto-Pinto (MP) hysteretic model (1973), accounting also for the fracture as reported by Uriz and Mahin (2008).

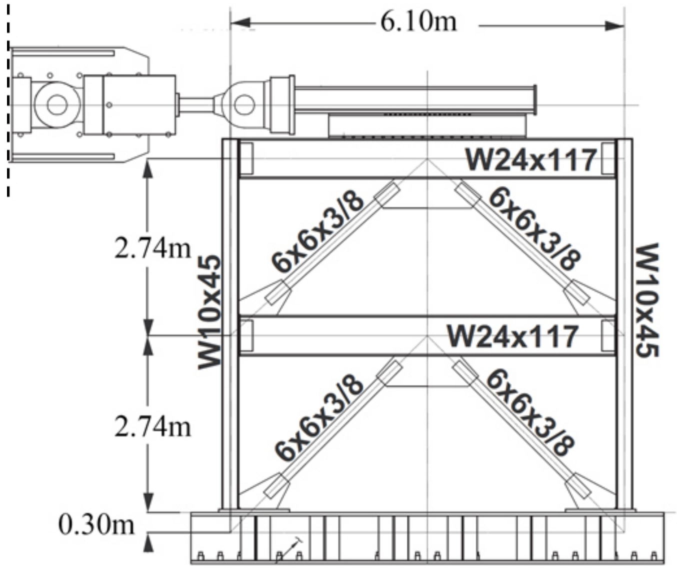

Figure 5.3 Test setup and geometry of the frame tested by Uriz and Mahin (2008).

Figures 5.4a,b show the comparison between numerical and experimental results in terms of failure mode at the same cycle, while the comparison in terms of base shear versus both roof and first storey drift ratios is shown in Figs. 5.4c,d. As it can be observed, the simulated behaviour satisfactorily matches the test results, thereby predicting buckling, post-buckling and fractures of braces.

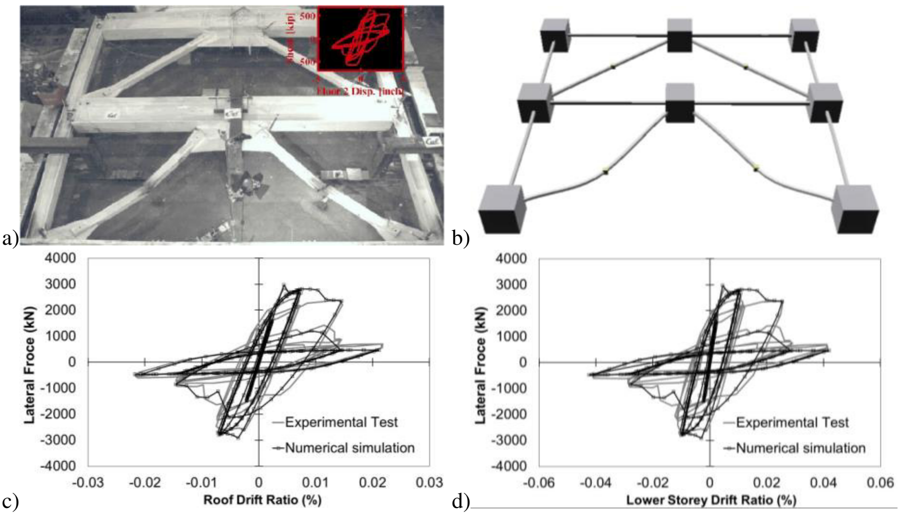

Figure 5.4 Numerical vs. experimental cyclic pseudo-static behaviour of the frame tested by Uriz and Mahin (2008).

5.4 PARAMETRIC STUDY: RESULTS AND DISCUSSION

5.4.1 *Ductility demand of bracing members*

Results obtained from both monotonic and cyclic analyses clearly show that the better braces performance, characterized by yielding in tension and limited damage in compression, is experienced for the structures with the higher values of beam-to-brace vertical stiffness ratio K_F. This feature can be explained considering that the stiffer the beam, the smaller is its vertical displacement, thus limiting the deformation demand in the brace under compression (see Fig. 5.5).

As a general remark, from Fig. 5.6 it can be observed that the higher the K_F value, the lower is the drift ratio for which yielding occurs. In the cases with $K_F = \infty$ the yielding of the brace in tension occurs at a drift ratio ranging from 0.1 % (for $tg\alpha = 1.33$) to 0.3% (for $tg\alpha = 0.6$).

Monotonic pushover analyses show that $K_F = 0.1$ is the threshold value that delimits two different structural performances. Indeed, for $K_F > 0.1$ brace yielding in tension can be observed at drift ratios within the range of 2-3%, depending on the frame aspect ratio $tg\alpha$ (see Fig. 5.6). On the contrary, for $K_F < 0.1$ the bracing does not yield in tension and at large drift ratios (e.g. $\theta > 2\%$) both diagonal elements can be subjected to compression forces. This behaviour is more evident for very flexible beams ($0 < K_F < 0.02$) (see Fig. 5.6).

Cyclic analyses confirm these results as shown in Fig. 5.7, where the peak ductility demand at each cycle is plotted for one of the bracing members. As it can be observed, the braces in structures with deformable beams are subjected to axial shortening in both directions of the cyclic action. Only for structures with $K_F > 0.02$ the bracings are subjected to alternate tension and compression.

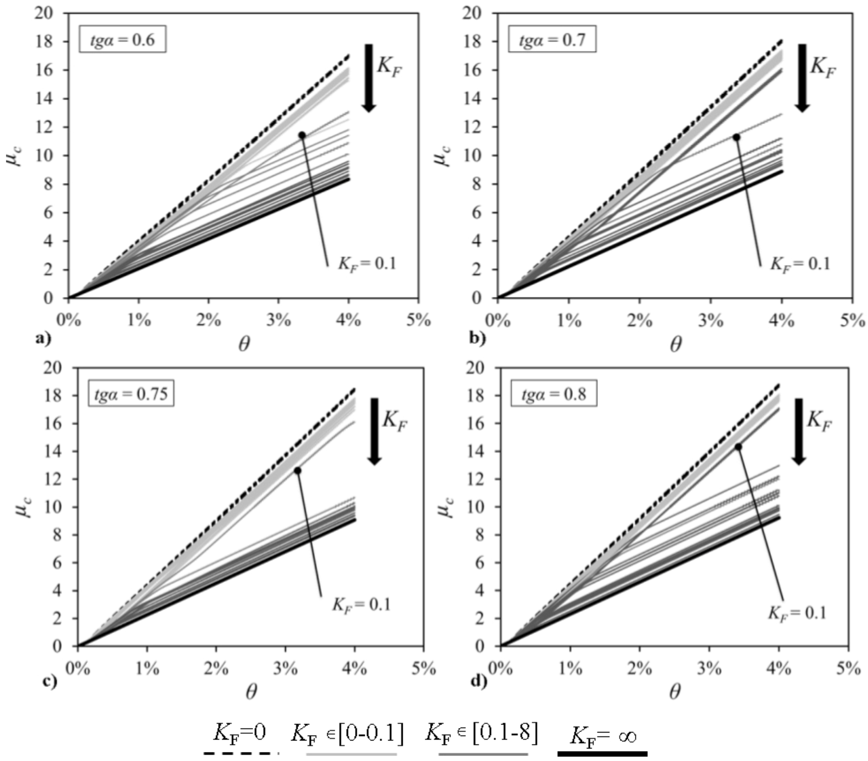

Figure 5.5 Brace ductility demand in compression.

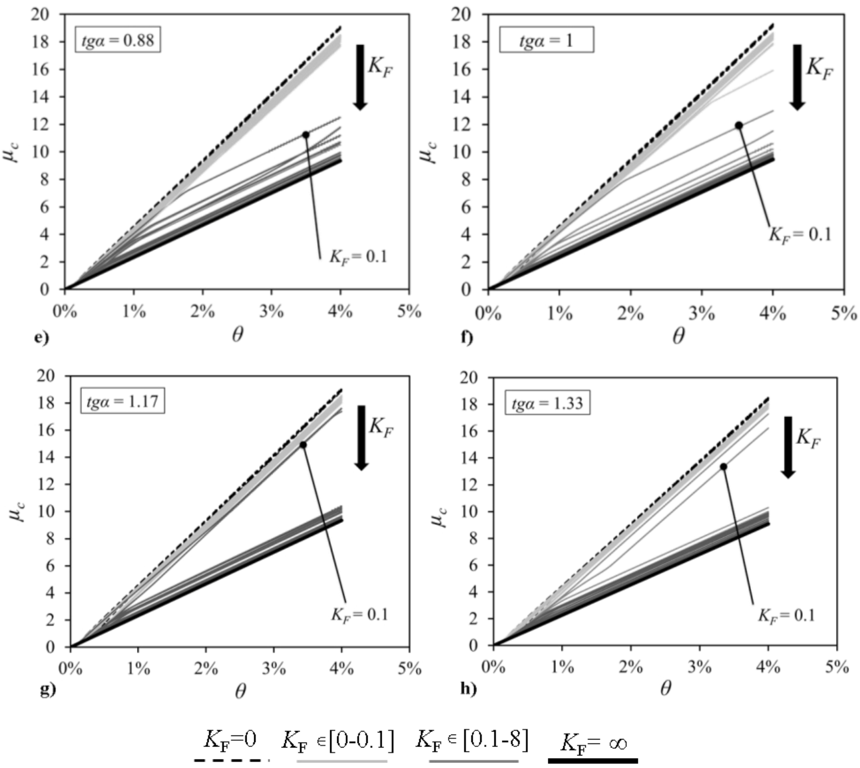

Figure 5.5 Brace ductility demand in compression.

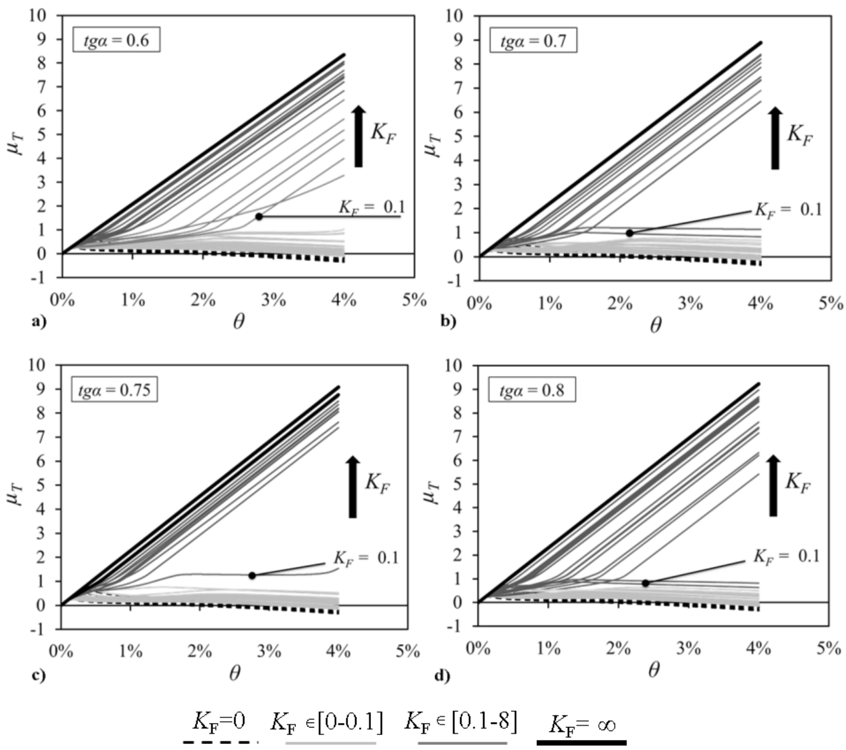

Figure 5.6 Brace ductility demand in tension.

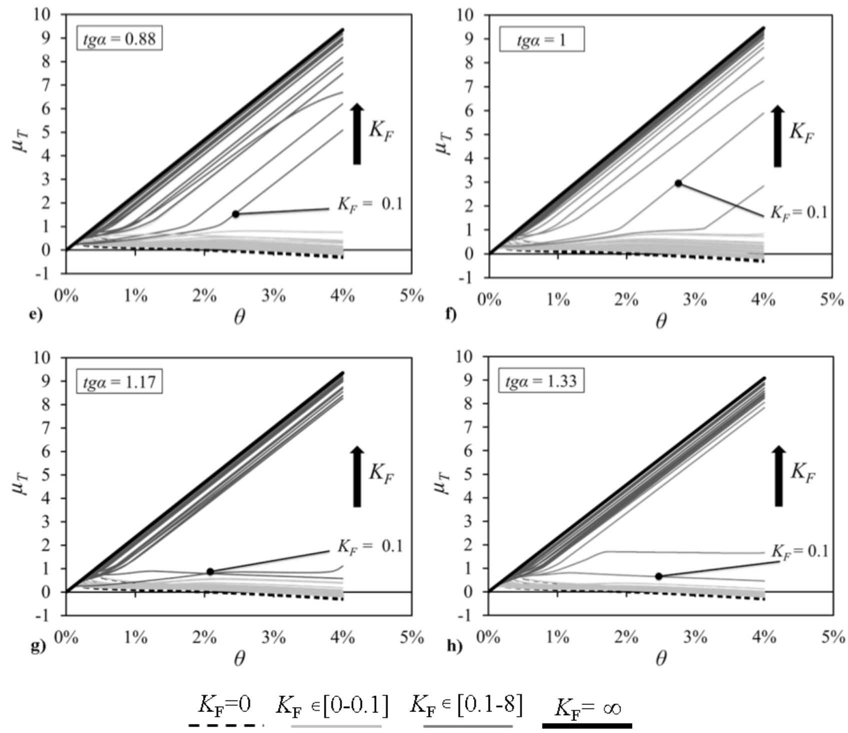

Figure 5.6 Brace ductility demand in tension.

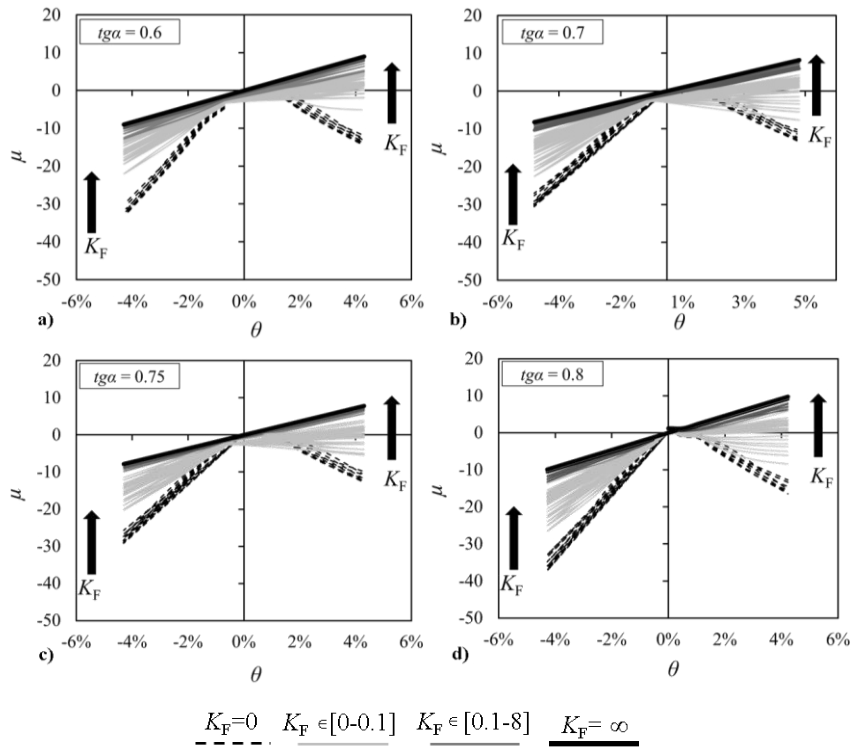

Figure 5.7 Brace ductility demand: cyclic response.

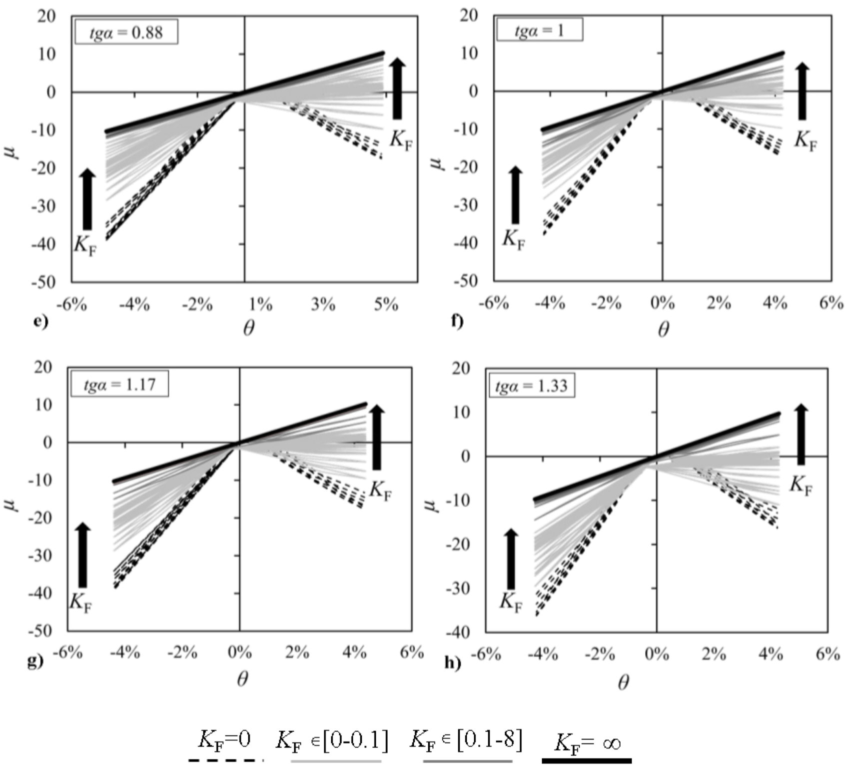

Figure 5.7 Brace ductility demand: cyclic response.

5.4.2 *Beam response*

The bending demand at the brace-intercepted section is mainly due to the vertical unbalanced force occurring after the buckling of the brace in compression and resulting from the axial forces transmitted by both braces.

In Fig. 5.8 the bending demand on the beam is represented by mean of the ratio M/M_{Rd} (given against the interstorey drift ratio θ) where M is the acting bending moment and M_{Rd} is the bending capacity accounting for the interaction with the axial force acting on the beam after the buckling of the brace under compression.

By observing the plots, three different performances can be recognized depending on the value of the beam-to-brace stiffness ratio K_F as follow:

(i) The plastic hinge develops in the beam for all the cases at about 2% of drift ratio for all cases with intermediate K_F within the range [0.02, 0.1].

(ii) For K_F within the range [0, 0.02] (very flexible beams) the beam behaves elastically even beyond the 4% of drift ratio. This result can be easily explained considering that both bracing members are under compression and negligible values of the unbalanced force can be developed even at very large storey displacements.

(iii) For $K_F > 0.1$ most of beams behave elastically because increasing the beam stiffness implies enlarging the flexural strength. In addition, as already shown, at larger K_F both the full yielding of the brace in tension and deterioration of brace in post-buckling range occur (see Section 5.4.1); in such condition, the unbalanced force cannot be larger than the value corresponding to the development of the plastic capacity of the connected braces, and the bending moment acting on the beam cannot increase.

However, by observing the Fig. 5.8, some exceptions can be recognized. Indeed, a very small group of cases with K_F ranging in [0.1-0.4] experience flexural yielding of the beam (see Fig. 5.8d,f,h,m,o). This feature can be easily explained considering the deterioration of the beam moment capacity due to the interaction with the axial force applied to the beam in the post-buckling range.

The exceptions specified in Fig. 5.8 correspond to cases characterized by stiff beams and stocky braces ($\overline{\lambda} \in [0.6, 0.8]$) inducing significant axial force on the beam. As a consequence deterioration of the beam plastic strength is recognized and combined axial-flexural yielding occurs at the brace-intercepted section.

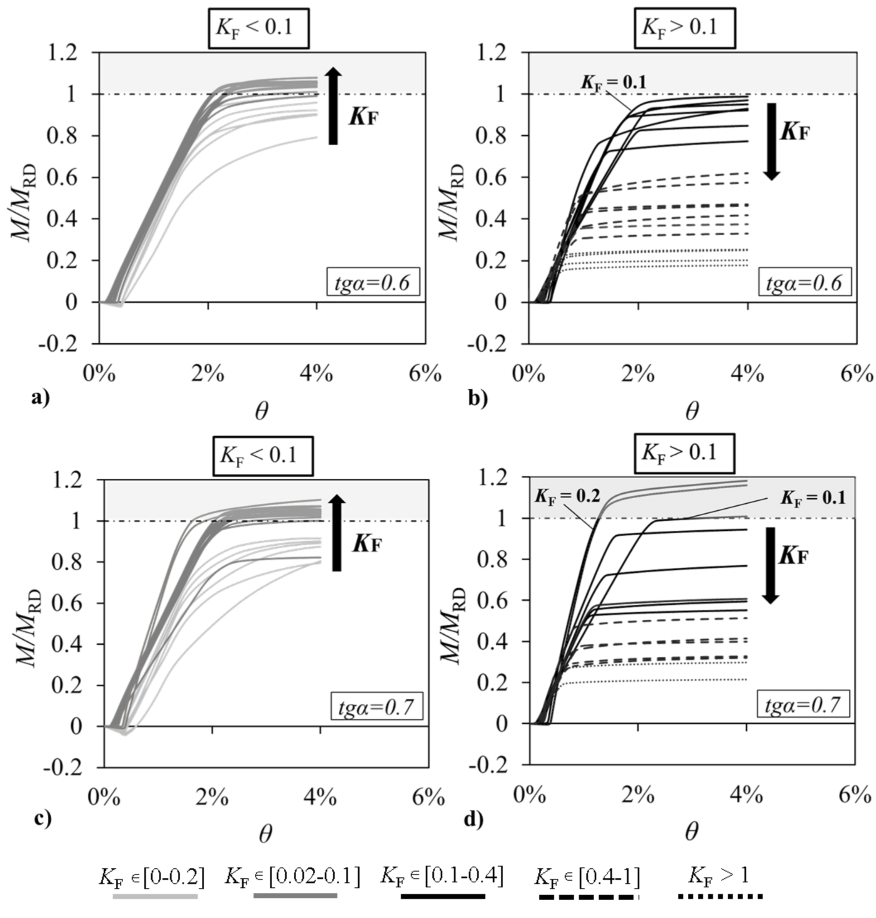

Figure 5.8 Brace-intercepted beam response.

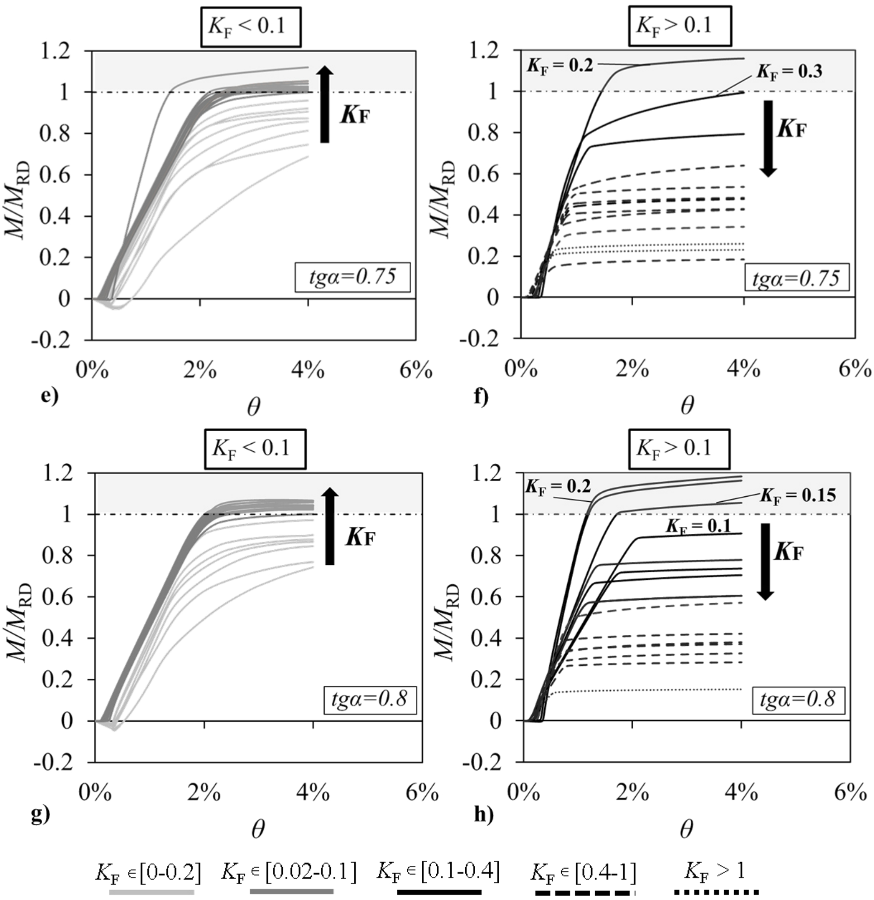

Figure 5.8 Brace-intercepted beam response.

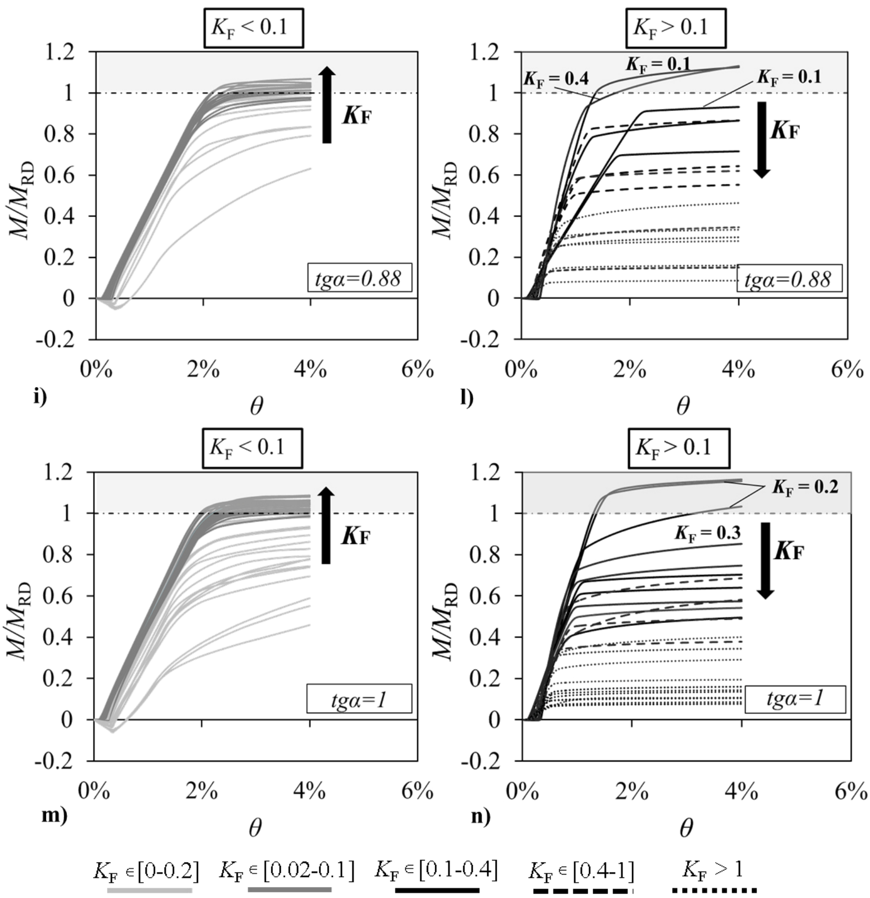

Figure 5.8 Brace-intercepted beam response.

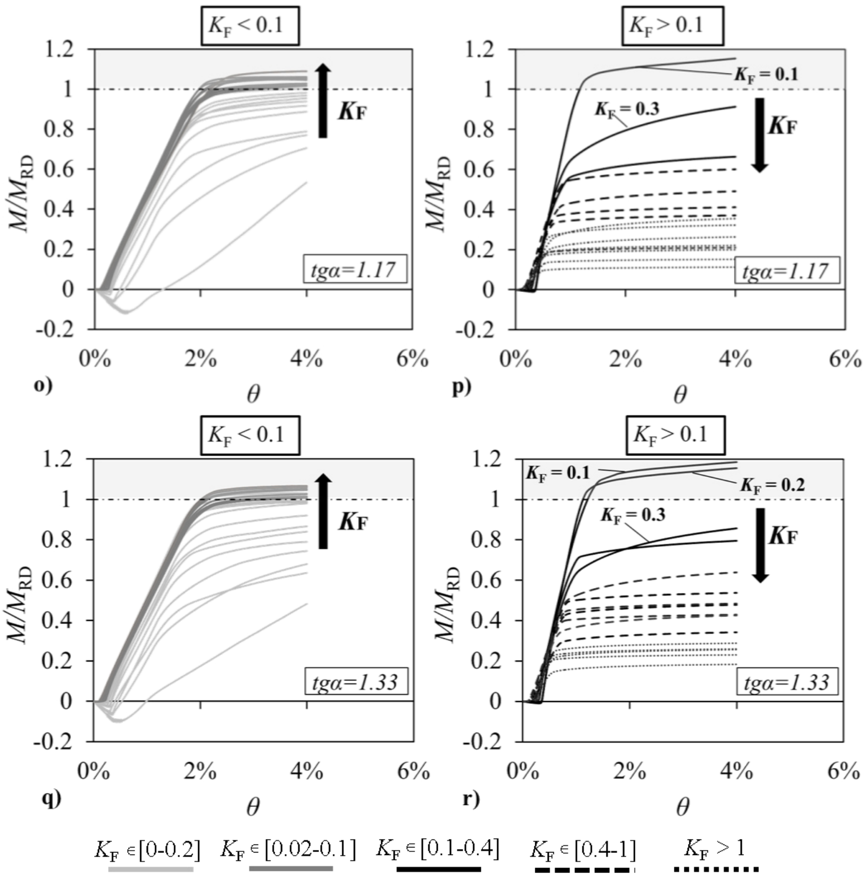

Figure 5.8 Brace-intercepted beam response.

5.5 EMPIRICAL EQUATIONS

The data obtained from numerical analyses were processed in order to obtain empirical equations correlating K_F to the performance parameters discussed previously in Section 5.2.2. The numerical results were analysed at specified drift ratios θ up to 4%, which was assumed as representative performance limit for multi-storey steel buildings under seismic actions.

5.5.1 *Ductility demand of bracing members*

Figure 5.9 shows the relationship between the drift ratio corresponding to the yielding of the brace in tension (θ_y) and K_F.

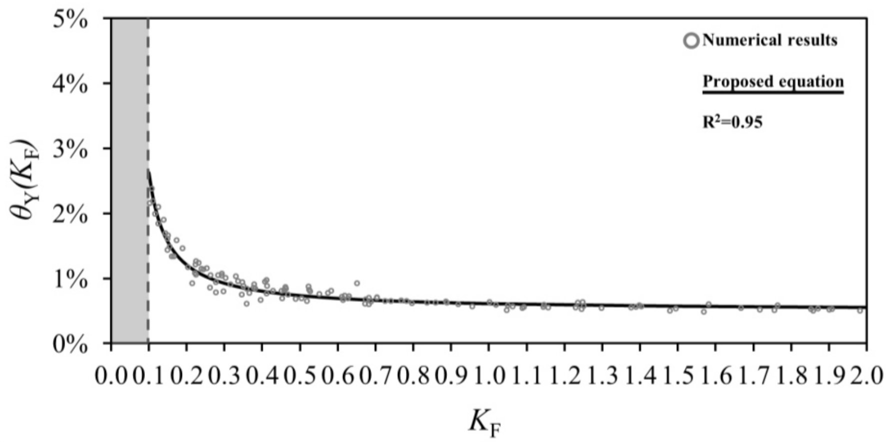

Figure 5.9 Brace yielding drift ratio vs. K_F: numerical results and proposed equation.

The interpolating curve fitting the numerical data is a hyperbolic function given as follows:

$$\theta_y(K_F) = \frac{0.008 \cdot K_F + 0.0013}{1.6 \cdot K_F - 0.08} \qquad \forall K_F \geq 0.1 \tag{5.7}$$

This equation is limited to $K_F > 0.1$, because bracing member cannot yield in tension for smaller K_F as previously discussed in Section 5.4.1.

Numerical data for drift ratios in the range of [0.01, 0.04] highlight that the brace ductility demand μ depends on both K_F and *tgα*. As shown in Figs. 5.10 and 5.11, the ductility demand for the braces in tension and compression (respectively) is satisfactorily matched by a hyperbolic equation given by Eq. (5.8) (see page 210), where the coefficients to be assumed are summarized in Table 5.2, while Table 5.3 reports coefficients of determination R^2 for Eq. (5.8) that show the accuracy of the proposed equation.

$$\mu(K_F, \mathrm{tg}\,\alpha, \theta) = \frac{\left[\left(k_3 \cdot \mathrm{tg}\,\alpha^3 + k_2 \cdot \mathrm{tg}\,\alpha^2 + k_1 \cdot \mathrm{tg}\,\alpha + k_0\right) \cdot \theta^2 + \left(p_3 \cdot \mathrm{tg}\,\alpha^3 + p_2 \cdot \mathrm{tg}\,\alpha^2 + p_1 \cdot \mathrm{tg}\,\alpha + p_0\right) \cdot \theta + \left(q_3 \cdot \mathrm{tg}\,\alpha^3 + q_2 \cdot \mathrm{tg}\,\alpha^2 + q_1 \cdot \mathrm{tg}\,\alpha + q_0\right)\right] \cdot K_F + (b_2 \cdot \theta^2 + b_1 \cdot \theta + b_0)}{(c_2 \cdot \theta^2 + c_1 \cdot \theta + c_0) \cdot K_F + (d_2 \cdot \theta^2 + d_1 \cdot \theta + d_0)}$$

(5.8)

$$K_F(\mu, tg\,\alpha, \theta) = \frac{(a_2 \cdot \theta^2 + a_1 \cdot \theta + a_0) \cdot \mu + (b_2 \cdot \theta^2 + b_1 \cdot \theta + b_0)}{[(k_3 \cdot tg\,\alpha^3 + k_2 \cdot tg\,\alpha^2 + k_1 \cdot tg\,\alpha + k_0) \cdot \theta^2 + (p_3 \cdot tg\,\alpha^3 + p_2 \cdot tg\,\alpha^2 + p_1 \cdot tg\,\alpha + p_0) \cdot \theta + (q_3 \cdot tg\,\alpha^3 + q_2 \cdot tg\,\alpha^2 + q_1 \cdot tg\,\alpha + q_0)] \cdot \mu + (d_2 \cdot \theta^2 + d_1 \cdot \theta + d_0)}$$

$$\forall\, 0 < \mu_T \leq \mu_{UB}(tg\,\alpha) \wedge \forall\, \mu_C \geq \mu_{UB}(tg\,\alpha)$$

(5.12)

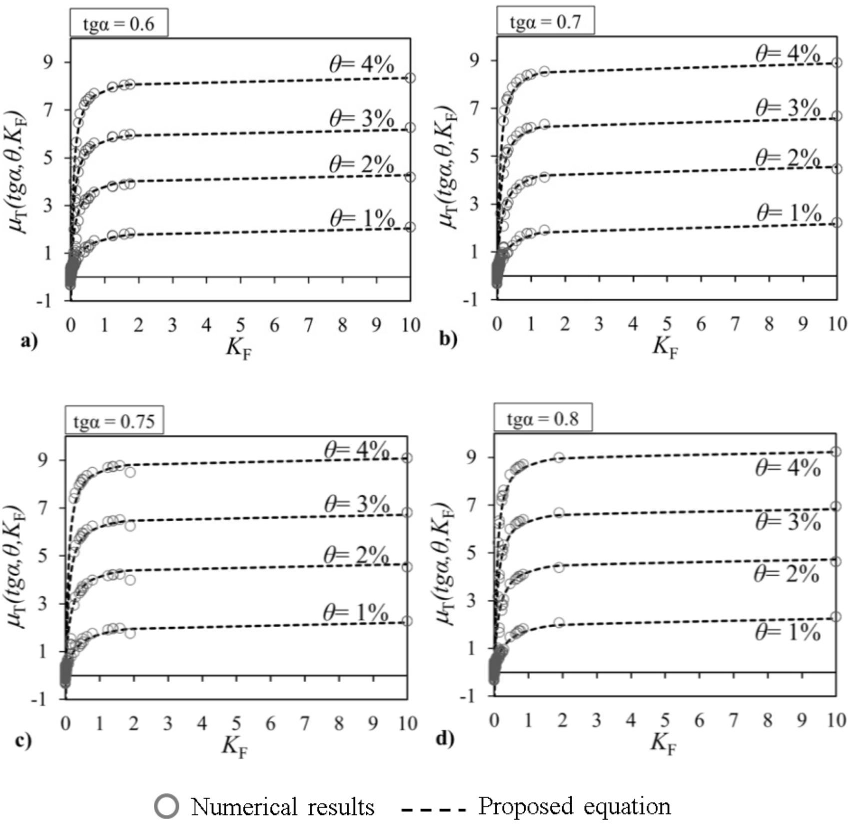

Figure 5.10 Brace ductility demand in tension (μ_T) vs. K_F.

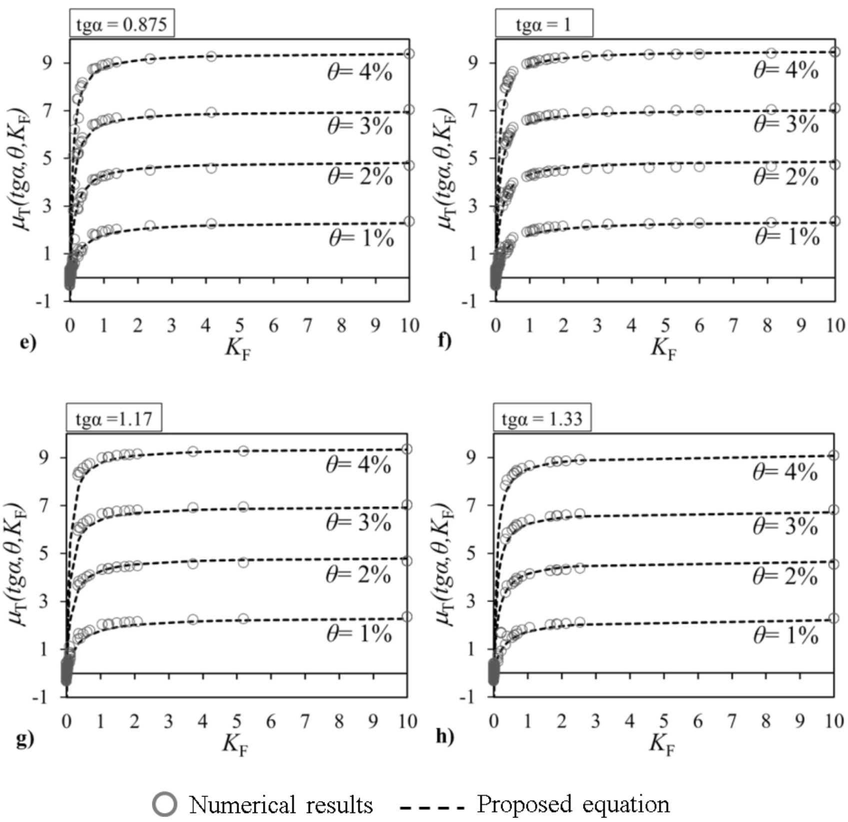

Figure 5.10 Brace ductility demand in tension (μ_T) vs. K_F .

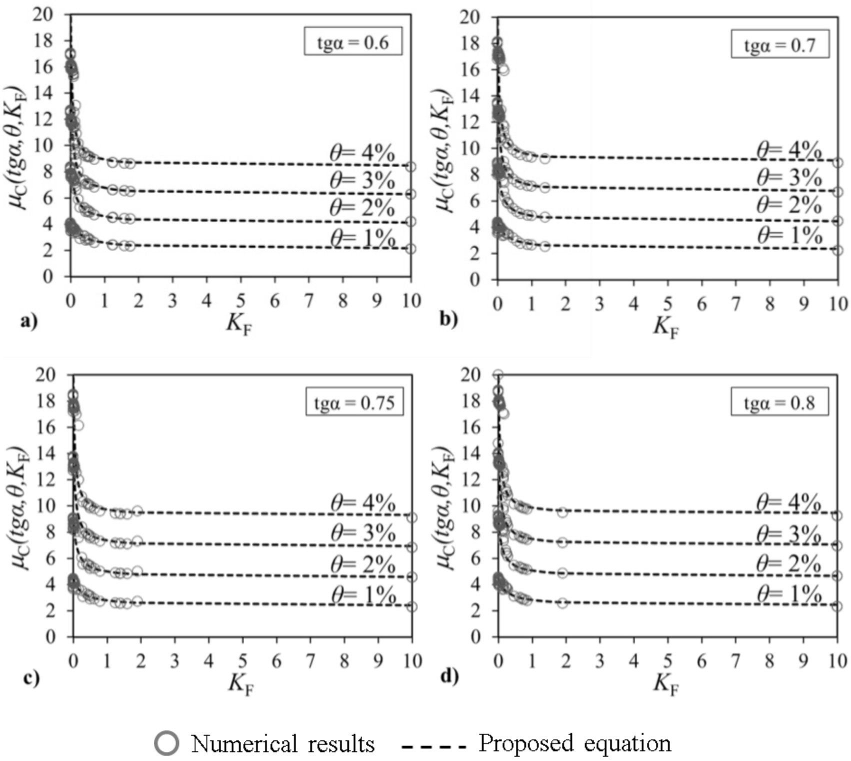

Figure 5.11 Brace ductility demand in compression (μ_C) vs. K_F.

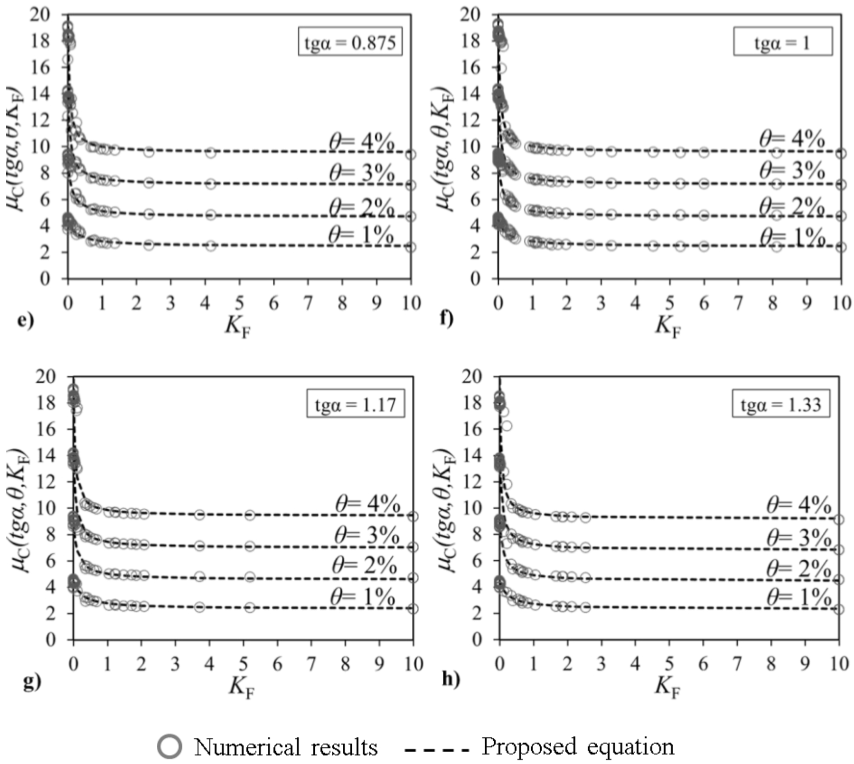

Figure 5.11 Brace ductility demand in compression (μ_C) vs. K_F.

Table 5.2 Values of the coefficients in the Eq. (5.8).

		μ_T vs. K_F			
k_3	482631.100	p_3	15226	q_3	-102.200
k_2	-1852640	p_2	-66050	q_2	444.820
k_1	2249364	p_1	86645	q_1	-584.500
k_0	-28087.600	p_0	-2438.500	q_4	24.775
b_2	-70000	c_2	-87500	d_2	7500
b_1	2200	c_1	10225	d_1	-885
b_0	-10.500	c_0	-8.750	d_0	38.250
		μ_C vs. K_F			
k_3	485389.9000	p_3	11668	q_3	17.012
k_2	-1908773	p_2	-37726	q_2	-57.565
k_1	2356294	p_1	38912	q_1	63.559
k_0	-1727.740	p_0	-12765	q_0	11.874
b_2	-25000	c_2	5000	d_2	5000
b_1	3950	c_1	3290	d_1	-460
b_0	22.500	c_0	19.5	d_0	17.500

Table 5.3 R^2 values for Eq.. (5.8).

μ_T vs. K_F				
tgα	***θ=1%***	***θ=2%***	***θ=3%***	***θ=4%***
0.6	0.98	0.962	0.93	0.887
0.7	0.976	0.952	0.888	0.825
0.75	0.985	0.975	0.934	0.895
0.8	0.979	0.953	0.898	0.841
0.875	0.987	0.976	0.953	0.924
1	0.984	0.97	0.932	0.894
1.17	0.984	0.975	0.943	0.909
1.33	0.99	0.978	0.944	0.912
μ_C vs. K_F				
tgα	***θ=1%***	***θ=2%***	***θ=3%***	***θ=4%***
0.6	0.928	0.93	0.894	0.847
0.7	0.899	0.915	0.845	0.775
0.75	0.945	0.954	0.905	0.857
0.8	0.937	0.934	0.879	0.819
0.875	0.944	0.948	0.918	0.878
1	0.963	0.954	0.905	0.859
1.17	0.965	0.961	0.919	0.877
1.33	0.975	0.967	0.927	0.89

It is interesting to note that the vertical asymptote of the hyperbolic curve given by Eq. (5.8) corresponds to the μ-axis, while the horizontal one is limited by the upper-bound cases with $K_F = \infty$. Indeed, for this ideal case no vertical deflection of the beam can occur and consequently the maximum elongation of the brace in tension and the minimum shortening of the brace in compression are obtained. Moreover, only for $K_F = \infty$, the brace axial deformation under tension and compression are symmetric, being:

$$\mu_{UB} = \mu_{T,MAX} = \mu_{C,MIN} \tag{5.9}$$

Where:

μ_{UB} is the brace ductility demand of the upper bound, for $K_F = \infty$;

$\mu_{T,MAX}$ is the maximum value of the brace ductility demand achieved by the brace in tension;

$\mu_{C,MIN}$ is the minimum value of the brace ductility demand experienced by the brace in compression.

The ductility demand μ_{UB} strictly depends on the storey drift ratio θ and the aspect ratio *tgα*. The ductility μ_{UB} was analytically derived by applying the large displacement theory imposing the relationship between brace axial lengthening and storey drift, as follows:

$$\mu_{UB}(\alpha) = \frac{\theta}{\varepsilon_y} \cdot \sin\alpha \cdot \cos\left(\alpha + arctg\left(\frac{\theta \cdot \sin^2\alpha}{1+\theta}\right)\right) \tag{5.10}$$

In order to verify the consistency of the models it was also derived μ_{UB} for each drift ratio within [0.01, 0.04], interpolating the numerical data obtained assuming beam with infinite stiffness as follows:

$$\mu_{UB}(tg\alpha) = \mu_{T,MAX} = -\mu_{c,MIN} = m_3 \cdot tg\alpha^3 + m_2 \cdot tg\alpha^2 + m_1 \cdot tg\alpha + m_0 \tag{5.11}$$

The terms m_i of Eq. (5.11) are reported in Table 5.4, where coefficients of determination R^2 are also presented to show the accuracy of the proposed equation.

Table 5.4 Coefficients m_i in the Eq. (5.11) and relevant R^2 indexes.

$\mu_{UB}(tg\alpha)$					
θ	m_3	m_2	m_1	m_0	R^2
1%	1.174	-4.858	6.201	-0.1456	0.999
2%	2.407	-9.784	12.344	-0.231	0.999
3%	3.690	-14.963	18.842	-0.463	0.999
4%	5.374	-21.146	25.756	-0.700	1.000

Figure 5.12 depicts the comparison between the analytical prediction, the interpolating function and the numerical results, which confirms the accuracy of the empirical formulation.

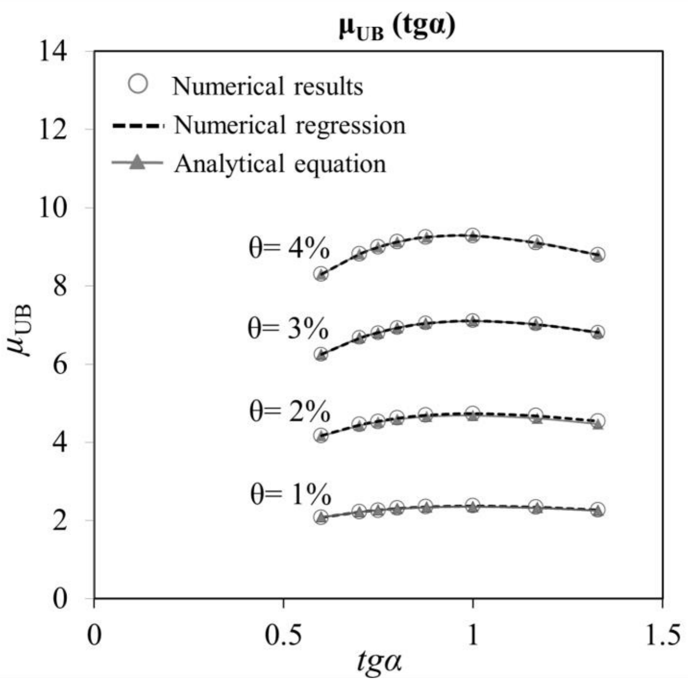

Figure 5.12 Brace ductility demand for $K_F = \infty$ vs. tgα.

Figure 5.11 shows that in the cases with low and medium values of K_F (i.e. those cases covering common configuraions made of IPE and HEA beam cross sections and intermediate brace slenderness ratio) for drift ratios generally accepted as satisfactory seismic performance (e.g. within 0.015-0.025) the corresponding damage in diagonal members is greater than the axial deformation limits provided by EN1998-3. With this regard, wide existing literature based on experimental tests (e.g. Tremblay (2002) and Goggins *et al.* (2006)) showed that the axial deformation limits recommended by EN1998-3 are too restrictive. A more rational criterion might be relating the brace deformation limits for CCBs to (i) the brace slenderness and (ii) the global performance in terms of drift ratio for each Limit State. F rom a design point of view it could be useful to relate K_F to the ductility demand (μ). Thereby, the inverse function (see Fig. 5.13 and Fig. 5.14) is given by Eq. (5.12) (see page 210). It should be noted that, being $\mu_{UB}(tg\alpha)$ the theoretical limit for ductility corresponding to $K_F=\infty$ (namely either the maximum possible ductility demand in tension or the minimum possible in compression), it also corresponds either to the upper bound of the interval of validity of Eq. (5.12) (if the tension brace ductility demand is used), or the lower bound (if the compression brace ductility demand is used), alternatively.

The coefficients to be assumed are summarized in Table 5.5, while Table 5.6 reports coefficients of determination R^2 for Eq. (5.12) that show the accuracy of the proposed equation.

Table 5.5 Values of the coefficients in the Eq. (5.12).

		K_F vs. μ_T			
a_2	25.000	b_2	-50.000	d_2	2500.000
a_1	-1.950	b_1	1.000	d_1	117.000
a_0	0.098	b_0	0.045	d_0	-0.700
k_3	8.770	p_3	-2.241	q_3	0.556
k_2	334.910	p_2	-26.742	q_2	-1.433
k_1	-714.510	p_1	61.666	q_1	1.165
k_0	699.230	p_0	-66.655	q_4	-0.277
		K_F vs. μ_C			
a_2	0.000	b_2	-50.000	d_2	1250.000
a_1	-0.100	b_1	-7.700	d_1	172.500
a_0	0.000	b_0	-0.115	d_0	-0.875
k_3	-185.230	p_3	20.242	q_3	0.107
k_2	773.750	p_2	-79.459	q_2	-0.415
k_1	-989.620	p_1	97.800	q_1	0.509
k_0	757.200	p_0	-70.425	q_4	-0.362

Table 5.6 R^2 values for Eq. (5.12).

K_F vs. μ_T				
tgα	***θ*=1%**	***θ*=2%**	***θ*=3%**	***θ*=4%**
0.600	0.990	0.989	0.996	0.974
0.700	0.980	0.987	0.988	0.977
0.750	0.895	0.898	0.882	0.889
0.800	0.966	0.979	0.996	0.966
0.875	0.977	0.921	0.999	0.890
1.000	0.951	0.857	0.995	0.816
1.170	0.964	0.899	0.995	0.879
1.330	0.982	0.968	0.992	0.976
K_F vs. μ_C				
tgα	***θ*=1%**	***θ*=2%**	***θ*=3%**	***θ*=4%**
0.600	0.978	0.993	0.966	0.980
0.700	0.958	0.986	0.969	0.974
0.750	0.899	0.898	0.890	0.894
0.800	0.976	0.989	0.942	0.958
0.875	0.927	0.983	0.862	0.902
1.000	0.896	0.987	0.806	0.860
1.170	0.891	0.971	0.823	0.862
1.330	0.982	0.994	0.951	0.970

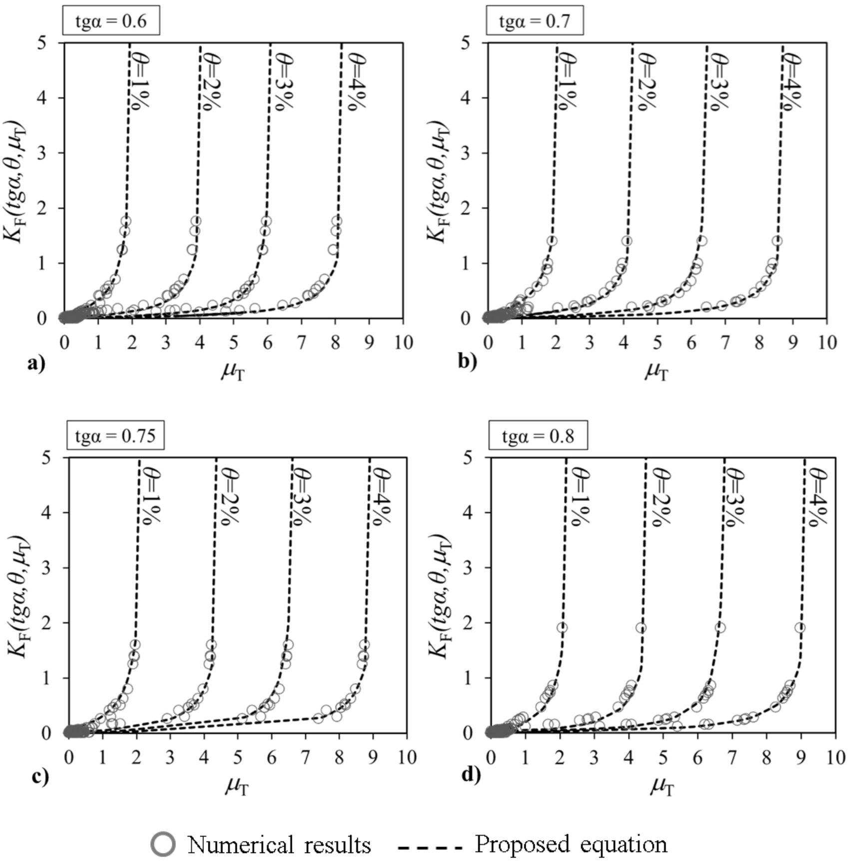

Figure 5.13 Beam-to-brace stiffness ratio K_F vs. brace ductility demand in tension (μ_T).

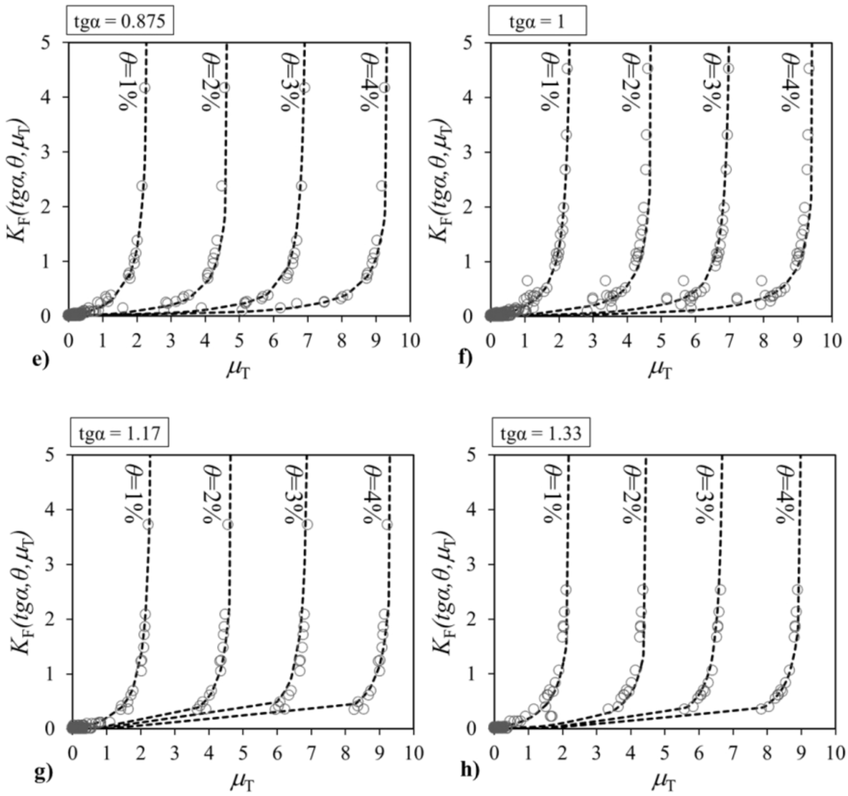

Figure 5.13 Beam-to-brace stiffness ratio K_F vs. brace ductility demand in tension (μ_T).

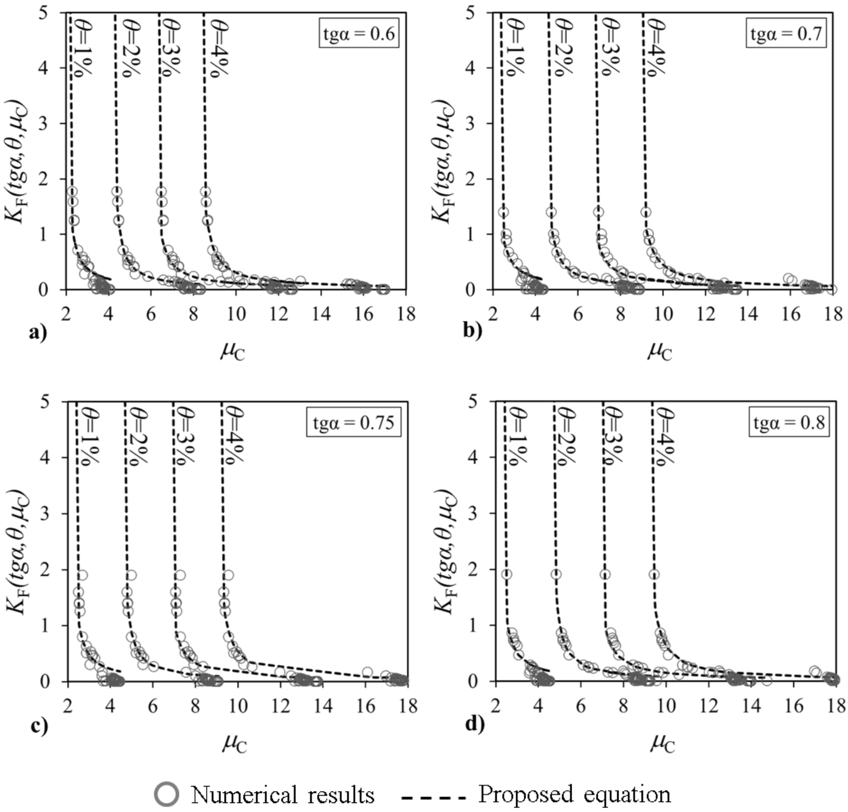

Figure 5.14 Beam-to-brace stiffness ratio K_F vs. brace ductility demand in compression (μ_C).

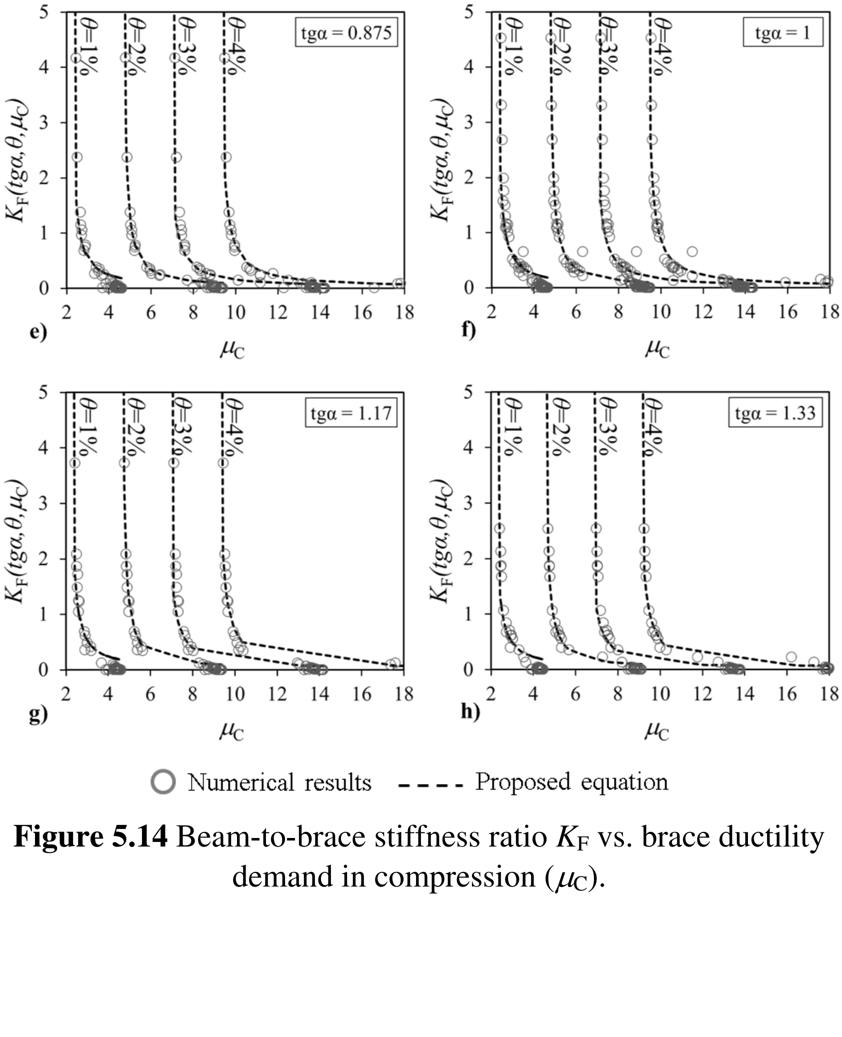

Figure 5.14 Beam-to-brace stiffness ratio K_F vs. brace ductility demand in compression (μ_C).

The Equations 5.8 - 5.13 have previously confirmed that the braces ductility demand both in tension and compression strictly depends on the stiffness ratio K_F, the aspect ratio $tg\alpha$ and the interstorey drift ratio θ.

By observing the results related to the lower bound limit cases (namely the ductility demand μ_{LB} experienced in the cases with K_F =0) it is interesting to note that the response of very flexible beams, is mostly affected by the braces slenderness ratio ($\bar{\lambda}$). Indeed, in these cases the beam deflection became dominant and the response is solely affected by the bending demand due to the unbalanced force applied at the brace-intercepted section. As already discussed in Chapter III (Section 3.3) the strength degradation of diagonal members subjected to cyclic action is strongly affected by their normalized slenderness $\bar{\lambda}$.

Figure 5.15 depicts the brace ductility demand for the lower bound cases μ_{LB} experienced both in tension $\mu_{LB,T}$ and compression $\mu_{LB,C}$ as function of the brace normalized slenderness $\bar{\lambda}$. The interpolating function is a polynomial relationship provided as:

$$\mu_{LB} = l_3 \cdot \bar{\lambda}^3 + l_2 \cdot \bar{\lambda}^2 + l_1 \cdot \bar{\lambda} + l_0 \tag{5.13}$$

The coefficients to be assumed are summarized in Table 5.7 that also reports coefficients of determination R^2 for Eq. (5.13) showing the accuracy of the proposed equation.

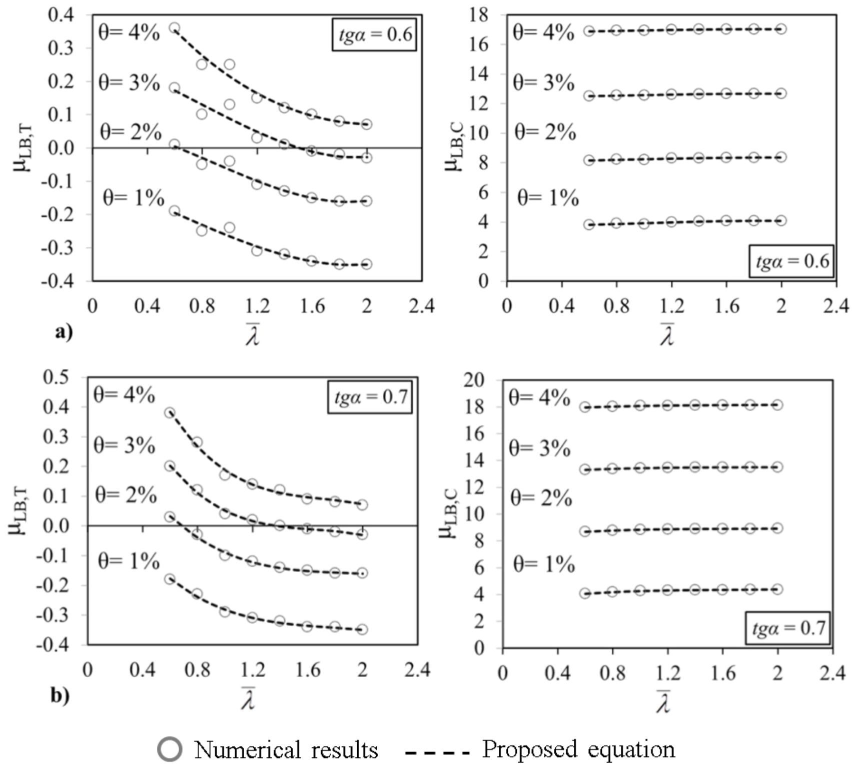

Figure 5.15 Brace ductility demand al lower bound in tension ($\mu_{LB,T}$) and compression ($\mu_{LB,C}$) vs. braces normalized slenderness $\bar{\lambda}$.

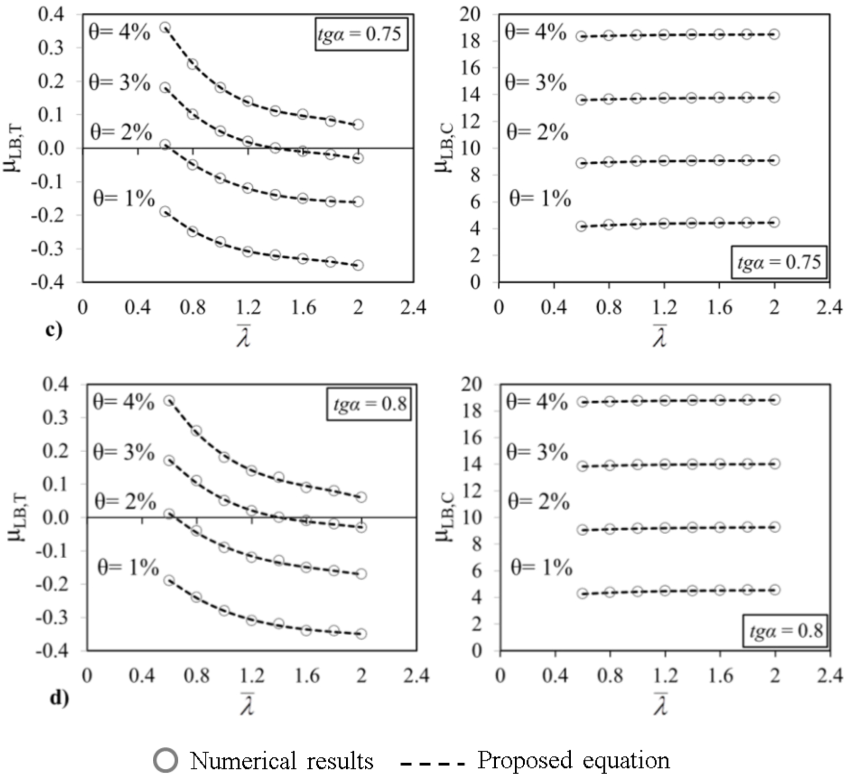

Figure 5.15 Brace ductility demand al lower bound in tension ($\mu_{LB,T}$) and compression ($\mu_{LB,C}$) vs. braces normalized slenderness $\bar{\lambda}$.

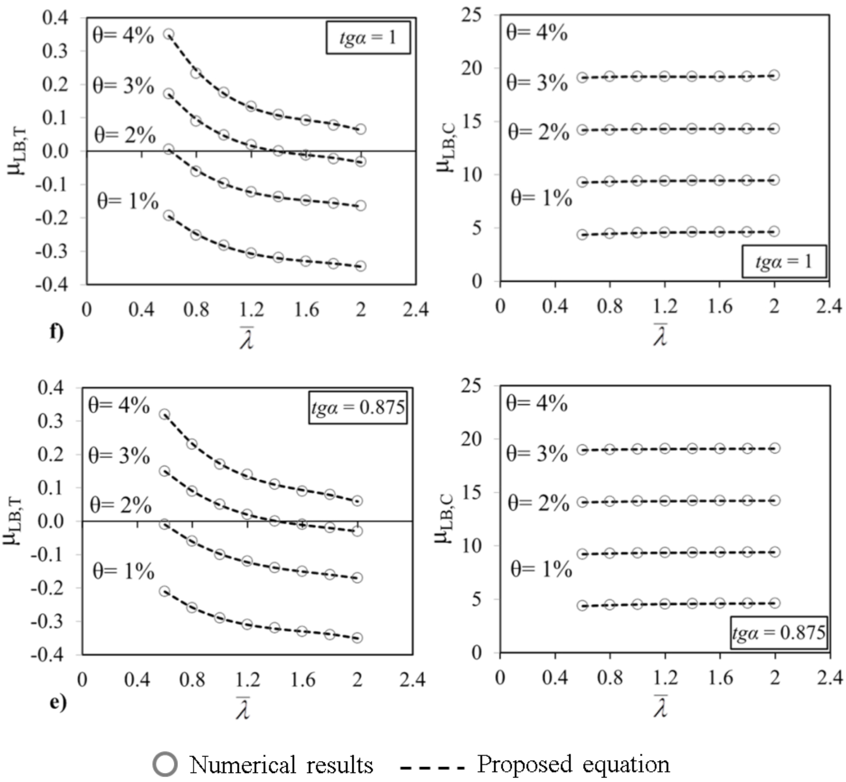

Figure 5.15 Brace ductility demand al lower bound in tension ($\mu_{LB,T}$) and compression ($\mu_{LB,C}$) vs. braces normalized slenderness $\bar{\lambda}$.

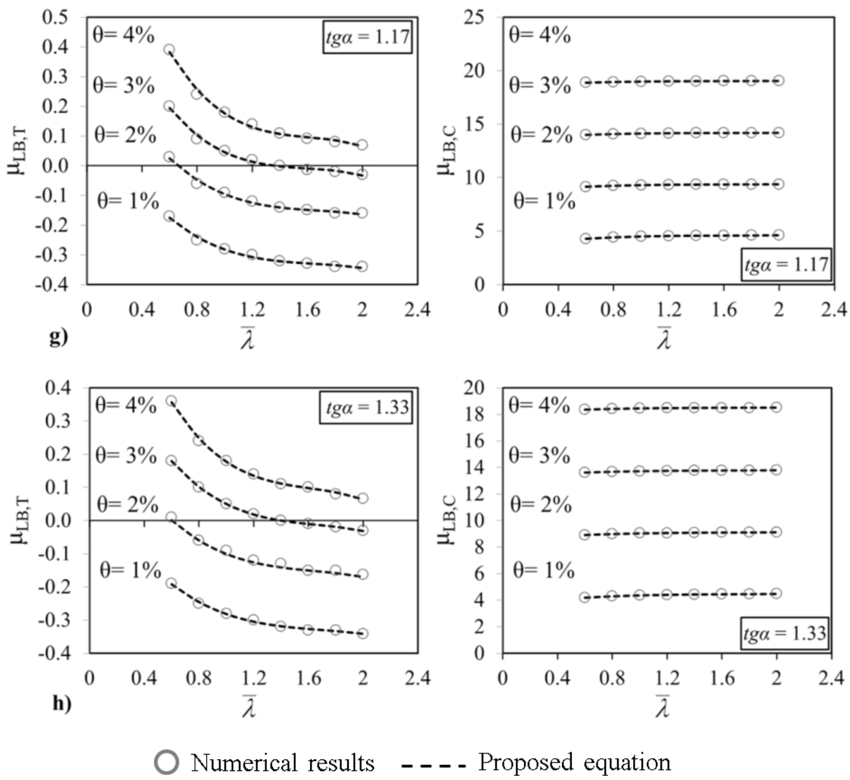

Figure 5.15 Brace ductility demand al lower bound in tension ($\mu_{LB,T}$) and compression ($\mu_{LB,C}$) vs. braces normalized slenderness $\bar{\lambda}$.

Table 5.7 Values of the coefficients and R^2 indexes for Eq. (5.13).

$\mu_{LB}(\bar{\lambda})$											
Demand in tension $\mu_{LB,T}(\bar{\lambda})$						**Demand in compression $\mu_{LB}(\bar{\lambda})$**					
***tgα* = 0.6**						***tgα* = 0.6**					
θ	**l_3**	**l_2**	**l_1**	**l_0**	**R^2**	**θ**	**l_3**	**l_2**	**l_1**	**l_0**	**R^2**
0.01	-0.01	0.19	-0.62	0.66	0.97	0.01	-0.14	0.41	-0.13	3.77	0.90
0.02	0.05	-0.13	-0.12	0.28	0.93	0.02	-0.05	0.12	0.12	8.05	0.93
0.03	0.06	-0.16	-0.04	0.07	0.96	0.03	-0.06	0.16	0.04	12.44	0.96
0.04	0.03	-0.06	-0.15	-0.09	0.95	0.04	-0.04	0.10	0.10	16.80	0.97
***tgα* = 0.7**						***tgα* = 0.7**					
θ	**l_3**	**l_2**	**l_1**	**l_0**	**R^2**	**θ**	**l_3**	**l_2**	**l_1**	**l_0**	**R^2**
0.01	-0.17	0.89	-1.57	1.04	0.99	0.01	0.21	-1.02	1.74	3.34	0.99
0.02	-0.16	0.78	-1.32	0.75	1.00	0.02	0.16	-0.78	1.32	8.15	1.00
0.03	-0.09	0.47	-0.90	0.42	0.99	0.03	0.09	-0.47	0.90	12.92	0.99
0.04	-0.08	0.43	-0.79	0.16	0.99	0.04	0.10	-0.49	0.87	17.59	0.99
***tgα* = 0.75**						***tgα* = 0.75**					
θ	**l_3**	**l_2**	**l_1**	**l_0**	**R^2**	**θ**	**l_3**	**l_2**	**l_1**	**l_0**	**R^2**
0.01	-0.17	0.84	-1.46	0.97	1.00	0.01	0.17	-0.84	1.46	3.55	1.00
0.02	-0.12	0.62	-1.07	0.62	1.00	0.02	0.12	-0.62	1.07	8.44	1.00
0.03	-0.05	0.31	-0.65	0.30	1.00	0.03	0.06	-0.34	0.67	13.31	1.00
0.04	-0.09	0.45	-0.77	0.13	1.00	0.04	0.09	-0.45	0.77	18.02	1.00
***tgα* = 0.8**						***tgα* = 0.8**					
θ	**l_3**	**l_2**	**l_1**	**l_0**	**R^2**	**θ**	**l_3**	**l_2**	**l_1**	**l_0**	**R^2**
0.01	-0.14	0.71	-1.27	0.89	1.00	0.01	0.12	-0.63	1.19	3.76	1.00
0.02	-0.09	0.46	-0.86	0.54	1.00	0.02	0.07	-0.39	0.78	8.72	1.00
0.03	-0.07	0.36	-0.69	0.31	1.00	0.03	0.09	-0.48	0.84	13.49	1.00
0.04	-0.05	0.31	-0.61	0.08	1.00	0.04	0.07	-0.34	0.64	18.39	1.00

Table 5.7 Values of the coefficients and R^2 indexes for Eq. (5.13).

$\mu_{LB}(\bar{\lambda})$											
Demand in tension $\mu_{LB,T}(\bar{\lambda})$						**Demand in compression $\mu_{LB}(\bar{\lambda})$**					
***tgα* = 0.6**						***tgα* = 0.6**					
θ	l_3	l_2	l_1	l_0	R^2	θ	l_3	l_2	l_1	l_0	R^2
0.01	-0.13	0.66	-1.16	0.80	1.00	0.01	0.14	-0.70	1.22	3.86	1.00
0.02	-0.07	0.39	-0.73	0.46	1.00	0.02	0.09	-0.45	0.80	8.90	1.00
0.03	-0.07	0.34	-0.64	0.26	1.00	0.03	0.08	-0.40	0.71	13.79	1.00
0.04	-0.09	0.41	-0.68	0.07	1.00	0.04	0.09	-0.41	0.68	18.69	1.00
***tgα* = 1**						***tgα* = 1**					
θ	**l_3**	**l_2**	**l_1**	**l_0**	**R^2**	**θ**	**l_3**	**l_2**	**l_1**	**l_0**	**R^2**
0.01	-0.18	0.86	-1.47	0.96	1.00	0.01	0.16	-0.83	1.43	3.77	1.00
0.02	-0.12	0.60	-1.03	0.60	1.00	0.02	0.12	-0.58	1.00	8.86	1.00
0.03	-0.09	0.47	-0.82	0.35	1.00	0.03	0.06	-0.37	0.68	13.90	0.84
0.04	-0.08	0.41	-0.71	0.10	1.00	0.04	0.44	-1.72	2.16	18.33	0.96
***tgα* = 1.17**						***tgα* = 1.17**					
θ	**l_3**	**l_2**	**l_1**	**l_0**	**R^2**	**θ**	**l_3**	**l_2**	**l_1**	**l_0**	**R^2**
0.01	-0.23	1.12	-1.85	1.14	0.99	0.01	0.26	-1.24	2.01	3.47	0.99
0.02	-0.18	0.85	-1.38	0.76	0.99	0.02	0.15	-0.76	1.27	8.63	0.99
0.03	-0.12	0.58	-1.00	0.44	0.99	0.03	0.14	-0.67	1.11	13.55	0.99
0.04	-0.11	0.53	-0.90	0.20	0.99	0.04	0.13	-0.60	0.98	18.48	1.00
***tgα* = 1.33**						***tgα* = 1.33**					
θ	**l_3**	**l_2**	**l_1**	**l_0**	**R^2**	**θ**	**l_3**	**l_2**	**l_1**	**l_0**	**R^2**
0.01	-0.19	0.92	-1.55	1.00	1.00	0.01	0.18	-0.86	1.46	3.59	1.00
0.02	-0.12	0.62	-1.07	0.63	1.00	0.02	0.12	-0.58	1.00	8.49	1.00
0.03	-0.10	0.48	-0.84	0.35	0.99	0.03	0.10	-0.50	0.85	13.27	1.00
0.04	-0.08	0.40	-0.71	0.11	1.00	0.04	0.08	-0.41	0.72	18.06	1.00

From the observation of the numerical data reported from Fig. 5.10 to 5.15 it can be recognized a relationship between ductility demands in tension and compression. Therefore, the correlation ratio $\omega = \frac{\mu_T}{\mu_C}$ is provided as follows:

$$\omega(K_F, \theta) = \frac{(a_2 \cdot \theta^2 + a_1 \cdot \theta + a_0) \cdot K_F + (b_2 \cdot \theta^2 + b_1 \cdot \theta + b_0)}{(c_2 \cdot \theta^2 + c_1 \cdot \theta + c_0) \cdot K_F + (d_2 \cdot \theta^2 + d_1 \cdot \theta + d_0)} \tag{5.14}$$

The values of the coefficients in Eq. (5.14) are given in Table 5.8, while the values of R^2 are reported Table 5.9. The correlation ratio ω given against the stiffness ratio K_F is depicted in Fig. 5.16

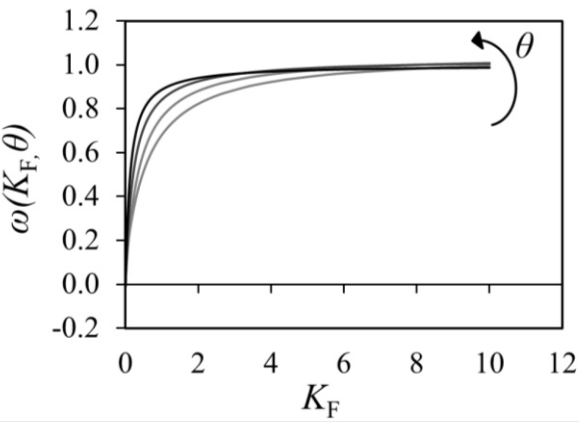

Figure 5.16 Correlation ratio ω between the brace ductility demand in tension and compression vs K_F.

Table 5.8 Values of the coefficients for Eq. (5.14).

$\omega(K_F,\theta)$							
a_2	-1250.00	b_2	5245.000	c_2	-500.000	d_2	2500.00
a_1	127.500	b_1	-165.970	c_1	107.000	d_1	-275
a_0	8.875	b_0	1.740	c_0	8.500	d_0	8.5

Table 5.9 R^2 values for Eq. (5.14).

$\omega(K_F,\theta)$	
θ	R^2
1%	0.989
2%	0.982
3%	0.965
4%	0.930

5.5.2 *Unbalanced force acting on the beam*

The normalized unbalanced force β (previously defined in Section 5.2.2) obtained from numerical analyses is plotted against K_F in Fig. 5.17. The regression function of the percentiles at 0.16, 0.5 and 0.84 has been obtained and given by the following:

$$\beta(K_F,\theta) = \frac{a \cdot K_F}{(c_2 \cdot \theta^2 + c_1 \cdot \theta + c_0) \cdot K_F + (d_3 \cdot \theta^3 + d_2 \cdot \theta^2 + d_1 \cdot \theta + d_0)} \tag{5.15}$$

The values of coefficients in Eq. (5.15) are reported in Table 5.10 for each percentile, while the relevant values of R^2 are given in Table 5.11.

It should be observed that the case of $\beta = 0.7$ corresponds to the unbalance force given by the capacity design rule recommended by EN1998-1 for symmetric CCB configuration. Figure 5.17 clearly highlights that in most of cases (those having $\beta > 0.7$) the EC8 requirement is not conservative.

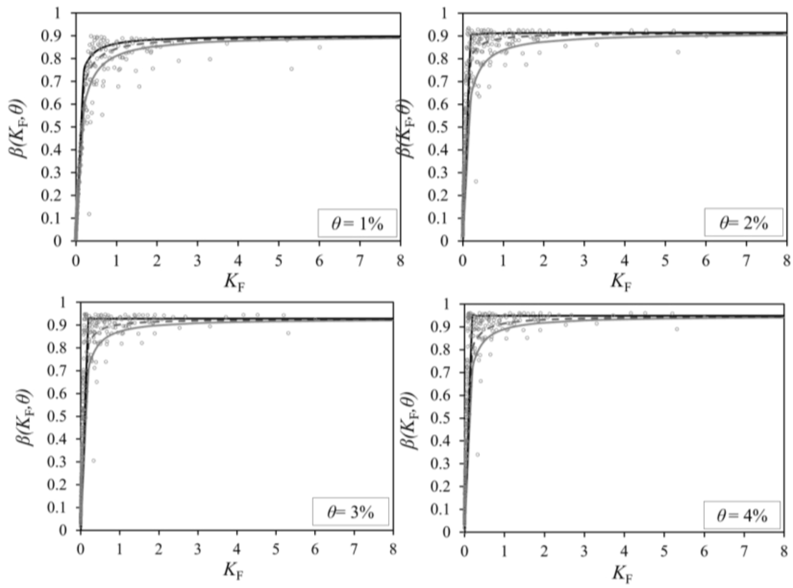

Figure 5.17 Unbalanced force β vs. K_F.

Table 5.10 Values of the coefficients for Eq. (5.15).

$\beta(K_F,\theta)$								
Percentile	**a**	**c_2**	**c_1**	**c_0**	**d_3**	**d_2**	**d_1**	**d_0**
0.16	650	-12500	-525	726.25	4166666.667	-275000	3833.333	65
0.5		-12500	-525	726.25	-4166666.670	400000	-12083.330	135
0.84		-12500	-525	726.25	-4033333.330	372500	-11151.667	108.3

Table 5.11 R^2 values for Eq. (5.15).

$\beta(K_F,\theta)$				
Percentile	**θ=1%**	**θ=2%**	**θ=3%**	**θ=4%**
0.16	0.934	0.957	0.957	0.973
0.5	0.967	0.988	0.988	0.991
0.84	0.978	0.998	0.998	0.998

5.6 DESIGN CRITERIA AND PROCEDURE FOR CCB$_S$.

5.6.1 *Proposed design criteria and procedure*

In literature, several sophisticated and refined design procedures have been developed aiming at control collapse mechanism by means of the application of the theory of limit plastic analysis (Mazzolani and Piluso, 1997; Longo *et al., 2008;* Giugliano *et al., 2010;* Giugliano *et al.*, 2011; Marino, 2014).

On the other hand, displacement based methodologies (which allows accounting for the displacement shape of the expected mechanism directly in the design process and obtaining the required base shear strength to meet the selected seismic performance objective) have been widely studied to achieve the same purpose (Priestley and Calvi, 1997; Della Corte *et al.*, 2010; Maley *et al.*, 2010)

In this Section, a design method is proposed aimed at enhancing the seismic performance of CCBs by controlling the beam-to-brace stiffness ratio and the ductility demand in the diagonal members, following the philosophy of EC8 (see Chapter III). In particular, the intent is to assign the appropriate K_F for the selected brace ductility. In general, this approach may drive the designer to select stiffer (namely deeper) beams than those usually obtained by EC8 procedure, thus leading to potentially huge and anti-economic girders. In order to limit the size of the beams, it is proposed to relax the design requirements for bracings under compression by verifying that the bracings resist solely the forces induced by gravity loads, disregarding the verification of the compression diagonals under seismic condition but keeping the limit on slenderness given by EN1998-1. Namely, under seismic loading the bracings under compression are assumed buckled with capacity depending on the expected ductility. This assumption requires controlling the displacement profiles in order to distribute the base shear along the building height coherently to the expected plastic mechanism, because it is well known that the earthquake-equivalent static forces are reasonably proportional to the displacement shape.

At design stage, the structural members are unknown. Hence, using both the lateral force and response spectrum method to calculate internal force needs, several iterations are necessary with a weak control of the final CCB response. Conversely, in this study it is proposed to apply a trial displacement shape to derive the horizontal forces to be internally distributed in a consistent way with the assumed displacement profiles. Since, the displacement shape of a structure is not known a priori, likewise the ratios of gravity to seismic axial forces in members are not known, some approximations have been introduced involving the design values for deformations (e.g. the column shortening, the brace lengthening, etc.). As shown in Fig. 5.18, the lateral displacement shape in terms of interstorey drift ratios (θ) of the braced cantilever can be decomposed in the sum of three terms (Della Corte *et al.*, 2010) i) the contribution of the diagonal braces (θ_{br}), ii) the contribution of the beam deflection (θ_b) and iii) the contribution of columns (θ_{col}). The first two contributions are strictly correlated as discussed in the previous Sections. It must be noted that only these contributions to the story drift angle (i.e. the θ_{br+b}) produce structural damage (brace buckling and yielding), while θ_{col} can produce damage to claddings and secondary elements. In any case, all terms must be considered to estimate the total displacement distributions, even though it can be argued that θ_{col} is generally smaller than θ_{br+b}.

Regarding the contribution due to braces and beams, once fixed the target performance value for θ_{br+b} and either K_F or μ_T the damage distribution is univocally determined using Eqs. (5.12) or (5.8), respectively.

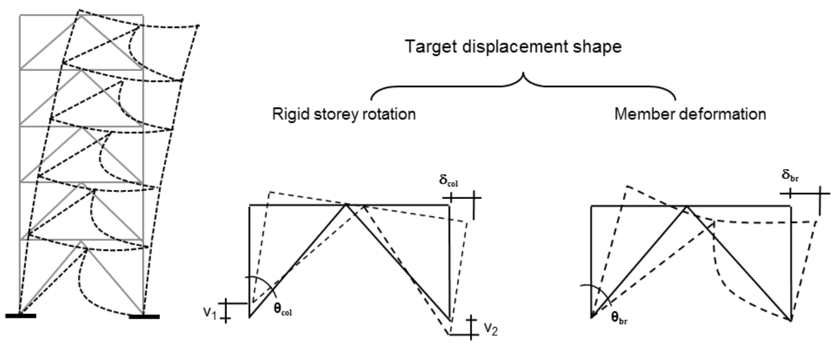

Figure 5.18 Target displacement shape.

Assuming pinned beams, a uniform distribution of brace in tension and column strains at each storey and neglecting the flexural deformation due to the continuity of the column along the building height, the generic lateral displacement at the i-th storey is given as follows:

$$\delta_i = \theta_i \cdot h_i + \sum_{1}^{i-1} \left(\theta_j \cdot h_j \right) \tag{5.16}$$

Where:

$$\theta_i = \frac{\Delta u_i}{h_i} = \theta_{\mathrm{col,i}} + \theta_{\mathrm{br+b,i}} = \left(\frac{v_{2,i} - v_{1,i}}{L} + \frac{2(\mu_{T,i} \cdot \varepsilon_{\mathrm{y,i}} + v_{b,i} \cdot sen\alpha_i)}{sen 2\alpha_i} \right) \tag{5.17}$$

$$v_{1,i} = \sum_j \left(\varepsilon_{\mathrm{c1,j}} \cdot h_{\mathrm{j}} \right) = \sum_j \left(\rho \cdot \chi \cdot \varepsilon_{\mathrm{y,j}} \cdot h_{\mathrm{j}} \right) \tag{5.18}$$

$$v_{2,i} = \sum_j \left(\varepsilon_{\mathrm{c2,j}} \cdot h_{\mathrm{j}} \right) = \sum_j \left(\chi_j \cdot \varepsilon_{\mathrm{y,j}} \cdot h_{\mathrm{j}} \right) \tag{5.19}$$

The term $v_{\mathrm{b,i}}$ is the vertical displacement at the mid-span of brace-intercepted beam. In the proposed procedure it is not necessary to specify both the target beam deflection $v_{\mathrm{b,i}}$ and the tension brace ductility $\mu_{\mathrm{T,i}}$, because the structural performance is ruled by $\theta_{\mathrm{br+b}}$ that directly accounts for both parameters.

The terms $v_{1,\mathrm{i}}$ and $v_{2,\mathrm{i}}$ correspond to the vertical deformations of the columns of the braced span. The former is related to the columns subjected to both gravity loads and the forces of the braces in tension, while the second to the columns subjected to both gravity loads and the forces of the braces in compression. Therefore, in Eq. (5.18) it was introduced a coefficient $\rho < 1$ to reduce the column compression strain. For residential medium rise frames reasonable trial values for ρ and χ could be assumed equal to 0.4 and 0.7, respectively.

The main phases of the proposed design procedure are described hereinafter by subdivision into steps:

Step 1: Performance objectives. Consistently with EN1998-1, this procedure considers the two limit states, namely the Damage Limitation (DL) and the Ultimate Limit or Significant Damage (SD) limit states corresponding to return periods of 95 and 475 years, respectively. In particular, the structure is first designed for SD limit state and then verified to satisfy the requirements at DL limit state. At the global level, the performance is fixed in terms of interstorey drift ratios θ_{br+b} for the considered earthquake intensities. At the local level the performance is fixed in terms of brace ductility in tension. It is worth noting that the performance objectives can be fixed *ad hoc* by the designers, which has to judiciously select the most appropriate for the behaviour to obtain. In the case study described in the next Section (namely Section 5.7), it was used $\theta_{br+b,DL} = 0.5\%$, $\theta_{br+b,SD} = 1\%$ as global performance target, while $\mu_{T,DL} < 1$ and $\mu_{T,SD} = 1.5$, as local performance target.

Step 2: Design values of key structural parameters. The steel yield strength and the value of K_F are fixed in this step. The first parameter can be arbitrarily selected by the designer. The second is obtained from Eq. (5.12) once fixed $\mu_{T,SD}$ and $\theta_{br+b,SD}$.

Step 3: Displacement shape at performance target (SD limit state). Once fixed $\mu_{T,SD}$ and $\theta_{br+b,SD}$ the displacement profile is obtained by Eq. (5.16).

Step 4: Calculation of seismic forces. The earthquake-equivalent static forces are approximated by the Equation:

$$F_i = \frac{m_i \delta_i}{\sum_1^n m_i \delta_i} = \frac{m_i (\delta_i / \delta_r)}{\sum_1^n m_i (\delta_i / \delta_r)} V_b = \frac{m_i \phi_i}{\sum_1^n m_i \phi_i} V_b \tag{5.20}$$

Where the storey displacements δ_i have been normalized ($\phi_i = \delta_i/\delta_r$) using a reference value δ_r, (usually, the roof displacement in case of buildings) and V_b is the base shear force calculated according to EC8.

Step 5: Calculation and verification of braces. The horizontal forces given by Eq. (5.20) are calculated having assumed that the diagonal under compression is buckled. Therefore, the tension brace is verified to resist the following design force:

$$N_{T,Ed,i} = \frac{V_i}{(2-\beta)\cos\alpha} \tag{5.21}$$

Where $N_{T,Ed,i}$ is the axial force in the tension brace at the i-th storey; V_i is the seismic shear acting at the i-th storey; α is the tilt angle of the brace respect to the horizontal direction; β is the parameter defined in Section 5.2.2 and calculated as $\beta(K_F, \theta_{br+b,SD})$ according to Eq. (5.4).

The brace cross sections are also designed in order to guarantee that the overstrength ratios $\Omega_i = N_{pl,br,Rd,i}/N_{T,Ed,i}$ respect the requirements of EC8. In addition, the limitation of brace slenderness (i.e. $\bar{\lambda} \leq 2.0$) should be verified. At this stage it is possible to calculate the bracing axial stiffness k_{br} (see Eq. (5.3)).

Step 6: Calculation and verification of columns. The columns belonging to the bracing system are designed to resist the following force:

$$N_{c,Ed,i} = N_{Ed,G} + \sum_{1}^{i} \frac{\beta \cdot N_{pl,br,Rd,i} \cdot \sin\alpha}{2} \tag{5.22}$$

Where $N_{c,Ed,i}$ is the axial force in the column at the i-th storey; $N_{Ed,G}$ is the contribution in the column at the i-th storey due to gravity loads in seismic loading combination; α is the tilt angle of the brace respect to the horizontal direction; β is the parameter defined in Section 5.2.2 and calculated as $\beta(K_F, \theta_{br+b,SD})$ according to Eq. (5.4). $N_{PL,br,Rd,i}$ is the plastic strength of the diagonal members at the i-th storey.

The columns behave as deformable supports for the beams of the braced span. The axial stiffness of the columns can be evaluated according to Eq. (5.6)

Step 7: Design and verification of the beams. Being known at the i-th storey both $K_{F,i}$ and $k_{br,i}$ and $k_{col,ji}$, the stiffness $k^*_{b,i}$ of the beam accounting for the deformability of columns is univocally obtained as $k^*_{b,i} = K_{F,i} / k_{br,i}$. Therefore, the unknown optimal beam flexural stiffness $k_{b,i}$ can be derived from Eq. (5.5).

Once calculated $k_{b,i}$, it is possible to select the beam on the basis of the second moment of area from Eq. (5.2) and then it is necessary to verify the beam strength against the following design actions:

$$N_{b,Ed,i} = \frac{(2-\beta)\cdot N_{pl,br,Rd,i}\cdot\cos\alpha}{2} \tag{5.23}$$

$$M_{b,Ed,i} = \frac{\beta\cdot N_{pl,br,Rd,i}\cdot\sin\alpha\cdot L_b}{4} \tag{5.24}$$

Where $N_{b,Ed,i}$ is the axial force in the beam at the i-th storey; $M_{b,Ed,i}$ is the bending moment in the beam at the i-th storey; α is the tilt angle of the brace respect to the horizontal direction; β is the parameter defined in Section 5.2.2 and calculated as $\beta(K_F, \theta_{br+b,SD})$ according to Eq. (5.4); $N_{PL,br,Rd,i}$ is the plastic strength of the diagonal members at the i-th storey; L_b is the beam length.

Step 8: Verification at DL. The displacements calculated according to EN1998-1 should verify both the requirements to limit non-structural damages and the condition $\theta_{DL} \leq \theta_y$ in order to avoid the yielding of braces, where θ_y is calculated according to Eq. (5.7)

5.7 APPLICATION TO A CASE STUDY

In order to verify the effectiveness of design criteria described in Section 5.6, the seismic performance of a multi-storey CCB frame, alternatively designed according to both EN 1998-1 and the proposed procedure, was analysed. In particular, both monotonic and dynamic time-history analyses were performed and the results are described and discussed hereinafter.

5.7.1 *Description and modelling assumptions*

The case study is a six-storey residential building equipped with CCBs. The interstorey height is equal to 3.50 *m* with exception of the first floor, which is 4.00 *m* high. The structural layout of the typical floor (rectangular shape plan 31 *m* x 24 *m*), illustrating the location of braces (indicated by the bold lines), and the CCB vertical configuration examined in this study are shown in Fig. 5.19.

At each floor, the rigid diaphragm transmitting the horizontal actions is made of composite slabs with profiled steel sheetings supported by the hot rolled "I-shaped" beams; the composite action is obtained for all beams by applying shear connectors between the slab and the beams.

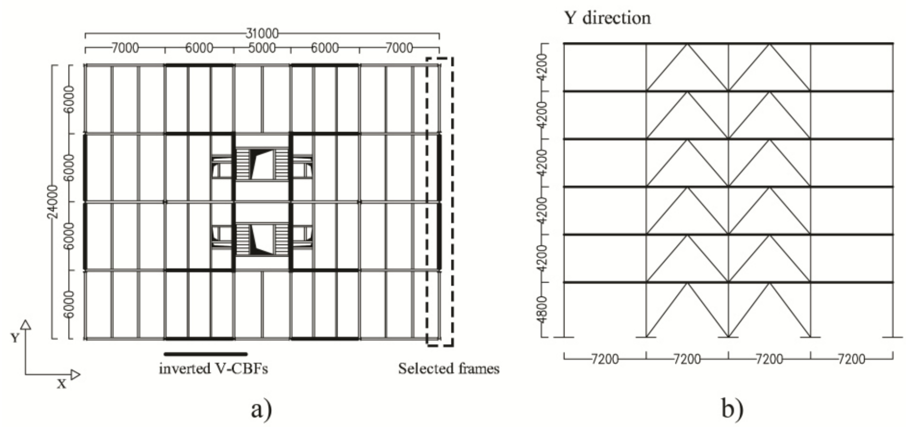

Figure 5.19 Structural layout of case study building: (a) plan and (b) vertical view.

Circular hollow cold formed sections were used for the diagonals members. All steel members (i.e. beams, bracings and columns) have cross section satisfying the Class 1 requirements according to EN 1993:1-1. In particular, for the EC8-compliant frame the dual steel concept (Dubina *et al.*, 2006; Dubina *et al.*, 2010; Vulcu *et al.*, 2014; Tenchini *et al.*, 2014) was used in order to reproduce an even more common design practice consisting in minimizing the beam depth to limit architectural interference.

Therefore, S 235 steel grade was used for the dissipative elements (i.e. diagonal members), S 460 steel grade for beams of the braced bays and S 355 steel grade for columns. On the contrary, S 355 steel grade was used for all members in the case designed with the proposed procedure.

The concept "DCH" (Ductility Class High) according to EN1998-1 was followed for both the code-compliant frame and the structure designed using the proposed procedure. A reference peak ground acceleration equal to a_{gR} = 0.25g, a soil type C, a type 1 spectral shape and a behaviour factor q = 2.5 were assumed.

Besides the seismic recommendations, the structural safety verifications are carried out according to the following European codes:

- EN 1990 (2001) Eurocode 0: Basis of structural design;
- EN 1991-1-1 (2002) Eurocode 1: Actions on structures - Part 1-1: General actions -Densities, self-weight, imposed loads for buildings;
- EN 1993-1-1 (2003) Eurocode 3: Design of steel structures - Part 1-1: General rules and rules for buildings;
- EN 1994-1-1 (2004) Eurocode 4: Design of composite steel and concrete structures - Part 1.1: General rules and rules for buildings.

The members resulting from both EC8 and proposed design procedures are reported in Table 5.12.

As it can be noted, the proposed criteria leads to heavier profiles for beams and columns than EC8; on the contrary the bracing members are more slender (i.e. $\bar{\lambda} \in [1.8 - 2.0]$) than those for EC8 (i.e. $\bar{\lambda} \in [0.5 - 1.3]$). Thus, this result corresponds to a structure with stiffer beams having K_F ranging within 0.49-0.70, while 0.10-0.15 for the EC8-compliant case. The numerical behaviour of the designed frames was simulated using a 2D planar model. The calculation models assume all pinned connections (brace-to-beam, brace–to-column and beam-to-column connections, column bases), but columns are considered continuous through each floor beam. The nonlinear behaviour of members was simulated as described in Section 5.2.3. Masses are considered as lumped into a selected master joint at each floor, because the floor diaphragms may be taken as rigid in their planes. The P–Δ effects were accounted for by assigning the gravity loads on the interior frames to fictitious column, connected to the main frame using pinned rigid links. In such a way, this column has no lateral stiffness but it carries all vertical loads from the gravity frames.

Concerning dynamic analyses a 2% Rayleigh tangent stiffness damping was used at both first and second modes

Table 5.12 Structural members of the designed frames.

	beam			column			bracings	
Storey	**Gravity load resisting**	**EC8**	**Proposed Criteria**	**Gravity load resisting**	**EC8**	**Proposed Criteria**	**EC8**	**Proposed Criteria**
6	IPE 330 (S355)	HEB260 (S460)	HEB 320 (S355)	HEA 180 (S355)	HEA180 (S355)	HEB 300 (S355)	127 x 6.3 (S235)	100 x 4 (S355)
5	IPE 330 (S355)	HEB 300 (S460)	HEB 450 (S355)	HEA 180 (S355)	HEA 180 (S355)	HEB 300 (S355)	193.7 x 8 (S235)	108 x 6 (S355)
4	IPE 330 (S355)	HEB 320 (S460)	HEB 500 (S355)	HEB220 (S355)	HEM 240 (S355)	HEB 340 (S355)	244.5 x 8 (S235)	113 x 8 (S355)
3	IPE 330 (S355)	HEB 360 (S460)	HEA 600 (S355)	HEB220 (S355)	HEM 240 (S355)	HEB 340 (S355)	244.5 x 10 (S235)	125 x 10 (S355)
2	IPE 330 (S355)	HEB 400 (S460)	HEB 600 (S355)	HEB260 (S355)	HEM 320 (S355)	HEB 450 (S355)	273 x 10 (S235)	125 x 10 (S355)
1	IPE 330 (S355)	HEB 450 (S460)	HEB 600 (S355)	HEB260 (S355)	HEM 320 (S355)	HEB 450 (S355)	323.9 x 10 (S235)	125 x 12 (S355)

5.7.2 *Results and comparison*

5.7.2.1 Pushover analyses

Static pushover analyses were performed according to EN 1998-1. Thereby, two different lateral force patterns were considered: the first proportional to the first vibration mode and the second proportional to the masses along frame height.

The monotonic response curves are plotted in Fig. 5.20, where it can be observed that the lateral strength of the two structures is substantially similar although the diagonal members in EC8-compliant case are stronger than those in the frame designed with the proposed criteria.

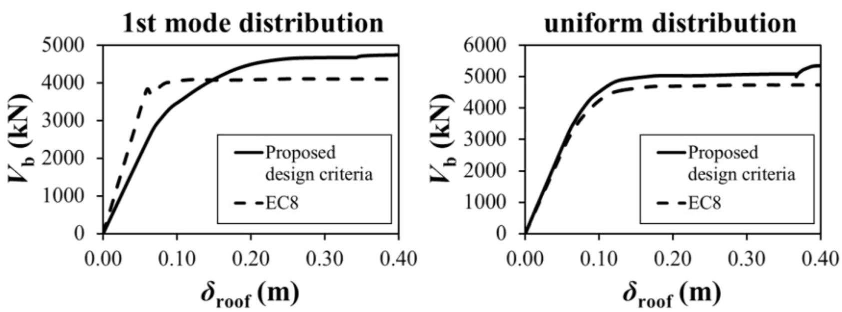

Figure 5.20 Comparison of pushover response curve: 1st mode and uniform load pattern distributions.

This result is mainly due to the fact that in the EC8-compliant frame, the lateral capacity is offered by both bracing members that work in compression being both buckled at larger roof displacement. On the contrary, in the case designed according to the novel procedure, the expected force transfer mechanism can develop in the bracings so that the one in tension can yield developing its full axial strength allowing also a more uniform distribution of damage along the building height.

In addition, both global (namely the displacements profile) and local (ductility demand on bracing members) response parameters were monitored at two displacement thresholds; the latter correspond to the attainment of the 0.01 and 0.02 values of the drift ratio θ, measured by dividing the roof displacement by the total height of the building from the top to the foundation.

Figures 5.21 show the displacement shapes of the examined cases in term of interstorey drift θ along the building height. Under the load distribution proportional to the shape of the first mode of vibration (see Fig. 5.21a), the frame designed according to the proposed procedure shows slightly large horizontal displacements , but a better response, characterized by more uniform distribution of drift demand along the building height. Indeed, different displacement shapes can be recognized, namely cantilever shape for EC8-compliant case (with soft-storey mechanism at the roof storey), and shear-type for the proposed criteria. No appreciable differences can be recognized under uniform load pattern (see Fig. 5.21b).

Consistently with the relevant displacement shapes, the ductility demand for braces shows different damage distribution (see Fig. 5.22).

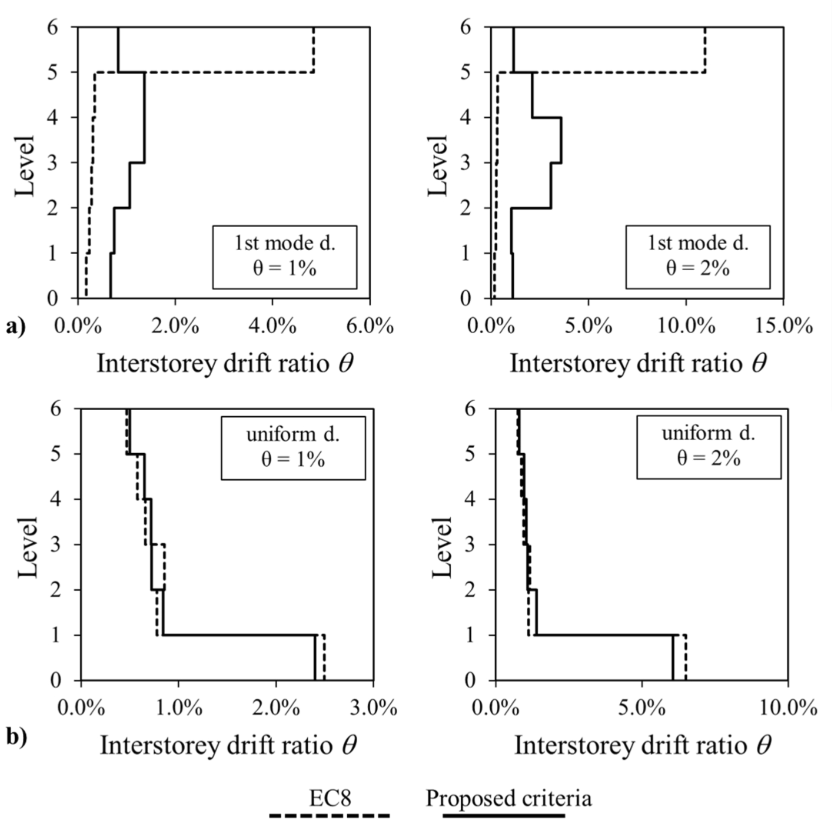

Figure 5.21 Results from monotonic analyses: interstorey drift ratios.

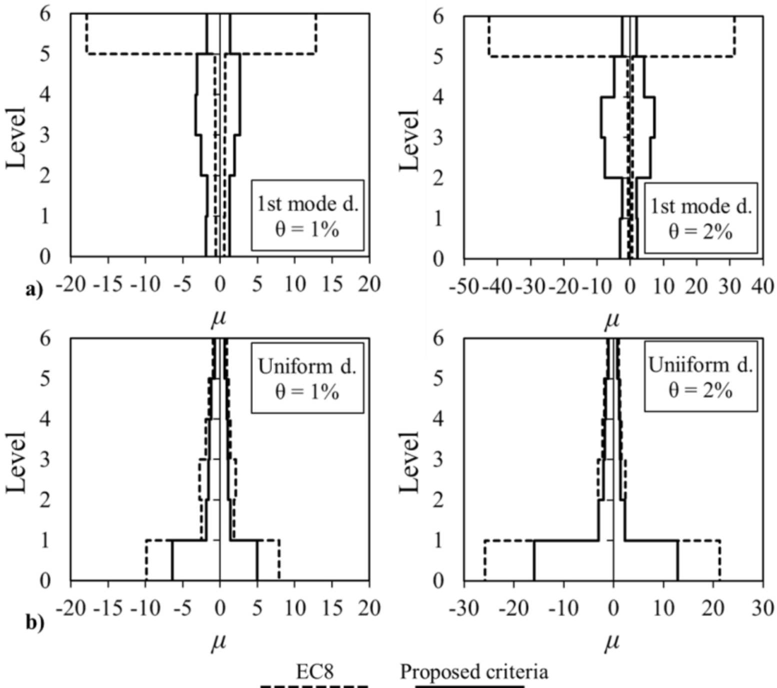

Figure 5.22 Results from monotonic analyses: braces ductility demand.

It should be noted that the structure designed according to the proposed design criteria exhibits larger plastic engagement in the braces under tension under 1^{st} mode-compliant load distribution (see Fig. 5.22a) and also experiences more uniform distribution of damage in compression along the building height. No significant differences can be recognized under uniform load pattern (see Fig. 5.22b).

5.7.3 *Dynamic time history analyses*

5.7.3.1 Seismic hazard levels

The seismic response obtained from time history analyses was evaluated for the three seismic hazard levels given by Eurocode 8, which are associated to different annual rates of exceedance: damage limitation (DL), severe damage (SD) and near collapse (NC).

In Eurocode 8, the seismic hazard is expressed in terms of the value of the reference peak ground acceleration a_{gR} on bedrock corresponding to the 10% probability of exceedance (i.e. a return period equal to 475years). To obtain the reference peak ground acceleration for different probabilities of exceedance in 50 years EC8 introduces an importance factor γ_I multiplying a_{gR} that is given as follows:

$$\gamma_I = \left(\frac{T_{LR}}{T_L} \right)^{-1/3} \tag{5.25}$$

being T_L the return period and T_{LR} the reference return period for which the reference seismic action may be computed.

According to Eurocode 8 the considered values of γ_I for DL SD and NC are 0.59, 1 and 1.73 respectively.

5.7.3.2 Records

A set of 14 natural earthquake acceleration records was considered to perform the dynamic time history analyses on the examined cases. The signals were obtained from the RESORCE ground motion database (Akkar *et al.*, 2014) and selected according to procedure described in (Fulop, 2010) in order to match the elastic acceleration spectrum provided for by EN 1998-1 corresponding to the seismic hazard level associated with the Severe Damage limit state (i.e. 10% probability of exceedance in 50 years). The data of the records are reported in Table 5.13, and the comparison between the natural signals and the design spectrum provided by EC8 is shown in Fig. 5.23 In addition, in order to calculate the residual inter-storey drift ratios from the dynamic time history analyses, each record was fictitiously extended by 10 seconds at zero acceleration.

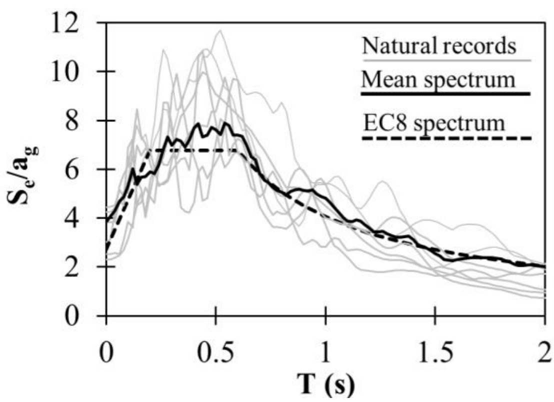

Figure 5.23 Comparison between natural signals and EC8 design spectrum.

Table 5.13 Basic data of the selected ground motions.

Earthquake name	Date	Station Name	Station Country	Magnitude Mw	Fault mechanism
Alkion	24.02.1981	Xylokastro-O.T.E.	Greece	6.6	Normal
Montenegro	24.05.1979	Bar-Skupstina Opstine	Montenegro	6.2	Reverse
Izmit	13.09.1999	Yarimca (Eri)	Turkey	5.8	Strike-Slip
Izmit	13.09.1999	Usgs Golden Station Kor	Turkey	5.8	Strike-Slip
Faial	09.07.1998	Horta	Portugal	6.1	Strike-Slip
L'Aquila	06.04.2009	L'Aquila - V. Aterno - Aquila Park In	Italy	6.3	Normal
Aigion	15.06.1995	Aigio-OTE	Greece	6.5	Normal
Alkion	24.02.1981	Korinthos-OTE Building	Greece	6.6	Normal
Umbria-Marche	26.09.1997	Castelnuovo-Assisi	Italy	6.0	Normal
Izmit	17.08.1999	Heybeliada-Senatoryum	Turkey	7.4	Strike-Slip
Izmit	17.08.1999	Istanbul-Zeytinburnu	Turkey	7.4	Strike-Slip
Ishakli	03.02.2002	Afyon-Bayindirlik ve Iskan	Turkey	5.8	Normal
Olfus	29.05.2008	Ljosafoss-Hydroelectric Power	Iceland	6.3	Strike-Slip
Olfus	29.05.2008	Selfoss-City Hall	Iceland	6.3	Strike-Slip

5.7.3.3 Seismic performance evaluation

The performance indicators monitored for all limit states are the following: i) peak transient interstorey drift ratios θ; ii) residual interstorey drift ratios θ_{RES}; iii) peak storey accelerations A; iv) braces ductility demand; v) beam flexural overstrength. The results are presented hereinafter.
Figure 5.24a depicts the average demand of θ along the building height for the three limit states. As a general remark, it can be observed that the structure designed according to the proposed criteria is characterized by a demand generally larger for all limit states but with a more uniform distribution. However, the performance is satisfactory being lower than the performance limits assumed at the design stage (see Section 5.6). The residual interstorey drift ratios θ_{RES} are shown in Fig. 5.24b, where no appreciably difference in terms of the amount of the residual out-of-verticality can be recognized, while a substantial difference in terms of distribution of damage is observed. The only additional minor difference can be recognized at DL limit state where the EC8-compliant frame shows slightly larger θ_{RES} because of the early damage in compression of both bracings at the top storey, which reduces the restoring capacity of the bracing system. Figure 5.25 shows the peak storey accelerations for both the examined cases: EC8-compliant frame is characterized by significant storey accelerations, whose peak average value (A) increases up to 3.5 times the peak record acceleration (A_d) at SD and 2 times at NC. On the contrary, the average peak storey accelerations are less than the half into the frame designed according to the proposed procedure, due to its larger dissipative capacity provided by the yielding of braces.

Figure 5.24 clearly shows that the two structures experience a (i) different displacement shape (i.e. cantilever shape the EC8-compliant frame and shear type the one designed with the proposed criteria) and (ii) different damage distribution. The latter is better clarified by observing Fig. 5.26, where the mean brace ductility demand is reported (being the positive μ-axis corresponding to the tension and the negative μ-axis to the compression).

It is worth noting that the proposed criteria allow obtaining a better plastic engagement of the brace in tension and avoiding the damage concentration in the brace under compression that occurs for EC8-compliant frame at SD and NC limit states. EC8-compliant frame is characterized by smaller drift demand except for the roof. This performance depends on the code requirements. Indeed, as previously discussed, the limit on the brace slenderness (namely $\bar{\lambda} \leq 2$) and the requirement on the variability of design overstrength ratios Ω_i lead to stocky bracing members characterized by large overstrength except for the top storey. A possible improvement of the code might be neglecting the control on overstrength Ω_i for braces at the top storey, as discussed by Landolfo (2013). However, this strategy is not able to guarantee the yielding in tension of braces. Indeed, if the bracing members are designed to avoid buckling under the design seismic forces without any requirement for the minimum stiffness of brace-intercepted beam, the designed structures might be characterized by stocky braces and flexible beams (e.g. using high strength steel for beams) in several cases.

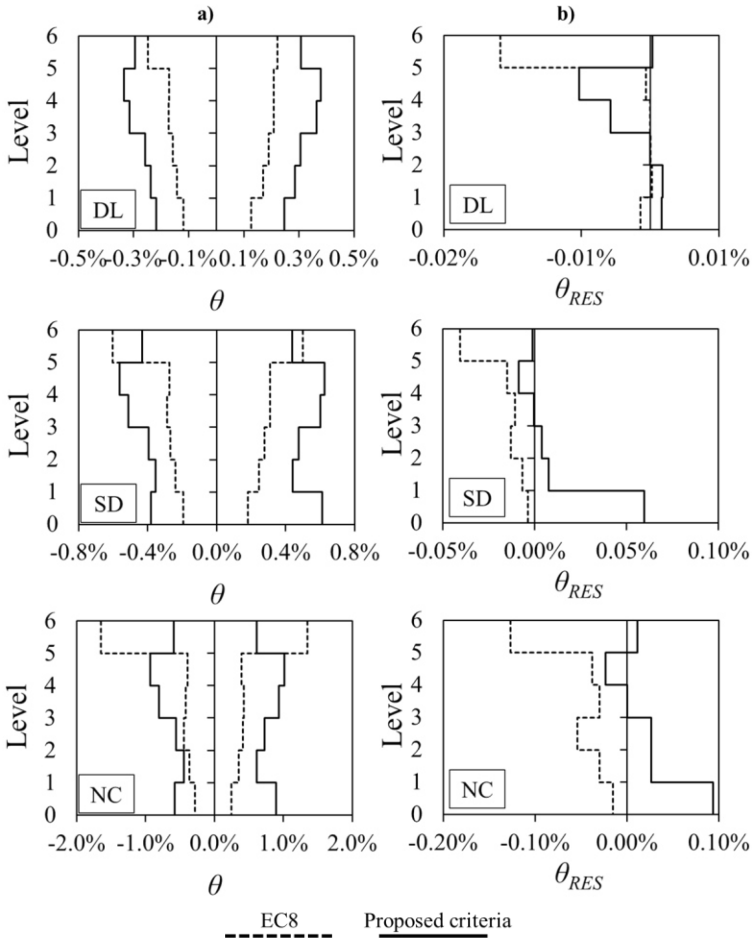

Figure 5.24 EC8 vs. proposed design criteria: transient (a) and residual (b) interstorey drift ratios.

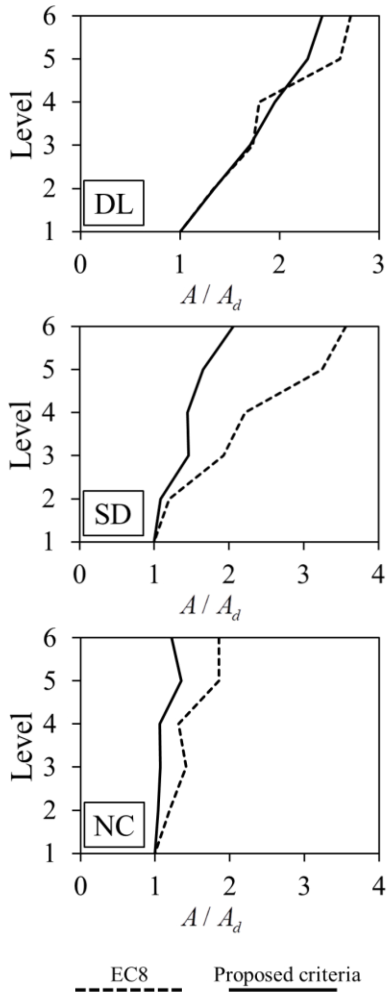

Figure 5.25 EC8 vs. proposed design criteria: peak storey accelerations.

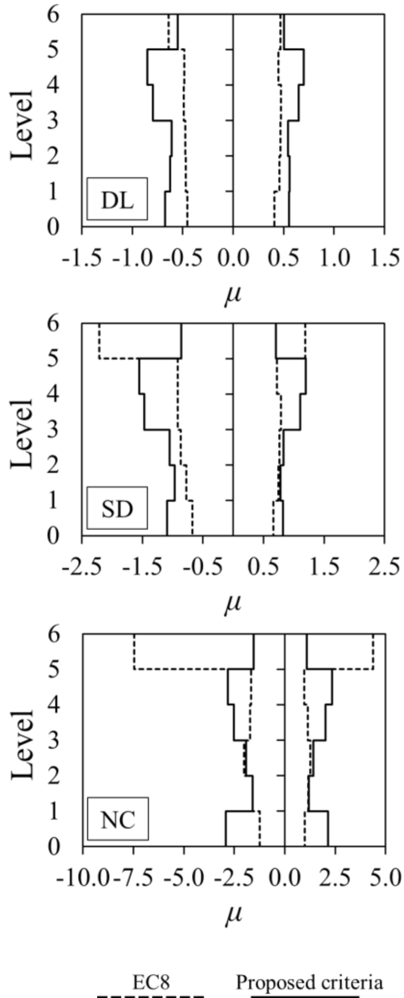

Figure 5.26 EC8 vs. proposed design criteria: braces ductility demand.

The structure designed according to the proposed procedure is more flexible than that compliant with EC8, as shown in Fig. 5.24. Nevertheless, the proposed procedure guarantees an adequate lateral stiffness, being the values of the interstorey drift ratios less than 1% up to NC limit state. In addition, the increased displacement demand plays a key role in improving the overall performance, because it allows the yielding of the braces in tension. Indeed, the axial deformation of the braces strictly depends on the horizontal storey displacement threshold achieved. With this regard Eq. (5.10) clearly highlights that at the interstorey drift ratios experienced by the EC8-compliant frame, the braces cannot yield in tension also in case of beam with infinitive flexural stiffness. As shown in Fig. 5.25, the brace yielding allows also reducing the storey accelerations, which is beneficial to minimize the no-structural damage.

It is also interesting to observe that although the proposed criteria disregard the verification of the brace under the compression forces due to seismic actions, the performance at DL limit state is satisfactory. Indeed, the interstorey drift ratio θ is smaller than the limit θ_{DL} = 0.5% and μ_T is smaller than 1 (namely the brace in tension is in the elastic range). Regarding the brace under compression, although for DL the buckling occurs at all storeys, the analyses showed that the average brace out-of-plane displacements "*w*" (calculated as described in Tremblay, 2002 and Goggins *et al.* 2006) do not compromise the functionality of common cladding walls (e.g. sandwich panels connected to the primary steel members of the structure by means of secondary light weight cold formed frames, as illustrated in Fig. 5.27a).

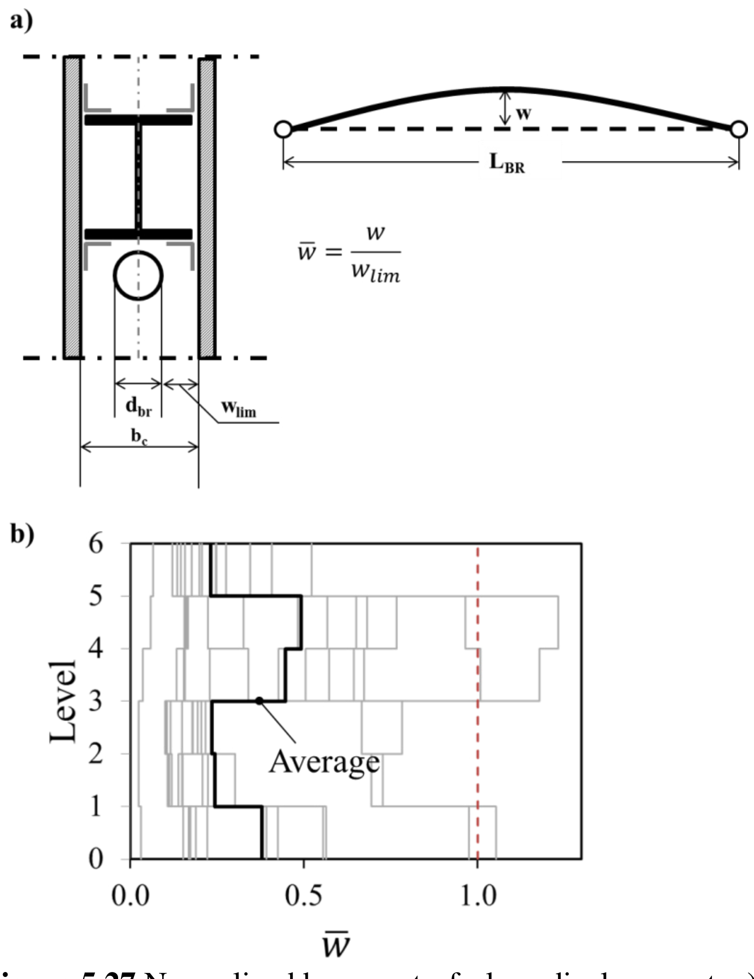

Figure 5.27 Normalized brace out-of-plane displacement: a) definition and b) average demand at DL limit state for the frame designed according to the proposed design criteria.

In Fig. 5.27b the average demand of the normalized brace out-of-plane displacements $\bar{w}$ (see the definition given in Fig. 5.27a) is reported and it can be noted than it is fairly below the limit (i.e. $w_{LIM} = 0.5 \cdot (b_c - d_{br})$, being b_c the width of the column flange and d_{br} the external diameter of the bracing member), thus preserving the cladding from the damage due to the trust forces generated by the contact between buckled brace and cladding wall.

Finally, Figure 5.28 shows the bending moment demand (*M*) normalized with the bending strength accounting for the axial interaction (M_{RD}) in the beams of the braced spans at SD and NC limit states. As it can be easily recognized, the EC8-compliant frame exhibits the formation of plastic hinge, while this detrimental response does not occur in the frame designed according to the proposed criteria.

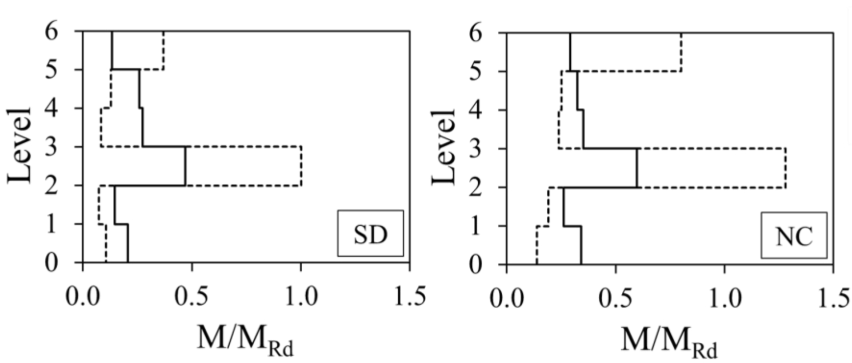

Figure 5.28 Normalized bending moment demand in the beams of the braced spans.

5.8 CONCLUSIVE REMARKS

In this chapter the influence of beam flexural stiffness on the seismic response of steel chevron concentrically braced frames has been investigated on the basis of a comprehensive numerical parametric study. In particular, the examined key parameter is the beam-to-brace stiffness ratio (K_F), which has been analysed varying both geometrical and mechanical parameters as the brace slenderness, the type of beam section (European IPE and HE hot-rolled profiles), the beam strength and stiffness, the span length, and the interstorey height.

The interpretation of numerical data inferred the following remarks:

- The higher the K_F value, the lower is the drift ratio for which yielding occurs. In the cases with $K_F = \infty$ the yielding of the brace in tension occurs at interstorey drift ratio ranging from 0.1 % to 0.3% depending on the slope of the bracing members.
- $K_F = 0.1$ is the threshold value that delimits two different structural performances. For $K_F > 0.1$ the brace yielding in tension can be observed, occurring at interstorey drift ratios within the range 2-3% depending on the tilt angle of the bracing members. On the contrary, for $K_F < 0.1$ the bracing cannot yield in tension and at larger interstorey drift ratios (e.g. $\theta > 2\%$) both diagonal elements can be subjected to compression. For $0 < K_F < 0.02$ both diagonal members are in compression at any interstorey drift ratio.
- The brace-intercepted beam can develop plastic hinge at about 2% of interstorey drift ratio for $0.02 < K_F < 0.1$. For

K_F larger than 0.1 the beam tends to behave elastically because increasing the beam stiffness implies enlarging the flexural strength. For $0 < K_F < 0.02$ the beam behaves elastically even beyond the 4% of interstorey drift ratio.

- The capacity design rule for beams given by EN 1998-1 is not conservative in the most of cases, being the unbalanced force resulting from the analyses larger than the value recommended by the code.
- The numerical analysis results allowed also developing empirical equations able (i) to predict with satisfactory accuracy the brace ductility demand and (ii) the drift ratio corresponding to brace yielding in tension, (iii) to provide the unbalance force acting on the beam of the braced span and (iv) to provide the appropriate beam flexural stiffness for the brace ductility corresponding to the required interstorey drift ratio.
- The obtained empirical formulations can be used as design aid to control the ductility demand of braces and the plastic mechanism at different performance levels.

5.9 REFERENCES

Abramowitz M, Stegun IA. (1964). Handbook of Mathematical Functions, National Bureau of Standards, Applied Math. Series.

Akkar S., Sandıkkaya M.A., Şenyurt M., Azari Sisi A., Ay B.Ö., Traversa P., Douglas J., Cotton F., Luzi L., Hernandez B., Godey S. (2014). Reference database for seismic ground-motion in Europe (RESORCE), *Bulletin of Earthquake Engineering*, 12(1): 311-339.

American Institute of Steel Construction, Inc. (AISC). (2010). Seismic Provisions for Structural Steel Buildings. ANSI/AISC Standard 341-10. AISC, Chicago, Illinois

Black G. R., Wenger B. A., Popov, E. P., (1980). Inelastic Buckling of Steel Struts Under Cyclic Load Reversals. UCB/EERC-80/40, Earthquake Engineering Research Center, Berkeley, CA.

Correia, A.A., Virtuoso, F.B.E. (2006). Nonlinear Analysis of Space Frames. *Proceedings of the Third European Conference on Computational Mechanics: Solids, Structures and Coupled Problems in Engineering*, Mota Soares et al. (Eds.), Lisbon, Portugal.

CSA. 2009. Design of Steel Structures, CSA-S16-09, Canadian Standards Association, Toronto, ON

D'Aniello M., La Manna Ambrosino G., Portioli F., Landolfo R. (2013). Modelling aspects of the seismic response of steel concentric braced frames. *Steel & Composite Structures*, An International Journal 15(5): 539-566.

D'Aniello M., La Manna Ambrosino G., Portioli F., Landolfo R., (2012). Seismic behaviour of dual steel concentric braced frames. *Proceedings of STESSA 2012. Conference – Steel Structures in Seismic Area*. Santiago, Chile – January 9-11.

D'Aniello M., La Manna Ambrosino G., Portioli F., Landolfo R., (2014). The influence of out-of-straightness imperfection in Physical-Theory models of bracing members on seismic performance assessment of concentric braced structures. *The Structural Design of Tall and Special Buildings* (published online 20April 2014). DOI: 10.1002/tal.1160

D'Aniello M., Portioli F.,Landolfo R., (2010). Modelling issues of steel braces under extreme cyclic actions. *Proceedings of COST-C26 Final Conference*, Naples 16-18 September: 335-341.

Della Corte G., Landolfo R., Mazzolani F.M., (2010). Displacement-based seismic design of braced steel structures. *Steel Construction* 3(3):134-139.

Dicleli M., Calik E. E., (2008). Physical Theory Hysteretic Model for Steel Braces. *Journal of Structural Engineering*, Asce, 134(7): 1215-1228.

Dubina D, Dinu F, Zaharia R, Ungureanu V, Grecea D., (2006). Opportunity and effectiveness of using high strength steel in seismic resistant building frames. *Proceedings of International Conference in Metal Structures*.

Dubina D, Stratan A, Dinu F., (2008). Dual high-strength steel eccentrically braced frames with removable links. *Earthquake Engineering and Structural Dynamic* 2008.

Dubina D., (2010). Dual-steel frames for multistory buildings in seismic areas. *Proceedings of International Colloquium Stability and Ductility of Steel Structures*.

ECCS-45. Recommended testing procedure for assessing the behaviour of steel elements under cyclic loads. European convention for constructional steelwork, Brussels; 1986.

EN 1993:1-1, Eurocode 3: Design of steel structures – Part 1-1: General rules and rules for buildings. CEN; 2005.

EN 1993-1-8, Design of steel structures - Part 1-8: Design of joints. CEN 2005.

EN 1998-1-1. Eurocode 8: Design of structures for earthquake resistance – Part 1: General rules, seismic actions and rules for buildings. CEN; 2005.

EN 1998-3, Eurocode 8: Design of structures for earthquake resistance – Part 3: Assessment and retrofitting of buildings. CEN; 2005.

Fulop L. (2010). Selection of earthquake records for the parametric analysis. Research report VTT-R-03238-10, VTT, Espoo.

Giugliano M.T., Longo A., Montuori R., Piluso V., (2010). Plastic design of CB-frames with reduced section solution for bracing members. *Journal of Constructional Steel Research*, 66(5): 611-621.

Giugliano M.T., Longo A., Montuori R., Piluso V., (2011). Seismic reliability of traditional and innovative concentrically braced frames. *Earthquake Engineering and Structural Dynamics*, 40(13):1455-1474.

Goggins J. M., Broderick B. M., Elghazouli A. Y., Lucas A. S., (2006). Behavior of tubular steel members under cyclic axial loading. *Journal of Constructional Steel Research*, 621(2): 121-131.

Hellesland J. 2007. Mechanics and effective length of columns with positive and negative end restraints. *Engineering Structures* 29: 3464–3474.

Ikeda K., Mahin S. A., (1986). Cyclic response of steel braces. *Journal of Structural Engineering*, ASCE, 112(2): 342-361.

Jain A.K., Goel S.C., Hanson R.D. (1978) Hysteresis behavior of bracing members and seismic response of braced frames with different proportions. UMEE 78R3, University of Michigan at Ann Arbor.

Khatib I.F., Mahin S.A., Pister K.S. (1988). Seismic behavior of concentrically braced steel frames. Report UCB/EERC-88/01, Earthquake Engineering Research Center, University of California, Berkeley, CA.

Landolfo Raffaele, editor. Assessment of EC8 provisions for seismic design of steel structures. Technical Committee 13—Seismic Design, No 131/2013. ECCS – European Convention for Constructional Steelwork; 2013.

Longo A., Montuori R., Piluso V., (2008). Failure mode control of X-braced frames under seismic actions. *Journal of Earthquake Engineering*, 12(5): 728-759.

Maley T.J., Sullivan T.J., Della Corte G. (2010). Development of a displacement-based design method for steel dual systems with buckling-restrained braces and moment-resisting frames. *Journal of Earthquake Engineering* 14 (S1): 106-140.

Marino E.M., (2014). A unified approach for the design of high ductility steel frames with concentric braces in the framework of Eurocode 8. *Earthquake Engineering and Structural Dynamics*, 43:97–118.

Mazzolani F.M., Piluso V., (1997). Plastic design of seismic resistant steel frames. *Earthquake Engineering and Structural Dynamics*, 26:167–191.

Menegotto M, Pinto PE. (1973). Method of analysis for cyclically loaded R.C. plane frames including changes in geometry and non-elastic behaviour of elements under combined normal force and bending. In: Symposium on the Resistance and Ultimate Deformability of Structures Acted on by Well Defined Repeated Loads.

Priestley M.J N., Calvi G. M., (1997). Concepts and procedures for direct displacement-based design. Seismic Design Methodologies for the Next Generation of Codes, Fajfar and Krawinkler (eds), Balkema, Rotterdam: 171-181.

Seismosoft (2011). SeismoStruct - A computer program for static and dynamic nonlinear analysis of framed structures. Available from URL: www.seismosoft.com.

Shen J., Wen R., Akbas B., (2015). Mechanisms in Two-story X-braced Frames. *Journal of Constructional Steel Research*, 106: 258-277.

Shen J., Wen R., Akbas B., Doran B., Uckan E., (2014). Seismic demand on brace-intersected beams in two-story X-braced frames. *Engineering Structures*, 76:295-312.

Spacone E., Ciampi V., Filippou F.C., (1996). Mixed formulation of nonlinear beam finite element. *Computer & Structure*, 58(I): 71-83.

Tenchini A., D'Aniello M., Rebelo C., Landolfo R., da Silva L.S., Lima L. (2014). Seismic performance of dual-steel moment resisting frames. *Journal of Constructional Steel Research*, 101: 437-454.

Tremblay R., (2002). Inelastic seismic response of steel bracing members, *Journal of Constructional Steel Research*, 58: 665-701.

Tremblay R., Robert N. (2000). Seismic design of low- and medium-rise chevron braced steel frames. *Canadian Journal of Civil Engineering*, 27: 1192–1206.

Tremblay R., Robert N. (2001). Seismic performance of low- and medium-rise chevron braced steel frames. *Canadian Journal of Civil Engineering*, 28: 699-714.

Uriz P, Mahin S.A. Toward Earthquake-Resistant Design of Concentrically Braced Steel-Frame Structures. PEER Rep. No.2008/08, Pacific Earthquake Engineering Research Center, College of Engineering, Univ. of California, Berkeley.

Vulcu C., Stratan A., Dubina D., D'Aniello M., Landolfo R., Cermelj B., Beg D., Comeliau L., Demonceau J.F., V. Long H., Kleiner A., Kuhlmann U., Fülöp L.A. (2014). Guidelines for seismic design and performance based evaluation of dual steel building frames. Deliverable WP6 High Strength Steel in Seismic Resistant Building Frames (HSS-SERF), Doc. ID: hss-d-0006-wp6-vtt-v13.

Chapter VI
Conceptual design issues and Dual CCBs

6.1 CONCEPTUAL DESIGN: CHEVRON VS X-CBF$_S$

Chevron concentrically braced frames are widely used as lateral resisting system in seismic design of steel buildings, due to their structural efficiency and architectural functionality.

Indeed, bracings in chevron configuration represent one of the most cost-effective solutions in low and mi-rise steel buildings, providing large lateral stiffness and requiring shorter diagonal members and fewer brace connections respect to X-CBFs, thus reducing cost of fabrication and construction.

Moreover, bracings in chevron configuration intrinsically offer architectural advantages owing to the possibility of easily include opens (windows, doorways, etc.) in bracing bents.

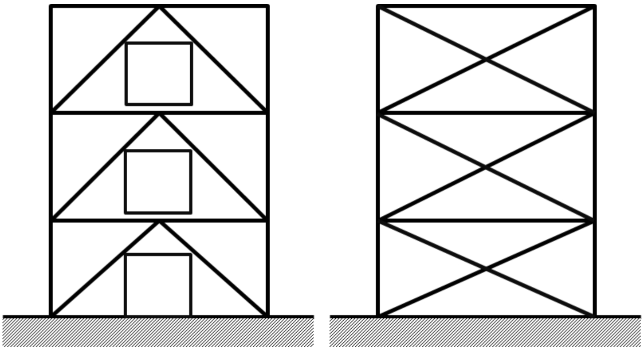

Figure 6.1 Chevon vs X CBFs

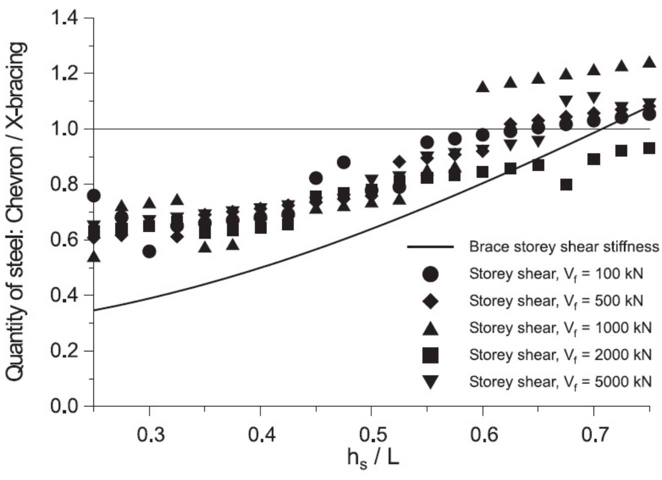

Figure 6.2 Comparison of the steel tonnage of the bracing members in chevron bracing and tension–compression X-bracing (from Tremblay and Robert, 2002)

Several authors previously suggested that braces arranged in chevron configuration are generally more structural effective respect to X-bracings (Allison, 1987; Stafford Smith and Coull, 1991; Tremblay and Robert, 2000).

For instance, in Fig. 6.2 (from Tremblay and Robert, 2000) the minimum steel tons required to resist various storey shears V_f with bracings in both chevron and X configuration are depicted; the figure illustrates that the chevron bracing configuration is more economical in providing storey shear strength over the practical range of h_s/L (from 0.3 to 0.6) being h_s the storey height and L the span length.

It is well known, that the seismic response of concentrically braced frames is significantly affected by the geometrical features of the bracing members, such as the slope of diagonal members, on which the lateral stiffness of the system directly depends on. In addition, the slope of the bracings is important also for technological and constructional reasons. Astaneh-Asl *et al.* (2006) suggest the range [30°-60°] as optimal value for the brace-to-beam angle, otherwise the gusset plate becomes too large (more details on this issue can be found in Section 3.5.5).

Figure 6.3 shows bracings slopes obtained by using chevron and cross concentrically bracings for values of storey height and span length commonly used in steel structural buildings: for the most of cases, arranging diagonal members in X-configurations enforces improper brace-to-beam angles (namely smaller than 30°) resulting in brace-to-beam/column connections impractical from constructional and technological points of view.

Another geometrical feature, limiting the use of concentric bracings in X-configuration, is related to the requirement on the normalized slenderness of bracings.

Indeed, within EC8, slenderness ratio limitation differs between X and chevron configuration: in the former case, the brace normalized slenderness $\bar{\lambda}$ must fall in the range [1.3, 2] (EN 1998-1 6.7.3(1)). Conversely, for bracing in chevron configuration no lower bound is provided and only the upper bound limit (namely, $\bar{\lambda} \leq 2$) is retained.

For X-CBFs, the lower bound limit is due to the simplified tension-only diagonal model assumed for structural analysis (see Fig. 3.2a), in order to avoid overloading of the column connected to the brace under compression.

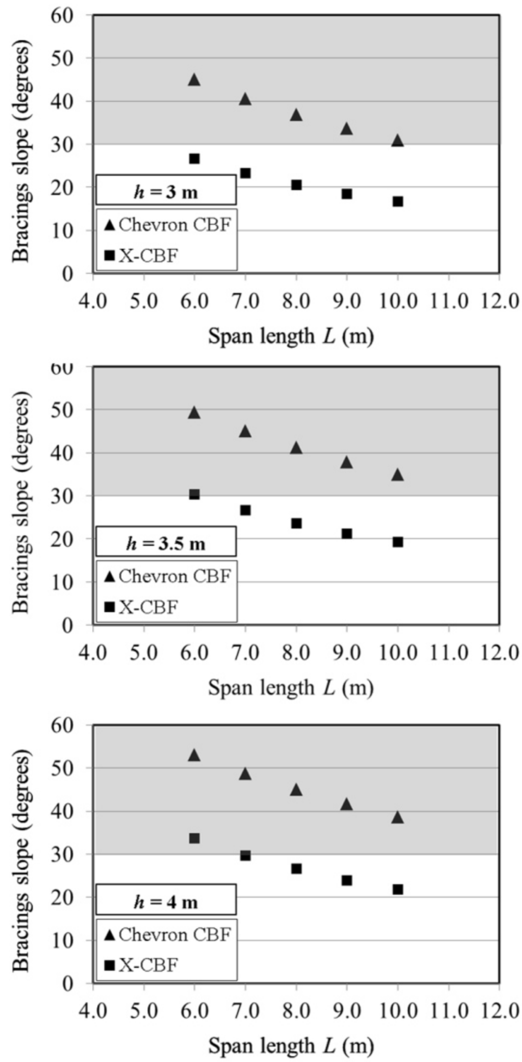

Figure 6.3 Bracings slope obtained for common h/L ratios: comparison between chevron and X configurations

6.2 CHEVRON BRACINGS IN DUAL FRAMES

Dual concentrically braced frames are characterized by the presence of concentrically braced system, acting together with a MRF part. The main benefit of this typology is due to the possibility to combine the advantages of the bracings with the moment resisting structures; indeed, the two different systems resist the seismic event behaving as a couple of mechanical springs acting in parallel.

Two different dissipative behaviours can be addressed by adopting different design strategies:

(i) A primary stiff braced frame with a secondary moment frame basically devoted to provide plastic distribution along the building height, thus avoiding formation of weak storey mechanism;

(ii) A primary ductile MRF stiffened by a secondary/sacrificial braced frame, designed to resist wind loads and to provide lateral stiffness to satisfy service-level drift control.

However, according to EN 1998, dual systems are expected to form an overall global ductile mechanism, with uniform formation of plastic zones along the building height, thus avoiding damage concentration in a limited number of storeys.

EN1998-1 does not provide specific design rules for dual configurations. Moreover, dual frames by combination of MRFs with bracings in chevron configuration are not properly addressed within current codes; indeed, the only type considered in EN1998-1 is “moment resisting frame combined with concentric bracing” (EN1998-1 Table 6.2), considering explicitly the X-bracings and not covering V and inverted-V bracings. The expected nonlinear behaviour of EC8-compliant dual structures is characterized by dissipation, simultaneously provided, by beams in MRF part and yielding of tension diagonals in the CBF. The behaviour factor recommended for DCH concept is slightly larger than that used for X-CBFs, thanks to the presence of MRF. The q_o is equal to 4 as that used for CBFs, while the ratio α_u/α_1 is 1.2.

6.2.1 *The influence of joint typology on the overall response of dual CBF$_s$*

EN 1998-1 6.6.4 allows locating dissipative zones in the connection in case of dual system. In detail, semi-rigid and/or partial strength joints can be used, provided the following conditions:

(i) the joints have a rotation capacity consistent with the global deformations;

(ii) members framing into the joints are stable at the ultimate limit state (ULS);

(iii) the effect of connection deformation on global drift is taken into account using nonlinear static (pushover) global analysis or non-linear time history analysis;

(iv) the rotation capacity of the dissipative joints θ_p is not less than 35 mrad for structures of ductility class DCH and 25 mrad for structures of ductility class DCM with q > 2.

(v) The rotation capacity of the joint has to be verified by performing qualification tests on joint sub-assemblages. The joint ductility is specified by the joint chord rotation $\theta_p = \delta/0{,}5L$, where δ is the beam deflection at mid-span and L is the beam span.

(vi) Stiffness and strength degradation smaller than 20% should be assured in the plastic hinge zone; moreover the column web panel shear deformation should not exceed the 30% of the total plastic rotation capacity of the joint.

However, the cyclic behaviour of beam-to-column joints has a crucial role on the overall seismic response of dual frames.

(Kazantzi *et al.*, 2008) highlighted the influence of joint rotation capacity on the seismic response of mid-rise MR frames designed according to EN 1998-1 (2005). At the present time, EN 1993-1-8 (2005) provides models to compute the strength and the stiffness of connections but no reliable and effective analytical tools are available to predict the rotation capacity and the cyclic performance in relation to the connection typology. On the other hand, in order to carry out the seismic assessment of frames with either partial strength or dissipative bolted joints it is necessary to account for the joint behaviour.

Several approaches, with different levels of complexity, can be considered for the modelling of beam-to-column joints in the framework of the component method (Da Silva, 2008; Gentili *et al*, 2015). In the following Sections, a refined modelling strategy was developed for a set of common used beam-to-column joint typologies.

Moreover, in order to assess the influence of joint typology on the overall response of dual concentrically braced frames, few benchmark dual frames were designed and non-linear dynamic time-history analyses were performed by implementing refined models for joints in frames.

6.2.1.1 Refined models of joints in frames

As mentioned in previous section, joints behaviour deeply affect the seismic response of dual systems; thereby, refined models in which the joints moment-rotation characteristics are properly accounted for, should be used in order to reliably assess the seismic performance of dual frames. With this regard, this Section is devoted to propose some modelling assumptions for a set of common used beam-to-column joint typologies which can be easily implemented for any beam-column assemblies.

In detail, modelling assumptions to simulate the nonlinear behaviour of both the connection zone and the web panel zone for full and partial strength joints are proposed and validated against some experimental results given by literature and finite element analyses. Finally, the effectiveness of the proposed refined modelling hypotheses is compared with the results obtained using simplified assumptions.

The nonlinear moment-rotation behaviour of bolted beam-to-column joints is influenced by the performance of three main contributions, namely the beam, the column web panel and connection response curves. In order to properly account for all these three components, a refined modelling approach was developed by using Seismostruct platform, providing the basic assumptions that can be implemented for a set of joint configurations by characterizing the strength and stiffness properties of each component.

Hereinafter, the modelling assumptions for all three macro-components are shown and verified against experimental tests available from literature.

6.2.1.1.1 Beam moment-rotation behaviour

The beam moment-rotation behaviour is modelled by using a force-based distributed inelasticity element in which the inelasticity is accounted for through integration of material response along the length of the element. The cross-section behaviour is also reproduced by means of the fibre approach, by assigning a uniaxial stress-strain relationship at each fibre; a number of fibres at least equal to 100 is considered for each cross-section. The numerical integration method used is based on the Gauss-Lobatto distribution and at least 5 integration sections are considered along the element.

The validity of the modelling assumptions has been verified against the experimental results carried out by D'Aniello *et al.* (2012) on steel beams, as depicted in Fig 6.4. It should be noted that the effectiveness and the accuracy of the numerical models is proved prior degradation phenomena may occur in the beams. According to experimental and analytical studies carried out by D'Aniello *et al.* (2012) and Carmelj and Bag (2014), the value of total beam rotation made of European profiles without degradation of maximal strength is larger than the stringent limit value of 0.035 rad from EN 1998-Moreover, if full strength and full rigid welded beam-to-column joints are designed in order to guarantee that plastic hinges develop away from the beam-to-column connections, the value of total joint rotation is larger than the limit value of 0.04 rad for structures classified as special moment resisting frames as in AISC 341-10. Therefore, it can be assumed that the models used in the present study may be considered valid within the range of ± 0.04 rad.

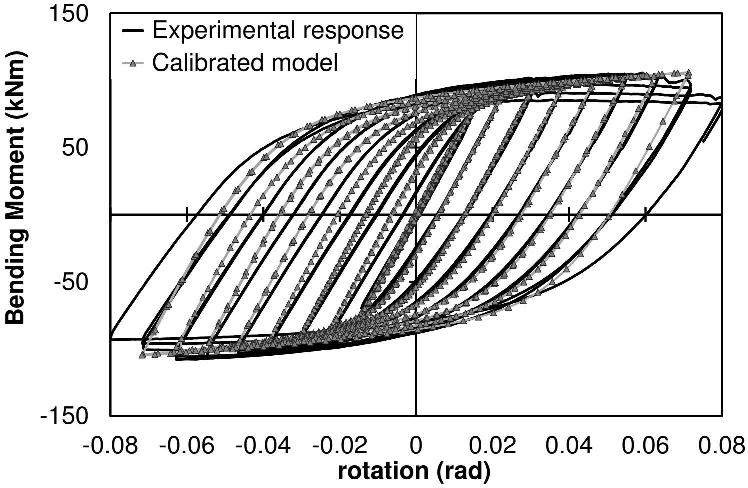

Figure 6.4 Comparison between numerical and experimental curves: cyclic tests on beams by D'Aniello *et al*. (2012)

6.2.1.1.2 Column web panel shear-distortion behaviour

The column web panel zone can be subjected to large stress and strain, especially in internal joints where shear demand larger than the case of external joint is expected, due to anti-symmetrical moments in the seismic condition. In order to simulate the shear response of panel zone, the geometrical size of the joint is accounted for by using a fictitious frame made of rigid elements reproducing the dimensions of the column web panel zone. Each rigid element is pinned at both ends, while at the upper corner two rotational springs (see Fig. 6.5) reproduce the shear-distortion behaviour of the column web panel.

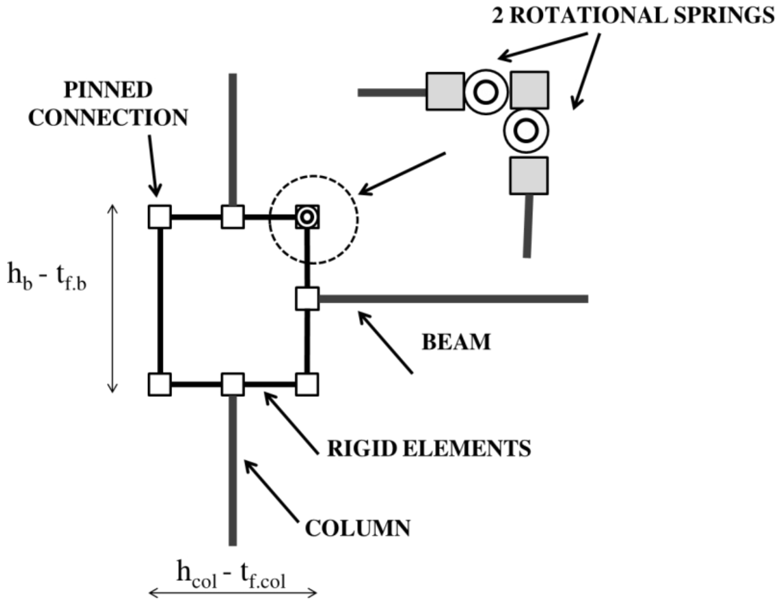

Figure 6.5 Refined model for the column web panel zone.

Several mathematical models are available in literature describing the shear-distortion relationship for the panel zone (Krawinkler *et al.*, 1971; Kim and Engelhardt, 1995; Gupta and Krawinkler, 1999). In the current study the springs are characterized by applying a hysteretic loop of Ramberg-Osgood type. In order to fully characterize the hysteretic response, the yielding parameters (namely yielding moment and yielding rotation) were defined analytically, while the remaining parameters (namely the Ramberg-Osgood parameter and the Convergence limit for the Newton-Raphson procedure) were calibrated on the basis of experimental results carried out by Dubina and Ciutina (2008). In detail, the yielding parameters have been defined similarly to what proposed by Gupta and Krawinkler (1999) and given by the following equations:

$$V_y = \frac{f_y}{\sqrt{3}} A_{eff} \tag{6.1}$$

$$M_y = V_y \cdot (h_b - t_{f.b}) \tag{6.2}$$

$$\gamma_y = \frac{f_y}{\sqrt{3} \cdot G} \tag{6.3}$$

Where:

M_y is the moment corresponding to the plastic shear V_y; A_{eff} is the shear area of the column given according to EN-1993 and accounting for eventually additional web plates; h_b is the beam height and $t_{f.b}$ is the beam flange thickness; γ_y is the distortion corresponding to the yielding of the panel in shear. The calibrated response of the Ramberg-Osgood hysteretic model of the flexural spring is shown in Fig.6.6, where the results are given in terms of spring moment against shear rotation; being θ_s given as:

$$\theta_s = \gamma_1^+ - \gamma_2^- \tag{6.4}$$

Where γ_1 and γ_2 are the contributions of the two rotational springs. The calibration parameters are given in Table 6.1.

As it can be recognized, the simulated response matches satisfactory the experimental curves up to a shear distortion equal to 0.05 rad. For larger rotation experimental results show some deterioration phenomena, while the numerical model is stable. Nevertheless, this level of shear distortion is quite large and generally excessively larger than the acceptable rotation compatible with the frame stability. Hence, the developed model can be considered suitable for the purpose of seismic assessment of building frame.

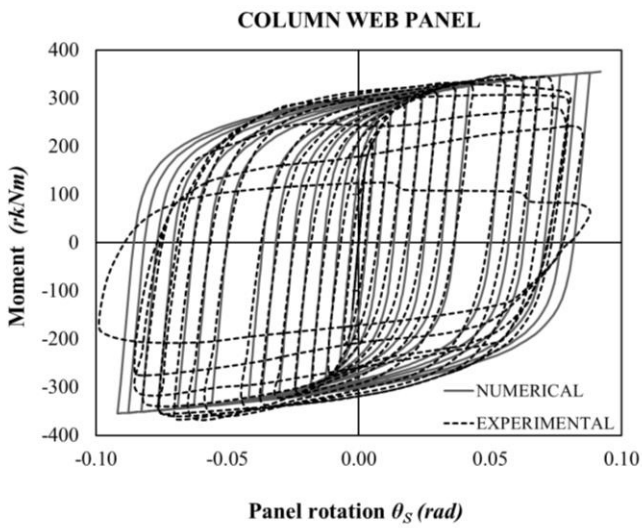

Figure 6.6 Column web panel: calibration of rotational springs.

Table 6.1 Calibration parameters for column web panel.

Parameter	Value
Ramberg-Osgood parameter	9-10
Convergence limit for the Newton-Raphson procedure	0.001

6.2.1.1.3 Connection moment-rotation behaviour

Different modelling assumptions have been proposed for different configurations of the connection zone, which depends on both the stiffness and strength properties to be simulated.

In case of full strength-full rigid connection, no source of deformability can be accounted for. Conversely, in case of partial-rigid connection, a further rotational spring (see Fig. 6.7) should be added between the beam end and the web panel in order to simulate the rigidity of the connection.

In detail, different connection configurations were considered, classified on the basis of simply capacity design criteria and of the expected failure mechanism. For sake of clarity, in the following, the definitions of "Full strength", "Equal strength" and "Partial strength" configurations considered for the calibration procedure are specified.

- Full strength connection: plastic deformations are expected only in the beam, while the connection should behave elastically; the joint should be able to develop a moment capacity at least 1.5 times larger than those experienced in the connected element.

-Equal strength connection: plastic deformations could contemporary occur both in the connection zone and in the connected beam.

- Partial strength connection: plastic deformations occur in the connection zone before the plastic resistance in the connected beam is reached.

These design criteria correspond to different actual joint configurations that are depicted in Fig. 6.8, namely haunched joint with full strength partial-rigid connection; rib-stiffened extended endplate joint with equal-strength partial-rigid connection; unstiffened extended endplate joint with partial-strength partial-rigid connection.

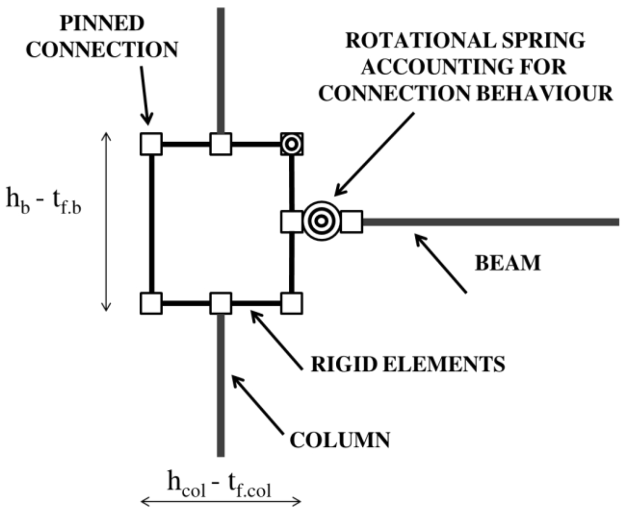

Figure 6.7 Refined model for partial rigid joints.

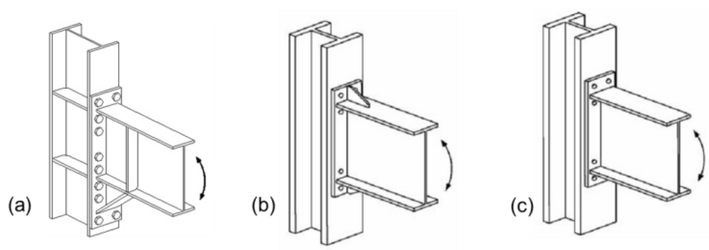

Figure 6.8 Joint configurations considered in the modelling procedure: (a) haunched joint with full strength partial-rigid connection; (b) rib-stiffened extended endplate joint with equal-strength partial-rigid connection; (c) unstiffened extended endplate joint with partial-strength partial-rigid connection.

The behaviour of full-strength partial-rigid joints can be easily defined by using a simple linear-symmetric relationship assuming the stiffness K_0 as the joint rigidity given according to EN-1993-8.

Conversely, for both equal and partial strength cases, plastic deformations are expected to occur in the connection zone and the refined model should be able to account for both strength and stiffness degradation experienced by the connection. Thereby a multi-linear relationship was selected for those cases.

In detail, the spring for the rib-stiffened extended endplate joint with equal-strength partial-rigid connection was calibrated on the basis of finite element analysis results carried out in the framework of research project “EQUALJOINTS RFSR-CT-2013-00021”.

The comparison between FEM results and numerical response of the spring is shown in Fig.6.9, where it can be easily recognized that the model seems to accuracy reproduce the connection behaviour expressed in terms of moment at column face against connection rotation (i.e. gap rotation). The relevant parameters of calibration are summarized in Table 6.2.

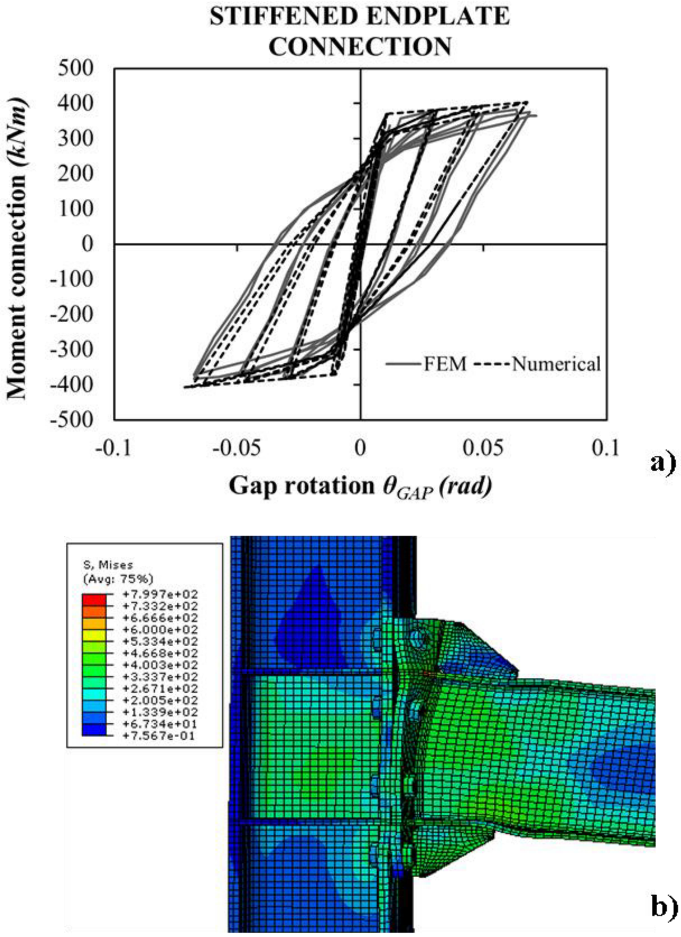

Figure 6.9 Spring calibration for rib-stiffened extended endplate equal-strength partial-rigid connection (a); FEA results (b).

Table 6.2 Parameters of calibration for rib-stiffened extended endplate equal-strength partial-rigid connection.

Parameter	Value
Analytically defined parameters	
Initial flexural rigidity (EI)	S_j*
Cracking moment (PC)	$0.25M_{pl}$*
Yield Moment (PY)	M_{pl}
Yield Curvature (UY)	M_{pl} / S_j
Ultimate Curvature(UU)	90UY
Post Yielding stiffness (EI3 a s% EI)	0.012
Calibrated parameters	
Stiffness degrading parameter (HC)	2
Ductility decay parameter (HBD)	0.1
Hysteretic energy decay parameter (HBE)	0.001
Slip parameter (HS)	0.85
trilinear/bilinear/vertex oriented (M)	0

*S_j is the secant stiffness according to EN-1993:1-8

*M_{pl} is the average plastic moment of the connection zone according to EN-1993:1-8

Finally, the spring for the unstiffened extended endplate joint with partial-strength and partial-rigid connection was calibrated on the basis of experimental tests carried out by Dubina et al. (2001). Figure 6.10 shows the comparison between the numerical prediction and the experimental response curve of the connection zone (namely in terms of moment at column face vs connection rotation). As it can be recognized the numerical model matches quite well the strength and stiffness degradation. The relevant parameters of calibration are reported in Table 6.3.

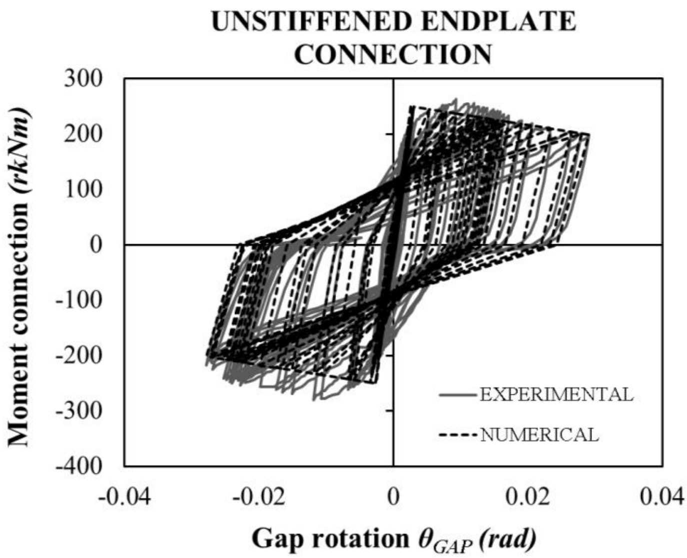

Figure 6.10 Spring calibration for unstiffened extended endplate partial-strength partial-rigid connection.

Table 6.3 Parameters of calibration for unstiffened extended endplate partial-strength partial-rigid connection.

Parameter	Value
Analytically defined parameters	
Initial flexural rigidity (EI)	S_j*
Cracking moment (PC)	$0.75M_{pl}$*
Yield Moment (PY)	M_{pl}
Yield Curvature (UY)	M_{pl} / S_j
Ultimate Curvature(UU)	35UY
Post Yielding stiffness (EI3 a % EI)	0.01
Calibrated parameters	
Stiffness degrading parameter (HC)	10
Ductility decay parameter (HBD)	1
Hysteretic energy decay parameter (HBE)	0.001
Slip parameter (HS)	0.7
trilinear/bilinear/vertex oriented (M)	0

*S_j is the secant stiffness according to EN-1993:1-8
*M_{pl} is the average plastic moment of the connection zone according to EN-1993:1-8

It is worth to note how both analytically defined and calibrated parameters affect the shape of the hysteretic loop. In both stiffened and unstiffened connections, the calibration exhibits a more accurate simulation of the connection behaviour by assuming the secant stiffness according to EN-1993:1-8 in place of the initial flexural rigidity. In all examined cases, assuming the initial stiffness of the analytical model by EN 1998:1-8 leads overestimating the connection rigidity.

6.2.1.1.4 The performance of the assembled refined model

In this section it is described and discussed the performance of an assembled refined model accounting for all sources of deformability (namely beam, column web panel and connection). In order to verify the effectiveness and the limits of the developed models, the numerical response is verified against some experimental results out by Dubina *et al*. (2001) The complete model (See Fig. 6.11) includes all the parts constituting the specimen assembly (i.e. beams, columns, and rotational springs accounting for column web panel and connection behaviour).

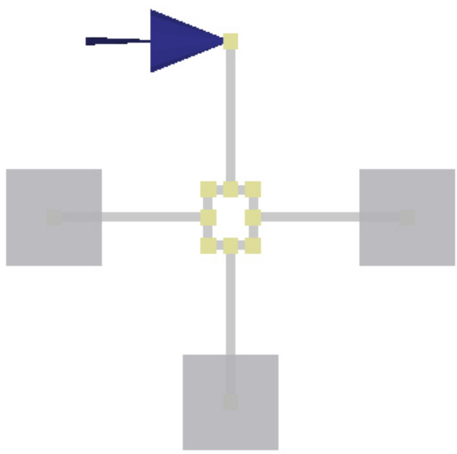

Figure 6.11 Assembled refined model of the joint tested by Dubina et al. (2001).

Figure 6.12 shows the comparison between experimental and numerical results in terms of overall response (namely applied force vs. top displacement), column web panel response and connection response.

As it can be observed, both the overall response (See Fig. 6.12a) and column web panel response (See Fig. 6.12b) match very well the experimental curves. Indeed, the failure mechanism experienced in the experimental test is successfully reproduced involving the yielding of both, column web panel and connection. However, the connection response (See Fig. 6.12c) highlights a limit of the complete model: indeed, fracture occurred in the beam during the test. Therefore, being the fracture propagation in the beam not accounted for in the numerical analysis, at the same imposed overall displacement the amount of rotation numerically applied to the connection results to be larger than the experimental case.

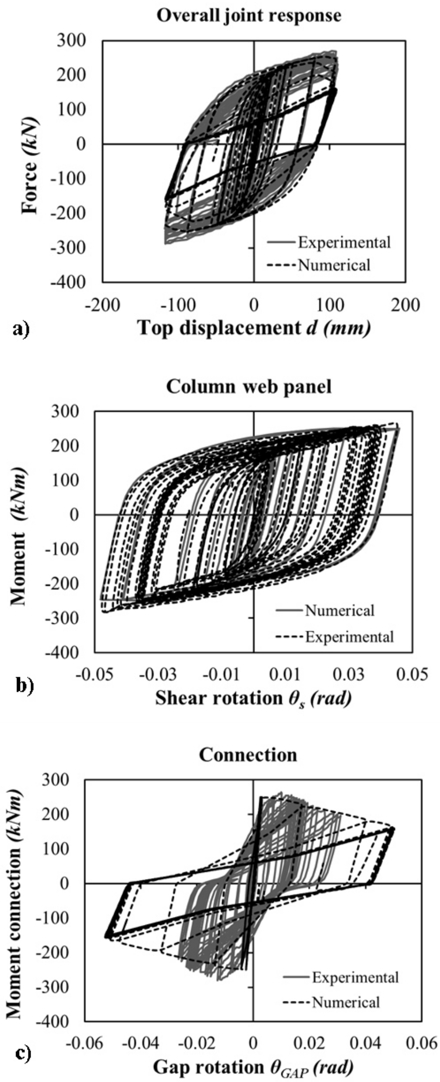

Figure 6.12 Comprehensive model calibration: (a) overall joint response (b) web panel response (c) connection response

6.2.1.1.5 Refined vs. simplified models.

In order to verify the effectiveness and the accuracy of the proposed modelling strategy, the refined modelling hypotheses are compared with the results obtained using simplified assumptions. In detail three different modelling approaches were considered as follows:

(i) a simplified model in which the influence of beam-to-column joint moment-rotation properties is totally neglected: the joint is assumed to be full-strength and full-rigid. Thus no spring is used to simulate the joint behaviour.

(ii) a second modelling approach where the joint behaviour is simulated by using a unique equivalent spring characterized by a bilinear relationship. In this case the required parameters (namely the initial flexural stiffness and the yielding moment) are defined according to EN-1993. At the light of the results previously discussed, the secant stiffness was used in place of the initial elastic rigidity.

(iii) The proposed refined model assumption proposed.

The comparison between the different modelling strategies is shown in Fig. 6.13. It can be easily observed that using a simplified model leads to a significant overestimation of the overall response (See Fig. 6.13a) expressed in terms of top displacements against applied force. On the contrary, by using the bilinear relationship characterised by parameters defined according to EN-1993, an underestimation of the joint moment-rotation properties can be recognized (See Fig. 6.13b). Conversely, as already shown, the proposed modelling assumptions exhibit a very good matching.

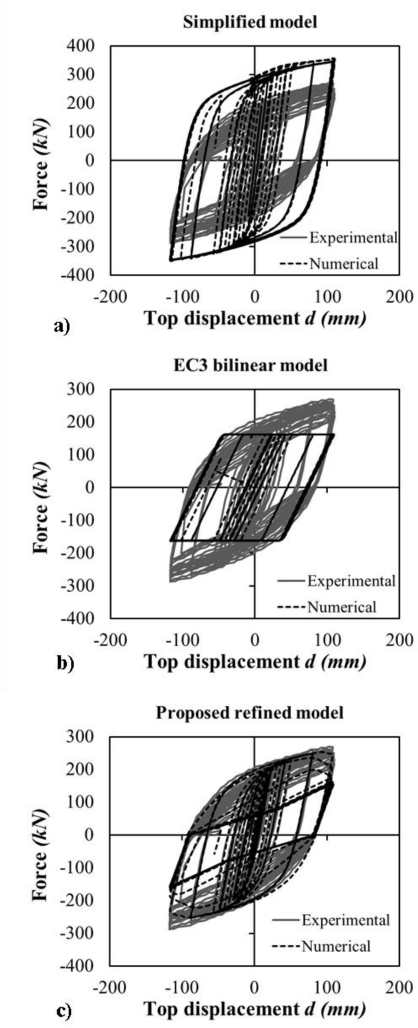

Figure 6.13 Comparison: simplified models against proposed refined model: (a) Simplified model (b) Bilinear model (c) Proposed refined model

6.2.2 *Examined study cases and design parameters.*

The examined dual configurations refer to primary chevron concentrically braced frame with a secondary moment frame basically devoted to provide plastic distribution along the building height, thus avoiding formation of weak storey mechanism. Therefore, the bracing system is designed to bear the 75% of seismic base shear force, while the remaining 25% is resisted by the MRF part.

2D frames were extracted from two different idealized indefinitely rectangular six-storey reference buildings in three and five bays configurations, respectively. In particular, perimetric frames were considered (see Fig. 6.14), in order to account for the necessity (very common in the design of buildings) of distributing the seismic resistant elements along the perimeter of the building to guarantee adequate torsional strength and stiffness.

The spacing of braced frames is equal to L_y, being L_y the span length (set equal to 8 *m*) in the longitudinal direction, as shown in Fig. 6.14. The typical analysed frame in *x* direction consists of three or five bays (each of 8 *m* span); the interstorey height is set equal to 3.5*m* and 4*m* at the *i*-th and roof storey, respectively.

The mid-bay is equipped with chevron bracings, while MRF bays are placed laterally; also in five bays configuration, only two bays are designed as lateral resisting system (namely MRF), while the interior frames are assumed to be gravity frames and their lateral load resisting capacity is neglected (see Fig. 6.14).

Four different typologies are considered to investigate the influence of joint moment-rotation behaviour on overall seismic response: (i) full strength full rigid, (ii) full strength partial rigid, (iii) equal strength partial rigid, (iv) partial strength and partial rigid. However, at design stage, simplified assumption considering the joint like a full strength full rigid point is adopted.

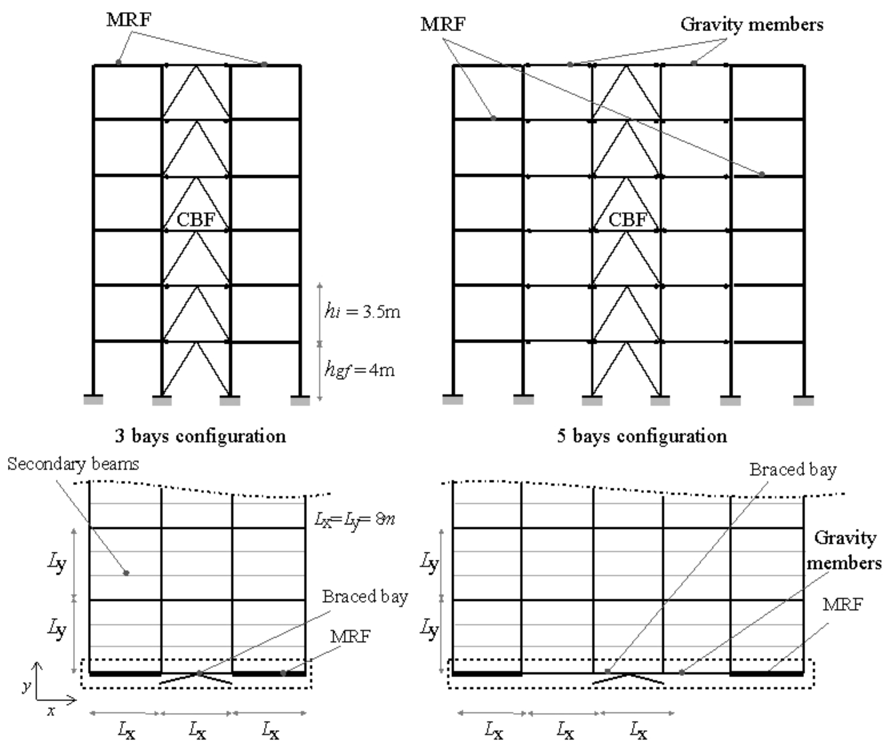

Figure 6.14 Structural layout of case study building: plan of idealized reference building and vertical configuration

EN 1998-1, Type 1 design spectra for soil C are used for calculating the seismic loads for a high seismicity level (0.35g). The lateral force method of analysis is employed for calculating the seismic action effects. A behaviour factor q=4.8 was assumed at design stage.

Besides rules given by Eurocode 8, the structural safety verifications were carried out according to the following European codes:

- EN 1990 (2001) Eurocode 0: Basis of structural design;
- EN 1991-1-1 (2002) Eurocode 1: Actions on structures - Part 1-1: General actions -Densities, self-weight, imposed loads for buildings;
- EN 1993-1-1 (2003) Eurocode 3: Design of steel structures - Part 1-1: General rules and rules for buildings;

Both permanent (G_k) and live loads (Q_k) are summarized in Table 6.4. As it can be observed, the same loads were assumed acting on both roof and i-th storey.

Table 6.5 shows the seismic weights per unit floor area and masses for each 2D frame. For all the examined cases the inertial effects in the seismic design situation were evaluated by taking into account the presence of the masses corresponding to the combination of permanent and variable gravity loads as given, in accordance with EN 1998-1 3.2.4 (2)P.

Table 6.4: Characteristic values of gravity loads**.**

	G_k (kN/m^2)	Q_k (kN/m^2)
Storey slab	5.20	2.00
Roof slab	5.20	2.00

Table 6.5: Seismic weights and masses.

	Seismic weight (kN/m^2)	Seismic mass for 3 bays case ($kN\ s^2/m$)	Seismic mass for 5 bays case ($kN\ s^2/m$)
i-th storey	5.5	80.73	134.56
Roof storey	5.68	83.38	138.96

Cold formed circular hollow profiles were used for the diagonals members; IPE and HE profiles were used for beams; HE and HD profiles were used for the columns. Tables 6.6 and 6.7 summarize the cross section properties of structural members of the frames in three and five bays configuration respectively.

Table 6.6: Cross section properties for 3 bays configurations

Storey	MRF		CBF		
	Beam	Column	Beam	Column	Brace
	S355	S355	S355	S355	S235
6	IPE 330	HE 240 B	HE 300 B	HE 280 B	114.3 x 8
5	IPE 330	HE 240 B	HE 360 B	HE 280 B	139.7 x 10
4	IPE 330	HE 280 B	HE 400 B	HE 280 M	168.3 x 10
3	IPE 330	HE 280 B	HE 450 B	HE 280 M	168.3x 12.5
2	IPE 330	HE 300 B	HE 450 B	HE 300 M	177.8 x12.5
1	IPE 330	HE 300 B	HE 500 B	HE 300 M	193.7 x12.5

Table 6.7: Cross section properties for 5 bays configurations

Storey	MRF		CBF			Gravity members	
	Column	Beam	Column	Beam	Brace	Column	Beam
	S355	S355	S355	S355	S235	S355	S355
6	HE300B	IPE330	HE600A	HE320B	139.7x8	HE260A	IPE330
5	HE300B	IPE330	HE600A	HE300M	168.3x10	HE260A	IPE330
4	HE300B	IPE360	HE600A	HE360M	168.3x16	HE260B	IPE330
3	HE300B	IPE400	HE600A	HE400M	177.8x16	HE260B	IPE330
2	HE340B	IPE400	HE650M	HE450M	219.1x16	HE300B	IPE330
1	HE340B	IPE400	HE650M	HE550M	219.1x16	HE300B	IPE330

6.2.3 *Seismic performance evaluation*

A set of incremental dynamic time-history analyses was performed in order to assess the influence of joints moment-rotation behaviour on the seismic performance of examined frames. 14 natural earthquake acceleration records were considered consistently to what described in Section 7.3.3.2, while the modelling assumptions can be found in Section 7.3.1.

The seismic response was evaluated for the three seismic hazard levels as given according to Eurocode 8, which are associated to different annual rates of exceedance: damage limitation (DL), severe damage (SD) and near collapse (NC) (See also Section 7.3.3.1).

Both global and local performance indicators were select to evaluate the seismic response of all the examined frames.

The monitored parameters for all limit states are summarized as follow:

- *Global response indicator:*

i) peak transient interstorey drift ratios θ (given by the horizontal relative displacement at each storey divided by the interstorey height)

ii) residual interstorey drift ratios θ_{RES}: it is defined as the average value of relative horizontal displacements at each storey experienced during the last 10 seconds at zero acceleration fictitiously added to each record, divided by the interstorey height.

- *Local performance indicators:*

i) braces ductility demand (μ) both in tension and compression is given by the ratio:

$$\mu = \frac{d}{d_y} \tag{6.5}$$

where d is the brace axial displacement and d_y the displacement of the brace at yielding.

ii) connection rotation θ_C (i.e. gap rotation)

iii) web panel zone rotation θ_{WP}

iii) beam chord rotation θ_b

The analyses results are presented hereinafter, by showing the average demand obtained by the 14 considered records per response indicator.

Figures 6.15 and 6.16 depict both transient (θ, see Figs. 6.15-16a) and residual (θ_{RES}, Figs. 6.15-16b) interstorey drift ratios for three and five bays cases, respectively. Both cases show significant lateral stiffness with limited displacement smaller than 1% at SD limit state. Moreover, it is trivial to observe that no appreciable differences can be recognized by varying the joints types; analogous behaviour can be observed in terms of braces ductility demand (see Figs. 6.17 and 6.18), with bracing members in tension practically behaving elastically up to NC limit state.

Figures from 6.15 to 6.18 basically show that for the examined hazard level the seismic demand on the analysed frames is very low: indeed, in dual-scheme the presence of stiff bracings significantly reduces the lateral drift demand beam-to-column joints belonging to the MRF part do not experience plastic engagement and the joint typology does not affect the overall response.

This feature is confirmed also by Figs. 6.19 to 6.20 were the rotation of beam-to-column joints of the MRF part are depicted; in detail the contributions of the three macro-components (namely connection zone in Figs. 6.19 to 6.20a, web panel zone in Figs. 6.19 to 6.20b and beam chord rotation in Figs. 6.19 to 6.20c) are separately shown, normalized on the relevant deformations at yielding. As it can be observed, no plastic engagement can be recognized until NC limit state.

Thereby, results from non-linear dynamic analysis show that moment-rotation properties of joints belonging to the MRF part, slightly affect the overall response of analysed dual-frames, and only small differences can be recognized at local level. These results suggest that semi-rigid connections can be used in dual-frames without affecting the overall response (provided that the deformability is correctly accounted for the design) also reducing the constructional costs. In addition, enforcing plasticity into the connections allows using deep beams that are beneficial for the lateral stiffness and stability, while avoiding the severe capacity design requirements for columns that will be designed for the strength of connections only.

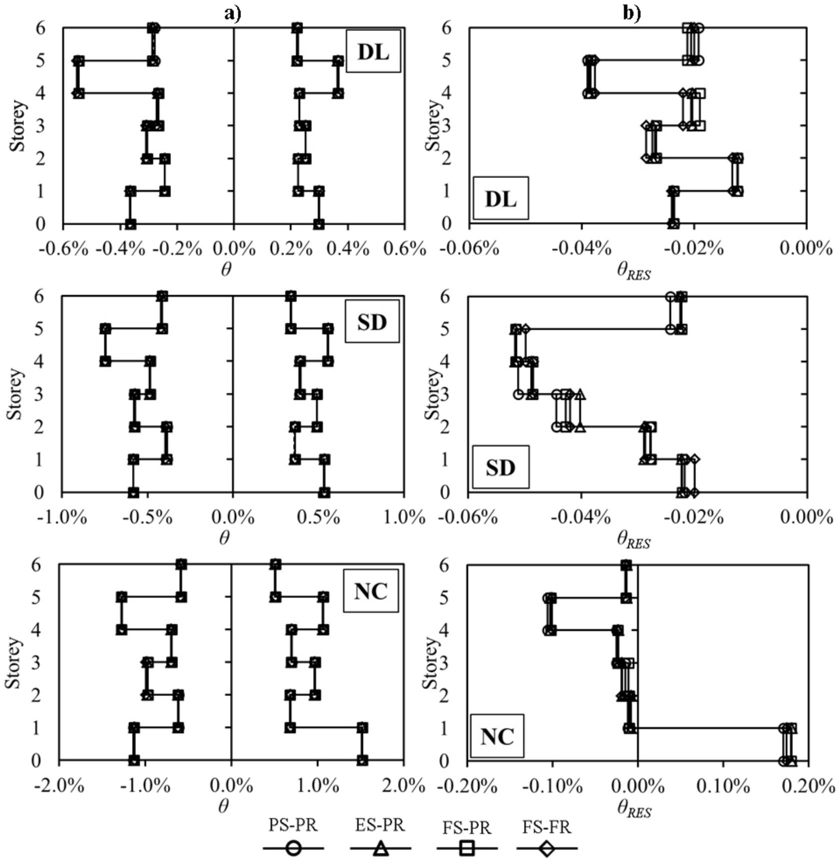

Figure 6.15 Interstorey drift transient (a) and residual (b): comparison between 3-bays frames with different joint types.

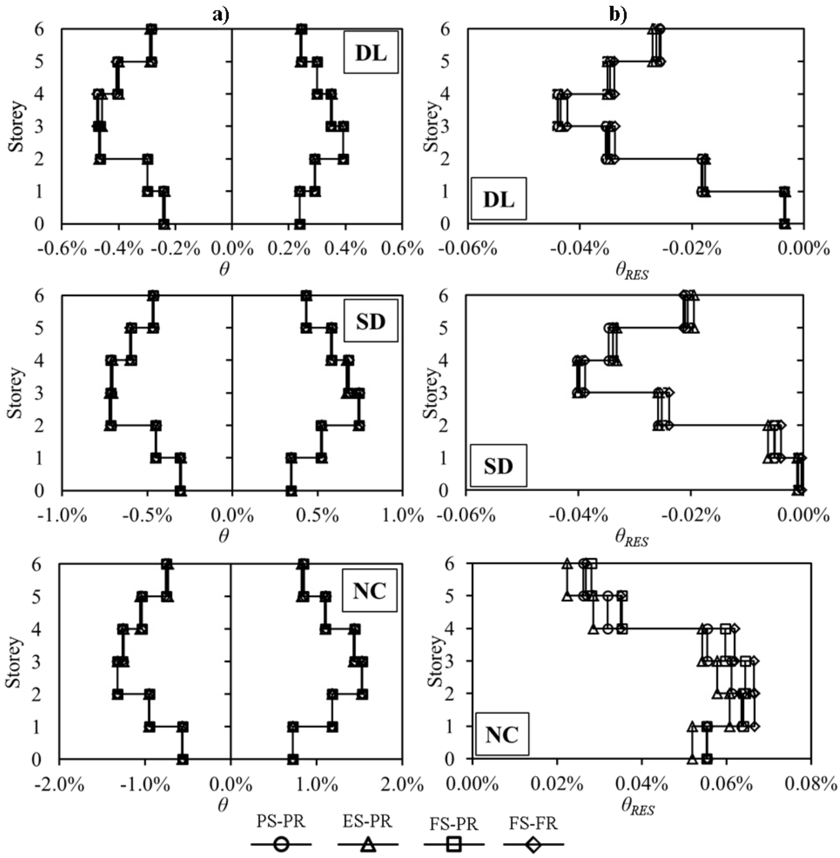

Figure 6.16 Interstorey drift transient (a) and residual (b): comparison between 5-bays frames with different joint types.

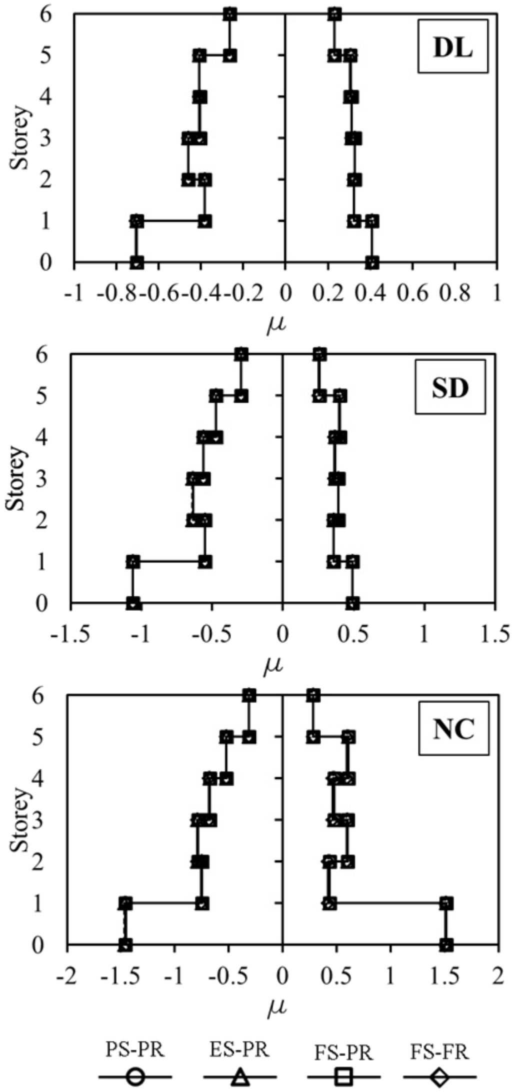

Figure 6.17 Braced ductility demand: comparison between 3-bays frames with different joint types.

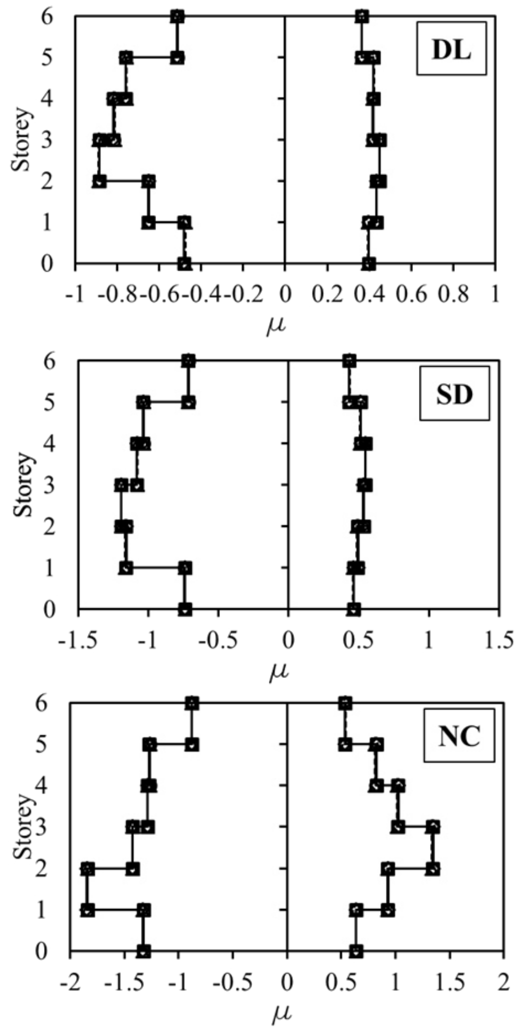

Figure 6.18 Braced ductility demand: comparison between 5-bays frames with different joint types.

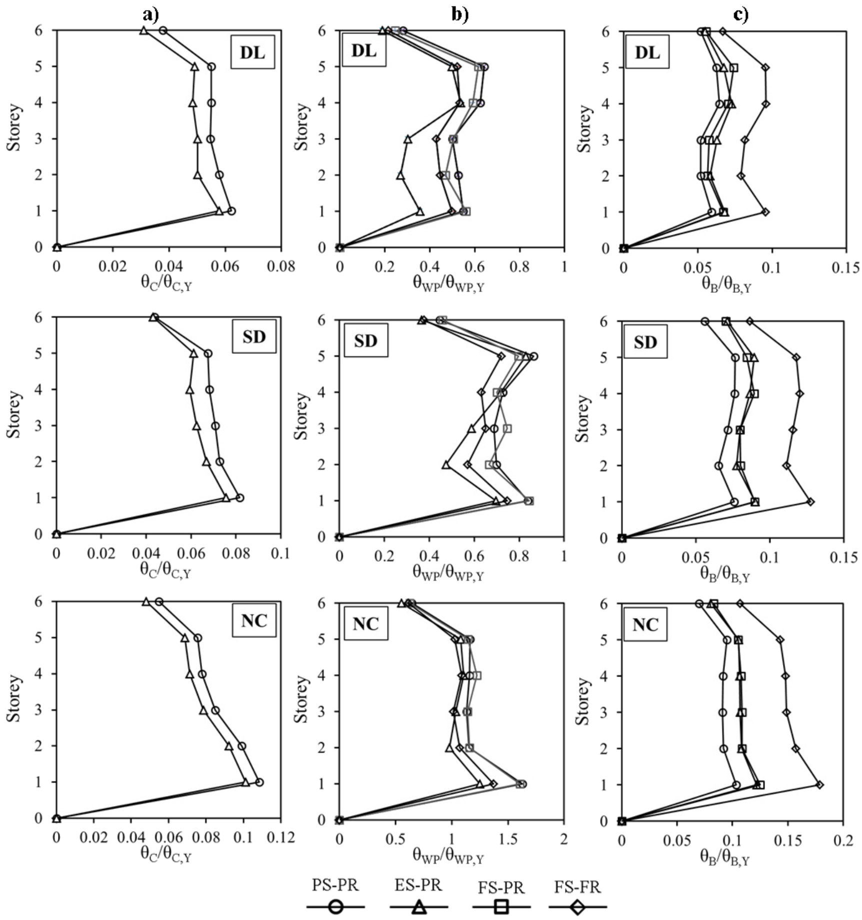

Figure 6.19 Seismic demand on joints for 3-bays frames with different joint types: (a) normalized connection rotation (b) normalized web panel shear rotation (c) beam normalized chord rotation.

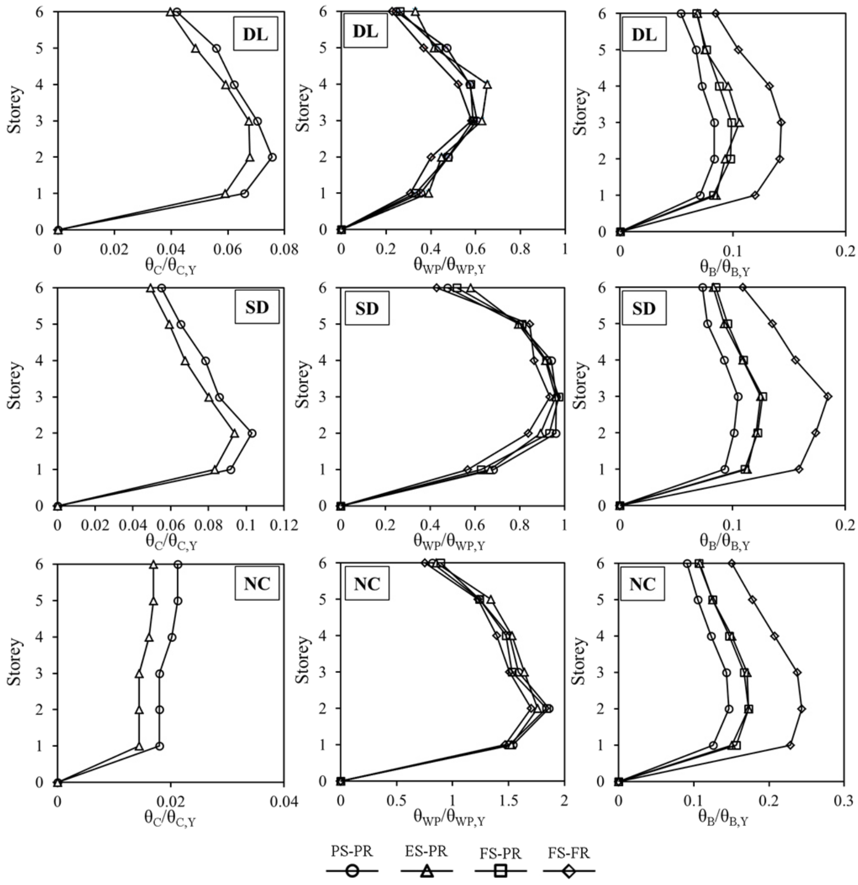

Figure 6.20 Seismic demand on joints for 5-bays frames with different joint types: (a) normalized connection rotation (b) normalized web panel shear rotation (c) beam normalized chord rotation.

6.3 CONCLUSIVE REMARKS

In this Chapter, conceptual design issues concerning the use of concentrically braced frames in seismic resistant steel building have been discussed.

The discussion showed that, even though, chevron bracings are expected to provide smaller ductility and dissipation capacity respect to X-CBFs, the first are generally more structural effective, considering the following remarks:

- chevron bracings provide large lateral stiffness requiring shorter diagonal members and fewer brace connection respect to X-CBFs, thus reducing cost of fabrication and construction.
- the arrangement of bracings in chevron configuration intrinsically offers architectural advantages owing to the possibility of easily include opens (windows, doorways, etc) in bracing bents
- geometrical features (as the slope of bracings and the requirements on normalized slenderness) limit the use of X-CBFs for storey height and span length dimensions commonly used in structural buildings.

In addition, the use of chevron bracings in dual-frames has been discussed; with this regard, the need to investigate the influence of joints behaviour on the overall response of steel multi-storey frames emerged and suggested developing refined models in which the moment-rotation behaviour of bolted end-plate moment resisting joints is specifically accounted for.

The proposed joint refined model is made of three macro-components, namely (i) the beam at intersection zone (ii) the column web panel (ii) the connection zone, thus allowing simulating the behaviour of different joint configurations by characterizing the strength and stiffness properties of each component. Specific modelling assumptions have been proposed for each zone; finally the three macro-components have been combined in a comprehensive model describing the overall moment-rotation response of the joint.

Three different connection configurations have been considered, classified on the basis of simply capacity design criteria and thus of the expected failure mechanism: (a) haunched joint with full strength partial-rigid connection; (b) rib-stiffened extended endplate joint with equal-strength partial-rigid connection; (c) unstiffened extended endplate joint with partial-strength partial-rigid connection.

The refined models developed according to the proposed assumptions generally match quite well the experimental results.

In order to verify the effectiveness of the proposed modelling strategy, the refined model has been compared with the results obtained using simplified models, showing the better accuracy respect to the simplified ones, whose response seems inadequate to reproduce the hysteretic behaviour of the joint.

The proposed refined model has been used to perform a set of non-linear dynamic analyses on few dual-frames taken as study cases in order to evaluate the influence of joints behaviour on the overall response.

Results from nonlinear analyses showed that joins properties slightly affect the overall response, and just small differences can be recognized at local level. Indeed, the presence of stiff bracing system significantly reduces the lateral drift demand on the MRF part and the joints do not experience plastic engagement.

Therefore, these outcomes suggest that semi-rigid connections can be used without affecting the overall response (provided that the deformability is correctly accounted for the design) also reducing the constructional costs.

6.4 REFERENCES

Allison, H. (1987). Steel design — special considerations. *In Building structural design handbook*. Edited by R. White and C.G. Salmon. John Wiley & Sons, New York, N.Y

American Institute of Steel Construction, Inc. (AISC) (2010). Seismic provisions for structural steel buildings. Standard ANSI/AISC 341-10, Chicago (IL, USA).

Astaneh-Asl A., Cochran M.L., Sabelli R. (2006). Seismic Detailing of Gusset Plates for Special Concentrically Braced Frames. *Structural Steel Educational Council- Steel TIPS*.

Cermelj B., Beg D. (2014) Cyclic behaviour of welded stiffened beam-to-column joints – experimental tests. *Steel Construction* 7(4): 221–229, 2014.

Ciutina A., Dubina D. (2008) Column Web Stiffening of Steel Beam-to-Column Joints Subjected to Seismic Actions. *Journal of Structural Engineering*, 134(3):505-510, 2008.

D'Aniello M, Landolfo R, Piluso V, Rizzano G. (2012) Ultimate Behaviour of Steel Beams under Non-Uniform Bending. *Journal of Constructional Steel Research* 78:144–158, 2012.

Dubina D., Ciutina A., Stratan A. (2001) Cyclic tests of double-sided beam-to-column joints. *Journal of Structural Engineering,* 127(2):129-136, 2001.

EN 1993-1-8, Design of steel structures - Part 1-8: Design of joints

EN 1998-1, Design of structures for earthquake resistance - Part 1: General rules, seismic actions and rules for buildings.

Gentile F., Shahbazian A., Rebelo C., Simões da Silva L. (2015) Influence of joint modelling strategies on the seismic response of dual-concentrically braced steel frames. *X Congresso de Construção Metálica e Mista Coimbra, Portugal*

Gupta A., Krawinkler H. (1999), Influence of column web stiffening on the seismic behaviour of beam-to-column joints. *Stanford University, Stanford, CA, 1999.*

Kazantzi A.K., Righiniotis T.D., Chryssanthopoulos M.K. (2008). The effect of joint ductility on the seismic fragility of a regular moment resisting steel frame designed to EC8 provisions. *Journal of Constructional Steel Research* 64: 987–996, 2008.

Kim, K., and Engelhardt, M. D. (1995). Development of analytical models for earthquake analysis of steel moment frames, *Report No. PMFSEL* 95-2, Dept. of Civil Eng., Univ. of Texas at Austin.

Krawinkler H., Bertero V. V., Popov E. P. (1971). Inelastic behavior of steel beam-to-column sub-assemblages. *Report No. UCB/EERC-71/07, Earthquake Engineering Research Center (EERC), University of California at Berkeley*

Seismosoft (2011). SeismoStruct – A computer program for static and dynamic nonlinear analysis of framed structures. Available from URL: www.seismosoft.com.

Simões da Silva L. (2008) Towards a consistent design approach for steel joints under generalized loading. *Journal of Constructional Steel Research* 64: 1059–1075.

Stafford Smith, B., and Coull, A. (1991) Tall building structures: analysis and design. John Wiley & Sons, New York, N.Y.

Tremblay R., Robert N. (2000) Seismic design of low- and medium-rise chevron braced steel frames. *Canadian Journal of Civil Engineering*. 27: 1192–1206

Chapter VII
Assessment of codified seismic design provisions for CCBs

7.1 INTRODUCTION

In this chapter a parametric study devoted to assess the effectiveness of seismic design provisions and codified criteria given by both European (EN-1998) and North-American (AISC 341 and CSA S16-09) codes is described and discussed. With this regard, a comprehensive set of non-linear dynamic analyses was performed on low, medium and high rise residential buildings. In addition further cases were added in order to evaluate the influence of some modifications applied to the requirements provided by EN-1998.

As already mentioned in Chapter III, both European and North-American (US and Canadian) seismic codes basically adopt the same approach (namely the capacity design philosophy), aimed at guaranteeing the plastic engagement is restrained into diagonal members and avoiding the damage in the remaining structural members. However, in order to achieve this purpose, different requirements and detailing rules are provided by the different codes, consequently affecting the overall performance and energy dissipation capacity.

It should be noted that the main purpose of this parametric study is to investigate the effectiveness of the different design criteria provided for both dissipative and non-dissipative members; with this aim, and in order to avoid misleading conclusions, the structures were designed according to same hazard level, (whose definition would differ in the three examined codes) and few requirements, mostly related to the beam-to-column connections, were disregarded in order to make easier the comparative reading of results.

The selection of the parameters to be observed at design stage and monitored during each analysis was addressed at the light of the results discussed in previous Chapters, in which the main issues influencing the seismic performance of concentric bracings in chevron configuration have been identified and deeply discussed.

7.2 DESIGN OF THE EXAMINED STRUCTURES

7.2.1 *Description of study cases*

7.2.1.1 Structural layout and archetypes

The analysed 2D frames were extracted from low, medium and high rise idealized reference buildings equipped with concentric bracings in chevron configuration, characterized by three, six and twelve storeys respectively; in particular, the alignments at the perimeter were considered (see Fig. 7.1), in order to account for the necessity (very common in the design of buildings) of distributing the seismic resistant elements along the perimeter of the building to guarantee adequate torsional strength and stiffness.

The spacing of braced frames is equal to $3L_y$, being L_y the span length (set equal to 6.5 *m*) in the longitudinal direction, as shown in Fig.7.1. The typical analysed frame in *x* direction consists of three bays (each of 8 *m* span).

The vertical configurations of the bracing members are shown in Fig. 7.2; the interstorey height is equal to 3.50 *m* with exception of the first floor, which is 4.00 *m* high. The frames extracted from low and medium rise buildings (namely three and six storey cases respectively) are equipped with a single braced bay per frame (see Fig. 7.2). Conversely, in twelve-storey cases two bays are equipped with chevron bracings in order to obtain reasonable cross section dimensions for the diagonal members.

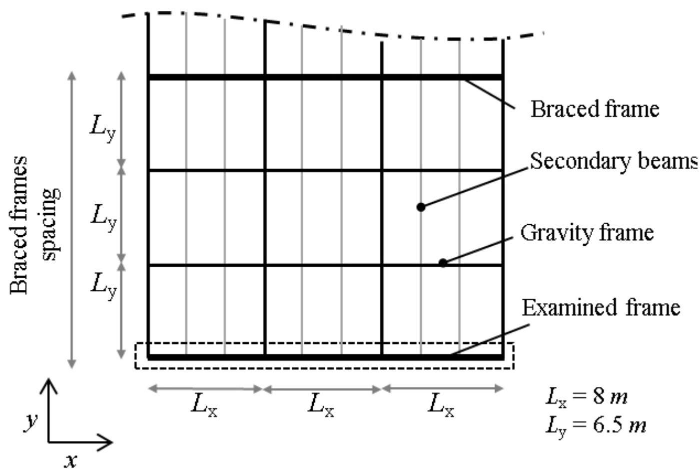

Figure 7.1 Structural layout of case study building: plan of idealized reference building.

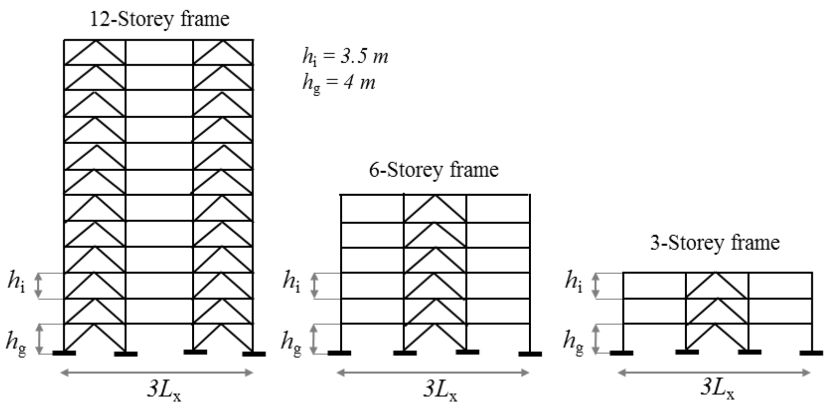

Figure 7.2 Structural layout of case study building: vertical configuration of bracing members.

At each floor, the rigid diaphragm transmitting the horizontal actions is realized by means of composite slabs with profiled steel sheetings supported by the hot rolled steel beams (primary and secondary), which are restrained to avoid flexural-torsional buckling; the composite action is obtained by applying shear connectors between the slab and the beams.

7.2.1.2 Normative references

Besides the seismic recommendations, the structural safety verifications were carried out according to the following European codes:

- EN 1990 (2001) Eurocode 0: Basis of structural design;
- EN 1991-1-1 (2002) Eurocode 1: Actions on structures - Part 1-1: General actions -Densities, self-weight, imposed loads for buildings;
- EN 1993-1-1 (2003) Eurocode 3: Design of steel structures - Part 1-1: General rules and rules for buildings;
- EN 1994-1-1 (2004) Eurocode 4: Design of composite steel and concrete structures - Part 1.1: General rules and rules for buildings.

The design of building was developed without reference to a specific National Annex. Hence, the calculation is carried out using the recommended values of the safety factors.

7.2.1.3 Design assumptions common to all examined cases

All the examined cases were designed by using European steel grades and the mechanical properties of the materials used for the structural members are summarized in Table 7.1, where the partial safety factors are also indicated.

Table 7.1 Material properties and partial safety factors.

Grade	f_y	$f_{y,m}$	γ_{ov}	γ_M	E
	(N/mm^2)	(N/mm^2)			(N/mm^2)
S 355	335	443.75	γ_{ov}=1.25	γ_{M0} = 1.00 γ_{M1} = 1.00 γ_{M2} = 1.25	210000
S 460	460	506	γ_{ov}=1.1		

It should be noted that the capacity of structural members was evaluated by accounting for the steel stress in compliance to what recommended by the different codes as described in Section 3.2.

Both permanent (G_k) and live loads (Q_k) are summarized in Table 7.2. As it can be observed, the same loads were assumed acting on both roof and *i*-th storey.

Table 7.3 shows the seismic weights per unit floor area and masses for each 2D frame. For all the examined cases the inertial effects in the seismic design situation were evaluated by taking into account the presence of the masses corresponding to the combination of permanent and variable gravity loads as given, in accordance with EN 1998-1 3.2.4 (2)P.

Table 7.2 Characteristic values of gravity loads**.**

	G_k (kN/m^2)	Q_k (kN/m^2)
Storey slab	5.20	2.00
Roof slab	5.20	2.00

Table 7.3 Seismic weights and masses.

	Seismic weight (kN/m^2)	Seismic mass (kN s^2/m)
i-th storey	5.5	131.19
Roof storey	5.68	135.49

In order to avoid misleading conclusions, the structures were designed according to same hazard level. Therefore both the elastic spectral shape and the reference peak ground acceleration a_{gR} are those described in EN-1998-1. The reference peak ground acceleration equal to $a_{gR} = 0.35g$ (being g the gravity acceleration), a type C soil, a type 1 spectral shape and importance factor γ_I equal to 1.0 were assumed. The design response spectra (see Fig. 7.3) were obtained for each examined seismic code by dividing the ordinates of elastic response spectrum by the relevant shear-reduction factor (see Section 3.2.1). For all the examined codes, the design of buildings was referred to the ductility classes expected to provide largest plastic engagement, namely (i) the concept “DCH” (Ductility Class High) was followed for the EC8-compliant frames (ii) the concept “SCBF” (Special Concentrically Braced Frames) was followed for the AISC-compliant frames (iii) the concept “MD CBF” (Moderate ductile CBF) was followed for the CSA-compliant frames.

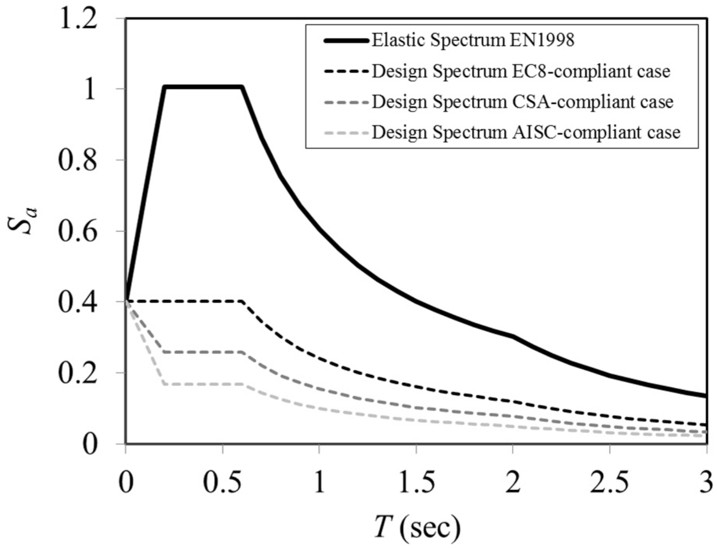

Figure 7.3 Elastic and design response spectra.

Cold formed circular hollow profiles were used for the diagonals members; IPE and HE profiles were used for beams; HE and HD profiles were used for the columns. Since European profiles were used for all the examined cases and to simplify the comparison between the examined codes, the width-to-thickness ratio limitations provided according to EN 1993:1-1 and devoted to control the local slenderness were extended also to the case designed in compliance to the North-American codes. Thereby, all steel members (i.e. beams, bracings and columns) have cross section satisfying the Class 1 requirements according to EN 1993:1-1.

In order to specifically assess the effectiveness of the detailing rules for both dissipative and non-dissipative members, at this stage the requirement provided by AISC 341 (see Section 3.2.4) on the beam-to-column connections of the braced bays to be MRF type, was disregarded with the aim to allow simply comparative reading of results in terms of seismic demand on members.

7.2.1.4 Modifications to EN-1998

Beside the EC8-compliant frames, further variations were added to the analysed set of structures in order to verify the possibility to improve the effectiveness of the codified design criteria by removing or modifying apparently inconsistent requirements. With this regard, six further frames (two per number of storeys) were obtained applying few revisions to the EN-1998 provisions. Both the applied modifications are related to the requirement on the variation of the overstrength factor Ω. Indeed, as deeply discussed in Section 3.2.3, EN-1998 states that the brace overstrength ratio $\Omega_i = N_{pl,br,Rd,i}/N_{Ed,br,i}$ should vary within the range Ω to 1.25Ω, being $\Omega = \min(\Omega_i)$. Such requirement, devoted to assure uniform distribution of damage along the building height, often enforces to oversize the diagonal members at lower storeys, being the upper storeys generally characterized by the highest value of Ω_i.

It should be noted that, beside leading uneconomical solutions, selecting stocky braces contributes to arouse unfavourable behaviour with diagonal members behaving elastically under tension (See Chapter 5). In order to mitigate this undesired effect, two alternative adjustments are proposed and investigated to obtain more effective configurations of bracing members along the building height:

(i) The requirement on Ω_i variation is retained, but the roof storey is excluded.

Therefore, considering an n-storey building, it is imposed that:

$$\left[(\Omega_i - \Omega) / \Omega \right] \leq 0.025 \tag{7.1}$$

Where Ω is the minimum overstrength ratio $\Omega = \min \left(\frac{N_{pl,br,Rd,i}}{N_{Ed,br,i}} \right)$ and Ω_i is the overstrength ratio at the i-th storey evaluated as:

$$\Omega_i = \frac{N_{pl,br,Rd,i}}{N_{Ed,br,i}} \quad i \in \left[1, (n-1) \right]. \tag{7.2}$$

The modified requirement here defined is referred in the following as “revised criterion 1” or “rev 1”, in order to make easier the reading of analyses results.

(ii) The requirement on Ω_i variation is retained as provided by EN-1998 (namely, including the roof storey); however the overstrength ratio Ω_i (in the following referred as $\Omega_{b,i}$) at each storey is defined considering the compression axial strength of the brace rather than the plastic capacity:

$$\Omega_{b,i} = \frac{N_{b,br,Rd,i}}{N_{Ed,br,i}} = \frac{\chi_i N_{pl,br,Rd,i}}{N_{Ed,br,i}} \tag{7.3}$$

This criterion is referred in the following as “revised criterion 2” or “rev 2”, As it can be easily recognized, such an approach considers that the buckling of the brace under compression is the actual first nonlinear event occurring at each storey, prior the yielding under tension is reached.

It should be noted that defining the overstrength ratio according to the Eq. (7.3) also makes easier to fit the distribution of diagonal strengths $N_{b,Rd,i}$ to the distribution of computed action effect $N_{Ed,i}$; indeed, with this aim, the designer can select the braces at each storey not only according to their cross section area, but also acting on the relevant geometrical properties (i.e. second moment of inertia and radius of gyration).

7.2.1.5 Designed Structures

Tables from 7.1 to 7.3 summarize the cross section properties of structural members of the three, six and twelve-storey buildings respectively, designed according to all the examined codes.

It is trivial to observe (see Fig. 7.4), that the frames designed according EN1998-1 are characterized by the stockiest braces with intermediate normalized slenderness $\bar{\lambda}$ varying between 1.14 to 1.21 for the three-storey case, 0.8 and 1.21 for the six-storey case and 0.91 to 1.46 for the twelve-storey case. The values of the normalized slenderness obtained for frames designed in compliance with the three examined codes are also reported in Tables from 7.4 to 7.6. In addition, the design procedure provided by EN1998-1 also leads to heavier profiles for beams and columns. This difference can be easily explained by considering the smaller value of the force reduction factor accounted for by the European code. Moreover, this difference is further exasperated considering that in the US and Canadian codes the dissipative members are designed according their “expected” and “probable” capacities respectively, namely evaluated using the average yield stress of the material, while the design value (namely the characteristic value also reduced by using a proper partial safety factor) is implemented in the calculation of the resistance of diagonal members according to EN1998-1.

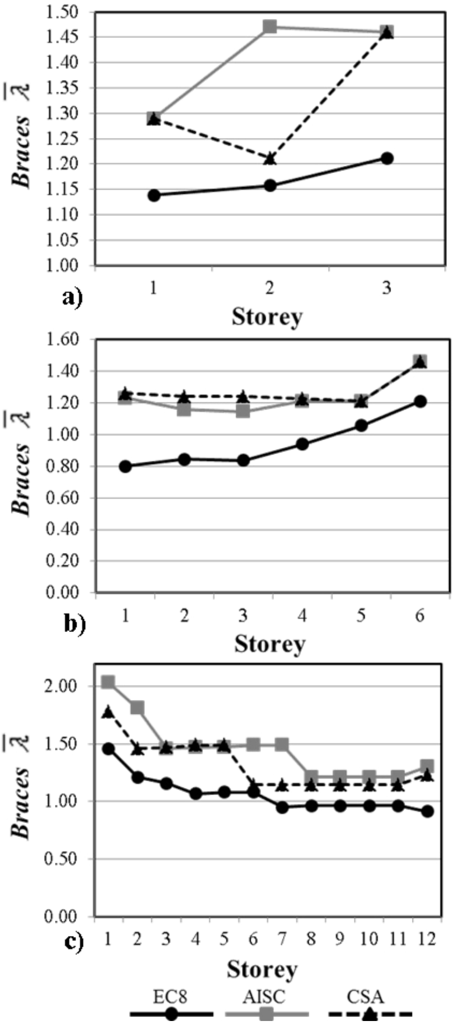

Figure 7.4 Normalized slenderness of braces at each storey: comparison between examined codes.

Table 7.1 Cross section properties of structural members of 3-storey cases: comparison between different codes.

	Columns			Beams			Braces (d x t)			Gravity members	
Storey	EC8	AISC	CSA	EC8	AISC	CSA	EC8	AISC	CSA	Columns	Beams
	S355	S355	S355	S460	S460	S460	S355	S355	S355	S355	S355
3	HE 200 B	HE 200 B	HE 200 B	HE 400 B	HE 400 A	HE 360 B	168.3 x 6	139.7 x 5	139.7 x 5	HE 200 B	IPE 330
2	HE 260 B	HE 240 B	HE 240 B	HE 400 B	HE 400 B	HE 400 B	177.8 x 8	139.7 x 6	168.3 x 6	HE 240 B	IPE 330
1	HE 260 B	HE 240 B	HE 240 B	HE 500 B	HE 450 B	HE 450 B	193.7 x 10	168.3 x 6	168.3 x 6	HE 240 B	IPE 330

Table 7.2 Cross section properties of structural members of 6-storey cases: comparison between different codes.

	Columns			Beams			Braces (d x t)			Gravity members	
Storey	EC8	AISC	CSA	EC8	AISC	CSA	EC8	AISC	CSA	Columns	Beams
	S355	S355	S355	S460	S460	S460	S355	S355	S355	S355	S355
6	HE 400 A	HE 320 A	HE 260 A	HE 400 A	HE 360 B	HE 400 A	168.3 x 6	139.7 x 5	139.7 x 5	HE 260 A	IPE 330
5	HE 400 A	HE 320 A	HE 260 A	HE 450 B	HE 450 B	HE 400 B	193.7 x 8	168.3 x 6	168.3 x 6	HE 260 A	IPE 330
4	HE 450 B	HE 360 A	HE 280 B	HE 500 B	HE 450 B	HE 500 B	219.1 x 10	168.3 x 6	168.3 x 8	HE 280 B	IPE 330
3	HE 450 B	HE 360 A	HE 280 B	HE 550 B	HE 500 A	HE 550 B	244.5 x 10	177.8 x 6	168.3 x 10	HE 280 B	IPE 330
2	HD 400 x 347•/+	HE 400 M	HE 280 M	HE 600 B	HE 500 B	HE 550 B	244.5 x 12	177.8 x 8	168.3 x 10	HE 280 M	IPE 330
1	HD 400 x 347•/+	HE 400 M	HE 280 M	HE 600 M	HE 550 B	HE 550 M	273 x 12	177.8 x 8	177.8 x 12	HE 280 M	IPE 330

Table 7.3 Cross section properties of structural members of 12-storey cases: comparison between different codes.

Storey	Columns			Beams*			Braces (*d* x *t*)		
	EC8	AISC	CSA	EC8	AISC	CSA	EC8	AISC	CSA
	S460	*S355*	*S355*	*S460*	*S460*	*S460*	*S355*	*S355*	*S355*
12	HE 320 M	HE 280 A	HE 300 A	HE 300 B	HE 320 B	HE 300 B	139.7 x 5	101.6 x 5	114.3 x 4
11	HE 320 M	HE 280 A	HE 300 A	HE 320 M	HE 360 B	HE 340 B	168.3 x 6	114.3 x 6	139.7 x 5
10	HE 320 M	HE 280 A	HE 300 A	HE 320 M	HE 360 B	HE 360 B	177.8 x 8	139.7 x 5	139.7 x 6
9	HD 400 x 347•/+	HE 320 A	HE 320 B	HE 320 M	HE 450 A	HE 450 B	193.7 x 10	139.7 x 6	139.7 x 8
8	HD 400 x 347•/+	HE 320 A	HE 320 B	HE 360 M	HE 450 A	HE 450 B	193.7 x 12	139.7 x 6.3	139.7 x 8
7	HD 400 x 347•/+	HE 320 A	HE 320 B	HE 400 M	HE 450 B	HE 450 B	193.7 x 12.5	139.7 x 8	177.8 x 6
6	HD 400 x 347•/+	HE 360 B	HE 340 M	HE 550 M	HE 450 B	HE 450 B	219.1 x 12.5	139.7 x 8	177.8 x 6
5	HD 400 x 347•/+	HE 360 B	HE 340 M	HE 550 M	HE 450 B	HE 450 B	219.1 x 16	168.3 x 6	177.8 x 6
4	HD 400 x 347•/+	HE 400 M	HE 340 M	HE 550 M	HE 450 B	HE 450 B	219.1 x 16	168.3 x 6	177.8 x 6
3	HD 400 x 509•/+	HE 400 M	HE 360 M	HE 550 M	HE 450 B	HE 450 B	219.1 x 16	168.3 x 6	177.8 x 6
2	HD 400 x 509•/+	HE 400 M	HE 360 M	HE 550 M	HE 450 B	HE 450 B	219.1 x 16	168.3 x 6	177.8 x 6
1	HD 400 x 509•/+	HE 400 M	HE 360 M	HE 650 M	HE 550 B	HE 500 B	244.5 x 16	168.3 x 8	177.8 x 8

*All gravity resistant beams are IPE 330

Table 7.4 Brace slenderness ratio in 3-storey cases: comparison between different codes.

	Brace normalized slenderness $\bar{\lambda}$		
Storey	EC8	AISC	CSA
3	1.21	1.46	1.46
2	1.16	1.47	1.21
1	1.14	1.29	1.29

Table 7.5 Brace slenderness ratio in 6-storey cases: comparison between different codes.

	Brace normalized slenderness $\bar{\lambda}$		
Storey	EC8	AISC	CSA
6	1.21	1.46	1.46
5	1.06	1.21	1.21
4	0.94	1.21	1.23
3	0.84	1.14	1.24
2	0.85	1.16	1.24
1	0.80	1.23	1.26

Table 7.6 Brace slenderness ratio in 12-storey cases: comparison between different codes.

	Brace normalized slenderness $\bar{\lambda}$		
Storey	EC8	AISC	CSA
12	1.46	2.03	1.78
11	1.21	1.81	1.46
10	1.16	1.46	1.47
9	1.07	1.47	1.49
8	1.08	1.47	1.49
7	1.08	1.49	1.14
6	0.95	1.49	1.14
5	0.97	1.21	1.14
4	0.97	1.21	1.14
3	0.97	1.21	1.14
2	0.97	1.21	1.14
1	0.91	1.30	1.23

However, beside the size of the members, it is interesting to note that, even though the EC8-compliant frame is characterized by smaller cross sections of the members, the relative beam-to-brace stiffness is smaller (namely in the range 0.07-0.13) if compared to the North-American cases (see Tables from 7.7 to 7.9). Figure 7.5 shows the beam-to-braces stiffness ratios K_F (as defined in Chapter 5) at each storey for all the examined cases. As it can be observed, both AISC341-10 and CSA S16-09 lead to similar values of K_F, larger respect to the European case. Beside the larger slenderness of bracing members, this feature is mainly due to the different values assumed to evaluate the post-buckling capacity of the brace under compression, directly affecting the unbalanced force applied to the beam in the non-linear range and thus its required strength. Indeed, as discussed in Section (3.2.4) EN-1998 assumes larger (and non-conservative in the most of cases) values of the post-buckling strength, leading to select weaker beams.

Table 7.7 Stiffness ratio for 3-storey cases: comparison between different codes.

	Beam to brace stiffness ratio K_F		
Storey	EC8	AISC	CSA
3	0.10	0.11	0.11
2	0.07	0.13	0.10
1	0.09	0.14	0.13

Table 7.8 Stiffness ratio for 6-storey cases: comparison between different codes.

	Beam to brace stiffness ratio K_F		
Storey	EC8	AISC	CSA
6	0.08	0.11	0.11
5	0.09	0.13	0.10
4	0.09	0.14	0.13
3	0.10	0.14	0.14
2	0.11	0.14	0.15
1	0.12	0.16	0.16

Table 7.9 Stiffness ratio for 12-storey cases: comparison between different codes.

	Beam to brace stiffness ratio K_F		
Storey	EC8	AISC	CSA
12	0.07	0.11	0.10
11	0.12	0.11	0.09
10	0.09	0.11	0.09
9	0.07	0.16	0.13
8	0.07	0.13	0.13
7	0.08	0.13	0.14
6	0.14	0.13	0.14
5	0.11	0.15	0.14
4	0.11	0.15	0.14
3	0.11	0.15	0.14
2	0.11	0.15	0.14
1	0.13	0.17	0.13

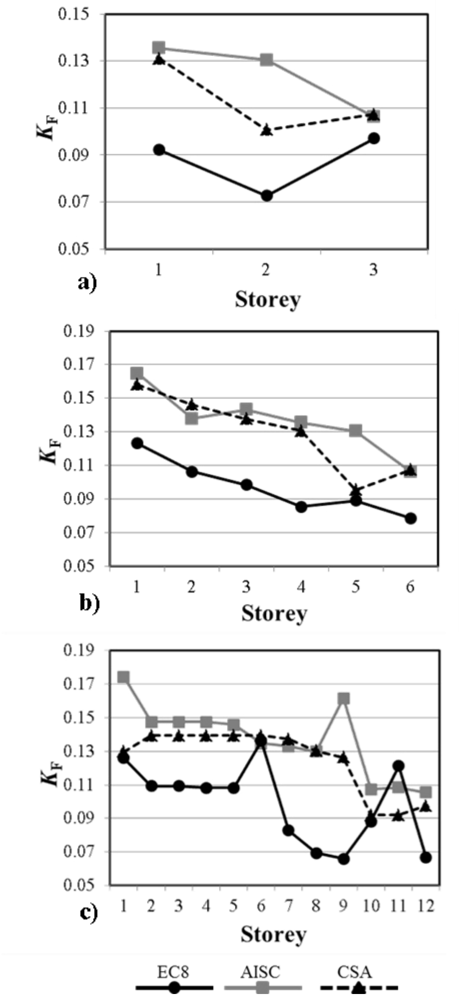

Figure 7.5 Beam-to-brace stiffness ratio: comparison between examined codes

The cross section properties of structural members for three, six and twelve-storey buildings designed accounting for the revised criteria to the EN-1998 provisions described in Section 7.2.1.4 are summarized and compared with the EC8-compliant frames in Tables from 7.10 to 7.12. The values of the normalized slenderness obtained in compliance with the three examined codes are also reported in Tables from 7.13 to 7.15, while the beam-to-brace stiffness ratios are summarized in Tables from 7.16 to 7.18.

As it can be easily noted, the CBFs designed introducing the two critical revisions slightly differs respect to the Eurocode 8-compliant cases. This feature can be explained considering that the modifications applied to the code provisions only refer to the requirement on the overstrength factor variation; thereby only the selection of bracing members (and thus their normalized slenderness) is slightly affected, particularly at the lower storeys. This effect is more evident for three and twelve-storey cases respect to the six-storey one.

Figure 7.6 depicts the normalized slenderness of diagonal members at each storey for three, six and twelve storey cases, while Figure 7.7 shows the relevant beam-to-brace stiffness ratio.

.

Table 7.10 Cross section properties of structural members for 3-storey cases: comparison between EN-1998 and proposed revisions.

Storey	Columns			Beams			Braces (*d* x *t*)			Gravity members	
	EC8	Rev 1	Rev 2	EC8	Rev 1	Rev 2	EC8	Rev 1	Rev 2	Columns	Beams
	S355	S355	S355	S460	S460	S460	S355	S355	S355	S355	S355
3	HE 200 B	HE 200 B	HE 200 B	HE 400 B	HE 400 A	HE 400 B	168.3 x 6	168.3 x 6	168.3 x 6	HE 200 B	IPE 330
2	HE 260 B	HE 240 B	HE 260 B	HE 400 B	HE 400 A	HE 450 B	177.8 x 8	193.7 x 6	177.8 x 8	HE 240 B	IPE 330
1	HE 260 B	HE 240 B	HE 260 B	HE 500 B	HE 450 B	HE 500 B	193.7 x 10	193.7 x 8	193.7 x 8	HE 240 B	IPE 330

Table 7.11 Cross section properties of structural members for 6-storey cases: comparison between EN-1998 and proposed revisions.

Storey	Columns			Beams			Braces (*d* x *t*)			Gravity members	
	EC8	Rev 1	Rev 2	EC8	Rev 1	Rev 2	EC8	Rev 1	Rev 2	Columns	Beams
	S355	S355	S355	S460	S460	S460	S355	S355	S355	S355	S355
6	HE 400 A	HE 340 B	HE 360 A	HE 400 A	HE 400 A	HE 400 A	168.3 x 6	168.3 x 6	168.3 x 6	HE 260 A	IPE 330
5	HE 400 A	HE 340 B	HE 360 A	HE 450 B	HE 450 B	HE 450 B	193.7 x 8	193.7 x 8	193.7 x 8	HE 260 A	IPE 330
4	HE 450 B	HE 400 B	HE 400 A	HE 500 B	HE 500 A	HE 450 B	219.1 x 10	219.1 x 8	219.1 x 8	HE 280 B	IPE 330
3	HE 450 B	HE 400 B	HE 400 A	HE 550 B	HE 550 B	HE 500 B	244.5 x 10	244.5 x 10	244.5 x 8	HE 280 B	IPE 330
2	HD 400 x 347•/+	HD 400 x 347•/+	HE 400 M	HE 600 B	HE 550 B	HE 550 B	244.5 x 12	244.5 x 10	244.5 x 10	HE 280 M	IPE 330
1	HD 400 x 347•/+	HD 400 x 347•/+	HE 400 M	HE 600 M	HE 550 M	HE 550 M	273 x 12	273 x 10	244.5 x 10	HE 280 M	IPE 330

Table 7.12 Cross section properties of structural members for 12-storey cases: comparison between EN-1998 and proposed revisions.

Storey	Columns			Beams*			Braces (*d* x *t*)		
	EC8	Rev 1	Rev 2	EC8	Rev 1	Rev 2	EC8	Rev 1	Rev 2
	S460	S460	S355	S460	S460	S460	S355	S355	S355
12	HE 320 M	HE 360 A	HE 320 B	HE 300 B	HE 320 A	HE 450 A	139.7 x 5	139.7 x 5	139.7 x 5
11	HE 320 M	HE 360 A	HE 320 B	HE 320 M	HE 400 A	HE 450 A	168.3 x 6	168.3 x 6	168.3 x 6
10	HE 320 M	HE 360 A	HE 320 B	HE 320 M	HE 450 A	HE 450 A	177.8 x 8	177.8 x 8	168.3 x 8
9	HD 400 x 347•/+	HE 400 B	HE 400 B	HE 320 M	HE 500 A	HE 500 A	193.7 x 10	177.8 x 10	168.3 x 10
8	HD 400 x 347•/+	HE 400 B	HE 400 B	HE 360 M	HE 500 A	HE 500 A	193.7 x 12	219.1 x 8	177.8 x 10
7	HD 400 x 347•/+	HE 400 B	HE 400 B	HE 400 M	HE 550 B	HE 500 A	193.7 x 12.5	219.1 x 10	219.1 x 8
6	HD 400 x 347•/+	HD 400 x 347•/+	HE 450 M	HE 550 M	HE 550 B	HE 500 A	219.1 x 12.5	244.5 x 10	219.1 x 8
5	HD 400 x 347•/+	HD 400 x 347•/+	HE 450 M	HE 550 M	HE 550 B	HE 500 A	219.1 x 16	244.5 x 10	219.1 x 8
4	HD 400 x 347•/+	HD 400 x 347•/+	HE 450 M	HE 550 M	HE 550 B	HE 550 A	219.1 x 16	244.5 x 10	244.5 x 8
3	HD 400 x 509•/+	HD 400 x 421•/+	HD 400 x 347•/+	HE 550 M	HE 600 B	HE 550 A	219.1 x 16	244.5 x 12	244.5 x 8
2	HD 400 x 509•/+	HD 400 x 421•/+	HD 400 x 347•/+	HE 550 M	HE 600 B	HE 550 A	219.1 x 16	244.5 x 12	244.5 x 8
1	HD 400 x 509•/+	HD 400 x 421•/+	HD 400 x 347•/+	HE 650 M	HE 650 B	HE 450 M	244.5 x 16	244.5 x 12	244.5 x 10

*All gravity resistant beams are IPE 330

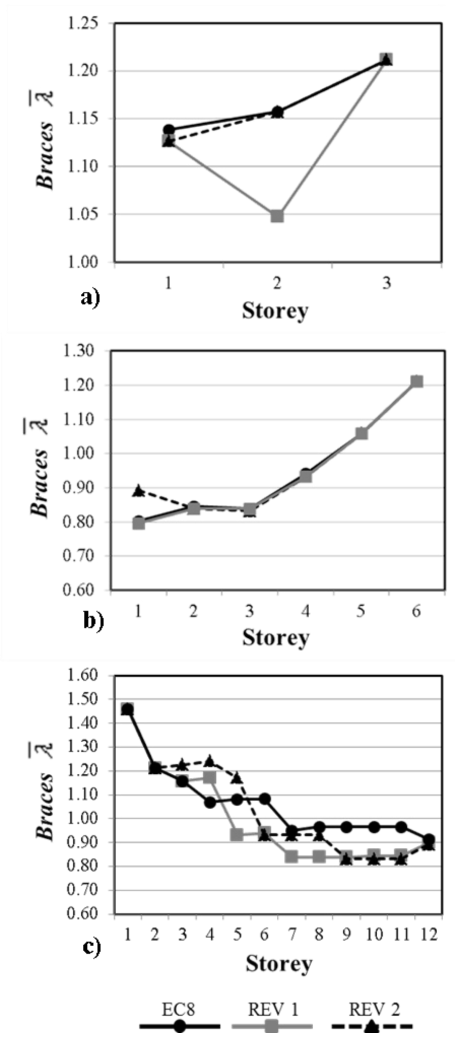

Figure 7.6 Braces normalized slenderness ratio: EN-1998 vs proposed revisions.

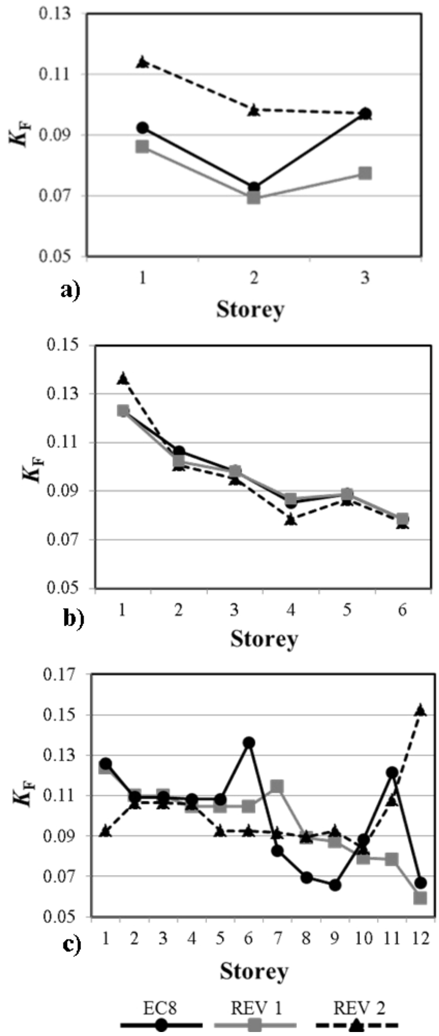

Figure 7.7 Beam-to-brace stiffness ratio: EN-1998 vs proposed revisions.

Table 7.13 Brace slenderness ratio for 3-storey cases: EN-1998 vs proposed revisions.

	Brace normalized slenderness $\bar{\lambda}$		
Storey	EC8	Rev 1	Rev 2
3	1.21	1.21	1.21
2	1.16	1.05	1.16
1	1.14	1.13	1.13

Table 7.14 Brace slenderness ratio for 6-storey cases: EN-1998 vs proposed revisions.

	Brace normalized slenderness $\bar{\lambda}$		
Storey	EC8	Rev 1	Rev 2
6	1.21	1.21	1.21
5	1.06	1.06	1.06
4	0.94	0.93	0.93
3	0.84	0.84	0.83
2	0.85	0.84	0.84
1	0.80	0.80	0.89

Table 7.15 Brace slenderness ratio for 12-storey cases: EN-1998 vs proposed revisions.

	Brace normalized slenderness $\bar{\lambda}$		
Storey	EC8	Rev 1	Rev 2
12	1.46	1.46	1.46
11	1.21	1.21	1.21
10	1.16	1.16	1.23
9	1.07	1.17	1.24
8	1.08	0.93	1.17
7	1.08	0.94	0.93
6	0.95	0.84	0.93
5	0.97	0.84	0.93
4	0.97	0.84	0.83
3	0.97	0.85	0.83
2	0.97	0.85	0.83
1	0.91	0.90	0.89

Table 7.16 Stiffness ratio for 3-storey cases: EN-1998 vs proposed revisions.

	Beam to brace stiffness ratio K_F		
Storey	EC8	Rev 1	Rev 2
3	0.10	0.08	0.10
2	0.07	0.07	0.10
1	0.09	0.09	0.11

Table 7.17 Stiffness ratio for 6-storey cases: EN-1998 vs proposed revisions.

	Beam to brace stiffness ratio K_F		
Storey	EC8	Rev 1	Rev 2
6	0.08	0.08	0.08
5	0.09	0.09	0.09
4	0.09	0.09	0.08
3	0.10	0.10	0.10
2	0.11	0.10	0.10
1	0.12	0.12	0.14

Table 7.18 Stiffness ratio for 12-storey cases: EN-1998 vs proposed revisions.

	Beam to brace stiffness ratio K_F		
Storey	EC8	Rev 1	Rev 2
12	0.07	0.06	0.15
11	0.12	0.08	0.11
10	0.09	0.08	0.08
9	0.07	0.09	0.09
8	0.07	0.09	0.09
7	0.08	0.11	0.09
6	0.14	0.10	0.09
5	0.11	0.10	0.09
4	0.11	0.10	0.11
3	0.11	0.11	0.11
2	0.11	0.11	0.11
1	0.13	0.12	0.09

Finally, Tables from 19 to 21 report the value of the overstrength ratio per storey for three, six and twelve-storey frames, respectively. It should be noted that consistently with the relevant criteria, the overstrength factor are evaluated according to Eq. (7.2) for the EN 1998-compliant frames and the “revision 1” and according to Eq. (7.3) for the “revision 2”.

As it can be observed, EN-1998 provisions generally lead to larger overstrength ratios respect to the proposed revisions. In detail, the “revision 1” (namely, excluding the roof storey from the requirement Ω on the variation) allows to avoid significant oversizing of the diagonal members at lower and intermediate storeys. As a consequence, also slightly smaller profiles for beams and columns can be selected respect to the EC8-compliant frames (see Tables from 10 to 12).

On the other hand, the “revision 2” allows obtaining smaller values of the overstrength ratios with $\Omega_1 < 1.5$, which obviously influence the design of columns, whose required strength is evaluated according to Eq. (3.2). Thereby smaller profiles can be selected, especially at intermediate storeys (see Tables from 10 to 12).

In addition, applying the “revision” 2 also allows reducing the overstrength percentage variation (namely the quantity $(\Omega_i - \Omega)/\Omega$) in medium and high rise buildings. Indeed, the percentage variation is equal to 0.17, for the six-storey frame and to 0.19 for the twelve-storey frames against the 0.18 and 0.24 obtained in the EC8-compliant frames, respectively.

Table 7.19 Overstrength ratio for 3-storey cases: EN-1998 vs proposed revisions.

	Overstrength ratios		
Storey	EC8*	Rev 1*	Rev 2**
3	2.34	2.34	1.23
2	2.02	1.67	1.13
1	2.14	1.73	1.00

* Ω_i evaluated according to Eq. (7.2)

** $\Omega_{b,i}$ evaluated according to Eq. (7.3)

Table 7.20 Overstrength ratio for 6-storey cases: EN-1998 vs proposed revisions.

	Overstrength ratios		
Storey	EC8*	Rev 1*	Rev 2**
6	2.05	2.05	1.07
5	1.77	1.77	1.11
4	1.85	1.49	1.07
3	1.73	1.73	1.09
2	1.86	1.56	1.21
1	1.86	1.56	1.03

* Ω_i evaluated according to Eq. (7.2)

** $\Omega_{b,i}$ evaluated according to Eq. (7.3)

Table 7.21 Overstrength ratio for 12-storey cases: EN-1998 vs proposed revisions.

	Overstrength ratios		
Storey	EC8*	Rev 1*	Rev 2**
12	3.34	3.34	1.30
11	2.72	2.72	1.42
10	2.72	2.72	1.32
9	2.93	2.68	1.27
8	2.94	2.28	1.24
7	2.69	2.49	1.43
6	2.79	2.53	1.30
5	3.25	2.35	1.21
4	3.08	2.22	1.39
3	2.95	2.54	1.34
2	2.87	2.47	1.30
1	3.00	2.29	1.42

* Ω_i evaluated according to Eq. (7.2)

** $\Omega_{b,i}$ evaluated according to Eq. (7.3)

7.3 SEISMIC PERFORMANCE EVALUATION

7.3.1 *Modelling assumptions*

The numerical behaviour of the designed frames was simulated using a 2D planar model. Indeed, EC8 allows using simplified modelling approach if the building is conforming to the criteria for regularity both in plan and in elevation.

Masses are considered as lumped into a selected masterjoint at each floor, because the floor diaphragms may be taken as rigid in their planes.

The calculation models assume pinned connections for beam-to-column connections; the bracing members are modelled as fixed in the plane of the frames and pinned in out-of-plane direction. Columns are considered continuous through each floor beam. The nonlinear behaviour of members was simulated as described in Section 5.2.3; the diagonal members behaviour is simulated by means of the physical theory model described in Chapter IV.

The P–Δ effects were accounted for by assigning the gravity loads on the interior frames to fictitious column, connected to the main frame using pinned rigid links. In such a way, this column has no lateral stiffness but it carries all vertical loads from the gravity frames.

The eigenvalue analyses are solved by using Jacobi algorithm with Ritz transformation.

Concerning dynamic analyses a 2% Rayleigh tangent stiffness damping was used at both first and second modes.

7.3.2 *Eigenvalue analyses*

Figure 7.8 depicts the period of vibration for the first (T_1) and the second (T_2) mode of vibration for all low, medium and high rise frames designed according to the three examined codes; the relevant participating mass percentages ($M_{x,1}$ and $M_{x,2}$ respectively) are shown in Fig. 7.9. Either periods of vibration and participating mass percentages are even summarized in Tables from 7.22 to 7.24.
It should be noted that both the North-American codes lead designing more deformable structures respect to the European one. In detail AISC-compliant frames exhibit the largest period of vibration (highlighted in bold in Tables from 7.22 to 724) for both first and second vibration mode. However, no appreciable differences can be recognized between the examined codes in terms of participating mass percentages (see Fig. 7.9).

In addition, Figures 7.10 and 7.11 show the periods of vibration and the participating mass percentages of the frames obtained applying the critical revisions to EN-1998 described in previous Sections, also compared with those obtained according to the codified criteria. Either periods of vibration and participating mass percentages are even summarized in Tables from 7.22 to 7.24.

It is worth noting that both the proposed revisions lead to slightly larger periods of vibration respect to the EC8-compliant cases (see Fig. 7.10). This feature can be easily explained considering that modifying the requirement on the overstrength variation allowed using more slender braces, resulting in more deformable frames; this effect is more evident for the first vibration mode and for the high rise building.

Also in this case no appreciable differences can be recognized in terms of participating mass percentages (see Fig. 7.11).

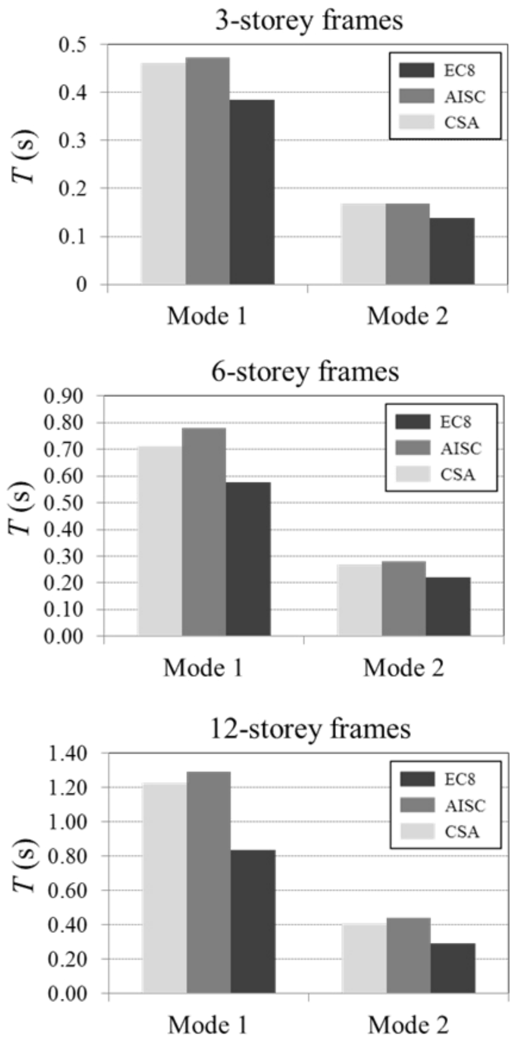

Figure 7.8 Periods of vibration: comparison between examined codes.

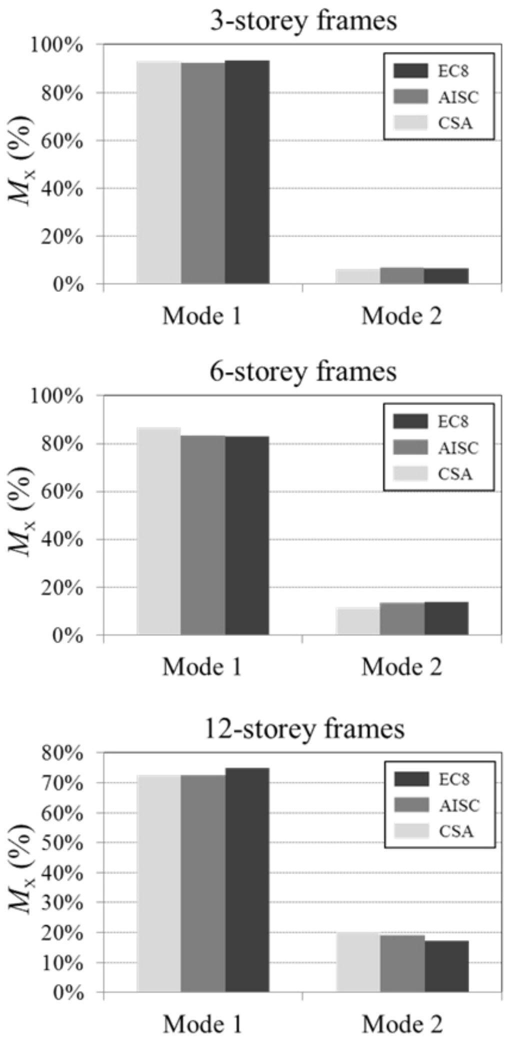

Figure 7.9 Participating mass percentages: comparison between examined codes.

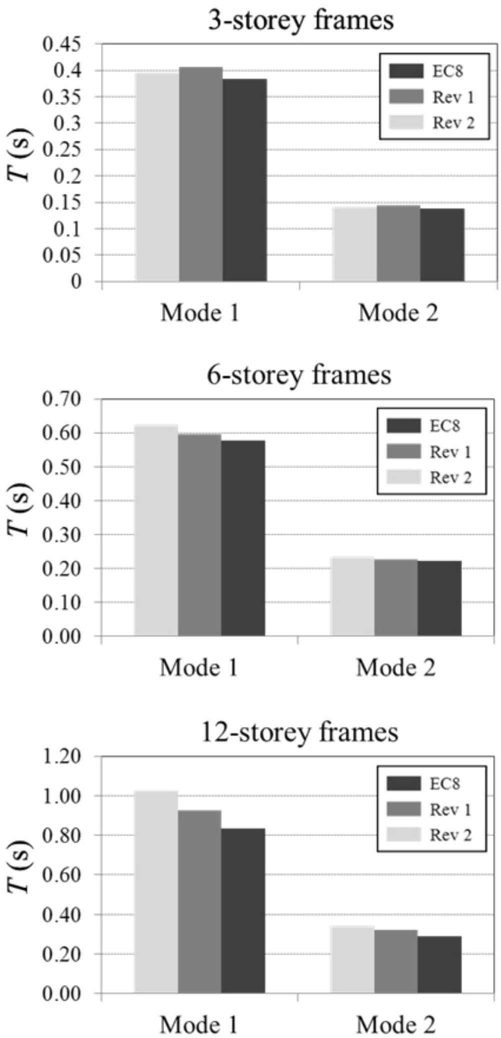

Figure 7.10 Periods of vibration: EN-1998 vs proposed revisions.

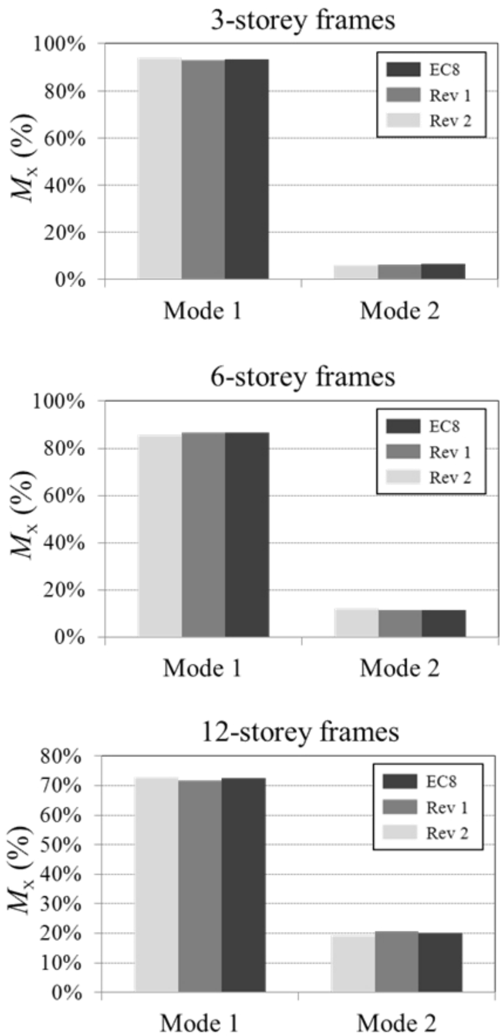

Figure 7.11 Participating mass percentages: EN-1998 vs proposed revisions.

Table 7.22 Dynamic characteristics of 3-storey cases.

Case	T_1 (sec)	T_2 (sec)	$M_{x,1}$ (%)	$M_{x,2}$ (%)
EC8	0.38	0.14	93.15%	6.69%
AISC	**0.47**	**0.17**	92.79%	6.43%
CSA	0.46	**0.17**	93.08%	6.17%
Rev 1	0.41	0.14	93.06%	6.31%
Rev 2	0.40	0.14	94.06%	5.75%

Table 7.23 Dynamic characteristics of 6-storey cases.

Case	T_1 (sec)	T_2 (sec)	$M_{x,1}$ (%)	$M_{x,2}$ (%)
EC8	0.58	0.22	86.54%	11.47%
AISC	**0.78**	**0.28**	83.47%	13.42%
CSA	0.71	0.27	82.93%	13.80%
Rev 1	0.60	0.23	86.58%	11.39%
Rev 2	0.62	0.23	85.51%	12.34%

Table 7.24 Dynamic characteristics of 12-storey cases.

Case	T_1 (sec)	T_2 (sec)	$M_{x,1}$ (%)	$M_{x,2}$ (%)
EC8	0.84	0.29	72.55%	20.26%
AISC	**1.29**	**0.44**	72.45%	19.10%
CSA	1.23	0.41	74.90%	17.13%
Rev 1	0.92	0.32	71.71%	20.71%
Rev 2	1.02	0.34	72.83%	19.39%

7.3.3 *Non-linear dynamic analyses*

7.3.3.1 Seismic hazard levels

The seismic response obtained for all the examined cases was evaluated for the three seismic hazard levels as given according to Eurocode 8, which are associated to different annual rates of exceedance: damage limitation (DL), severe damage (SD) and near collapse (NC).

In Eurocode 8, the seismic hazard is expressed in terms of the value of the reference peak ground acceleration a_{gR} on bedrock corresponding to the 10% probability of exceedance (i.e. a return period equal to 475years). To obtain the reference peak ground acceleration for different probabilities of exceedance in 50 years EC8 introduces an importance factor γ_I multiplying a_{gR} that is given as follows:

$$\gamma_I = \left(\frac{T_{LR}}{T_L} \right)^{-1/3} \tag{7.4}$$

being T_L the return period and T_{LR} the reference return period for which the reference seismic action may be computed.

According to Eurocode 8 the considered values of γ_I for DL SD and NC are 0.59, 1 and 1.72 respectively.

7.3.3.2 Records

A set of 14 natural earthquake acceleration records was considered to perform the dynamic time history analyses on the examined cases. The signals were obtained from the RESORCE ground motion database (Akkar *et al.*, 2014) and selected according to procedure described in (Fulop, 2010) in order to match the elastic acceleration spectrum provided for by EN 1998-1 corresponding to the seismic hazard level associated with the Severe Damage limit state (i.e. 10% probability of exceedance in 50 years). The data of the records and the comparison with the design spectrum provided by EC8 can be found in (Section 5.7.3.2). In addition, in order to calculate the residual inter-storey drift ratios from the dynamic time history analyses, each record was fictitiously extended by 10 seconds at zero acceleration.

7.3.3.3 Seismic performance evaluation

Both global and local performance indicators were select to evaluate the seismic response of all the examined frames.

The monitored parameters for all limit states are summarized as follow:

- *Global response indicator:*

i) peak transient interstorey drift ratio θ (given by the horizontal relative displacement at each storey divided by the interstorey height)

ii) residual interstorey drift ratios θ_{RES}: it is defined as the average value of relative horizontal displacements at each storey experienced during the last 10 seconds at zero acceleration fictitiously added to each record, divided by the interstorey height.

iii) peak storey accelerations A normalized to the design ground acceleration A_d

- *Local performance indicators:*

i) braces ductility demand (μ) both in tension and compression is given by the ratio:

$$\mu = \frac{d}{d_y} \tag{7.5}$$

where d is the brace axial displacement and d_y the displacement of the brace at yielding.

ii) brace axial deformation under compression (μ_χ) normalized to the buckling. It is given by the ratio:

$$\mu_\chi = \frac{d}{d_b} \tag{7.6}$$

where d is the brace axial displacement and d_b the displacement of the brace at buckling (namely equal to χd_y).

iii) brace out-of-plane deflection expressed in terms of: both brace out-of-plane rotation θ_{BR} and normalized displacement w. The brace rotation is defined as:

$$\theta_{br} = \frac{w}{0.5 \cdot L_{br}} \tag{7.7}$$

being w the out-of-plane displacement at the mid-length and L_{br}, the length of the diagonal member.

The normalized brace out-of-plane displacement is defined in Fig. 5.27a in Section 5.7.3.3 of Chapter V.

ii) normalized unbalanced force (β) applied on the beam

- The normalized unbalanced force applied to the beam when the buckling of the brace in compression occurs. This parameter is defined as:

$$\beta = \frac{N_{T,br} - N_{C,br}}{N_{pl,br}} \tag{7.8}$$

iii) beam chord rotation θ_b defined as:

$$\theta_b = \frac{d_{z,b}}{0.5 L_b} \tag{7.9}$$

where $d_{z,b}$ is the beam vertical displacement at the beam mid length and L_b is the beam length.

The analyses results are presented hereinafter, by showing the average demand obtained by the 14 considered records per response indicator.

Figure 7.12 depicts both transient (θ, see Fig. 7.12a) and residual (θ_{RES}, Fig. 7.12b) interstorey drift ratios for the three-storey frames, for the three considered performance levels. EC8-compliant frame experiences the largest lateral stiffness with interstorey drift ratios lesser than 0.5% up to NC limit state. However, all the examined three-storey frames exhibit satisfactorily performance at DL limit state according to the interstorey drift ratios limitation provided by EN 1998-1 for buildings having ductile non-structural elements and for buildings having non-structural elements fixed in a way so as not to interfere with structural deformations or without non-structural elements (namely 0.75% and 1%, respectively).

Both US and Canadian codes lead to larger residual interstorey drift ratios respect to the EC8-compliant case. However, acceptable values (lesser than 0.1%) at SD are experienced for all the frames.

The same response parameters are shown in Figs. 7.13a,b and 7.14a,b for both six and twelve-storey frames, respectively.

By observing Fig. 7.13a, different displacement shape profiles can be recognized for the six-storey cases between European and North-American codes, namely cantilever shape for EC8-compliant case, and shear-type for CSA and AISC-compliant frames. Also for six-storey frames, slightly larger residual interstorey drift ratios are experienced for the North-American codes, respect to the European case.

Similar behaviour can be recognized for twelve-storey frames: EC8-compliant case shows the largest lateral stiffness and a typical cantilever displacement shape characterized by drift demand concentration at upper storeys. CSA and AISC-compliant frames exhibit very similar responses with larger horizontal displacements but more uniform distribution of drift demand along the building height until NC limit state, for which demand concentration can be recognized at storey from 2nd to 5th.

Figures from 7.15 to 7.17 show the profiles of peak storey accelerations for three, six and twelve-storey frames, respectively: EC8-compliant frame is characterized by significant storey accelerations, whose peak average value (A) increases up to over 20 times the peak record acceleration (A_d) at both SD and NC limit state for the three-storey frame. This feature is even more evident in the six-storey case where the peak storey acceleration is amplified by 35 times respect to the ground acceleration $A_{d.}$ On the contrary, the significantly smaller average peak storey accelerations are less than the half into the three-storey frame designed according to the North-American codes, and even about 10 times lesser in the six-storey frames due to the larger dissipative capacity provided by the yielding of braces (see Figs. from 7.18 to 7.20).

For all the examined codes, the peak storey accelerations reach smaller value for the twelve-storey frames respect to the low and medium rise buildings; this feature can be easily explained considering that the high rise building are characterized by larger value of the fundamental period, and thus natural frequencies to which smaller spectral accelerations correspond.

Figures from 7.18 to 7.20 depict the braces ductility demand (μ) both in tension and in compression, for low, medium and high rise buildings, respectively.

The EC8-compliant frames show the smallest energy dissipation capacity: the three-storey case cannot experience any yielding phenomena under tension up to NC limit state; also for six and twelve-storey cases very limited plastic engagement can be recognized at upper storeys. Indeed, the cantilever-type behaviour entails significant engagement at the top of the building where also severe deterioration in the braces under compression can be recognized.

CSA and AISC-compliant cases exhibit slightly larger energy dissipation capacity with larger number of braces under tension attaining their plastic strength; these results confirm the outcomes previously described in Chapter V, being the frames designed according to the North-American codes characterized by larger values of beam-to-brace stiffness ratio K_F. However, also significant concentration of damage under compression occurs mainly due to the increased lateral deformability respect to the European cases.

Figures from 7.21 to 7.23 show the axial deformation of diagonal members under compression, normalized to the displacement at the brace buckling (see Eq. 7.6). It is interesting to note that all the examined frames, even those designed according to the Eurocodes, exceed the limits for axial deformation capacity provided by EN1998-3 (namely $\mu_{\chi,lim}$ = 0.25 at DL, $\mu_{\chi,lim}$ = 4 at SD and $\mu_{\chi,lim}$ = 6 at NC limit state for class of cross section 1). Indeed, by observing the figures, significantly larger engagement can be recognized at all the three considered limit states.

This consideration is in line with the literature. In particular, several experimental studies (e.g. Tremblay, 2002 and Goggins *et al*., 2006) show that the axial deformation limits recommended by EN1998-3 are too restrictive.

Regarding the brace under compression, Figures 7.24-26 show the brace out-of-plane deformations, expressed in terms of both, out of plane rotation θ_{br} (a) and normalized displacement $\overline{w}$ (b) (see Fig. 5.27a in Section 5.7.3.3). Coherently with the displacement shape and the brace ductility demand profiles, larger out-of-plane deformations can be recognized for the North-American code-compliant frames being equipped with more slender bracings respect to the European ones.

In detail, the normalized displacement $\overline{w}$ (calculated as described Fig. 5.27a in Section 5.7.3.3) shows that in most of cases $\overline{w} > 1$ also for DL limit state, so that the functionality of cadding walls is compromised. The only exception is constituted by the EC8-compliant cases for three and twelve-storey frames, attaining $\overline{w} \leq 1$.

The beam response is assessed by means of the normalized unbalanced force β (see Eq. 7.8) occurring after the brace buckling under compression; in addition the beam chord rotation ($\theta_{b,}$ see Eq. 7.9) is monitored in order to highlight eventual flexural yielding phenomena. Figures from 7.27 to 7.29 report the normalized unbalanced force β. It is trivial to observe that the bending demand on the brace-intercepted beam is strongly related to the unbalanced force and thus to the post-buckling behaviour of the compression brace; as already discussed in Chapter III, it is well known that the degradation of compression strength under repeated cyclic loadings is affected, among other parameters, by the braces slenderness ratio. As highlighted in Section 7.2, the frames designed according to EN 1998 are characterized by stockier bracings respect to the other cases. By observing Figs. from 7.27 to 7.29 it can be recognized that the unbalanced force acting at the brace-intercepted section is significantly smaller for the EC8-compliant frames. However, this apparently desirable behaviour is actually due to poor plastic engagement of the braces under tension, rather than to limited degradation of their compression strength. This feature is confirmed by observing the results for the twelve-storey frames in Fig. 7.29.

Indeed, the high rise frames designed according to AISC and CSA exhibit low β values at the intermediate storey, although characterized by more slender braces respect to the European case. In order to clarify this aspect, Figure 7.30 reports the distribution of both braces normalized slenderness $\bar{\lambda}$ (see Fig. 7.30a) and normalized unbalanced force β (see Fig. 7.30b) achieved at the three considered limit state for the AISC-compliant case: no direct relationship can be observed between the slenderness ratios of the bracing members and the unbalanced force occurring in the post-buckling range, being the latter also affected by the level of plastic engagement and the dynamic characteristics (namely the displacement shape profile) of the structure.

Moreover, comparing these results with those depicted in Fig. 7.20, it can be noted that the most stressed beams are located at levels where poor plastic engagement is experienced by the braces under both tension and compression. Indeed, the bending demand on the beam increases with the increasing of the unbalanced force due to the resultant of vertical components of axial forces transmitted by both bracings in tension and compression.

Figures from 7.31 to 7.33 show the beam chord rotation (see Eq. 7.9) for three, six and twelve-storey frames, respectively; moreover the normalized beam rotation is reported (Figs. 7.31-33b) in order to identify eventual yielding phenomena. The bending demand distribution on the beams along the building height is basically consistent to the normalized unbalanced force profiles; no plastic hinge occurs in the beams belonging to all low, medium and high rise buildings. However, the EC8-compliant frames experience large rotation, very close to the yielding at the upper stories in both six and twelve-storey frames (see Figs. 7.32b and 7.33b).

Moreover, it is worth to note that twelve-storey frames experience negative bending demand on the beam at the first storey; indeed at this level, the braces basically behave elastically and acting as intermediate support for the beam, thus resulting in negative bending moment.

Beside the beam chord rotation, Figures from 7.34 to 7.36 show the beam vertical displacement $d_{z,beam}$ normalized to the relative horizontal displacement at each storey ($d_{x,i}$). This parameter clarifies that the larger values of beams chord rotation recognized for CSA and AISC compared to the EC8-compliant three and six-storey frames (see Figs. 7.31 and 7.32) are actually due to the increased overall lateral deformability of the structures designed according to the North-American codes, rather than to the flexural deformability of the beams. Indeed, by observing Figs. 7.34 and 7.36 more flexible beams can be recognized in EC8-compliant frames, whose contribution to the overall deformability (see Fig. 5.1) is larger in percentage respect to the CSA and AISC-compliant cases.

Such behaviour cannot be recognized for twelve-storey cases, for which the profiles of vertical displacement normalized to the relative horizontal displacement at each storey are consistent with the relevant chord rotation profiles.

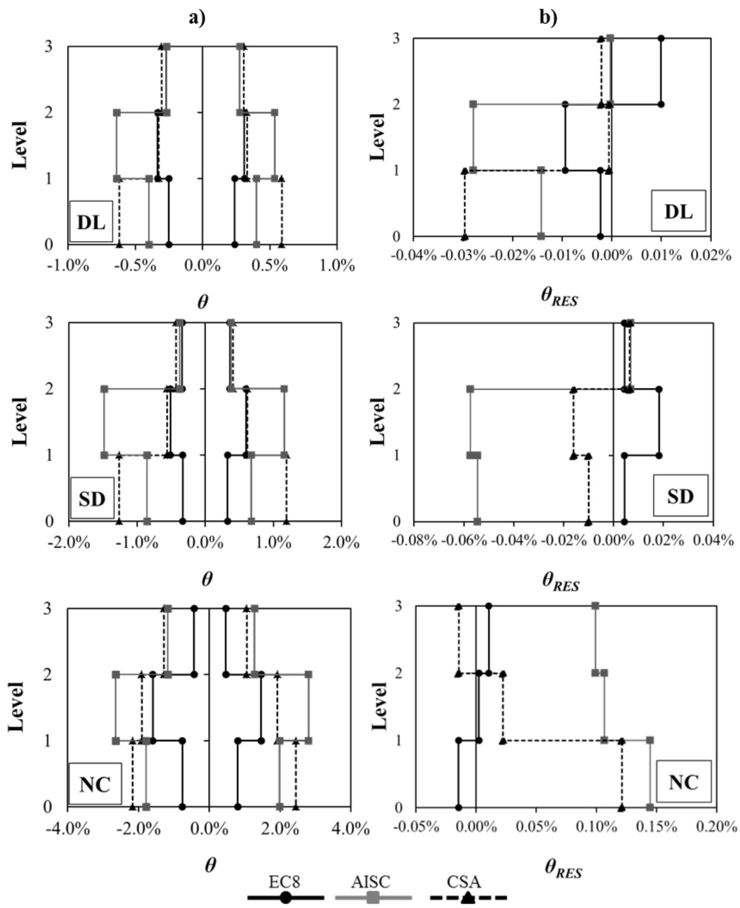

Figure 7.12 Interstorey drift transient (a) and residual (b) for 3-storey cases: comparison between examined codes.

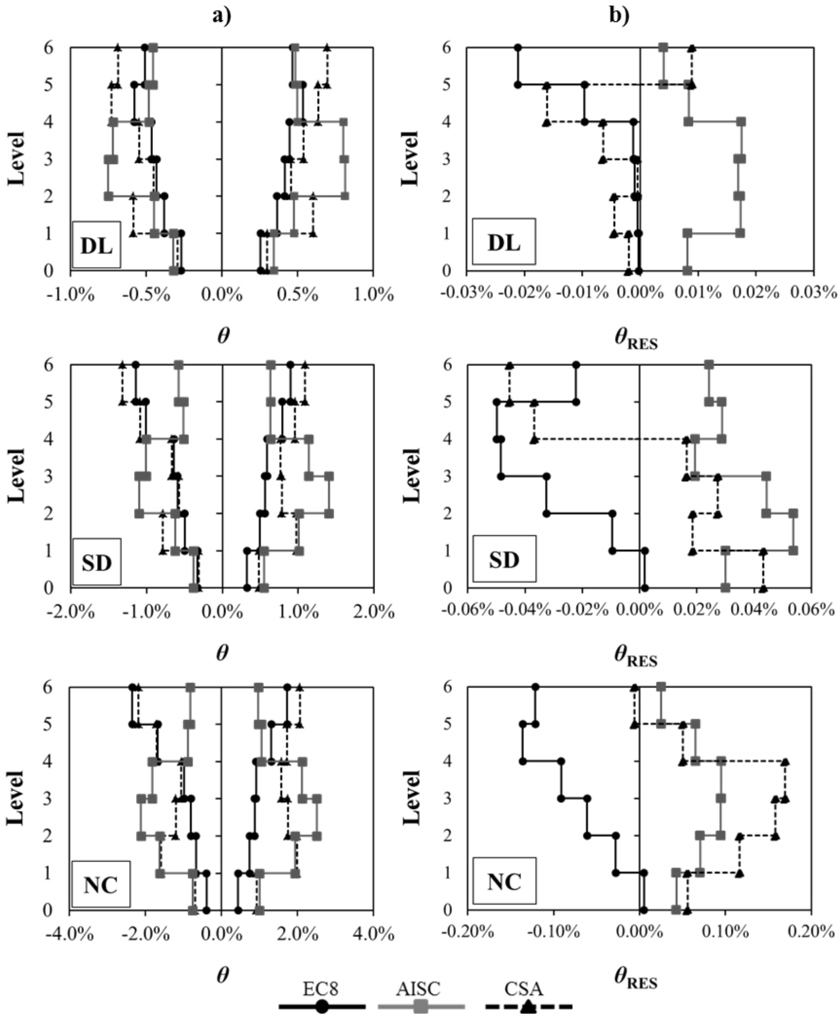

Figure 7.13 Interstorey drift transient (a) and residual (b) for 6-storey cases: comparison between examined codes.

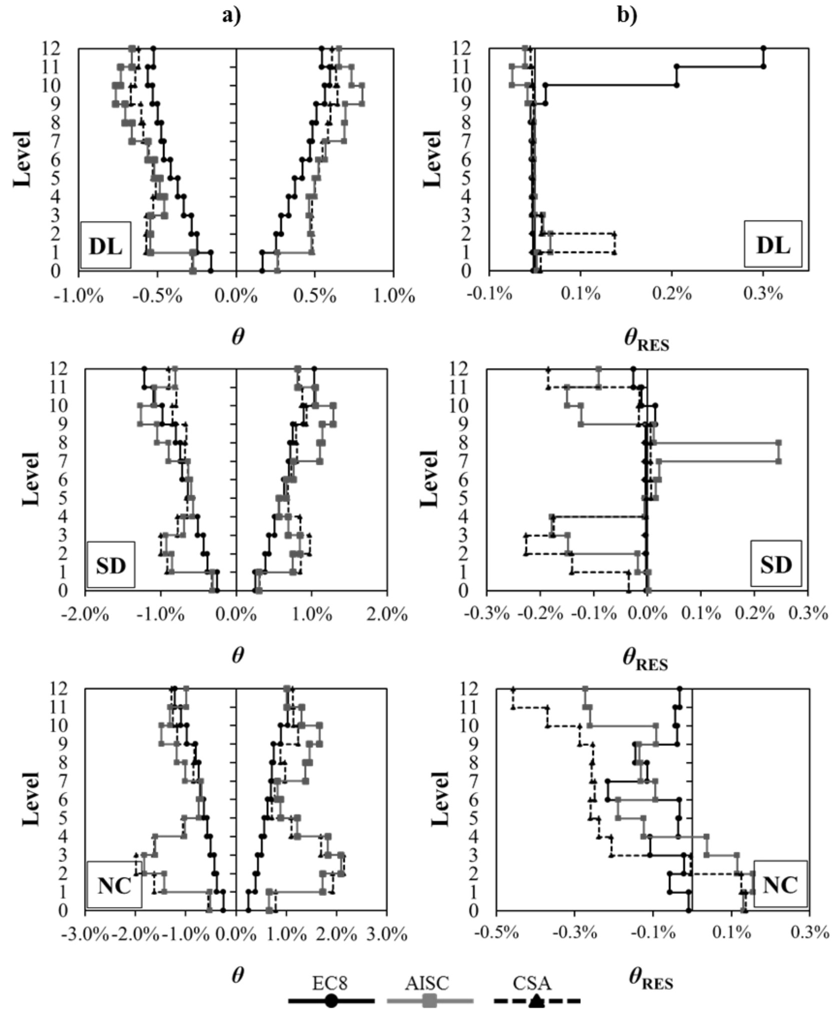

Figure 7.14 Interstorey drift transient (a) and residual (b) for 12-storey cases: comparison between examined codes.

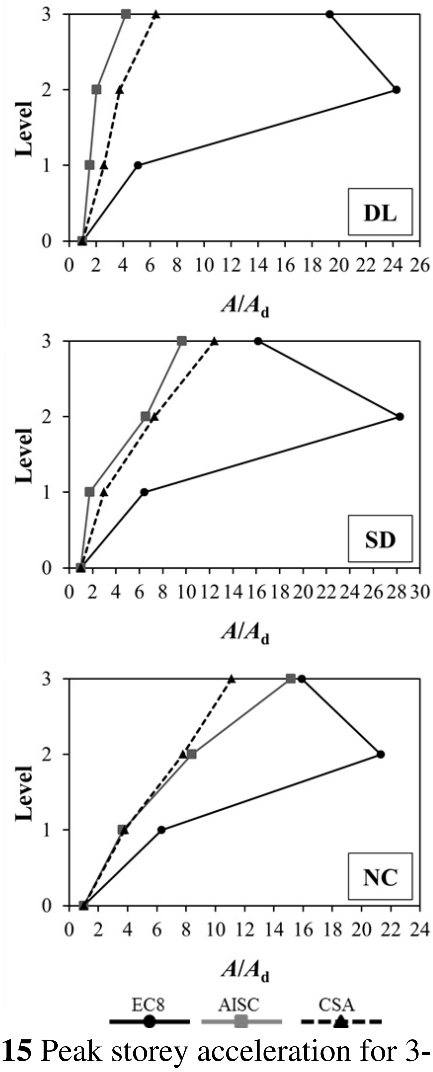

Figure 7.15 Peak storey acceleration for 3-storey cases: comparison between examined codes.

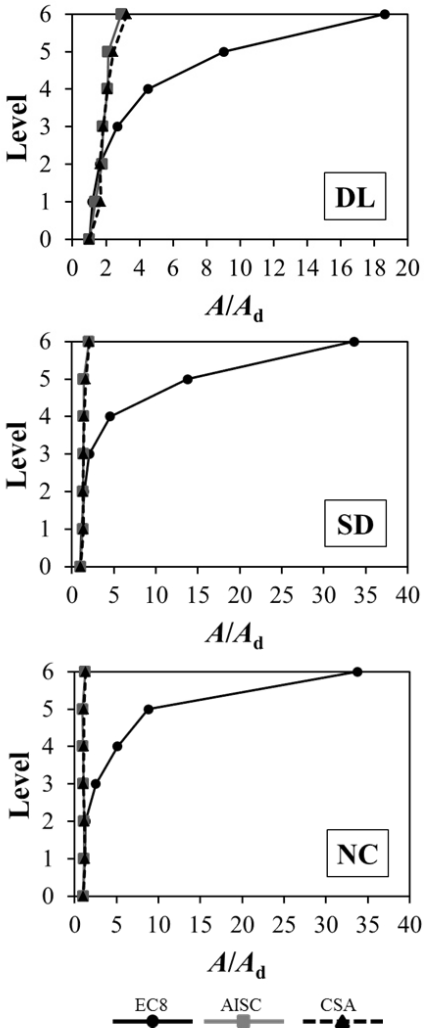

Figure 7.16 Peak storey acceleration for 6-storey cases: comparison between examined codes.

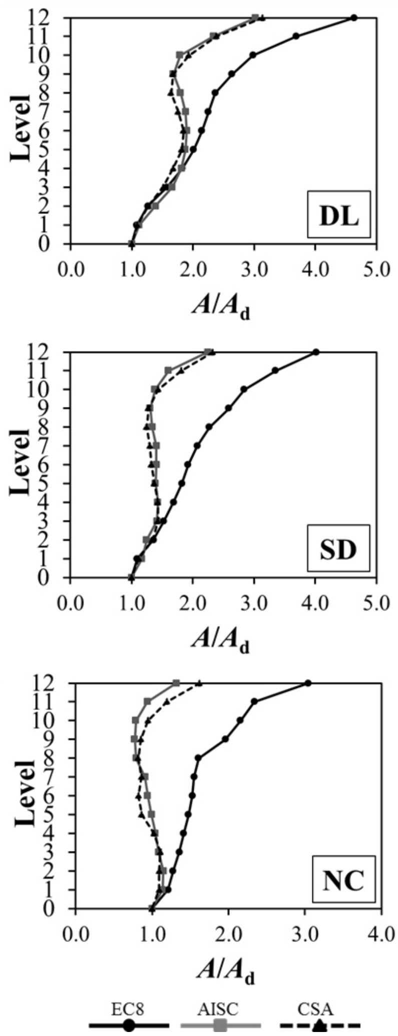

Figure 7.17 Peak storey acceleration for 12-storey cases: comparison between examined codes.

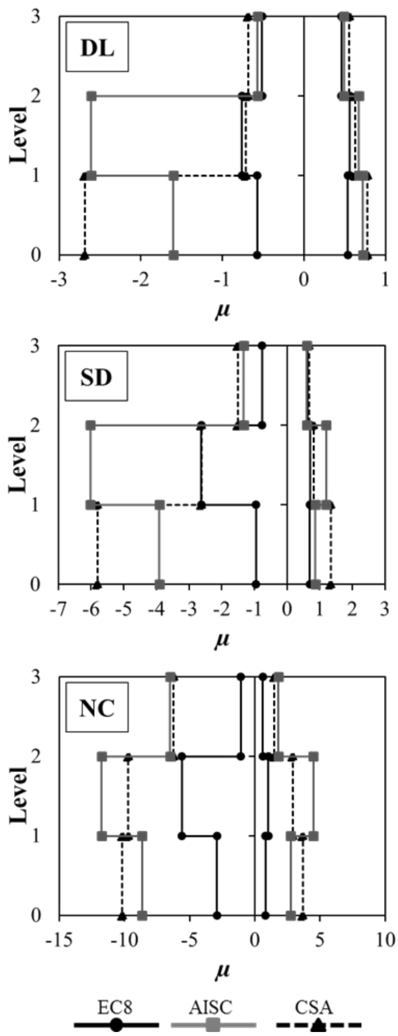

Figure 7.18 Braces ductility demand for 3-storey cases: comparison between examined codes.

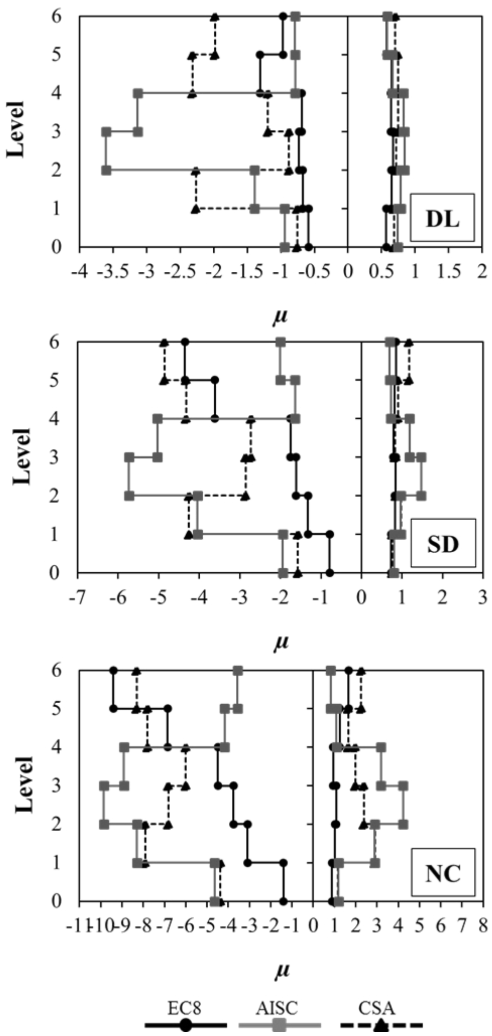

Figure 7.19 Braces ductility demand for 6-storey cases: comparison between examined codes.

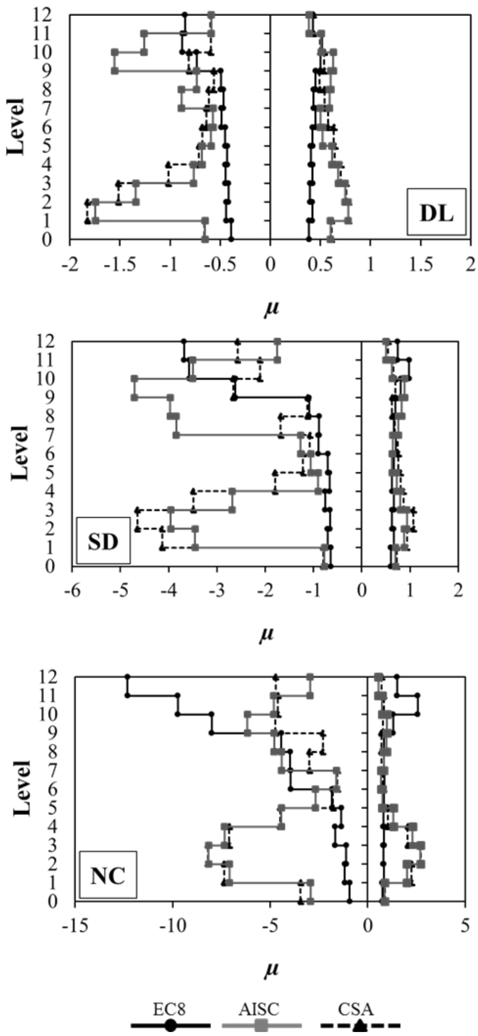

Figure 7.20 Braces ductility demand for 12-storey cases: comparison between examined codes.

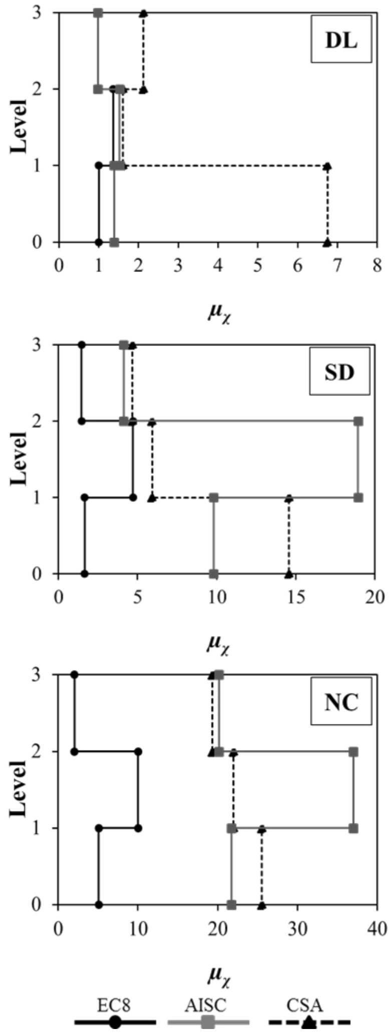

Figure 7.21 Ductility demand in compression for 3-storey cases: comparison between examined codes.

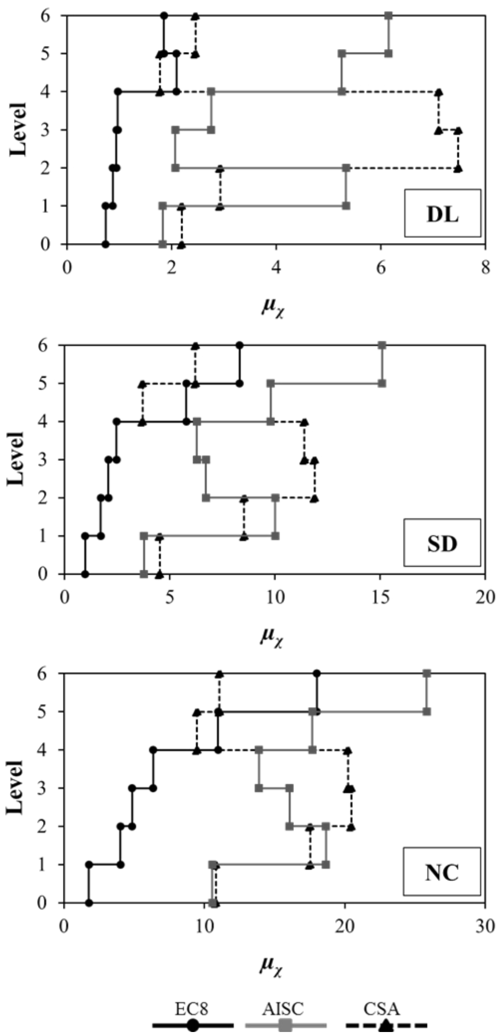

Figure 7.22 Ductility demand in compression for 6-storey cases: comparison between examined codes.

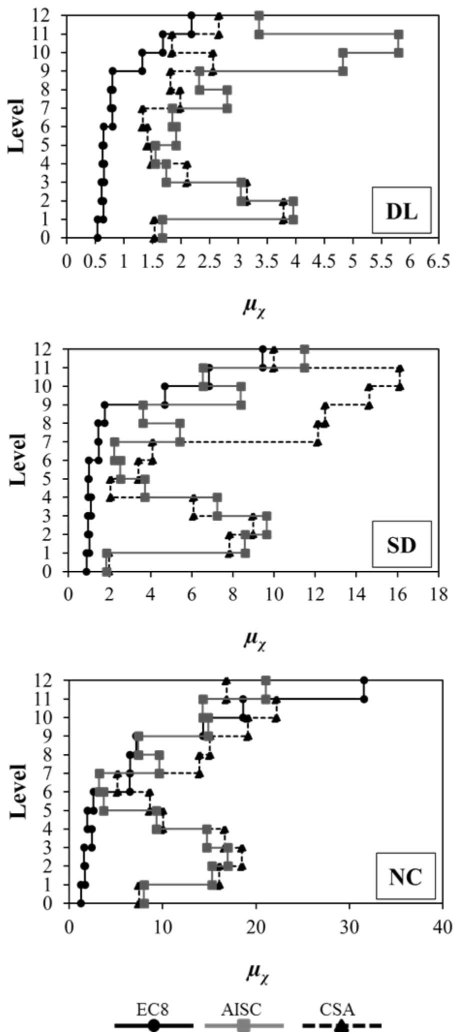

Figure 7.23 Ductility demand in compression for 12-storey cases: comparison between examined codes

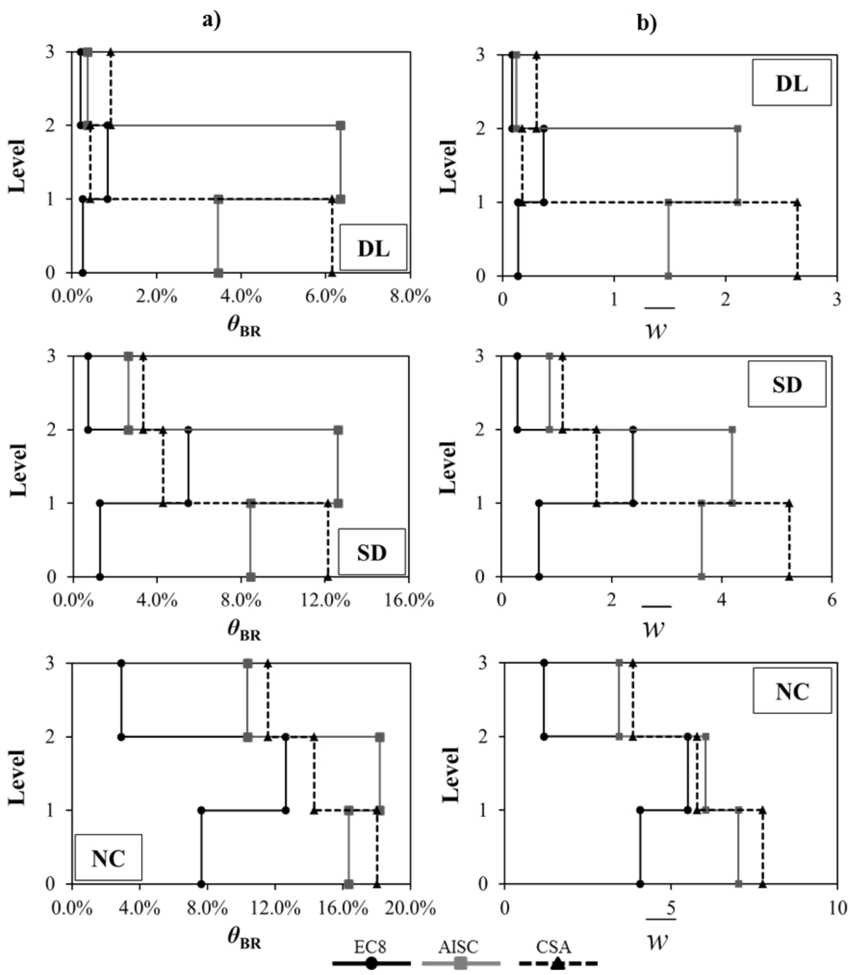

Figure 7.24 Braces out-of-plane rotations (a) and normalized displacements (b) for 3-storey cases: comparison between examined codes.

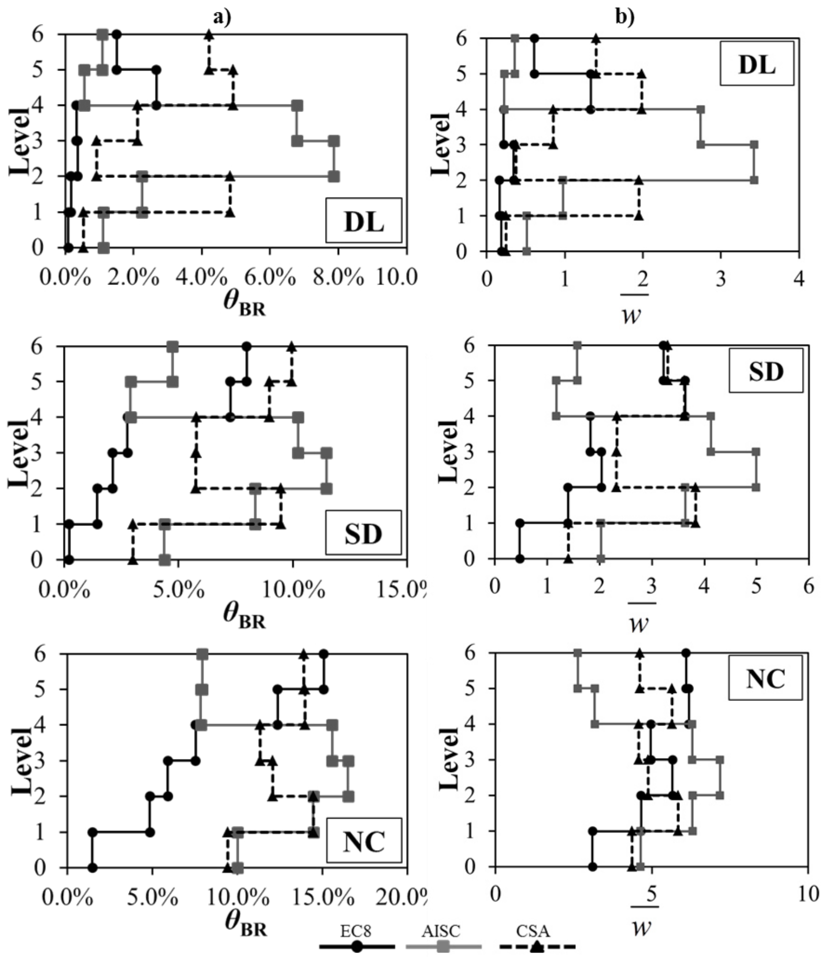

Figure 7.25 Braces out-of-plane rotations a) and normalized displacements (b) for 6-storey cases: comparison between examined codes.

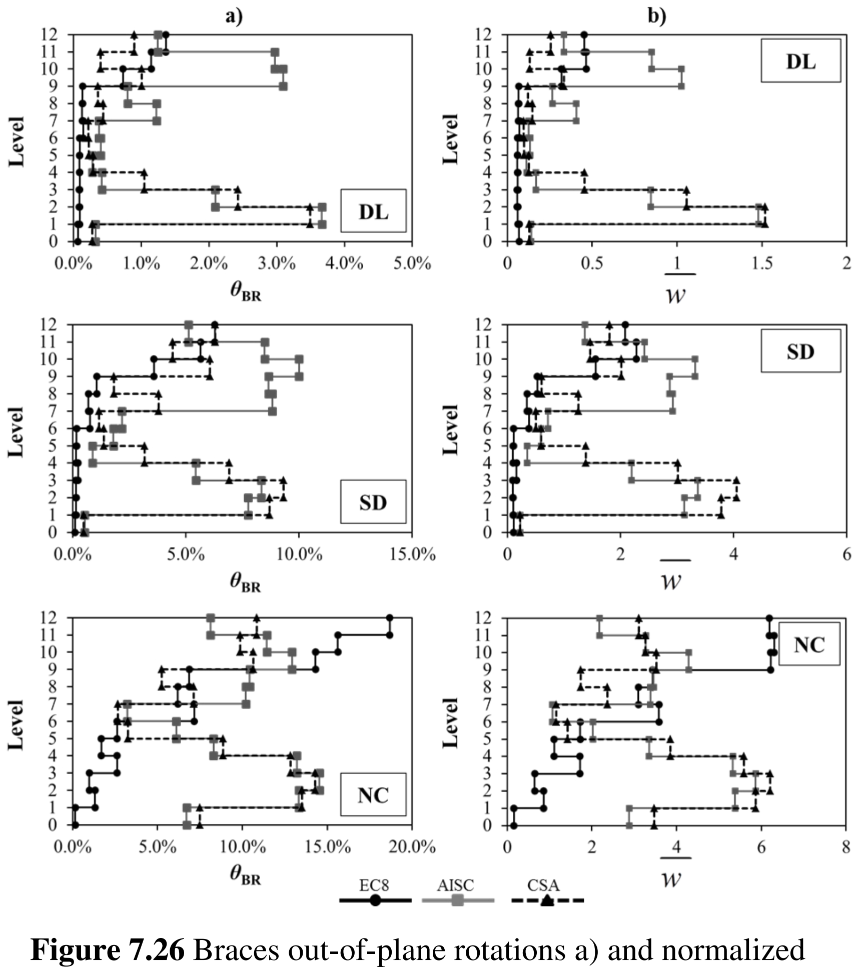

Figure 7.26 Braces out-of-plane rotations a) and normalized displacements (b) for 12-storey cases: comparison between examined codes.

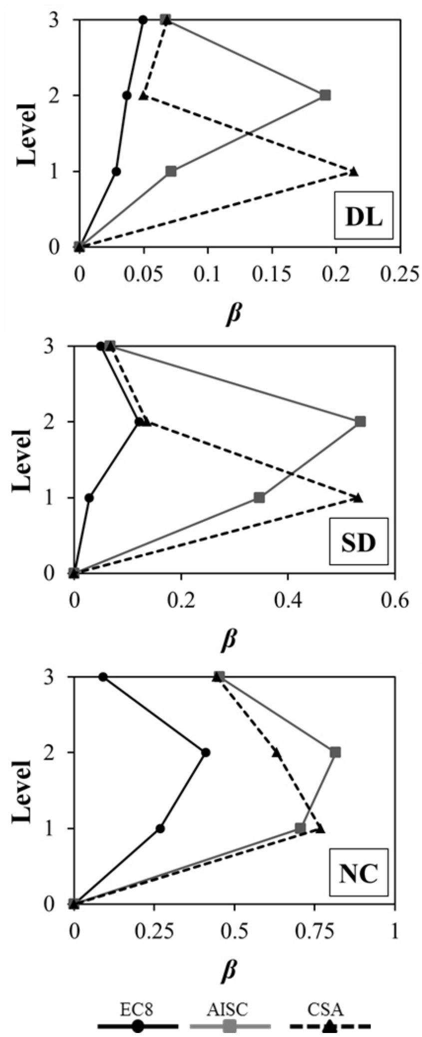

Figure 7.27 Unbalanced force applied on the beam for 3-storey cases: comparison between examined codes.

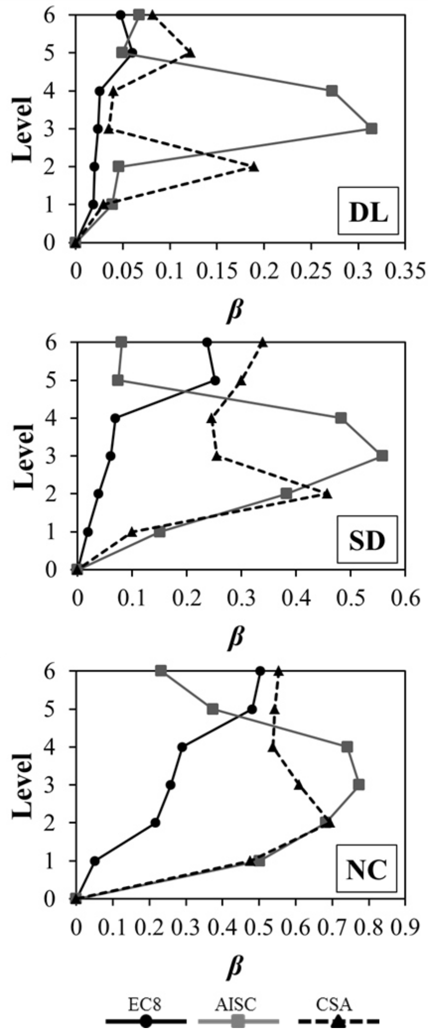

Figure 7.28 Unbalanced force applied on the beam for 6-storey cases: comparison between examined codes.

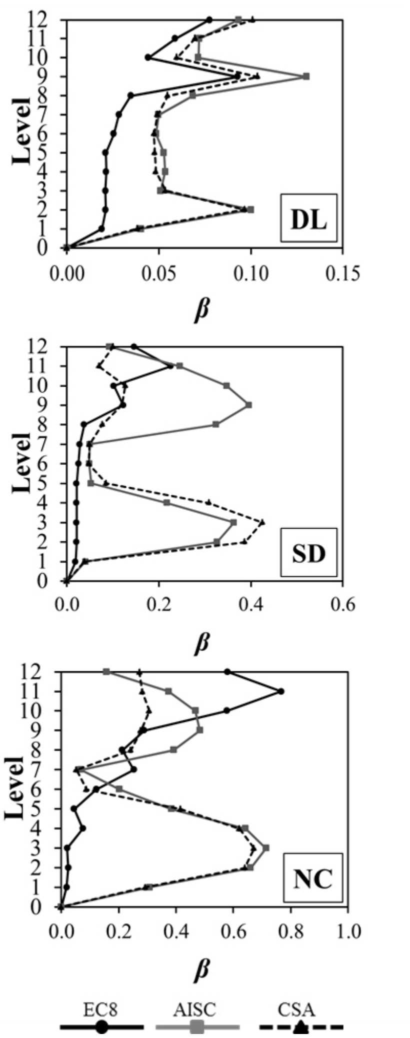

Figure 7.29 Unbalanced force applied on the beam for 12-storey cases: comparison between examined codes.

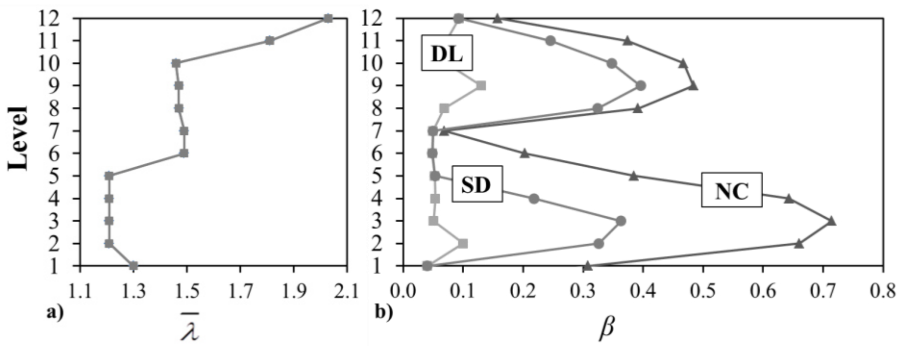

Figure 7.30 Relationship between brace slenderness ratio (a) and normalized unbalanced force (b) profiles for AISC-compliant 12-storey cases.

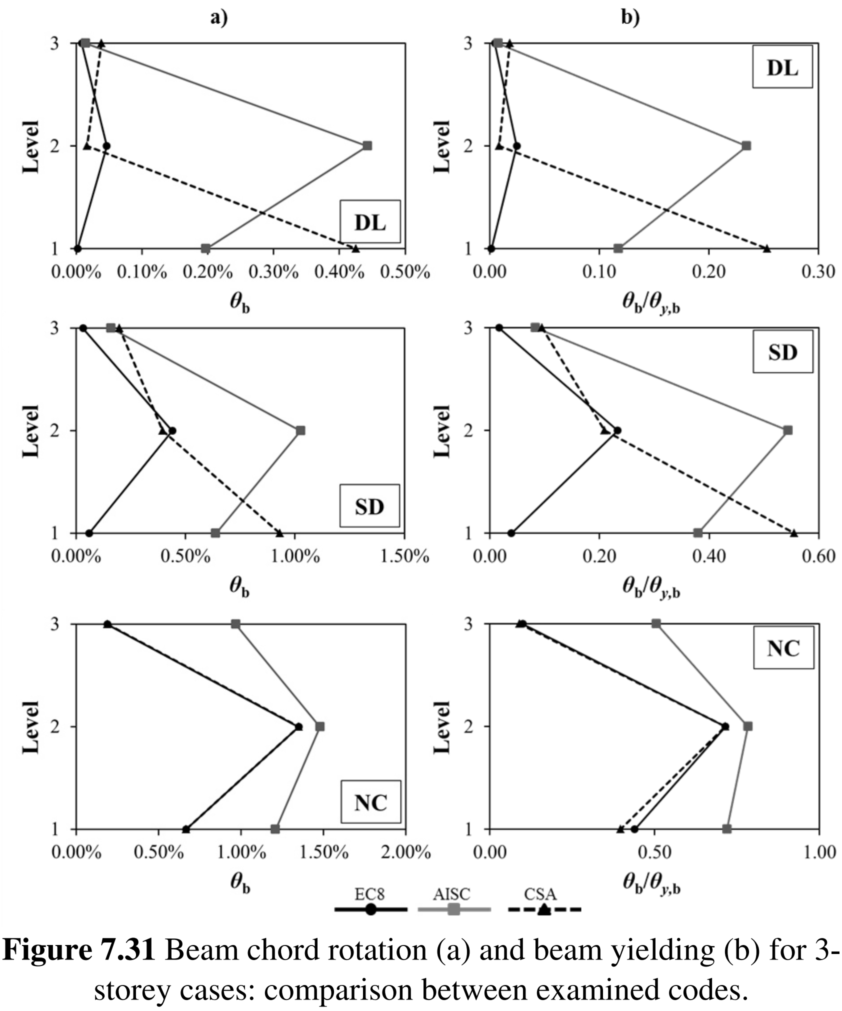

Figure 7.31 Beam chord rotation (a) and beam yielding (b) for 3-storey cases: comparison between examined codes.

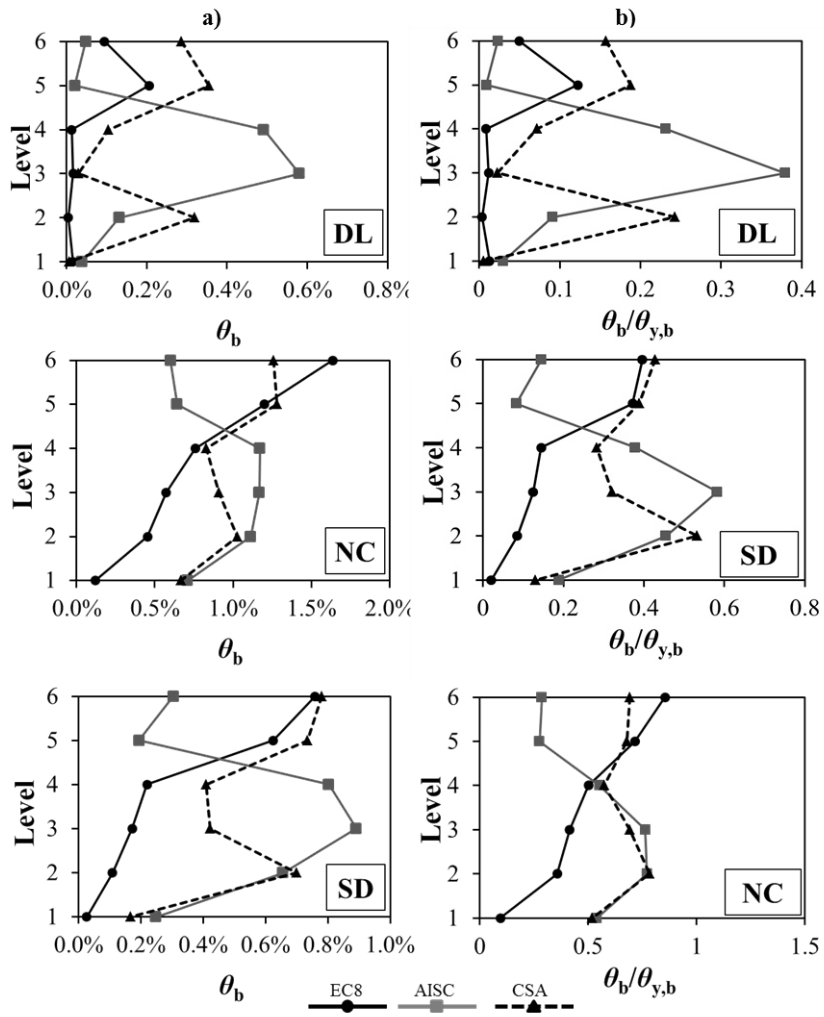

Figure 7.32 Beam chord rotation (a) and beam yielding (b) for 6-storey cases: comparison between examined codes.

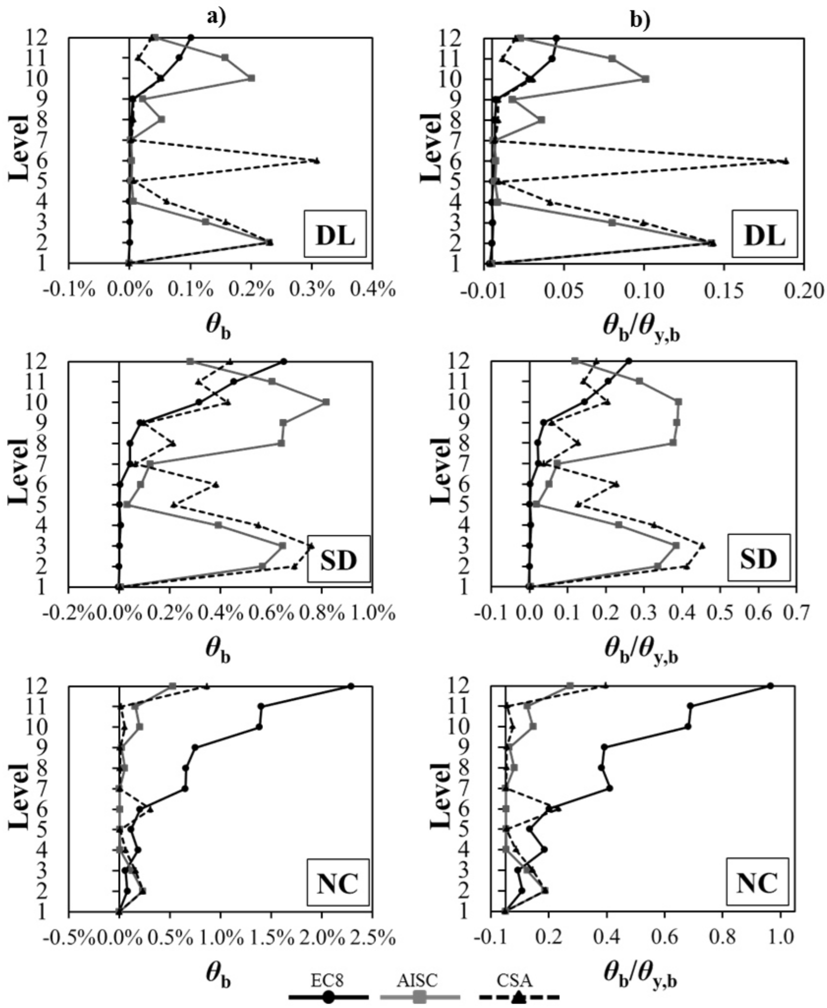

Figure 7.33 Beam chord rotation (a) and beam yielding (b) for 12-storey cases: comparison between examined codes.

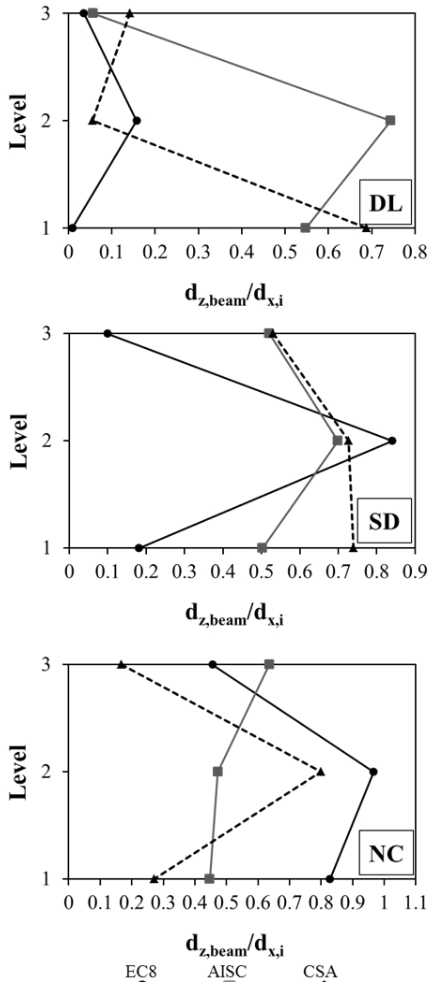

Figure 7.34 Beam vertical displacements-to-horizontal displacement ratio for 3-storey cases: comparison between examined codes.

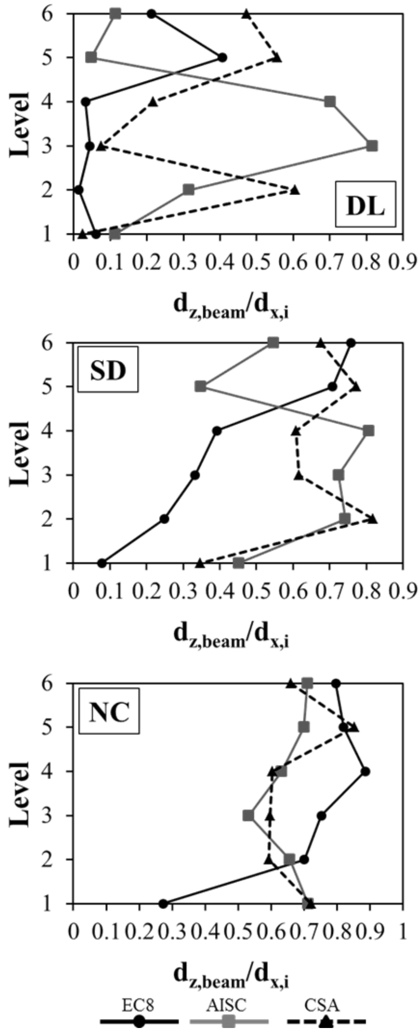

Figure 7.35 Beam vertical displacements-to-horizontal displacement ratio for 6-storey cases: comparison between examined codes.

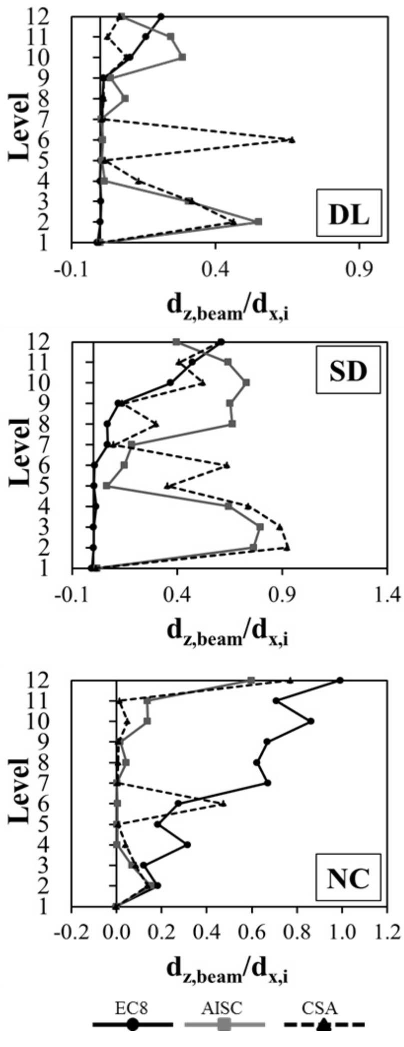

Figure 7.36 Beam vertical displacements-to-horizontal displacement ratio for 12-storey cases: comparison between examined codes.

Figure from 7.37 to 7.39 report both transient (θ, see Fig. 7.37-39a) and residual (θ_{RES}, Fig. 7.37-39b) interstorey drift ratios for the frames designed according to the proposed revisions (see Section 7.2.1.4) to EN-1998, compared with the codified criteria. No significant differences can be recognized from quantitative point of view in terms of interstorey drift ratio. All frames exhibit satisfactorily performance at DL limit state, being met the requirement provided by EN 1998-1 in terms of interstorey drift ratios limitation.

However, by applying the proposed revisions (see Section 7.2.1.4) more uniform distribution of drift ratios along the building height is obtained, especially for medium and high rise buildings; indeed shear-type displacement shape can be recognized for the frames designed according to both “revision 1” and “revision 2”.

Also satisfactorily performance in terms of residual interstorey drift ratios can be recognized for all three, six and twelve-storey frames (see from Fig. 7.37b to 7.39b), with θ_{RES} smaller than 0.15%, 0.2% and 0.5%, respectively, up to NC limit state.

Figures from 7.40 to 7.42 show the profiles of peak storey accelerations for three, six and twelve-storey frames, respectively: as well as EN-1998, “revision 1” leads to significant storey accelerations, for both three and six-storey buildings. Conversely, reduced peak average values (A) can be recognized for the Rev 2-compliant cases due to the slightly larger dissipation capacity.

For all examined codes, the peak storey accelerations reach smaller value for the twelve-storey frames respect to the low and medium rise buildings. Such result can be explained by the larger values of the fundamental period.

Figures from 7.43 to 7.45 depict the braces ductility demand (μ) both in tension and compression, for low, medium and high rise buildings, respectively. No significant differences can be recognized between codified criteria and proposed revisions for the three-storey cases (see Fig. 7.43); six and twelve-storey frames confirm the different distribution of deformation along the building height (see also Figs. from 7.46 to 7.48), namely cantilever-type for "revision 1" and shear-type for "revision 2". However no case experience yielding under tension until NC limits state.

Figures from 7.49 to 7.51 show the brace out-of-plane deformations, expressed in terms of both, out of plane rotation θ_{br} (a) and normalized displacement (b) $\overline{w}$ (see Fig. 5.27a in Section 5.7.3.3). Coherently with the displacement shapes and the brace ductility demand profiles, no significant differences can be recognized for low building case; conversely different distribution out-of-plane deformation along the building heigh can be observed comparing "revion 2" to "revision 1" for six and twelve-storey cases.

In detail, the normalized displacement $\overline{w}$ (calculated as described Fig. 5.27a in Section 5.7.3.3) shows that both "revision 1" and "revision 2" guarantee the functionality of cadding walls (namely for $\overline{w} \leq 1$), in most of cases at DL limit state for both three and twelve-storey cases; conversely six-storey frames experience damage (namely for $\overline{w} > 1$) at the non-structural components also under serviceability earthquake.

No significant differences can be recognized in terms of normalized unbalanced force applied to the beams for three-storey cases (see Fig. 7.52); the β distribution along the six and twelve-storey buildings height also reflects the different displacement shapes (see Figs. 7.53-4).

Figures from 7.55 to 7.57 show the beam chord rotation (see Eq. 7.9) for three, six and twelve-storey frames respectively, designed according to the proposed revisions and compared with the EC8-compliant ones; moreover the normalized beam rotation is reported (Figs. 7.55-57b) in order to identify eventual yielding phenomena. No plastic hinge occurs in the beams belonging to all low, medium and high rise buildings.

Beside the beam chord rotation, Figures from 7.58 to 7.60 show the beam vertical displacement $d_{z,beam}$ normalized to the relative horizontal displacement at each storey ($d_{x,i}$) which are consistent with the relevant chord rotation profiles.

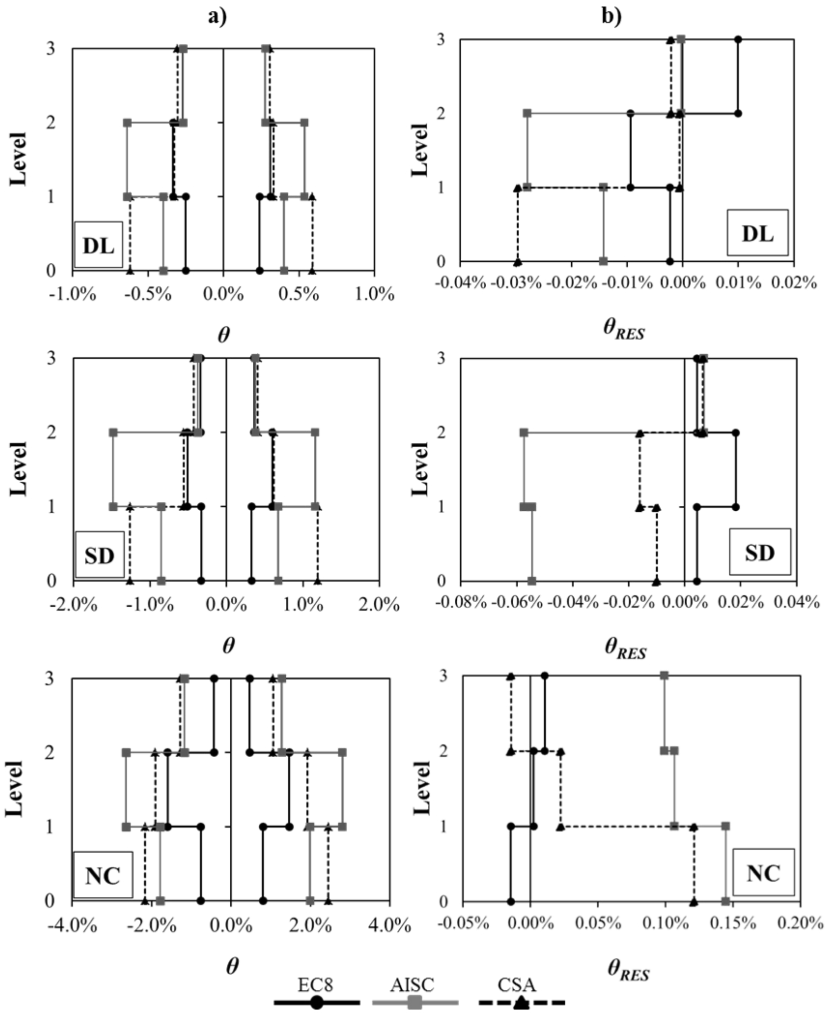

Figure 7.37 Interstorey drift transient (a) and residual (b) for 3-storey cases: comparison between EN-1998 and proposed revisions. (continued)

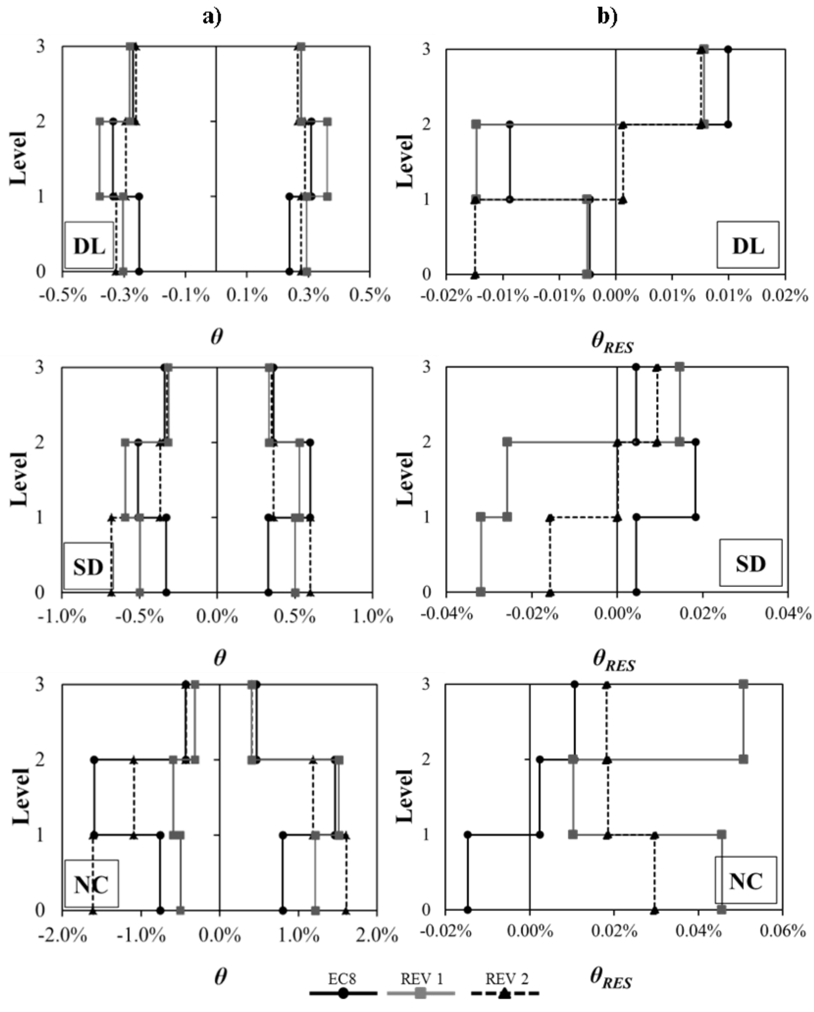

Figure 7.37 Interstorey drift transient (a) and residual (b) for 3-storey cases: comparison between EN-1998 and proposed revisions.

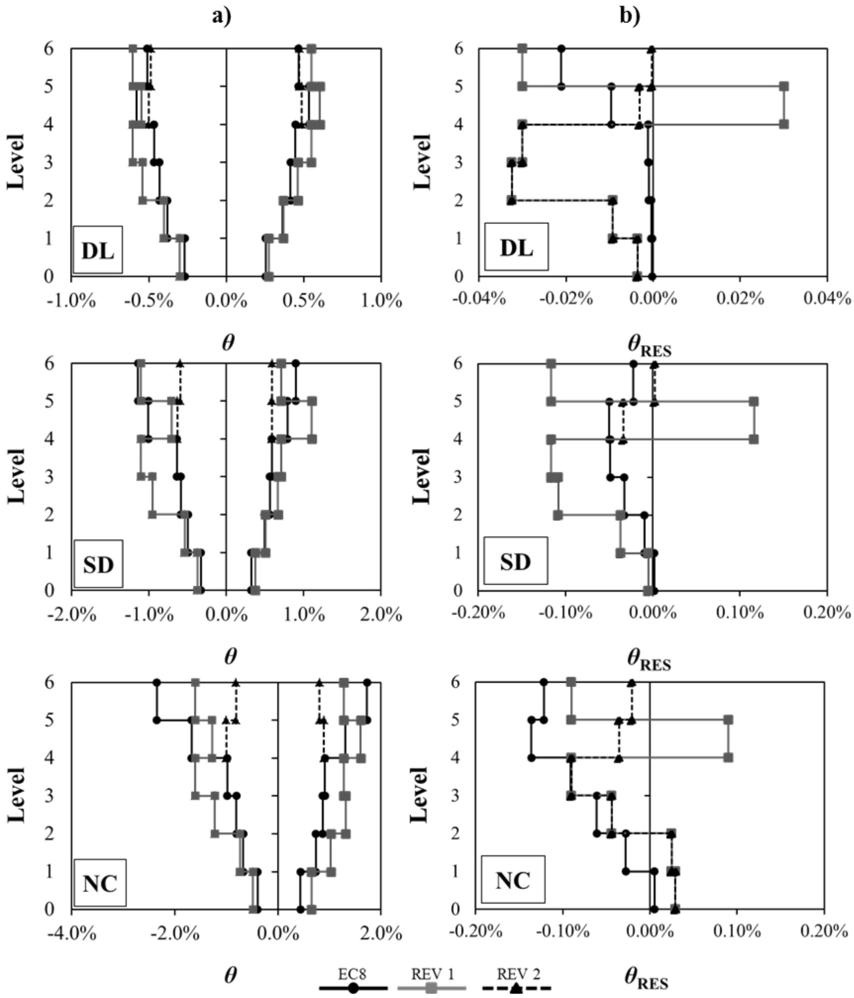

Figure 7.38 Interstorey drift transient (a) and residual (b) for 6-storey cases: comparison between EN-1998 and proposed revisions.

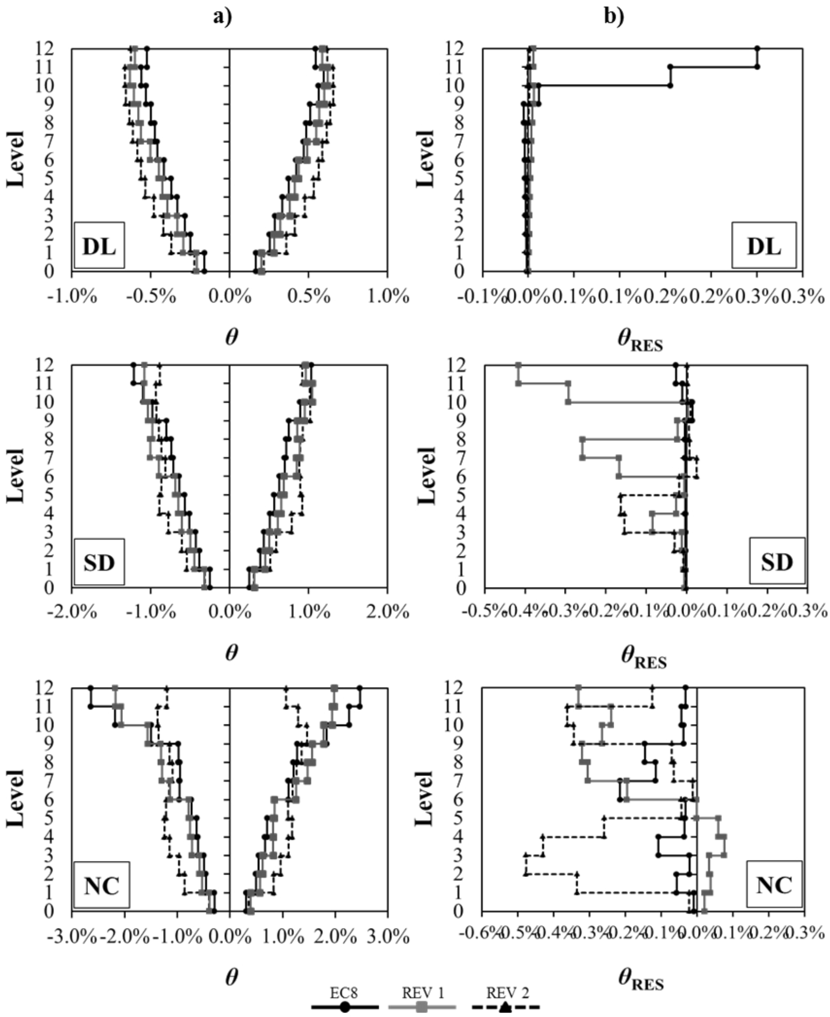

Figure 7.39 Interstorey drift transient (a) and residual (b) for 12-storey cases: comparison between EN-1998 and proposed revisions.

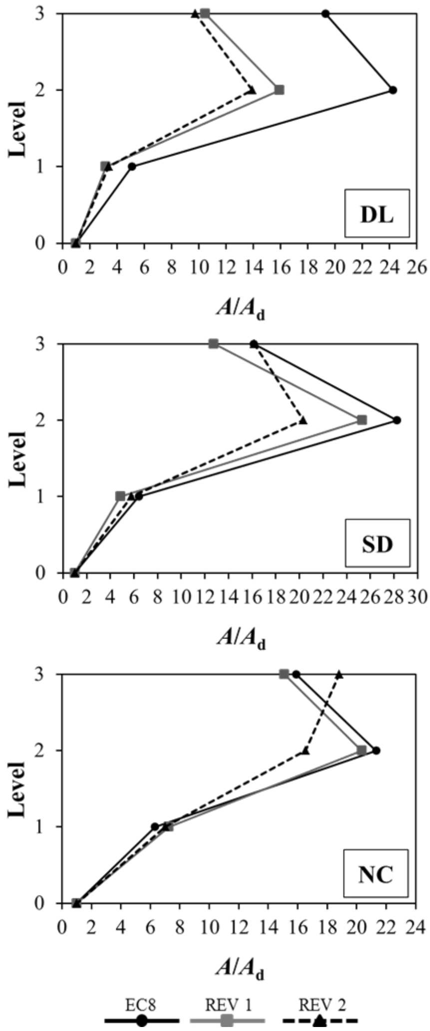

Figure 7.40 Peak storey accelerations for 3-storey cases: comparison between EN-1998 and proposed revisions.

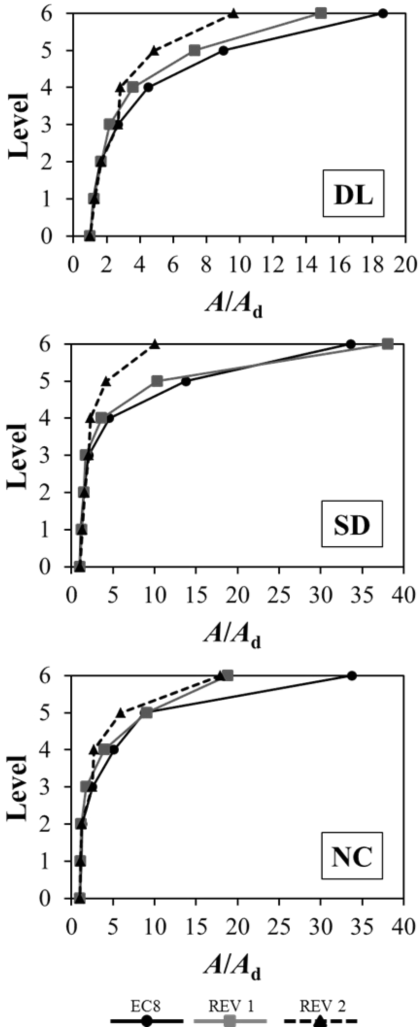

Figure 7.41 Peak storey accelerations for 3-storey cases: comparison between EN-1998 and proposed revisions.

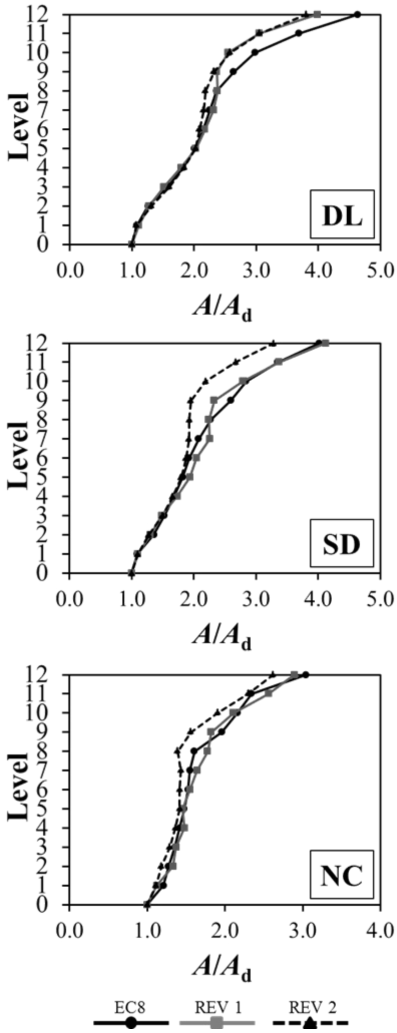

Figure 7.42 Peak storey accelerations for 3-storey cases: comparison between EN-1998 and proposed revisions.

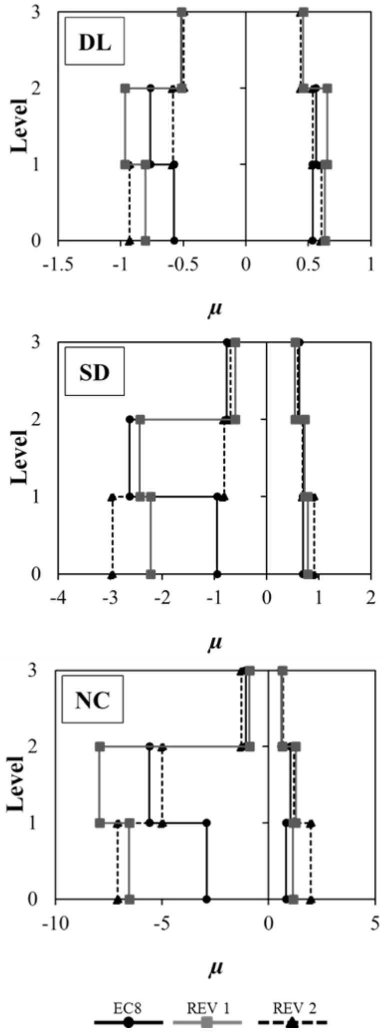

Figure 7.43 Braces ductility demand for 3-storey cases: comparison between EN-1998 and proposed revisions.

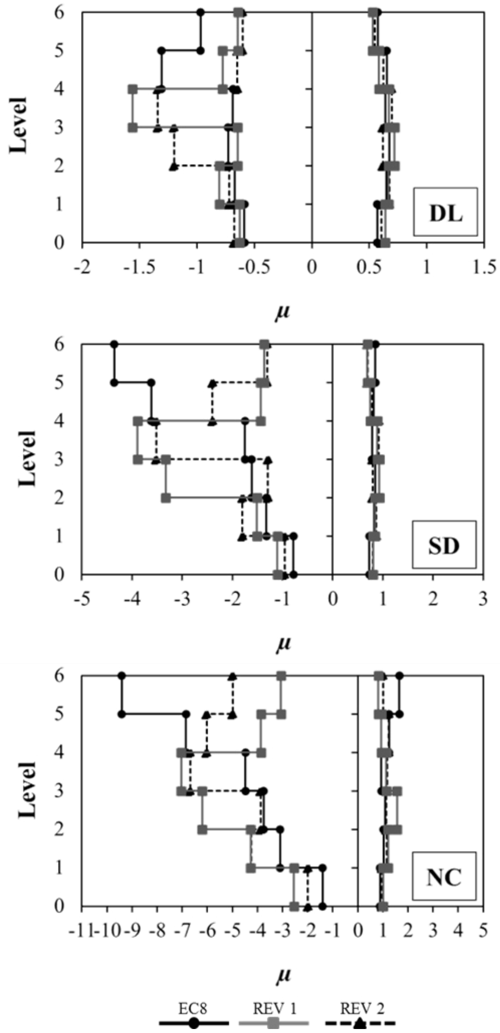

Figure 7.44 Braces ductility demand for 6-storey cases: comparison between EN-1998 and proposed revisions.

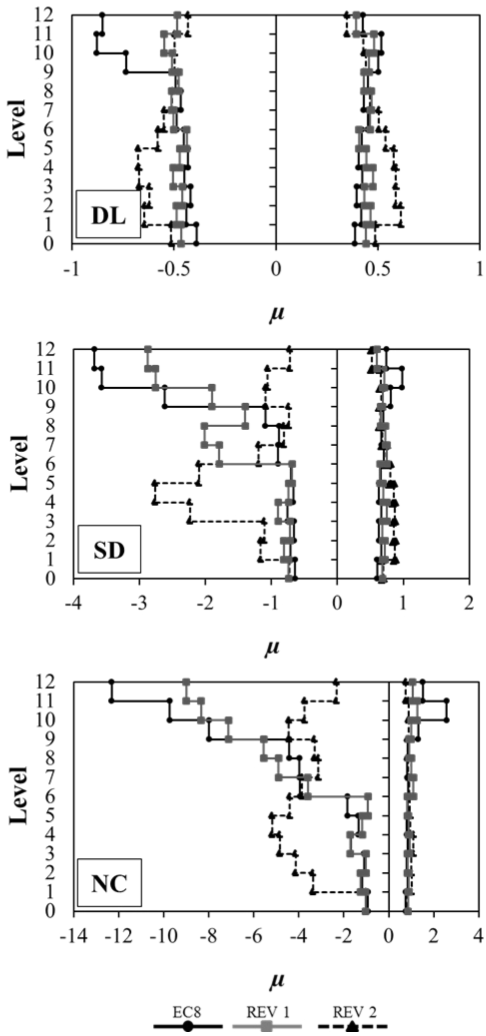

Figure 7.45 Braces ductility demand for 12-storey cases: comparison between EN-1998 and proposed revisions.

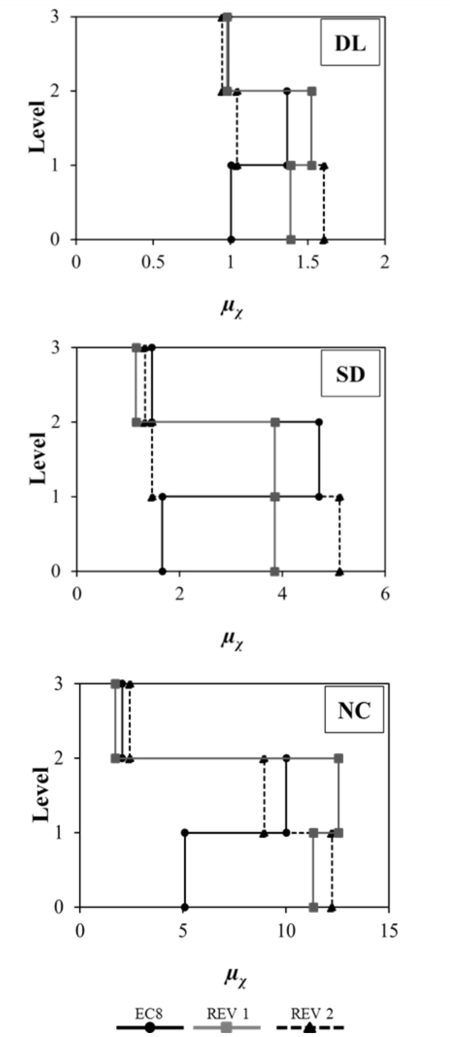

Figure 7.46 Ductility demand in compression for 3-storey cases: comparison between EN-1998 and proposed revisions.

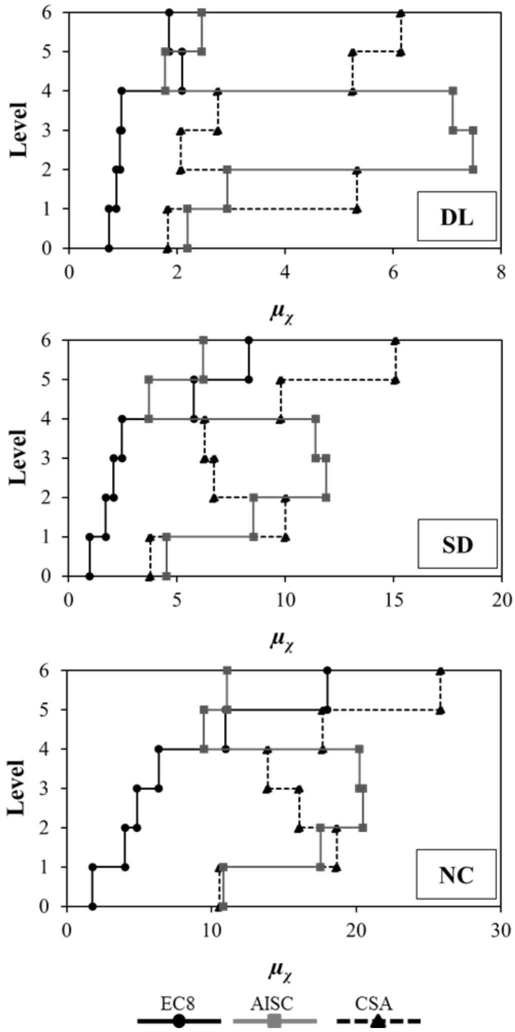

Figure 7.47 Ductility demand in compression for 6-storey cases: comparison between EN-1998 and proposed revisions.

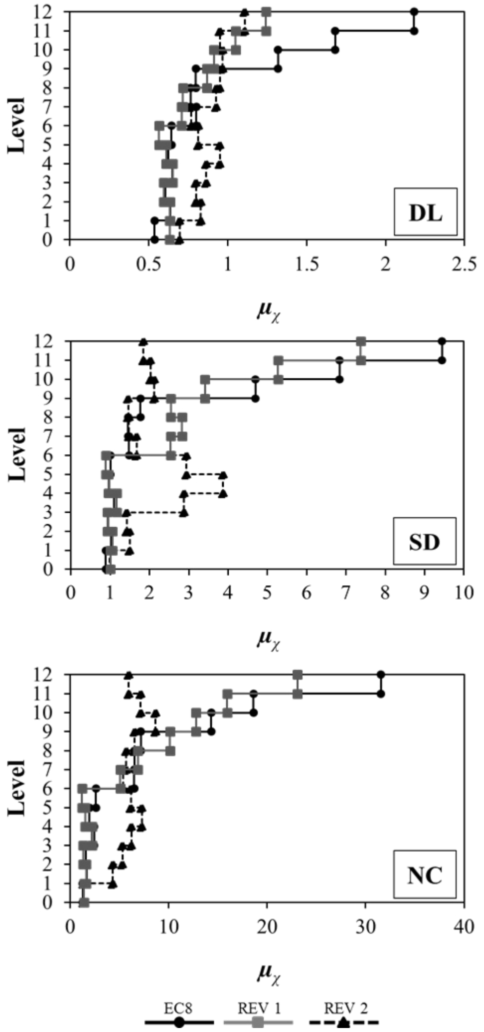

Figure 7.48 Ductility demand in compression for 12-storey cases: comparison between EN-1998 and proposed revisions.

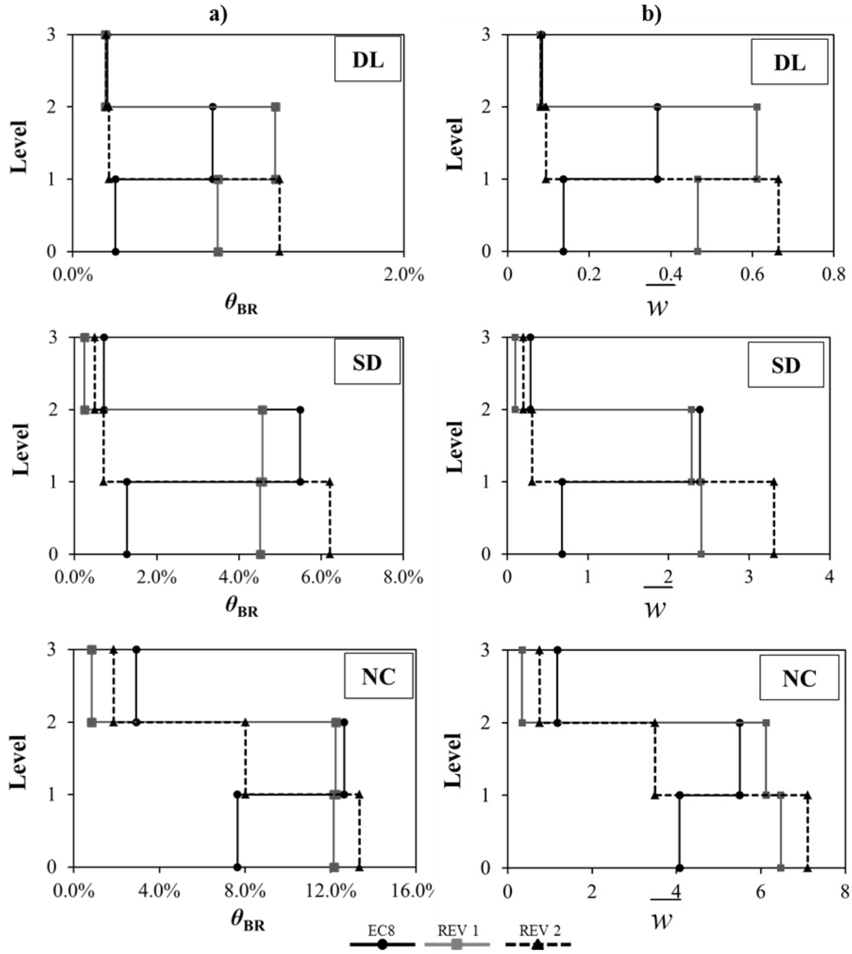

Figure 7.49 Braces out-of-plane rotations a) and normalized displacements (b) for 3-storey cases: comparison between EN-1998 and proposed revisions.

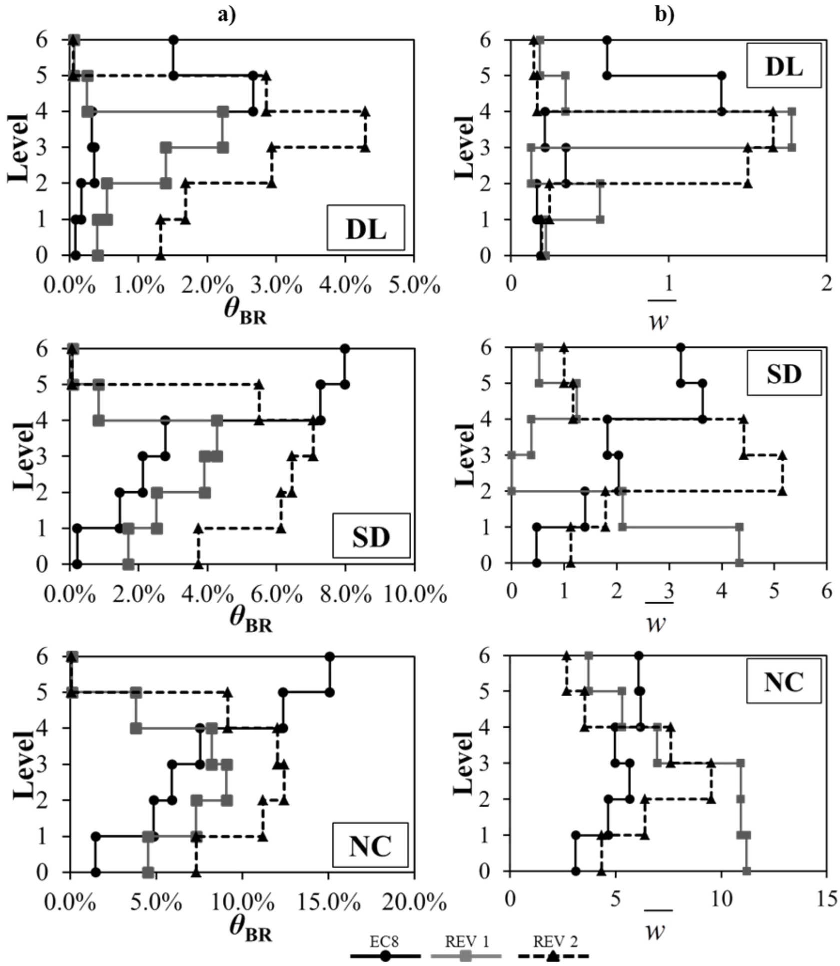

Figure 7.50 Braces out-of-plane rotations a) and normalized displacements (b) for 6-storey cases: comparison between EN-1998 and proposed revisions.

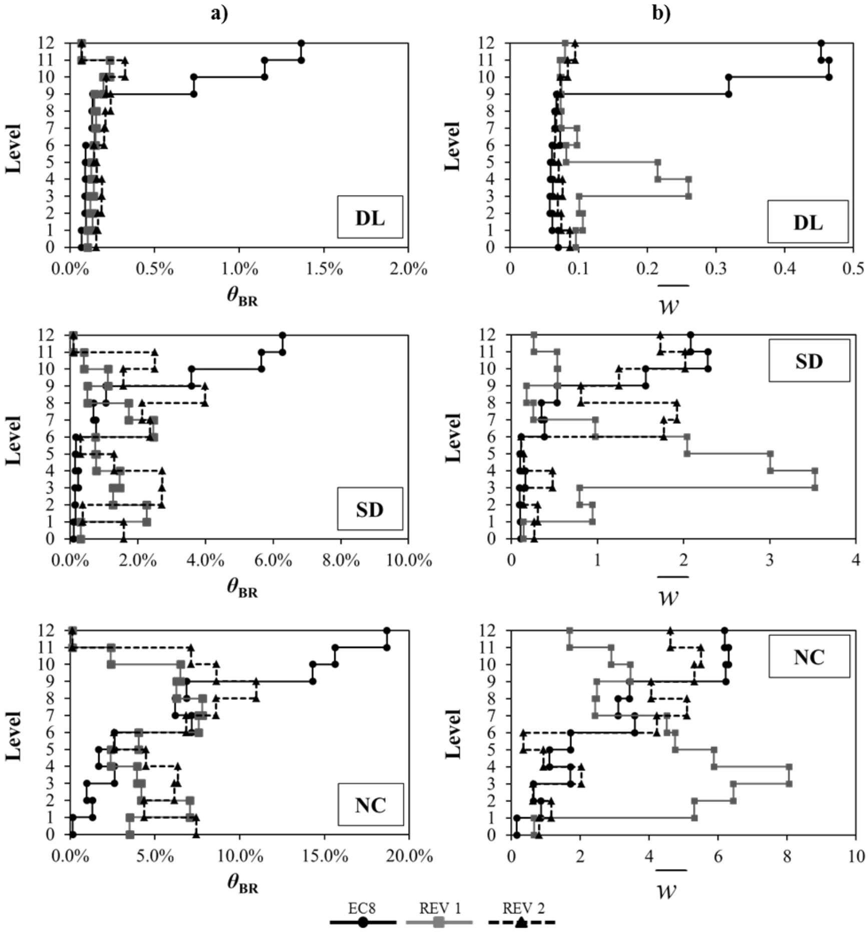

Figure 7.51 Braces out-of-plane rotations a) and normalized displacements (b) for 12-storey cases: comparison between EN-1998 and proposed revisions.

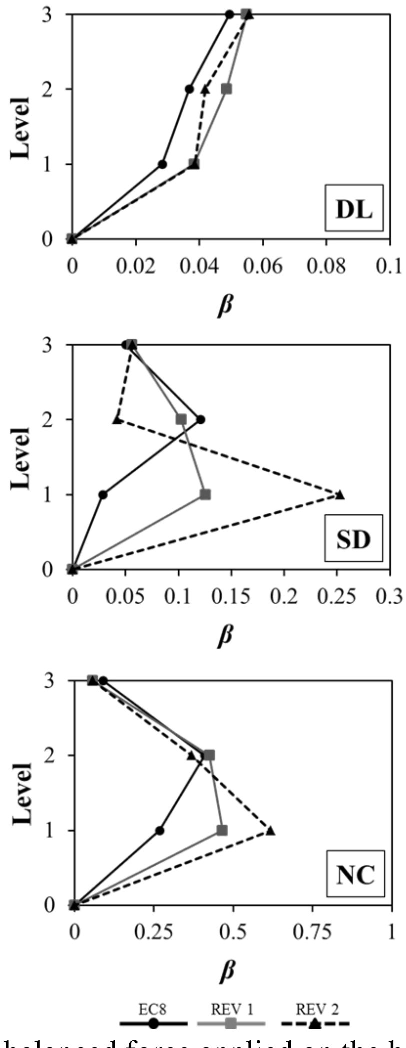

Figure 7.52 Unbalanced force applied on the beam for 3-storey cases: comparison between EN-1998 and proposed revisions.

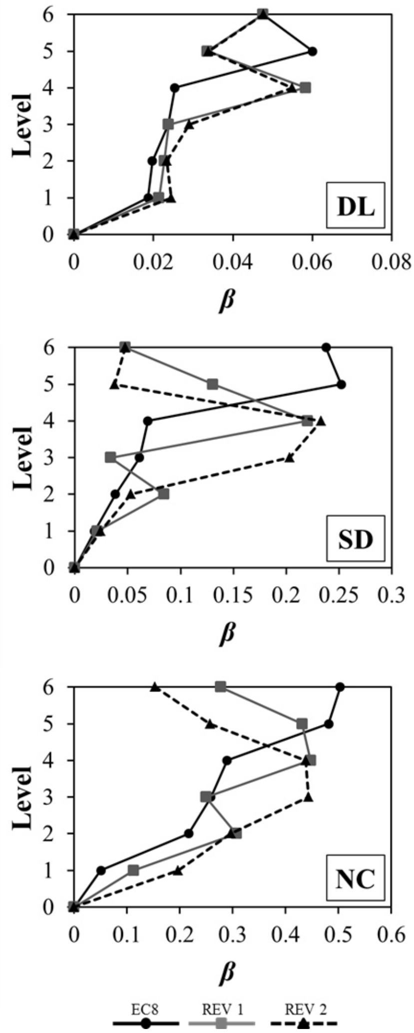

Figure 7.53 Unbalanced force applied on the beam for 6-storey cases: comparison between EN-1998 and proposed revisions.

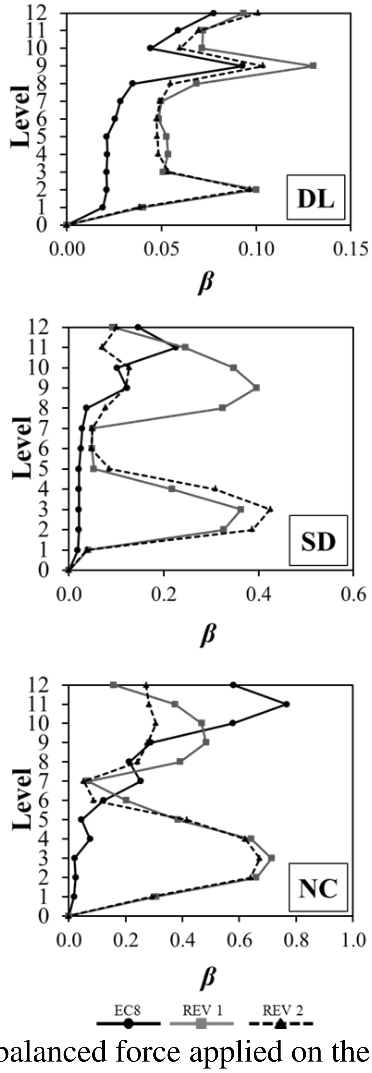

Figure 7.54 Unbalanced force applied on the beam for 12-storey cases: comparison between EN-1998 and proposed revisions.

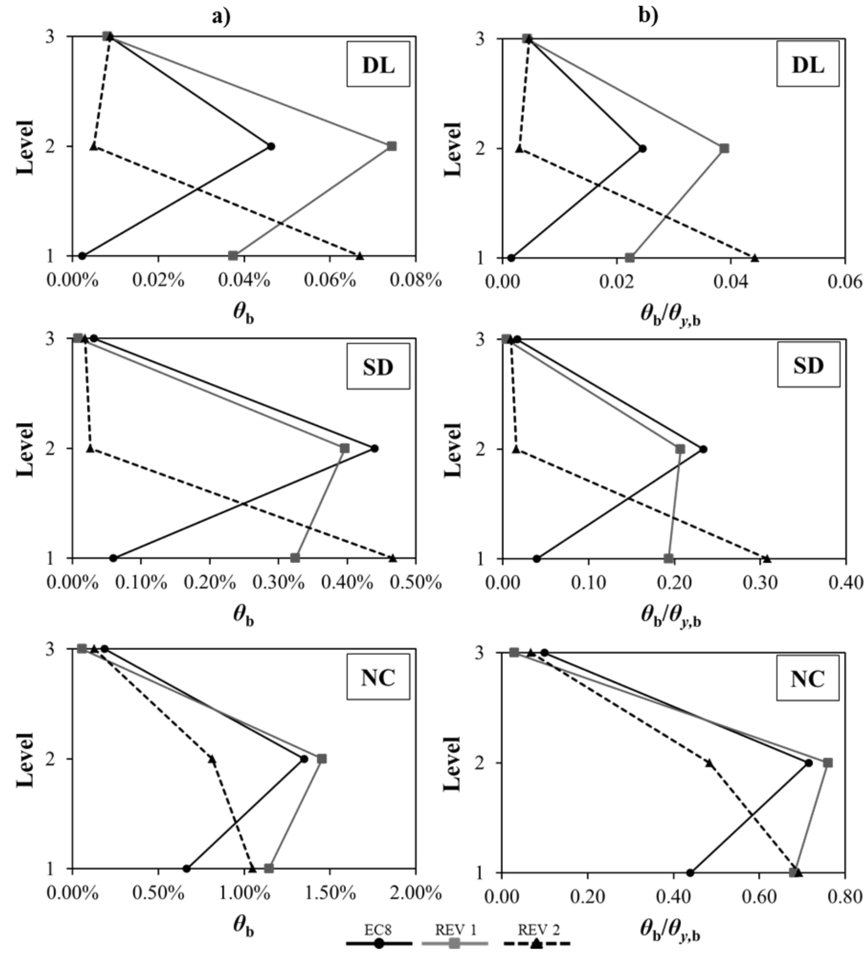

Figure 7.55 Beam chord rotation (a) and beam yielding (b) for 3-storey cases: comparison between EN-1998 and proposed revisions.

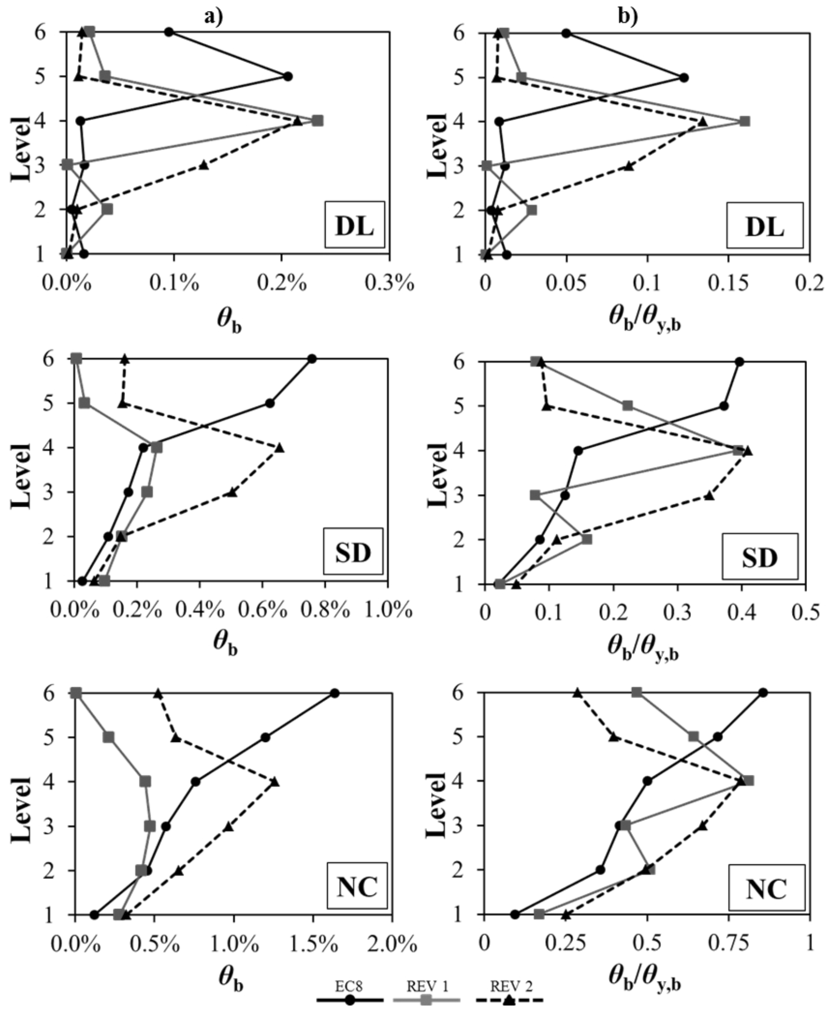

Figure 7.56 Beam chord rotation (a) and beam yielding (b) for 6-storey cases: comparison between EN-1998 and proposed revisions.

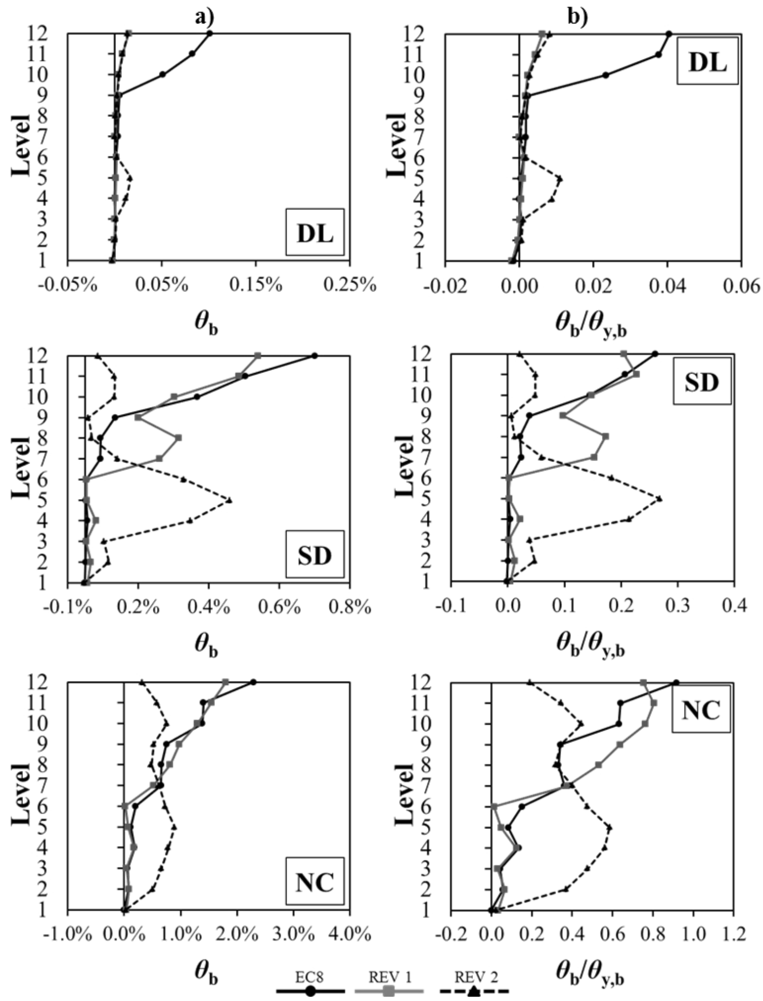

a

Figure 7.57 Beam chord rotation (a) and beam yielding (b) for 12-storey cases: comparison between EN-1998 and proposed revisions.

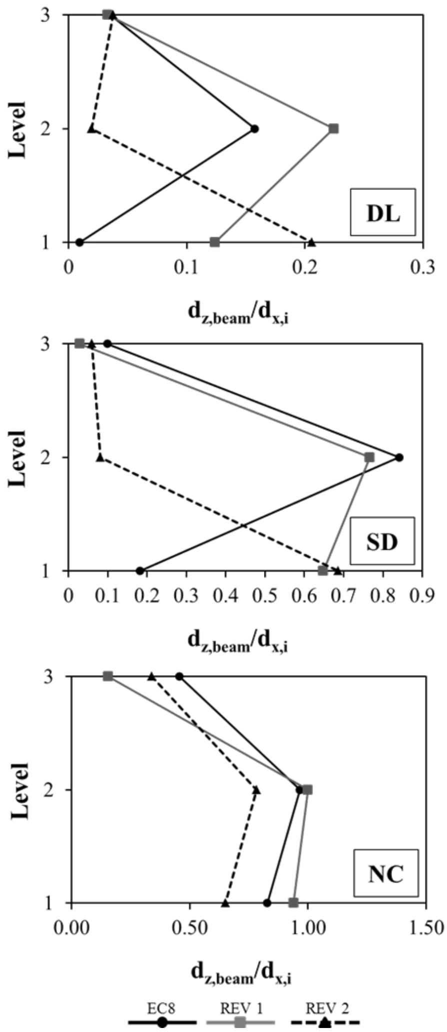

Figure 7.58 Beam vertical displacements-to-horizontal displacement ratio for 3-storey cases: comparison between EN-1998 and proposed revisions.

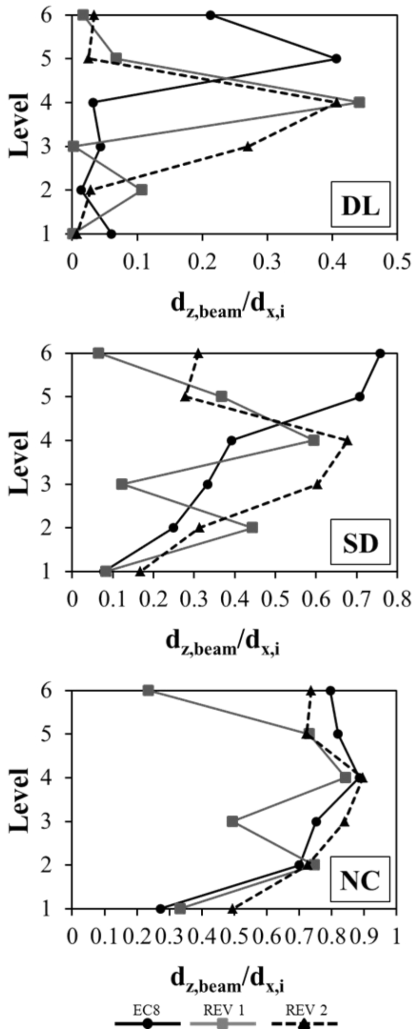

Figure 7.59 Beam vertical displacements-to-horizontal displacement ratio for 6-storey cases: comparison between EN-1998 and proposed revisions.

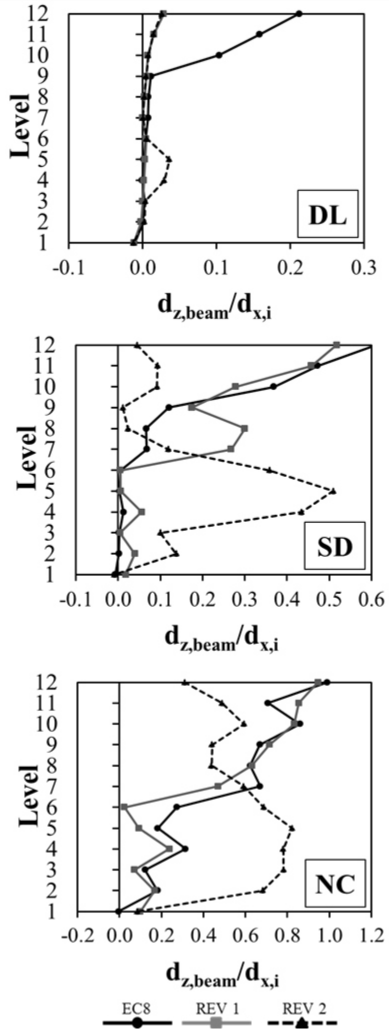

Figure 7.60 Beam vertical displacements-to-horizontal displacement ratio for 12-storey cases: comparison between EN-1998 and proposed revisions.

7.4 ECONOMICAL ASPECTS

Beside the seismic performance, the assessment of the effectiveness of codified and proposed design criteria needs to be completed by providing few remarks dealing with the economical aspects. Indeed, it is trivial to observe that different design criteria lead to different structural configurations and thus different constructional costs. Thereby, in this section the structural weights of frames obtained designing according to the examined criteria are evaluated and the relevant structural costs are analysed in terms of cost of construction (namely, the amount of steel necessary to realize the seismic resistant system); moreover, few considerations are provided concerning eventual repairing cost, by considering damage occurred at both structural and non-structural elements.

Figure 7.61 shows the total amount of steel tons estimated for either the frames designed according to the three examined seismic code (see Fig. 7.61a) and the proposed revisions (see Fig. 7.61b). The amount of steel is evaluated as the sum of the weights of the structural members (namely columns, beams, braces) neglecting the contribution due to the connections and to the secondary elements (namely cladding walls, etc.).

The EC8-compliant frames have the largest structural weight for all low, medium, and high rise buildings, while the cheapest system is given according to AISC 341 (see Fig. 7.61a).

A reduced amount of steel can also be obtained by applying both the proposed revisions (see Fig. 7.61b).

Moreover, Figure 7.62 reports the weight of structural members P_j separately, as a percentage of the total weight P_{tot}. By observing the histograms, it emerges that the frames designed according to the North-American codes exhibit larger percentage of steel employed for the manufacturing of beams, respect to the EC8-compliant cases, which conversely show increased amount for diagonal members and columns.

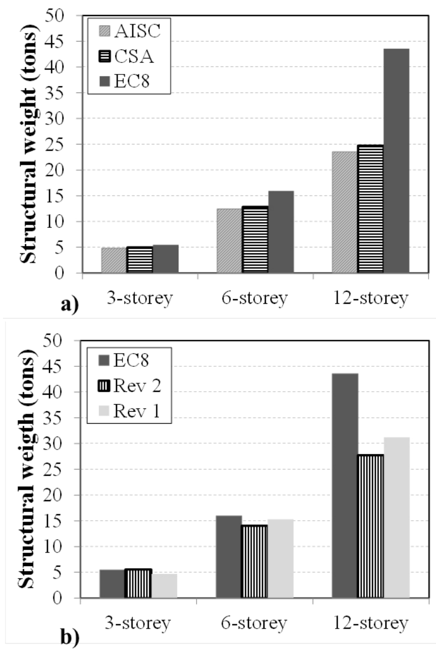

Figure 7.61 Structural weight: examined codes (a) EN 1998 and proposed revisions (b) comparison

The different distributions can be explained considering the larger behaviour factor stated by EN 1998, leading to stockier braces which also affect the design of columns through the overstrength factor Ω.

No significant differences can be observed comparing EN 1998 and the proposed revisions for three and twelve-storey cases; the six-storey frame designed according to “revision 2” presents a weight distribution close to that previously observed for the North-American code-compliant cases (see Fig. 7.63).

In light of the above considerations, the frames designed according to EN 1998 are characterized by the largest constructional cost.

However, beside the cost of construction, the response parameters previously discussed in Section 7.3 also provide information (although purely qualitative) on the need to sustain eventually repairing cost in order to restore eventual damaged zones.

The frames designed according to North-American codes requested smaller initial cost of construction; however, Figures from 7.21 to 7.23 show larger damage occurred in the compression braces and thus to the cladding walls (see Figs. from 7.24 to 7.26). On the other hand, EC8-compliant frames experienced very large peak storey accelerations at upper storeys (see Figs. from 7.15 to 7.17), presuming extensive damage to the non-structural elements contained in the buildings, whose impact would also compromise the human safe.

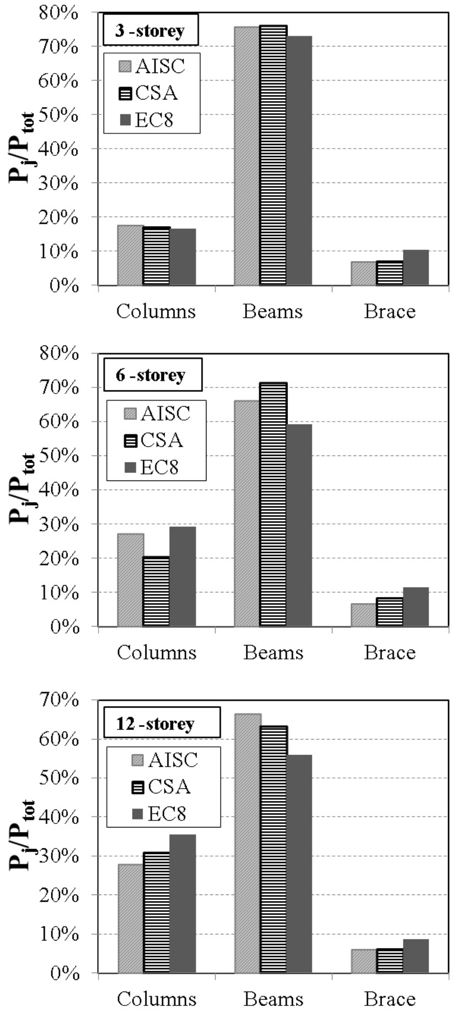

Figure 7.62 Weights of structural members as percentage of total amount: comparison between examined codes

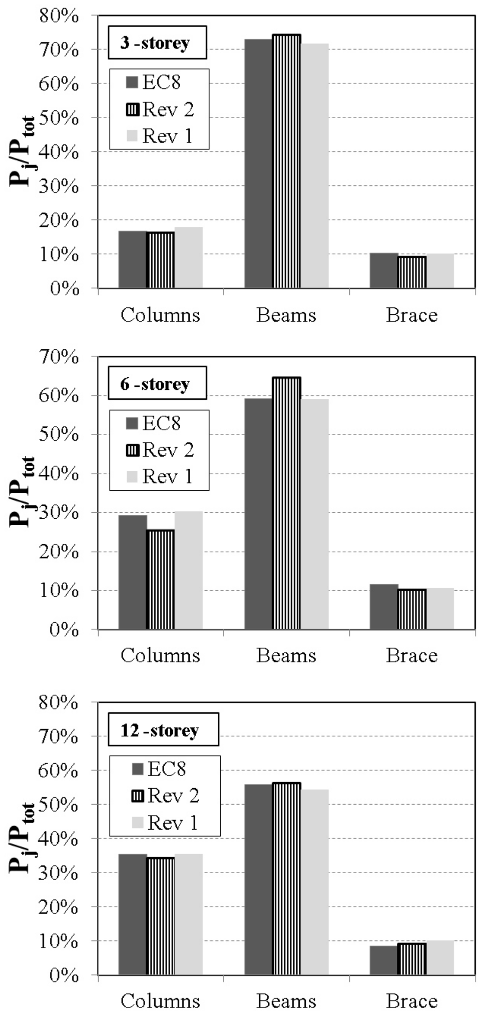

Figure 7.63 Weights of structural members as percentage of total amount: comparison between EN 1998 and proposed revisions

7.5 CONCLUSIVE REMARKS

In this Chapter a parametric study devoted to assess the effectiveness of seismic design provisions and codified criteria given by both European (EN-1998) and North-American (AISC 341 and CSA S16-09) has been described and discussed.

A comprehensive set of non-linear dynamic analyses has been performed on low, medium and high rise residential buildings designed according to the examined codes. Moreover, further cases have been analysed in order to evaluate the influence of some modifications applied to the requirements provided by EN-1998. The discussion of results suggests the following conclusive remarks:

- EN 1998 states to assume the smaller behaviour factor, leading to design heavier structural members; as consequence EC8-compliant frames are stiffer than those designed according to North-American codes. However, both CSA and AISC-compliant frames exhibit more uniform distribution of lateral displacements along the building height. Indeed, EC8-compliant cases show cantilever-type displacement shape with significant damage concentration at the upper storeys. Moreover, they suffer very large storey accelerations, whose peak significantly increases respect to the ground acceleration. On the contrary, smaller average peak storey accelerations are experienced by the frames designed according to North-American codes, due to the larger dissipative capacity provided by the yielding of braces.
- EC8-compliant frames show the smallest energy dissipation capacity with the most of bracing members

behaving elastically in tension up to NC limit state. CSA and AISC-compliant cases exhibit slightly larger energy dissipation capacity with larger number of braces under tension attaining their plastic strength; however, also significant concentration of damage under compression occurs, mainly due to the larger slenderness ratio of bracing members and to the increased lateral deformability respect to the European cases.

- All examined frames, even those designed according to the Eurocodes, largely exceed the axial deformation capacity limitations provided by EN1998-3. Indeed, significantly larger engagement can be recognized at all the three considered limit states.
- No improvement can be recognized in terms of energy dissipation capacity by applying the proposed revisions to EN-1998 design criteria; however, more uniform distribution of damage along the building height is obtained, particularly according to “revision 2”.
- The different design criteria lead to different structural configurations and thus different costs. EN 1998 leads designing more massive systems entailing the largest cost of construction; the frames designed according to North-American codes request smaller initial cost of construction, while they show more extent damage in compression braces and at cladding walls. EC8-compliant frames experienced very large peak storey accelerations at upper storeys presuming extensive damage to the non-structural elements.

7.6 REFERENCES

Akkar S., Sandıkkaya M.A., Şenyurt M., Azari Sisi A., Ay B.Ö., Traversa P., Douglas J., Cotton F., Luzi L., Hernandez B., Godey S. (2014). Reference database for seismic ground-motion in Europe (RESORCE), Bulletin of Earthquake Engineering, 12(1): 311-339

American Institute of Steel Construction, Inc. (AISC). (2010). Seismic Provisions for Structural Steel Buildings. ANSI/AISC Standard 341-10. AISC, Chicago, Illinois

CSA. 2009. Design of Steel Structures, CSA-S16-09, Canadian Standards Association, Toronto, ON

Goggins J.M., Broderick B.M., Elghazouli A.Y., Lucas A.S. (2006) Behaviour of tubular steel members under cyclic axial loading. *Journal of Constructional Steel Research* 62 121-131.

EN 1998-1-1. Eurocode 8: Design of structures for earthquake resistance – Part 1: General rules, seismic actions and rules for buildings. CEN; 2005.

Fulop L. (2010). Selection of earthquake records for the parametric analysis. Research report VTT-R-03238-10, VTT, Espoo.

Tremblay R. (2002) Inelastic seismic response of steel bracing members. *Journal of Constructional Steel Research* 58:665–701.

Chapter VIII
Proposal of seismic design criteria for CCBs for the next generation of Eurocodes

8.1 INTRODUCTION

In the previous Sections the seismic behaviour of chevron concentrically braced frames has been characterized by identifying the main parameters affecting the performance against lateral loadings. Moreover the framework of existing codes has been deeply discussed and described and the effectiveness of design criteria for chevron bracings codified within both European and North-American frameworks have been assessed by means of a comprehensive parametric study based on nonlinear dynamic analyses. The numerical results highlighted several criticisms in the current European codified rules, leading to limited dissipative capacity and poor seismic performance under severe seismic action.

In light of these results, new design criteria for chevron concentrically braced frames are proposed hereinafter, devoted to improve the ductility and the structural efficiency of this type of systems under severe earthquake.

A wide numerical parametric study was performed to validate the design assumptions and to verify the effectiveness of proposed design criteria.

With this regard, low, medium and high rise residential buildings were designed according to the proposed procedure and the relevant seismic response was monitored and compared to the performance exhibited by frames designed according to the requirement currently provided by EN-1998.

8.2 PROPOSAL FOR DUCTILE AND DISSIPATIVE CCB$_S$

8.2.1 *Proposed design provisions*

8.2.1.1 Ductility classes and behaviour factors.

According to the proposed design rules, chevron concentrically braced frames can be designed with reference to both medium ductility class (DCM) and high ductility class (DCH). Different force reduction factors are associated at each class, namely q=4.0 is assumed for DCM, while q=6.0 is considered for DCH.

Consistently to the requirements currently provided by EN-1998, the EC3 cross section classification is retained, relating it to the value assumed for behaviour factor q: cross-sectional class 1 or 2 is required for q in a range [2.0, 4.0], while only class 1 is allowed for DCH (q = 6.0).

8.2.1.2 Design of dissipative member: bracing elements

The diagonal members shall be placed in such a way that the structure exhibits similar load deflection characteristics at each storey in opposite senses of the same braced direction under load reversals; with this regard the requirements currently provided by EN 1998-1 clause 6.7.1 (3) is retained.

The design forces of bracing members are evaluated by performing a simple linear elastic analysis in which both braces are active in tension and compression (see Fig. 3.3a in Section 3.2.2).

Thereby, the bracing members should be designed in order to fulfill the following requirement:

$$N_{\mathrm{b,br,Rd},i} \geq N_{Ed,\mathrm{br}} \tag{8.1}$$

Where:

$N_{\mathrm{b,br,Rd,i}}$ is the factored buckling capacity of the bracing members evaluated according to EN 1993-1;

$N_{\mathrm{Ed,br}}$ is the axial force acting in the bracing members evaluated according to the following expressions:

(i) in order to enforce a shear-type lateral response, at the roof storey the braces should be designed to resist the following forces:

$$N_{Ed,br,\mathrm{rf}} = N_{Ed,br,\mathrm{E,rf}} \cdot q + N_{Ed,br,\mathrm{G,rf}} \tag{8.2}$$

Where:

$N_{\mathrm{Ed,br,rf}}$ is the required strength in compression of bracings at the roof storey;

$N_{\mathrm{Ed,br,E,rf}}$ is the axial force contribution at the roof storey due to the seismic action;

$N_{\mathrm{Ed,br,G,rf}}$ is the axial force contribution at the roof storey due to the non-seismic actions included in the combination of actions for the seismic design situation;

q is the behaviour factor assumed.

(ii) the brace design force at the i-th storey is given as follows:

$$N_{Ed,br,i} = N_{Ed,br,\mathrm{E,i}} + N_{Ed,br,\mathrm{G,i}} \tag{8.3}$$

Where:

$N_{\mathrm{Ed,br,i}}$ is the required strength in compression of bracings at the roof storey;

$N_{\mathrm{Ed,br,E,i}}$ is the axial force contribution at the i-th storey due to the seismic action;

$N_{\mathrm{Ed,br,G,i}}$ is the axial force contribution at the i-th storey due to the non-seismic actions included in the combination of actions for the seismic design situation;

In low rise buildings up to three storeys, the requirement (8.2) can be disregarded and the required strength for bracings at the roof storey can be evaluated according to Eq. (8.3).

The non-dimensional slenderness $\bar{\lambda}$ should be less than or equal to 2.0.

Moreover, in order to satisfy a homogeneous dissipative behaviour of the diagonals, the following condition should be satisfied:

$$\left[(\Omega_i - \Omega)/\Omega\right] \leq 0.02 \tag{8.4}$$

Where Ω is the minimum overstrength ratio $\Omega = \min\left(\frac{\chi \cdot N_{pl,br,Rd,i}}{N_{Ed,br,i}}\right)$ and Ω_i is the overstrength ratio at the i-th storey evaluated as:

$$\Omega_i = \frac{\chi \cdot N_{pl,br,Rd,i}}{N_{Ed,br,i}} \quad i \in \left[1,(n-1)\right] \tag{8.5}$$

It should be noted that for low rise buildings up to three storeys, the overstrength factor at the roof storey should be included in the check of the Ω variation, if the bracing members at the same storey are not designed to behave in the elastic range (See Eq. (8.3)).

The connections of the diagonals to any member should satisfy the following design rule:

$$R_d \leq 1.1 \cdot \gamma_{ov} \cdot R_{fy} \tag{8.6}$$

where:

R_d is the resistance of the connection in accordance with EN 1993;

R_{fy} is the plastic resistance of the connected dissipative member based on the design yield stress of the material as defined in EN 1993.

γ_{ov} is the material randomness coefficient;

8.2.1.3 Design of non-dissipative members

As a general remark non-dissipative members should be designed considering the most unfavorable situation between:

(i) the earthquake-induced effects calculated by means the former elastic (see Fig. 3.3a in Section 3.2.2) analysis and magnified by overstrength factor Ω.

(ii) the internal forces calculated performing a plastic mechanism analysis, namely considering a free-body distribution of plastic forces transmitted by the braces yielded under tension and those under compression behaving in the post-buckling range (see Fig. 3.3b in Section 3.2.2).

In detail, the beams should be designed to resist:

- all non-seismic actions without considering the intermediate support given by the diagonals;
- the unbalanced vertical seismic action effect applied to the beam by the braces after buckling of the compression diagonal.

The latter design force is calculated considering the brace under tension attaining its full plastic strength (namely given by

$\gamma_{ov}N_{pl,br,Rd}$) and the brace under compression transmitting its average post-buckling capacity assumed equal to $\gamma_{ov} \cdot 0.3 \cdot \chi \cdot N_{pl,br,Rd}$.

In addition, in order to assure adequate flexural stiffness, the beam should be designed in order to fulfill the following requirement:

$$K_F \geq 0.2 \tag{8.7}$$

being K_F the beam-to-brace stiffness ratio as defined by Eq. (5.1).

The requirement given by Eq. (8.7) should be disregarded for beams at roof storeys, except for low rise buildings up to three storeys, where the bracings are designed to resist the force calculated according to Eq. (8.3).

The columns belonging to the braced bays should be designed in order to satisfy the following requirement:

$$N_{b,Rd,col,i} \geq N_{Ed,\mathrm{col,i}} \tag{8.8}$$

Where: $N_{b,Rr,col,i}$ is the factored buckling capacity of the column at the *i*-th storey, and $N_{Ed,col,i}$ is the relevant design axial force, taken as the maximum deriving between situation (i) and (ii).

In detail, according to situation (i), the required strength can be evaluated as:

$$N_{Ed,col} = N_{Ed,G,col} + 1.1 \cdot \gamma_{ov} \cdot \Omega \cdot N_{Ed,E,col} \tag{8.9}$$

where:

$N_{\mathrm{Ed,col,el}}$ is the design resistance to axial force of the beam or column calculated in accordance to the situation (i);

$N_{\mathrm{Ed,G,col}}$ is the axial force in the column due to the non-seismic actions included in the combination of actions for the seismic design situation;

$N_{\mathrm{Ed,E,col}}$ is the axial force in the column evaluated by means of elastic analyses.

γ_{ov} is the material randomness coefficient;

Ω is the minimum overstrength ratio $\Omega_{\mathrm{i}} = N_{\mathrm{pl,br,Rd,i}} / N_{\mathrm{Ed,br,c,i}}$

According to situation (ii) the required strength is given as:

$$N_{Ed,\mathrm{col,i}} = N_{Ed,\mathrm{G,col,i}} + \\ + \left[\frac{\left[(1-0.3\cdot\chi)\cdot N_{pl,br,\mathrm{m}} \cdot \sin\alpha \right]}{2} \right]_{(i-1)} + \left[\frac{\left[(1-0.3\cdot\chi)\cdot N_{pl,br,\mathrm{m}} \cdot \sin\alpha \right]}{2} \right]_{i} + \left[0.3\cdot\chi\cdot N_{pl,br,\mathrm{m}} \cdot \sin\alpha \right]_{(i-1)} \tag{8.10}$$

where:

$N_{\mathrm{Ed,col,,i}}$ is the design resistance to axial force of the column at the i-th storey calculated in accordance to the situation (ii);

$N_{\mathrm{Ed,G,col,i}}$ is the axial force in the column due to the non-seismic actions included in the combination of actions for the seismic design situation;

$N_{\mathrm{pl,br,m}}$ is the plastic strength of the connected bracing member calculated by considering the average stress of the material equal to $\gamma_{\mathrm{ov}} N_{\mathrm{pl,br,Rd}}$ (see also Fig. 3.3b in Section 3.2.2).

8.2.1.4 Beam-to-column connections of the braced bays

Only for concentrically braced frames in DCH, it is additionally required that beam-to-column connections belonging to the braced bays should be full-strength and full-rigid.

8.3 VALIDATION OF PROPOSED DESIGN CRITERIA

8.3.1 *Parametric study*

The analysed 2D frames were conceived consistently to the frames analysed in Chapter VII; moreover, beside the frames described in Section 7.2.1.1, a further configuration was investigated considering another twelve-storey building equipped with chevron bracings only in the central bay (see Fig. 8.1). It should be noted that frames in such configurations could be designed only according to the proposed design criteria; indeed, to arrange bracing members only within one bay, led to too massive and non-reasonable structures if requirements currently given by EN 1998-1 are considered.

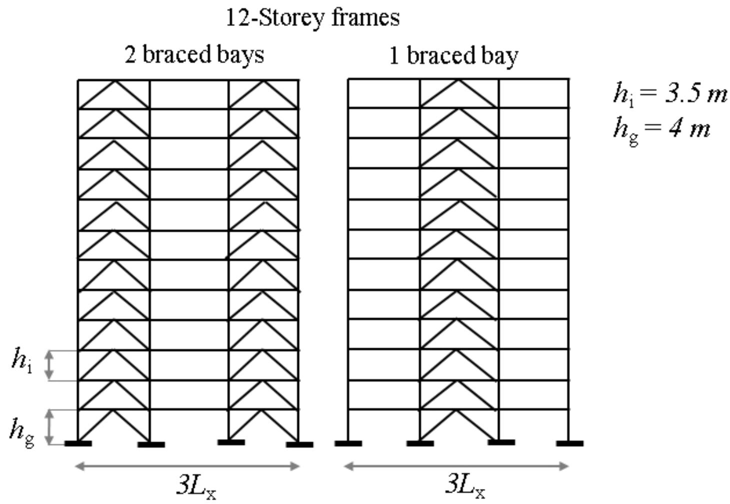

Figure 8.1 Two possible 12-storey configurations considered designing according to the proposed design criteria.

In order to verify the effectiveness of the proposed design criteria the set including all three-storey frames, six-storey frames and both the two different twelve-storey configurations was designed and analysed by varying the following parameters:

- the behaviour factor q: three variations, namely q=2.5, q=4, q=6, were considered.
- the degree of end restraints of the brace-intercepted beam, i.e. full-pinned, semi-rigid restraints and full-fixed restraints.
- With this aim, the rotational stiffness K_j of the beam-to-column joints belonging to the braced bays was varied considering the three variation, K_j=0 (corresponding to pinned-connected beams), $K_j = 0.5 \frac{EI_b}{L_b}$ (corresponding to

the lower bound limit for semi-rigid connections) and $K_j = \infty$ (corresponding to full-fixed beams).

Besides the proposed design rules, the structural safety verifications were carried out according to the following European codes:

- EN 1990 (2001) Eurocode 0: Basis of structural design;
- EN 1991-1-1 (2002) Eurocode 1: Actions on structures - Part 1-1: General actions -Densities, self-weight, imposed loads for buildings;
- EN 1993-1-1 (2003) Eurocode 3: Design of steel structures - Part 1-1: General rules and rules for buildings;
- EN 1994-1-1 (2004) Eurocode 4: Design of composite steel and concrete structures - Part 1.1: General rules and rules for buildings.

The design of building was developed without reference to a specific National Annex. Hence, the recommended values of the safety factors are used.

Cold formed circular hollow profiles were used for the diagonals members; IPE and HE profiles were used for beams; HE and HD profiles were used for the columns.

Incremental dynamic time-history analyses were performed in order to assess the seismic performance of all the examined cases. With this regard, the same set of 14 natural earthquake acceleration records described in Section 7.3.3.2 have been adopted, as well as the modelling assumptions shown in Section 7.3.1.

8.3.2 *Seismic performance evaluation*

8.3.2.1 Building structures designed for medium ductility class (DCM)

8.3.2.1.1 Designed structures

Structures for DCM were designed considering alternatively the behaviour factor q equal to 2.5 (consistently with the value recommended by current codes) and equal to 4 (consistently with the proposed design criteria).

Tables from 8.1 to 8.4 summarize the cross section properties of structural members of the three, six and twelve-storey buildings compared with the frames designed according to EN 1998-1.

By observing Fig. 8.2 it is trivial to note that frames designed according to the proposed criteria generally lead to more slender bracing members, also if a behaviour factor q=2.5 is used. This feature can be explained considering that evaluating the overstrength factor according to Eq. (8.5) allows to better distribute the plasticity along the building height, practically eliminating the need to oversize the diagonals at lower storeys in order to satisfy the requirement on Ω variation (see Section 3.2.3).

Stockier bracings can be recognized in the 3-storey frames designed according to the proposed criteria, respect to the EC8-compliant case; indeed, higher steel grade was necessary in the frames design according to current code provisions, leading to relatively smaller diagonal members.

The values of the normalized slenderness obtained for both proposed criteria and EN 1998 are also reported in Tables from 8.5 to 8.7.

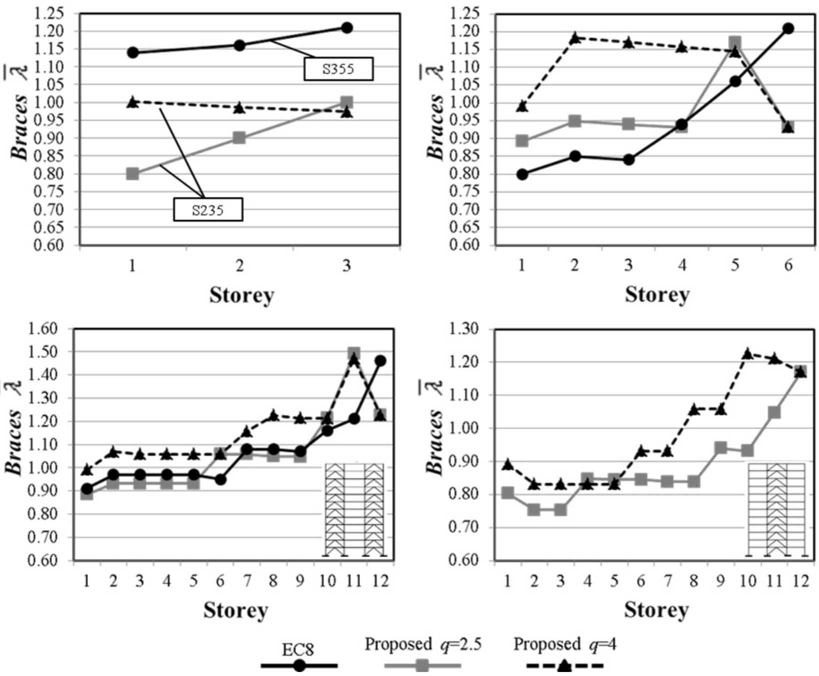

Figure 8.2 Normalized slenderness of braces at each storey: comparison between EN 1998-1 and proposed criteria.

Table 8.1 Cross section properties of structural members of 3-storey cases: proposed criteria vs EN-1998

Storey	Columns			Beams			Braces (d x t)			Gravity members	
	EC8	Proposed q=2.5	Proposed q=4	EC8	Proposed q=2.5	Proposed q=4	EC8	Proposed q=2.5	Proposed q=4	Columns	Beams
	S355	S355	S355	S460	S355	S355	S355	S235	S235	S355	S355
3	HE 200 B	HE 220 B	HE 220 B	HE 400 B	HE 550 B	HE 550 A	168.3 x 6	168.3 x 6	168.3 x 4	HE 200 B	IPE 330
2	HE 260 B	HE 260 B	HE 260 B	HE 400 B	HE 550M	HE 550 B	177.8 x 8	193.7 x 8	168.3 x 6	HE 240 B	IPE 330
1	HE 260 B	HE 260 B	HE 260 B	HE 500 B	HE 600M	HE 550M	193.7x 10	219.1 x 8	177.8 x 8	HE 240 B	IPE 330

Table 8.2 Cross section properties of structural members of 6-storey cases: proposed criteria vs EN-1998

Storey	Columns			Beams			Braces (d x t)			Gravity members	
	EC8	Proposed q=2.5	Proposed q=4	EC8	Proposed q=2.5	Proposed q=4	EC8	Proposed q=2.5	Proposed q=4	Columns	Beams
	S355	S355	S355	S460	S355	S355	S355	S355	S355	S355	S355
6	HE 400 A	HE 300 B	HE 300 B	HE 400 A	HE 500 M	HE 500 M	168.3 x 6	219.1 x 8	219.1 x 8	HE 260 A	IPE 330
5	HE 400 A	HE 300 B	HE 300 B	HE 450 B	HE 600 M	HE 450 M	193.7 x 8	177.8 x 10	177.8 x 6	HE 260 A	IPE 330
4	HE 450 B	HE 400 B	HE 340 B	HE 500 B	HE 600 M	HE 550 M	219.1 x 10	219.1 x 8	177.8 x 8	HE 280 B	IPE 330
3	HE 450 B	HE 400 B	HE 340 B	HE 550 B	HE 650 M	HE 550 M	244.5 x 10	219.1 x 10	177.8 x 10	HE 280 B	IPE 330
2	HD400x 347	HE 400 M	HE 340 M	HE 600 B	HE 700 M	HE 600 M	244.5 x 12	219.1 x 12	177.8 x 12	HE 280 M	IPE 330
1	HD400x 347	HE 400 M	HE 340 M	HE 600 M	HE 700 M	HE 600 M	273 x 12	244.5 x 10	219.1 x 8	HE 280 M	IPE 330

Table 8.3 Cross section properties of structural members of 12-storey-2braced bays cases: proposed criteria vs EN-1998

Storey	Columns			Beams*			Braces (d x t)		
	EC8	Proposed q=2.5	Proposed q=4	EC8	Proposed q=2.5	Proposed q=4	EC8	Proposed q=2.5	Proposed q=4
	S460	S355	S355	S460	S355	S355	S355	S355	S355
12	HE 320 M	HE 300 B	HE 300 B	HE 300 B	HE 600 B	HE 600 B	139.7 x 5	168.3 x 8	168.3 x 8
11	HE 320 M	HE 300 B	HE 300 B	HE 320 M	HE 550 B	HE 500 B	168.3 x 6	139.7 x 8	139.7 x 6
10	HE 320 M	HE 300 B	HE 300 B	HE 320 M	HE 550 B	HE 550 B	177.8 x 8	168.3 x 6.3	168.3 x 6
9	HD400x 347	HE 400 B	HE 400 B	HE 320 M	HE 600 A	HE 550 B	193.7 x 10	193.7 x 6	168.3 x 6.3
8	HD400x 347	HE 400 B	HE 400 B	HE 360 M	HE 600 B	HE 600 B	193.7 x 12	193.7 x 6.3	168.3 x 8
7	HD400x 347	HE 400 B	HE 400 B	HE 400 M	HE 600 B	HE 600 B	193.7x 12.5	193.7 x 8	177.8 x 8
6	HD400x 347	HE 400 M	HE 400 M	HE 550 M	HE 550 M	HE 600 B	219.1x 12.5	193.7 x 8	193.7 x 8
5	HD400x 347	HE 400 M	HE 400 M	HE 550 M	HE 550 M	HE 600 B	219.1 x 16	219.1 x 8	193.7 x 8
4	HD400x 347	HE 400 M	HE 400 M	HE 550 M	HE 550 M	HE 600 B	219.1 x 16	219.1 x 8	193.7 x 8
3	HD400x509	HD400x347	HD400x347	HE 550 M	HE 550 M	HE 600 B	219.1 x 16	219.1 x 8	193.7 x 8
2	HD400x509	HD400x347	HD400x347	HE 550 M	HE 550 M	HE 600 M	219.1 x 16	219.1 x 8	193.7 x 10
1	HD400x509	HD400x347	HD400x347	HE 650 M	HE 650 M	HE 600 M	244.5 x 16	244.5 x 8	219.1 x 8

*All gravity resistant beams are IPE 330

Table 8.4 Cross section properties of structural members of 12-storey-1braced bay cases

	Columns			Beams*		Braces (d x t)	
Storey	Gravity	P. q=2.5	P. q=4	P. q=2.5	P. q=4	P. q=2.5	P. q=4
	S355	S355	S355	S460	S355	S355	S355
12	HE 200 A	HE 400 B	HE 400 B	HE 600 M	HE 600 M	177.8 x 10	177.8 x 10
11	HE 200 A	HE 400 B	HE 400 B	HE 600 B	HE 550 B	193.7 x 6	168.3 x 6
10	HE 200 A	HE 400 B	HE 400 B	HE 600 M	HE 500 M	219.1 x 8	168.3 x 8
9	HE 220 B	HE 400 M	HE 400 M	HE 650 M	HE 550 M	219.1 x 10	193.7 x 8
8	HE 220 B	HE 400 M	HE 400 M	HE 650 M	HE 550 M	244.5 x 10	193.7 x 8
7	HE 220 B	HE 400 M	HE 400 M	HE 650 M	HE 550 M	244.5 x 10	219.1 x 8
6	HE 260 B	HD400x347	HD400x347	HE 700 M	HE 550 M	244.5 x 12	219.1 x 8
5	HE 260 B	HD400x347	HD400x347	HE 700 M	HE 600 M	244.5 x 12	244.5 x 8
4	HE 260 B	HD400x347	HD400x347	HE 700 M	HE 600 M	244.5 x 12.5	244.5 x 8
3	HE 300 B	HD400x509	HD400x421	HE 800 M	HE 600 M	273 x 12	244.5 x 8
2	HE 300 B	HD400x509	HD400x509	HE 800 M	HE 600 M	273 x 12	244.5 x 8
1	HE 300 B	HD400x509	HD400x509	HE 800 M	HE 700 M	273 x 12.5	244.5 x 10

*All gravity resistant beams are IPE 330

Table 8.5 Brace slenderness ratios in 3-storey cases: comparison between proposed criteria and EN 1998

	Brace normalized slenderness $\bar{\lambda}$		
Storey	EC8	Proposed q=2.5	Proposed q=4
3	1.21	1	0.97
2	1.16	0.9	0.99
1	1.14	0.8	1.00

Table 8.6 Brace slenderness ratios in 6-storey cases: comparison between proposed criteria and EN 1998

	Brace normalized slenderness		
Storey	EC8	Proposed q=2.5	Proposed q=4
6	1.21	0.93	0.93
5	1.06	1.17	1.14
4	0.94	0.93	1.16
3	0.84	0.94	1.17
2	0.85	0.95	1.18
1	0.8	0.89	0.99

Table 8.7 Brace slenderness ratios in 12-storey cases: comparison between proposed criteria and EN 1998

	Brace normalized slenderness				
	2 braced bays			1 braced bay	
Storey	EC8	Proposed q=2.5	Proposed q=4	Proposed q=2.5	Proposed q=4
12	1.46	1.23	1.23	1.17	1.17
11	1.21	1.49	1.47	1.05	1.21
10	1.16	1.21	1.21	0.93	1.23
9	1.07	1.05	1.21	0.94	1.06
8	1.08	1.05	1.23	0.84	1.06
7	1.08	1.06	1.16	0.84	0.93
6	0.95	1.06	1.06	0.85	0.93
5	0.97	0.93	1.06	0.85	0.83
4	0.97	0.93	1.06	0.85	0.83
3	0.97	0.93	1.06	0.75	0.83
2	0.97	0.93	1.07	0.75	0.83
1	0.91	0.88	0.99	0.80	0.89

Figure 8.3 reports the values of the beam-to-brace stiffness ratio K_F (see Eq. (5.1)) at each storey for the frames designed according to the proposed design rules compared to those obtained in compliance with EN 1998-1.

The structures designed according to the proposed design criteria (considering both q=2.5 and q=4), are characterized by significantly larger beam-to-brace stiffness ratios, generally twice the corresponding values in EC8-compliant cases. Indeed, according the proposed procedure, the design of the brace-intercepted beam is directly affected by to the additional requirement on the flexural stiffness given by Eq (8.7).

The values the beam-to-brace stiffness ratio K_F obtained for both proposed criteria and EN 1998 are also reported in Tables from 8.5 to 8.7, for all three, six and twelve-storey cases, respectively.

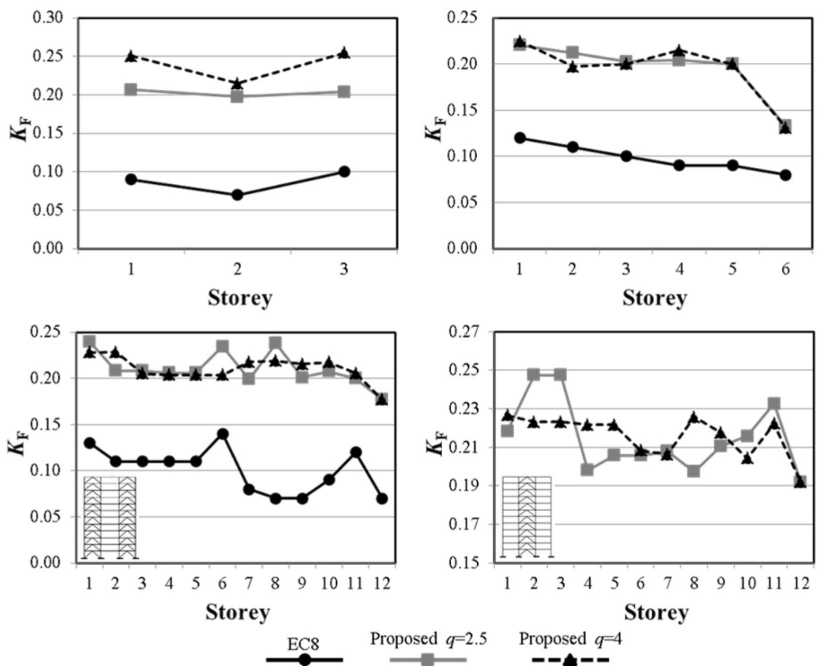

Figure 8.3 Beam-to-brace stiffness ratio at each storey: comparison between EN 1998-1 and proposed criteria.

8.3.2.1.2 Eigenvalue analyses

Figure 8.4 depicts the periods of vibration for the first (T_1) and the second (T_2) mode of vibration for all low, medium and high rise frames designed according to both EN 1998 and proposed design rules; the relevant participating mass percentages ($M_{x,1}$ and $M_{x,2}$ respectively) are shown in Fig. 8.5. Either periods of vibration and participating mass percentages are even summarized in Tables from 8.8 to 8.11.

Slightly larger periods of vibration can be recognized designing according to the proposed criteria (especially by assuming q=4) respect to the European one for the first vibration mode; similar values of periods of vibration can be recognized for all the cases for the second vibration mode. No appreciable differences can be noted in terms of participating mass percentages (see Fig. 8.5).

Table 8.8 Dynamic characteristics of 3-storey cases.

Case	T_1 (sec)	T_2 (sec)	$M_{x,1}$ (%)	$M_{x,2}$ (%)
EC8	0.38	0.14	93.15%	6.69%
Proposed q=2.5	0.38	0.14	93.83%	6.00%
Proposed q=4	0.42	0.15	92.61%	7.19%

Table 8.9 Dynamic characteristics of 6-storey cases.

Case	T_1 (sec)	T_2 (sec)	$M_{x,1}$ (%)	$M_{x,2}$ (%)
EC8	0.58	0.22	86.54%	11.47%
Proposed *q*=2.5	0.61	0.22	87.04%	11.47%
Proposed *q*=4	0.66	0.24	86.32%	11.92%

Table 8.10 Dynamic characteristics of 12-storey-2 braced bays cases.

Case	T_1 (sec)	T_2 (sec)	$M_{x,1}$ (%)	$M_{x,2}$ (%)
EC8	0.84	0.29	72.55%	20.26%
Proposed *q*=2.5	1.19	0.36	72.02%	20.91%
Proposed *q*=4	1.20	0.36	72.19%	20.57%

Table 8.11 Dynamic characteristics of 12 storey-1 braced bay-storey cases.

Case	T_1 (sec)	T_2 (sec)	$M_{x,1}$ (%)	$M_{x,2}$ (%)
Proposed *q*=2.5	1.19	0.00	75.63%	19.97%
Proposed *q*=4	1.34	0.00	76.55%	18.20%

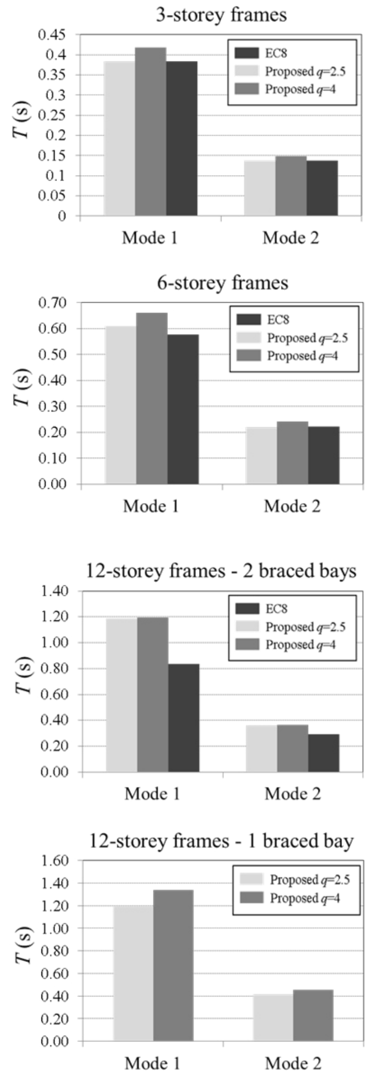

Figure 8.4 Periods of vibration: comparison between EN 1998-1 and proposed criteria.

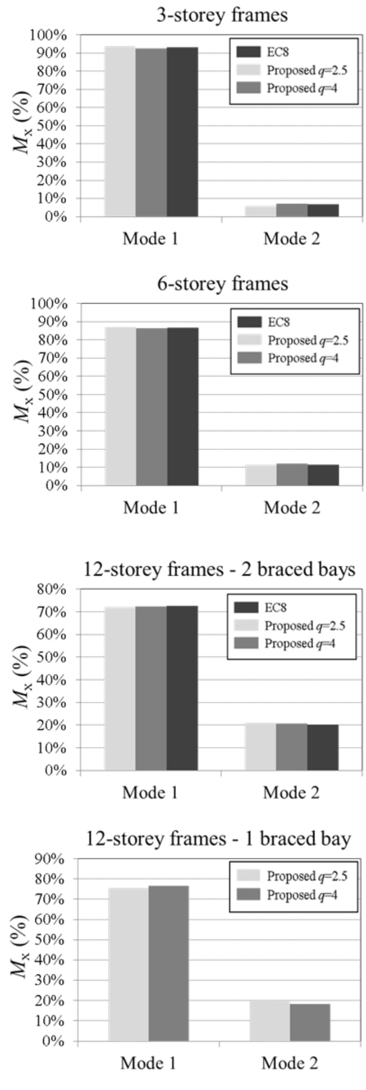

Figure 8.5 Participating mass percentages: comparison between EN 1998-1 and proposed criteria.

8.3.2.1.3 Nonlinear dynamic analyses

In this Section results from nonlinear analyses performed on building structures designed for DCM are presented and discussed in comparison with the seismic performance exhibited by the frames designed according to the current code.

Both global and local performance indicators were selected to evaluate the seismic response of all the examined frames; the monitored parameters for all limit states are summarized and described in Section 7.3.3.3.

Hereinafter, the results are presented showing the average demand obtained by the 14 considered records per response indicator, with reference to the three hazard levels as defined in Section 7.3.3.1.

Figures from 8.6 to 8.9 depicts both transient (θ, see Fig. 7.8.6-8.9a) and residual (θ_{RES}, Fig. 78.6-8.9b) interstorey drift ratios for low, medium and high rise frames, related to the considered performance levels. All frames designed according to the proposed procedure exhibit satisfactorily performance with adequate lateral stiffness. In addition, in the most of cases, more uniform distribution of deformations along the building height can be recognized for the systems designed according to the proposed design rules, respect to the EC8-compliant cases: by observing Figs from 8.6 to 8.9, different displacement shape profiles can be recognized, namely cantilever-type for EC8-compliant case, while shear-type is obtained for frames designed according to the proposed procedure. Indeed, according to the proposed design criteria, the diagonal members at the roof storeys are designed to remain in the elastic range (See Eq. 8.2); as a consequence the damage concentration at upper storeys typically obtained in the EC8-compliant cases, is avoided. Moreover, the revision applied to the requirement on the overstrength factor variation (See Eq. 8.5), namely to define the Ω factor at the i-th storey considering the buckling capacity of the diagonal member as first nonlinear event in place of the plastic strength considered according to the current code, allows to better control the distribution of plasticity along the building height, contributing to obtain more favourable displacement profiles respect to the EC8-compliant cases.

However, all examined frames exhibit satisfactorily performance at DL limit state, because the interstorey drift ratios do not exceed the limit values required by EN 1998-1 for buildings having ductile non-structural elements and for buildings having non-structural elements fixed in a way so as not to interfere with structural deformations or without non-structural elements (namely 0.75% and 1%, respectively).

Figures from 8.10 to 8.13 show the profiles of peak storey accelerations for three, six and twelve-storey frames, respectively: EC8-compliant frames are characterized by significant storey accelerations, whose peak average value (A) at SD limit state increases up to over 20 times, 35 times and 4 times the peak record acceleration (A_d) for the three, six and twelve storey frames respectively. On the contrary, the significantly smaller average peak storey accelerations can be recognized for frames designed according to the proposed procedure, due to the larger dissipative capacity provided by the yielding of braces (see also Figs. from 8.14 to 8.17). The better response in terms of acceleration profiles is obtained assuming the behaviour factor q equal to 4, with values of the ratio A/A_d close to the unit.

The peak storey accelerations reach smaller value for the twelve-storey frames respect to the low and medium rise buildings, mainly due to the larger values of the fundamental period, and thus natural frequencies to which smaller spectral accelerations correspond.

Figures from 8.14 to 8.17 depict the braces ductility demand (μ) both in tension and in compression, for low, medium and high rise buildings, respectively.

As discussed in previous Chapter, the EC8-compliant frames experience very limited plastic engagement, with braces under tension behaving elastically up to NC limit state; moreover, the cantilever-type behaviour entails significant damage concentration at the top of the building where also severe deterioration in the braces under compression can be recognized.

At the contrary, frames designed according to the proposed design rules, exhibit significantly better performance with braces yielded in tension and less severe damage concentration under compression. These results confirm the outcomes previously described in Chapter V, and the need to introduce design requirements to control not only the beam strength, but rather its flexural stiffness, which significantly modifies the demand on bracing members.

Figures from 8.18 to 8.21 show the axial deformation of diagonal members under compression, normalized to the displacement at the brace buckling (see Eq. 7.6), while Figures 8.22 to 8.25 show the brace out-of-plane deformations, expressed in terms of both, out of plane rotation θ_{br} (a) and normalized displacement $\bar{w}$ (see Fig. 5.27a in Section 5.7.3.3). Similar values of brace out-of-plane rotation can be recognized between EN 1998 and proposed criteria, except for the the three-storey cases in which, slightly larger braces out of plane rotations can be recognized ad DL limit states designing according to proposed criteria. Coherently with the displacement shape and the brace ductility demand profiles, different distribution of out-of-plane deformation along the building heigth can be recognized, with the most severe demand at the upper storeys for EC8 compliant frames, and for intermediate storey for proposed procedure.

The beam response is assessed by means of the normalized unbalanced force β (see Eq. 7.8) occurring after the brace buckling under compression; in addition, the beam chord rotation ($\theta_{b,}$ see Eq. 7.9) is monitored in order to verify the occurrence of flexural yielding. Figures from 8.26 to 8.29 show the average normalized unbalanced force β value occurring on the beam at each storey. As deeply discussed in previous Sections, the bending demand on the brace-intercepted beam is strongly related to the unbalanced force and thus to the post-buckling behaviour of the compression brace; from Figures 8.26 to 8.29 it can be recognized that the unbalanced force acting at the brace-intercepted section is smaller for the EC8-compliant frames owing to poor plastic engagement of the braces under tension, rather than to limited degradation of their compression strength. Indeed, comparing these results with those depicted in Figs from 8.14 to 8.17, it can be noted that the most stressed beams are located at levels where poor plastic engagement is experienced by the braces under both tension and compression.

Figures from 8.30 to 8.33 show the beams chord rotation (see Eq. 7.9) for three, six and twelve-storey frames, respectively; moreover, the normalized beam rotation was monitored (See Figs 8.30-33b) in order to identify eventual yielding phenomena. The bending demand distribution on the beams along the building height is basically consistent to the normalized unbalanced force profiles; no plastic hinge occurs in the beams belonging to all low, medium and high rise buildings. However, it should be noted that at both SD and NC limit states, the EC8-compliant frames experience the largest rotation, even though limited unbalance force occurs on the beams (See Fig.s 8.30-33b). Indeed, the additional requirement stating the lower bound limit for beam flexural stiffness (See Eq. 8.7) provided within the proposed design rules, allows avoiding significant vertical deflection and consequent detrimental effects on braces ductility demand.

These results are also confirmed by Figs. from 8.34 to 8.37, where beam vertical displacement $d_{z,beam}$ normalized to the relative horizontal displacement at each storey ($d_{x,i}$) is showed. This parameter clarifies that even though the smaller unbalanced forces occur on beams, in EC8-compliant frames the contribution of the beams vertical deflection to the overall lateral deformability (see Fig. 5.1) is significantly larger respect to the frames designed according to the proposed design rules and even becomes dominant at upper storeys.

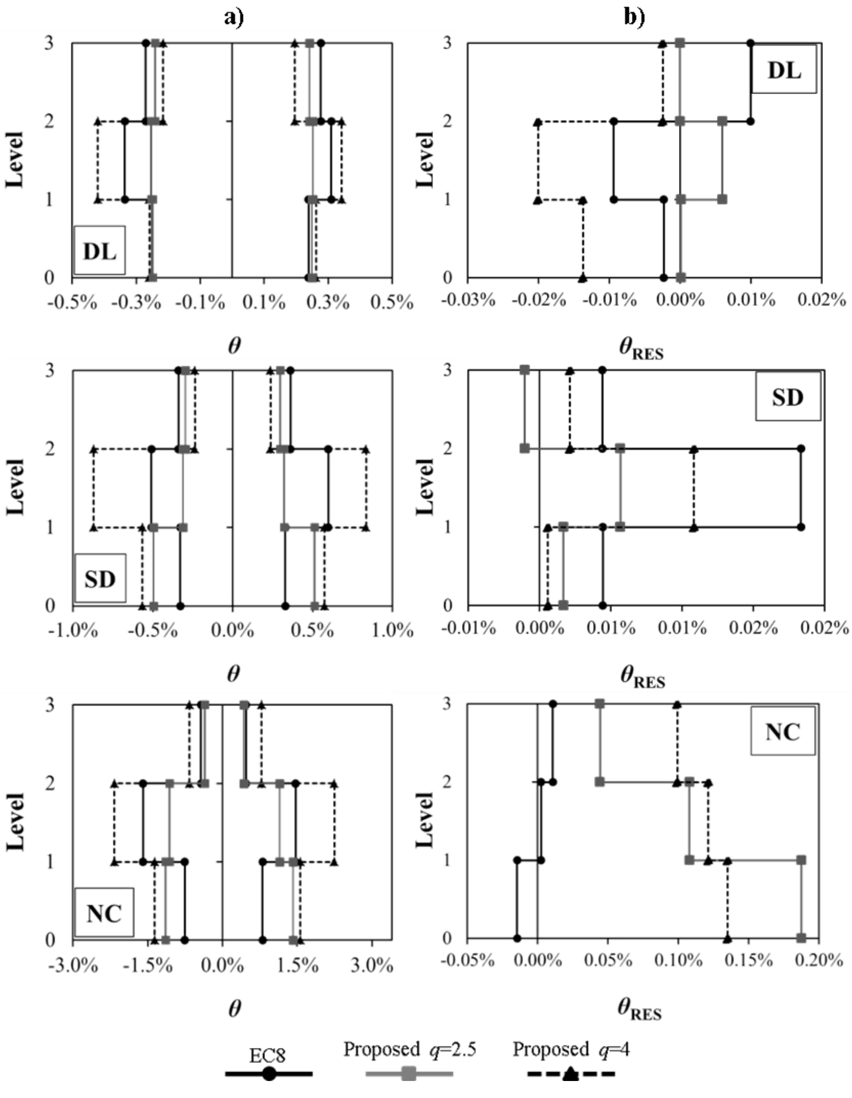

Figure 8.6 Interstorey drift transient (a) and residual (b) for 3-storey cases: proposed criteria vs EN 1998.

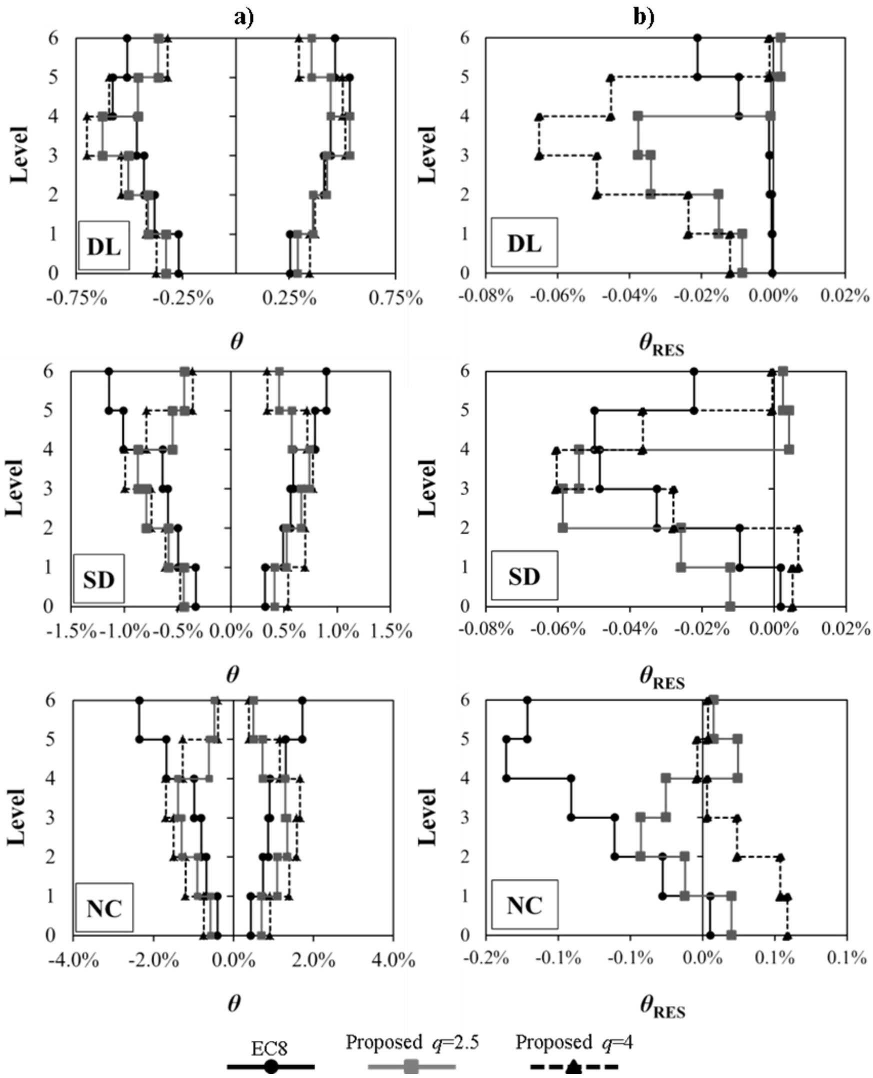

Figure 8.7 Interstorey drift transient (a) and residual (b) for 6-storey cases: proposed criteria vs EN 1998.

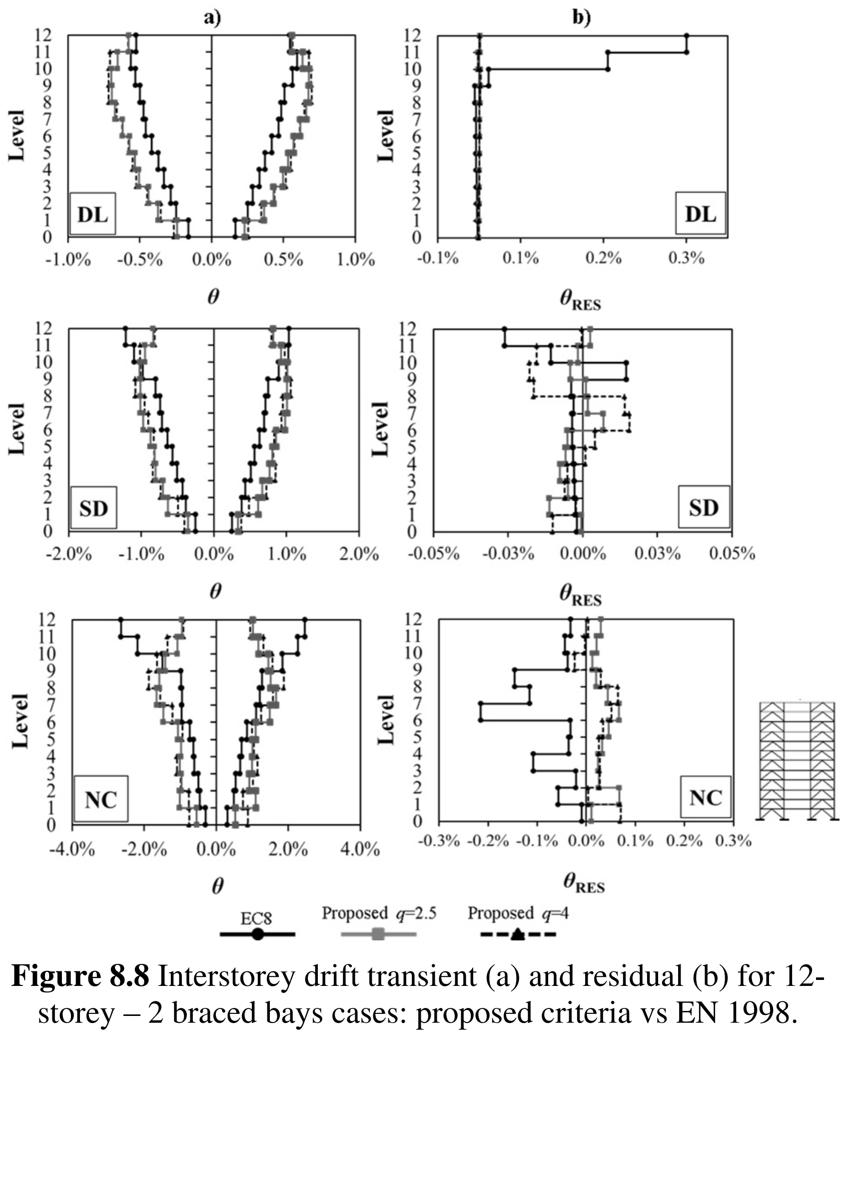

Figure 8.8 Interstorey drift transient (a) and residual (b) for 12-storey – 2 braced bays cases: proposed criteria vs EN 1998.

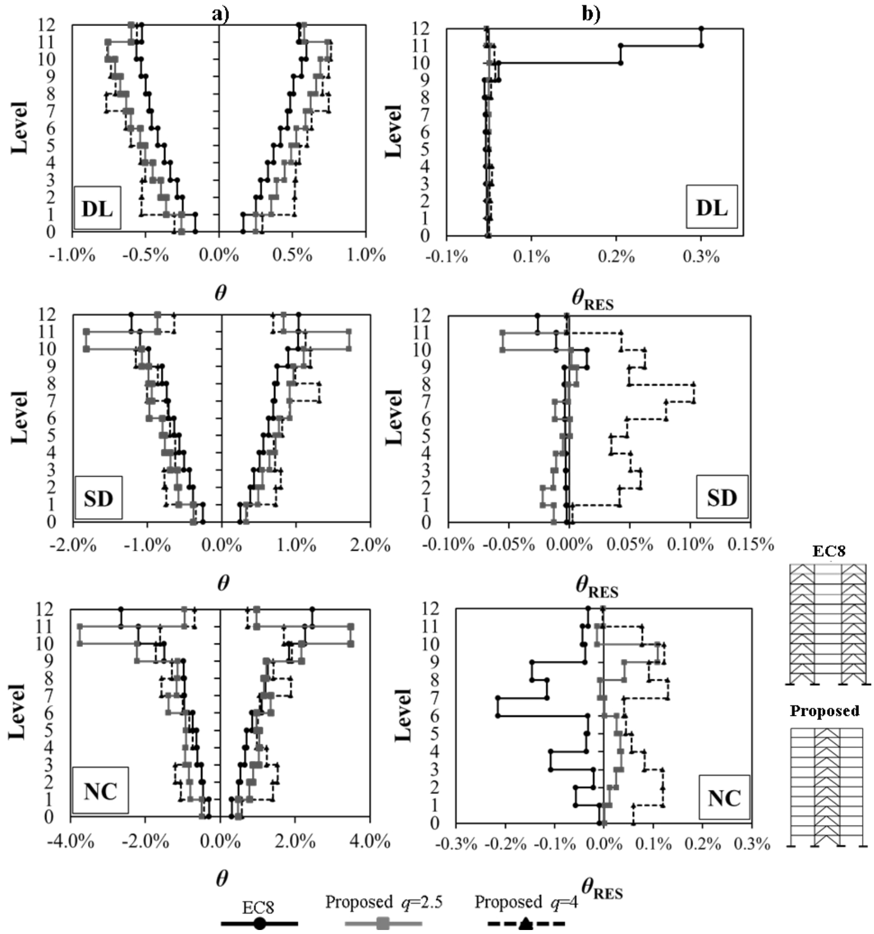

Figure 8.9 Interstorey drift transient (a) and residual (b) for 12 storey – 1 braced bay cases: proposed criteria vs EN 1998.

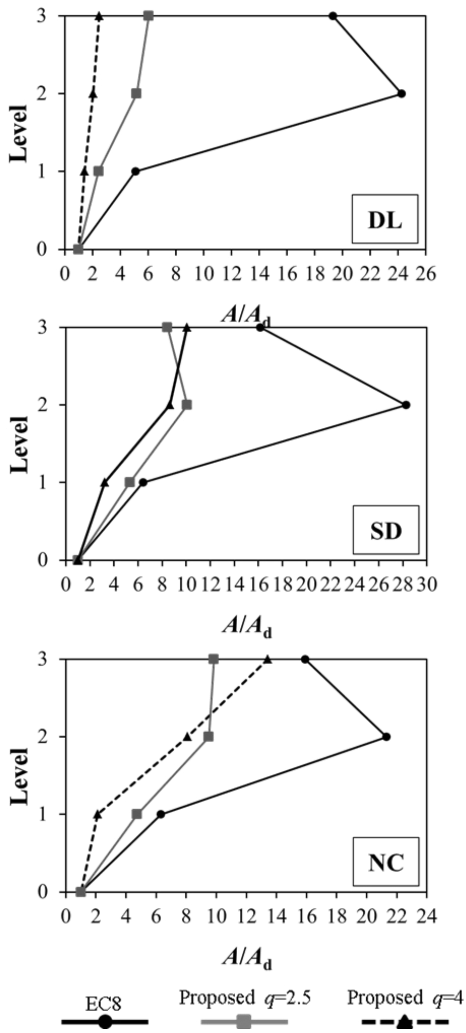

Figure 8.10 Peak storey acceleration for 3-storey cases: proposed criteria vs EN 1998.

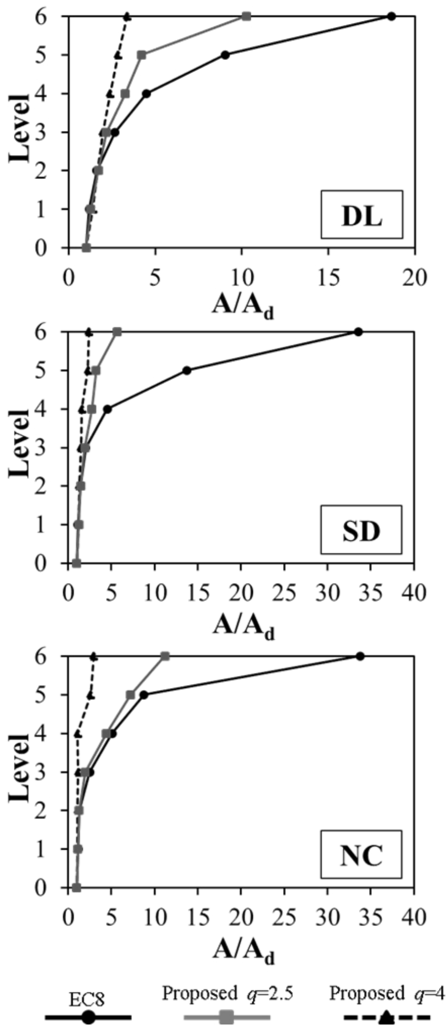

Figure 8.11 Peak storey acceleration for 6-storey cases: proposed criteria vs EN 1998.

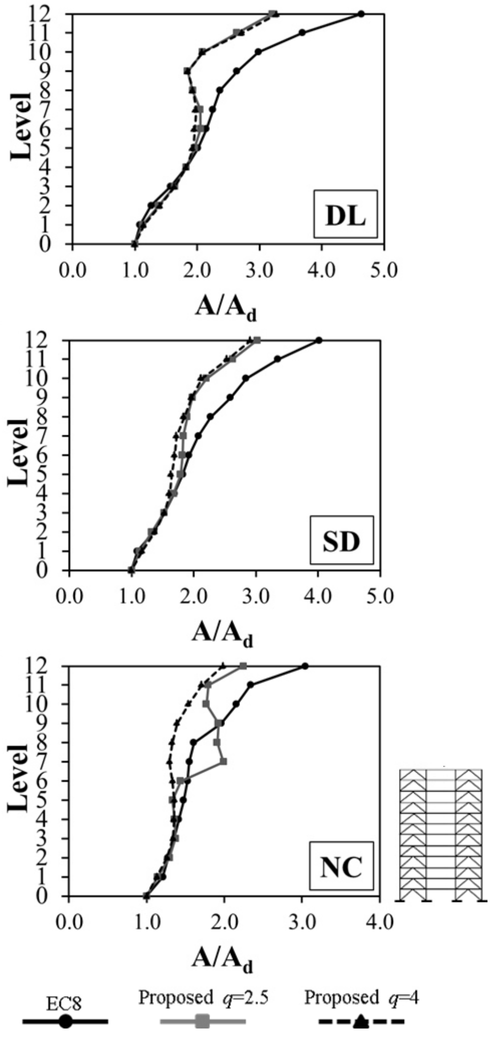

Figure 8.12 Peak storey acceleration for 12-storey – 2 braced bays cases: proposed criteria vs EN 1998.

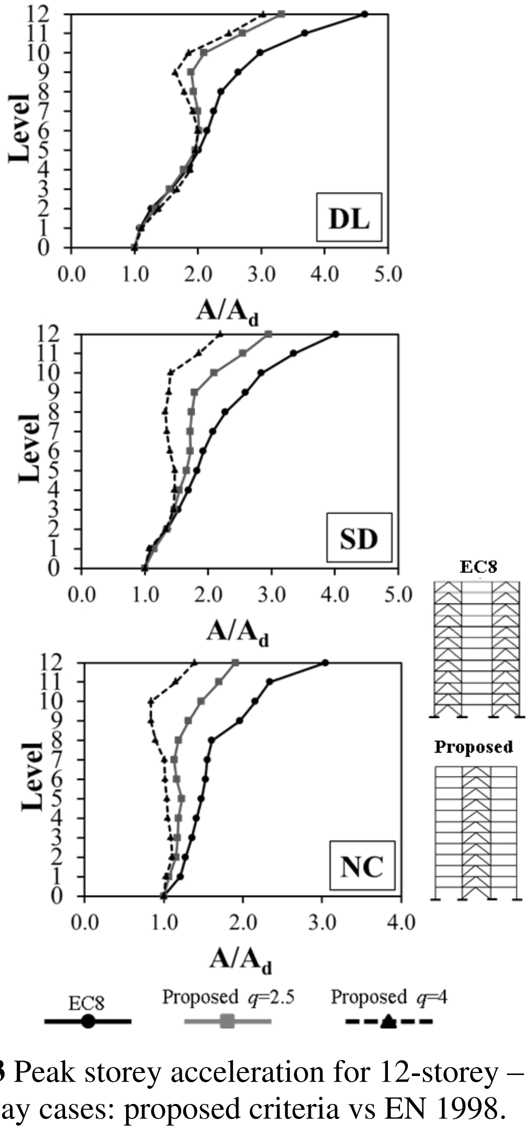

Figure 8.13 Peak storey acceleration for 12-storey – 1 braced bay cases: proposed criteria vs EN 1998.

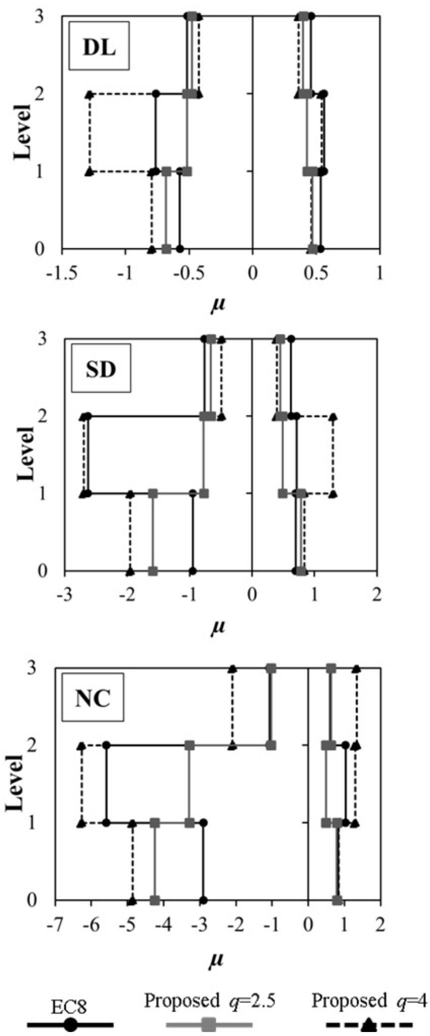

Figure 8.14 Braces ductility demand for 3-storey cases: proposed criteria vs EN 1998.

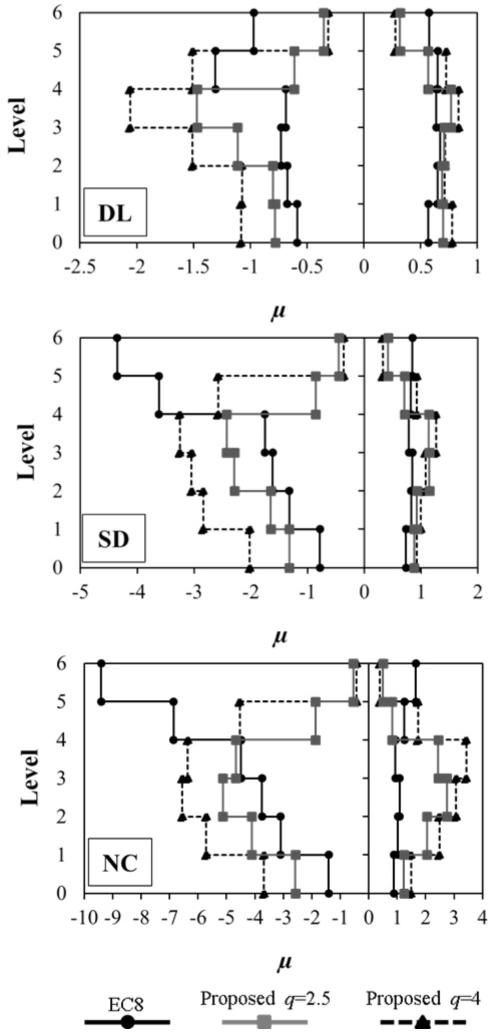

Figure 8.15 Braces ductility demand for 6-storey cases: proposed criteria vs EN 1998.

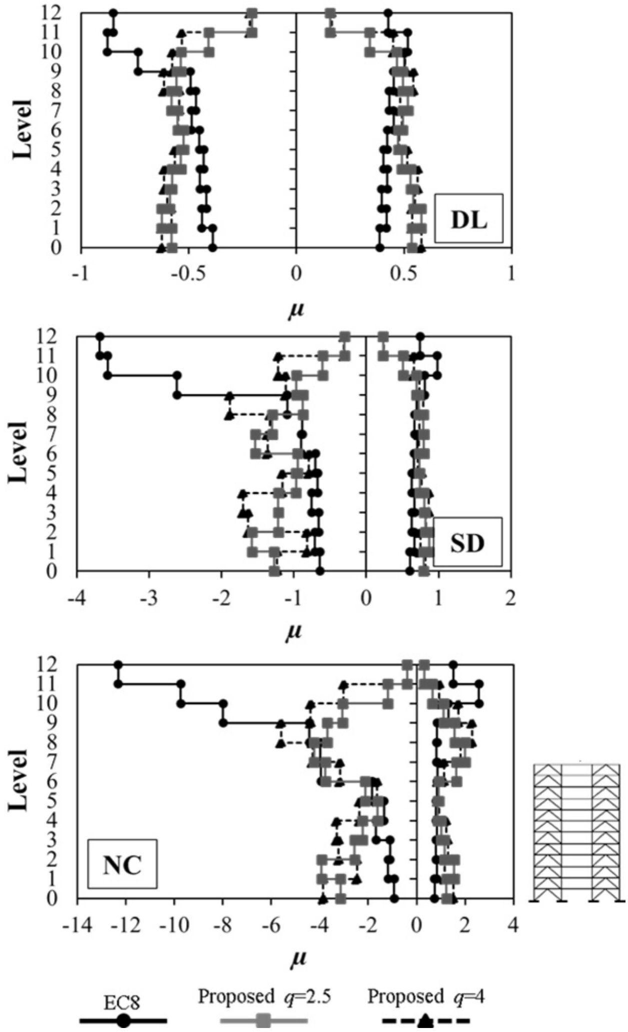

Figure 8.16 Braces ductility demand for 12-storey – 2 braced bays cases: proposed criteria vs EN 1998.

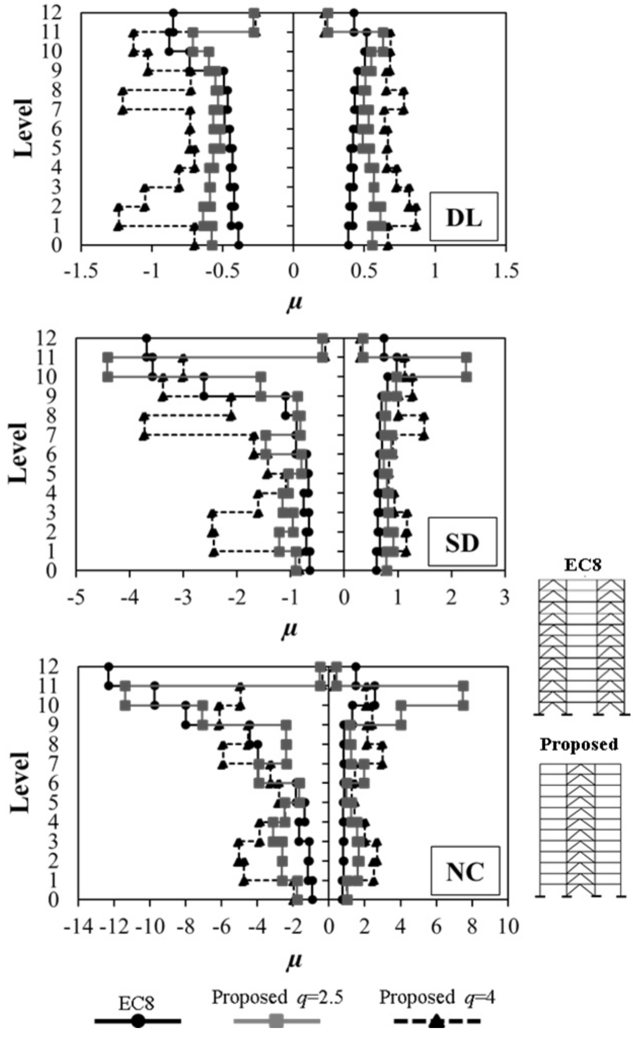

Figure 8.17 Braces ductility demand for 12-storey – 1 braced bay cases: proposed criteria vs EN 1998.

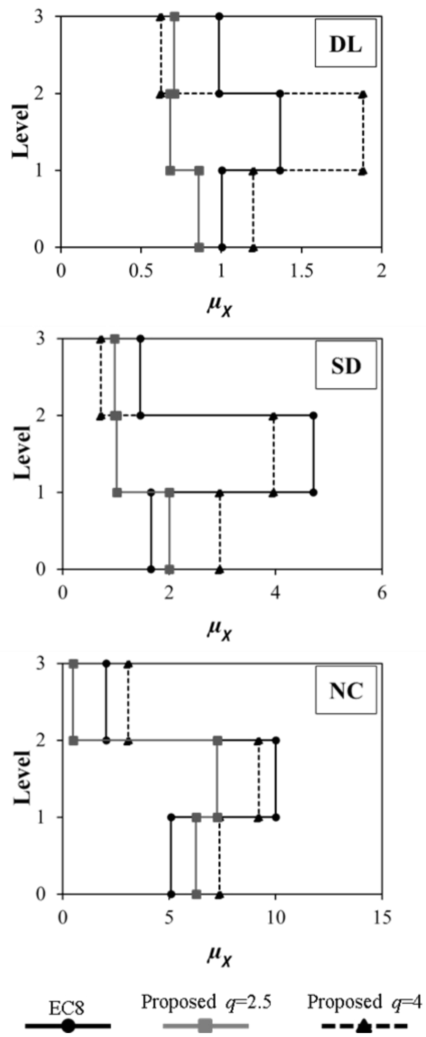

Figure 8.18 Braces ductility demand in compression for 3-storey cases: proposed criteria vs EN 1998.

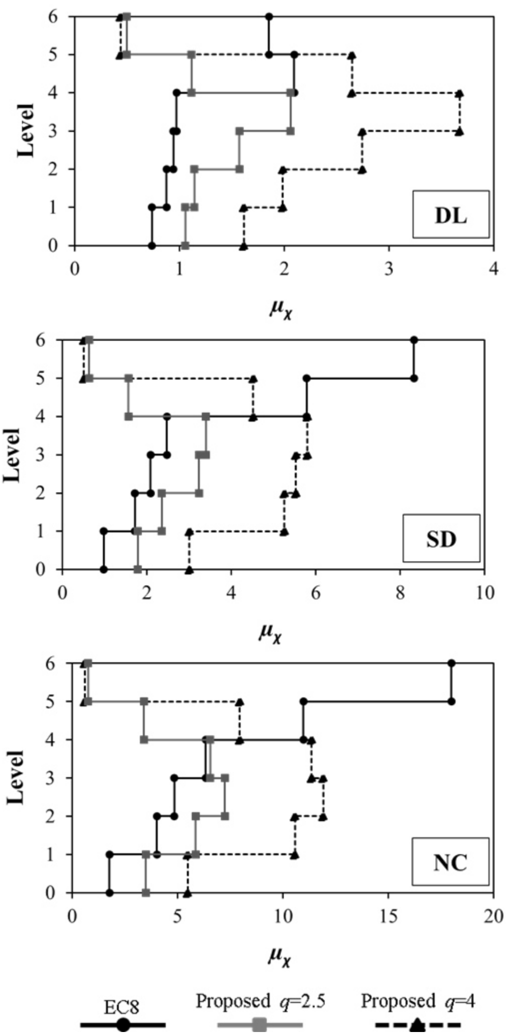

Figure 8.19 Braces ductility demand in compression for 6-storey cases: proposed criteria vs EN 1998.

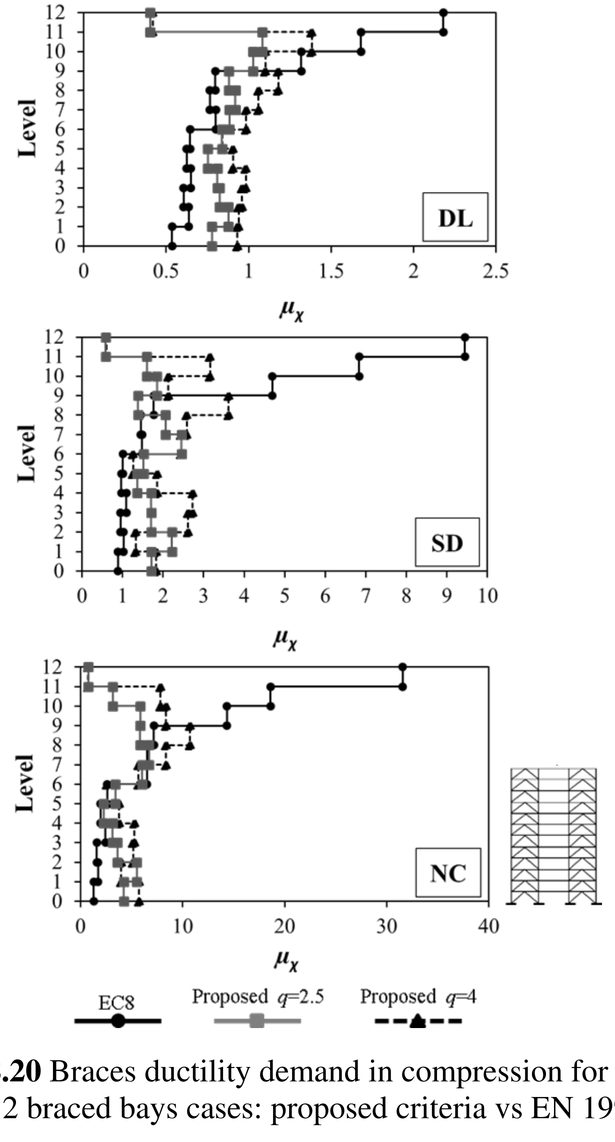

Figure 8.20 Braces ductility demand in compression for 12-storey – 2 braced bays cases: proposed criteria vs EN 1998.

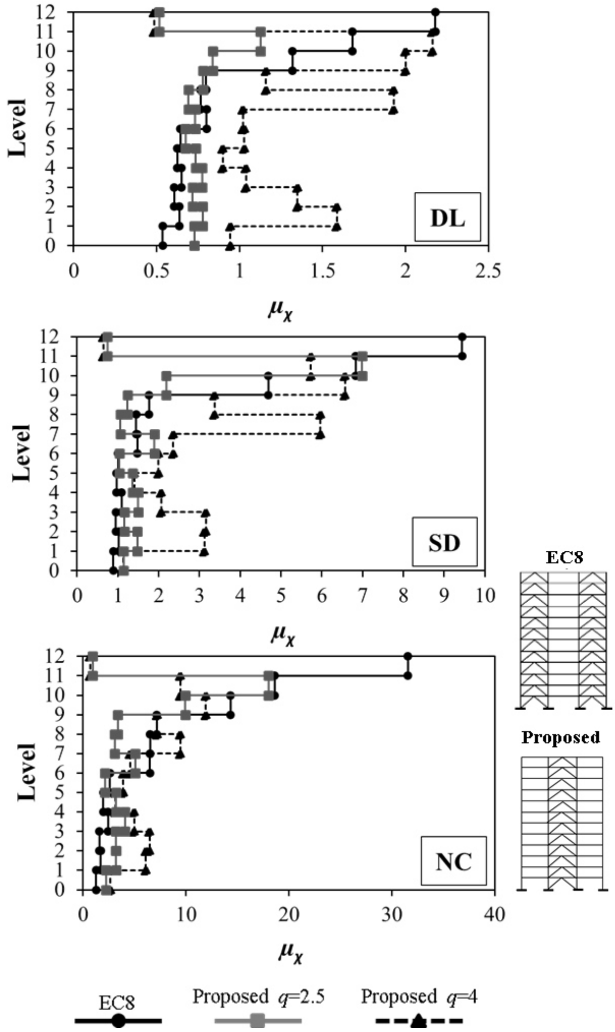

Figure 8.21 Braces ductility demand in compression for 12-storey – 1 braced bay cases: proposed criteria vs EN 1998.

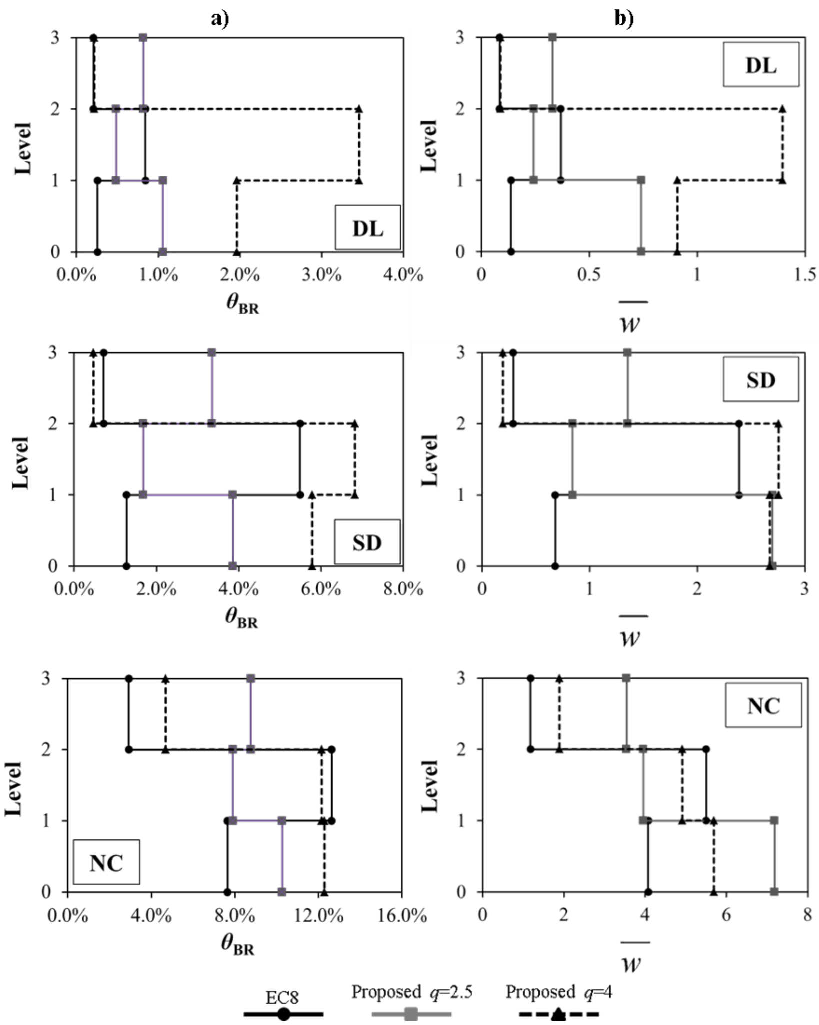

Figure 8.22 Braces out-of-plane rotations (a) and normalized displacements (b) for 3-storey cases: proposed criteria vs EN 1998.

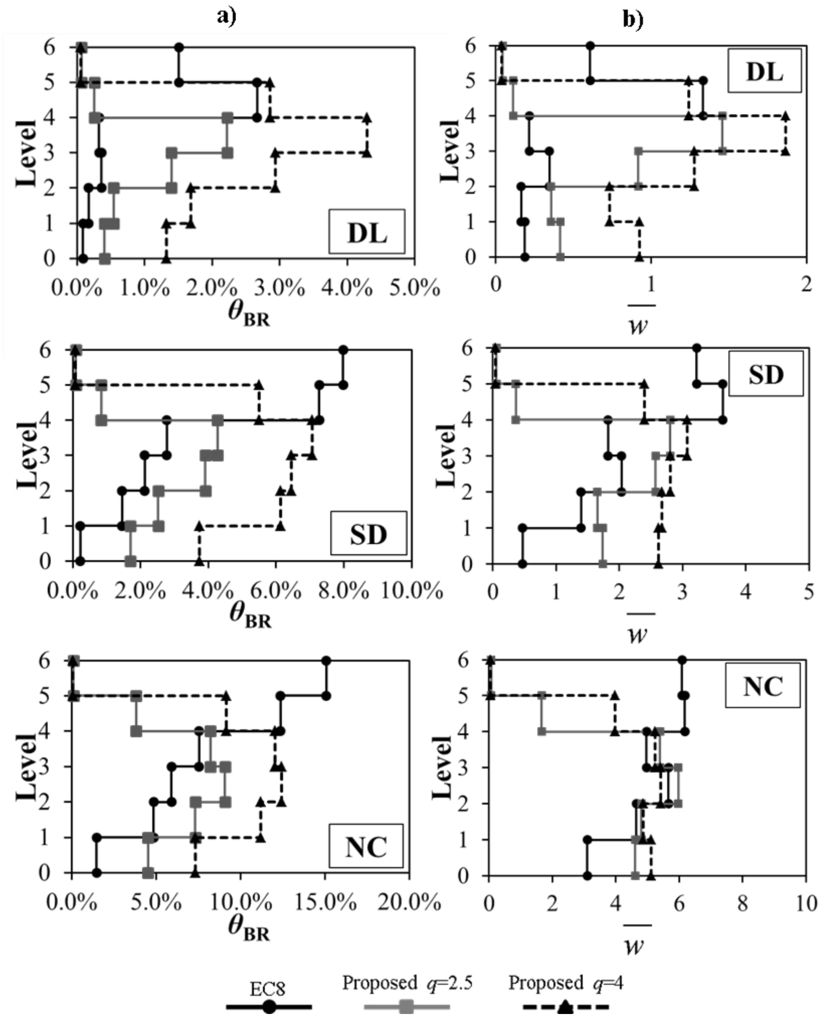

Figure 8.23 Braces out-of-plane rotations (a) and normalized displacements (b) for 6-storey cases: proposed criteria vs EN 1998.

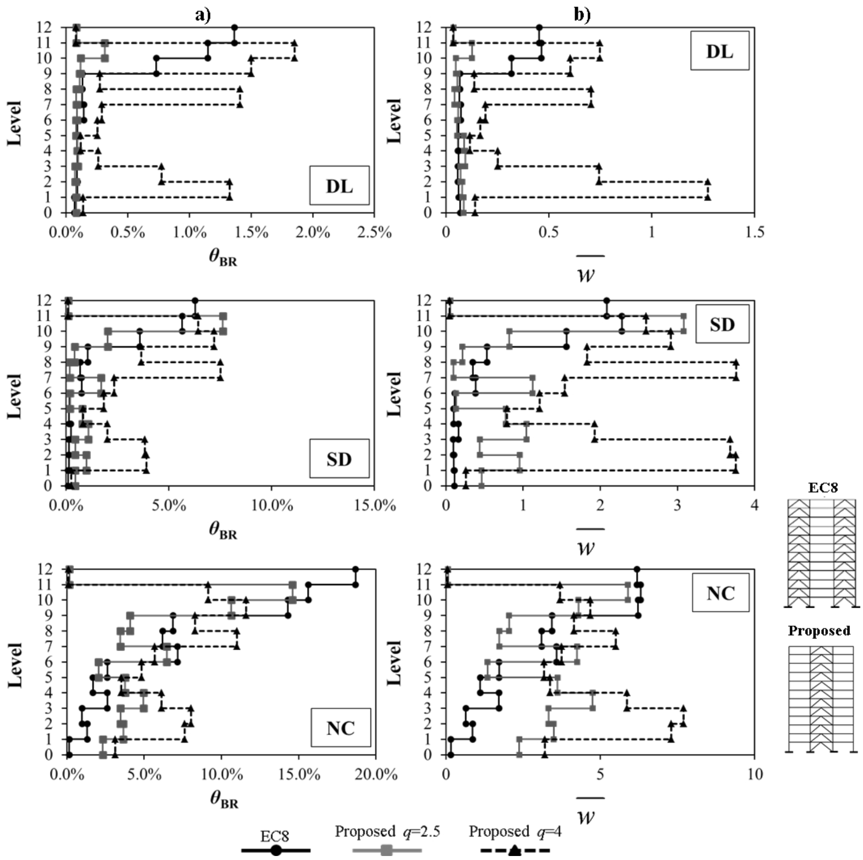

Figure 8.24 Braces out-of-plane rotations (a) and normalized displacements (b) for 12-storey – 2 braced bays cases: proposed criteria vs EN 1998.

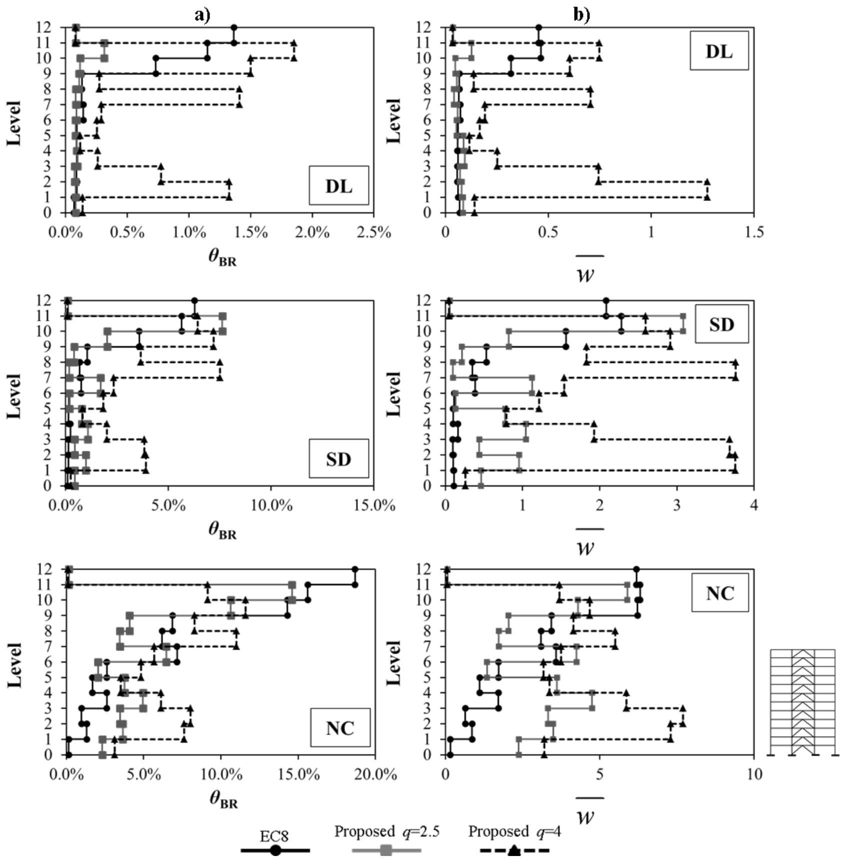

Figure 8.25 Braces out-of-plane rotations (a) and normalized displacements (b) for 12-storey – 1 braced bay cases: proposed criteria vs EN 1998.

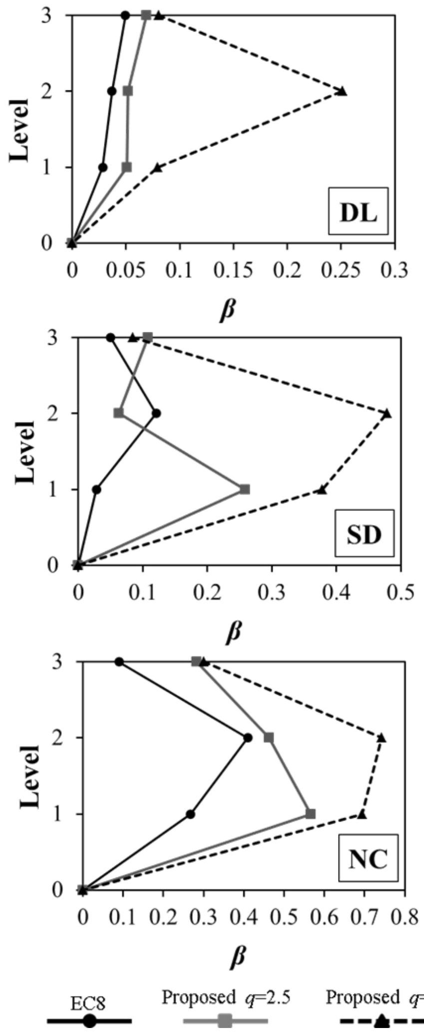

Figure 8.26 Unbalanced force applied on the beam for 3-storey cases: proposed criteria vs EN 1998.

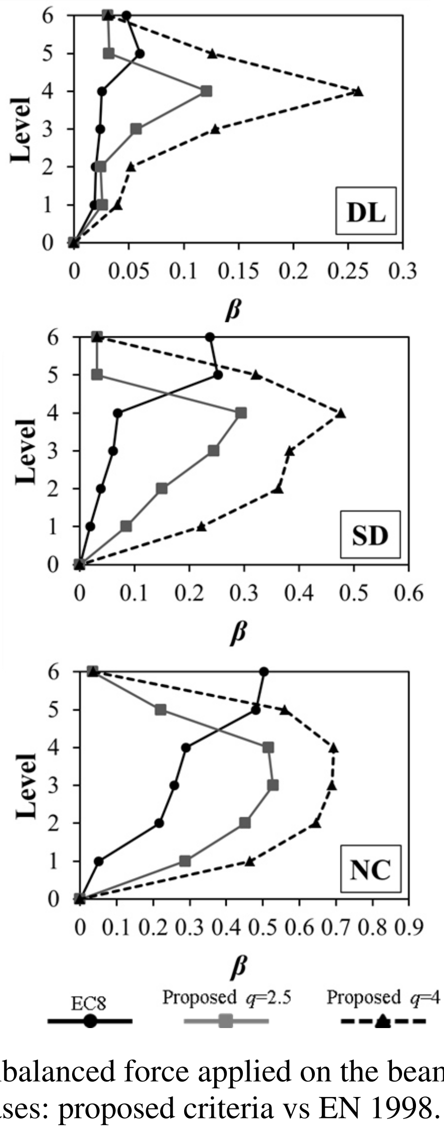

Figure 8.27 Unbalanced force applied on the beam for 6-storey cases: proposed criteria vs EN 1998.

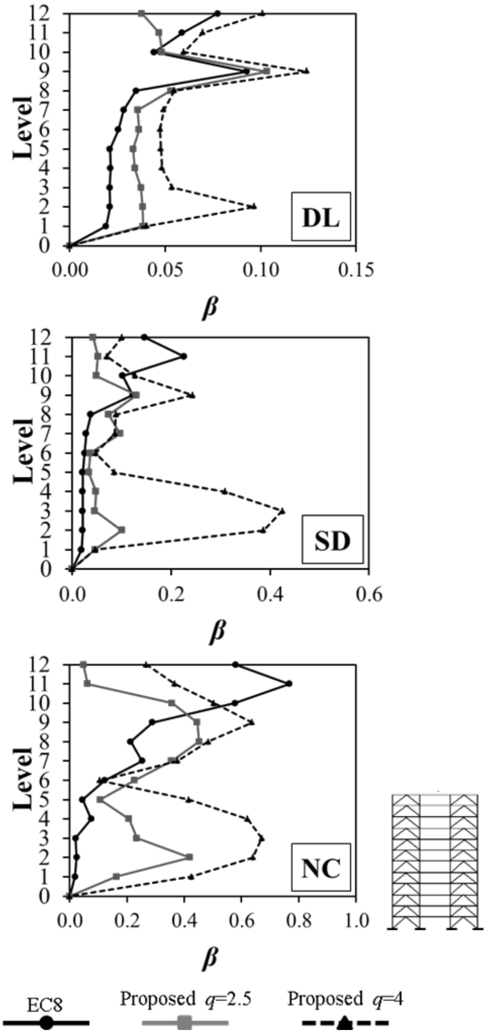

Figure 8.28 Unbalanced force applied on the beam for 12-storey – 2 braced bays cases: proposed criteria vs EN 1998.

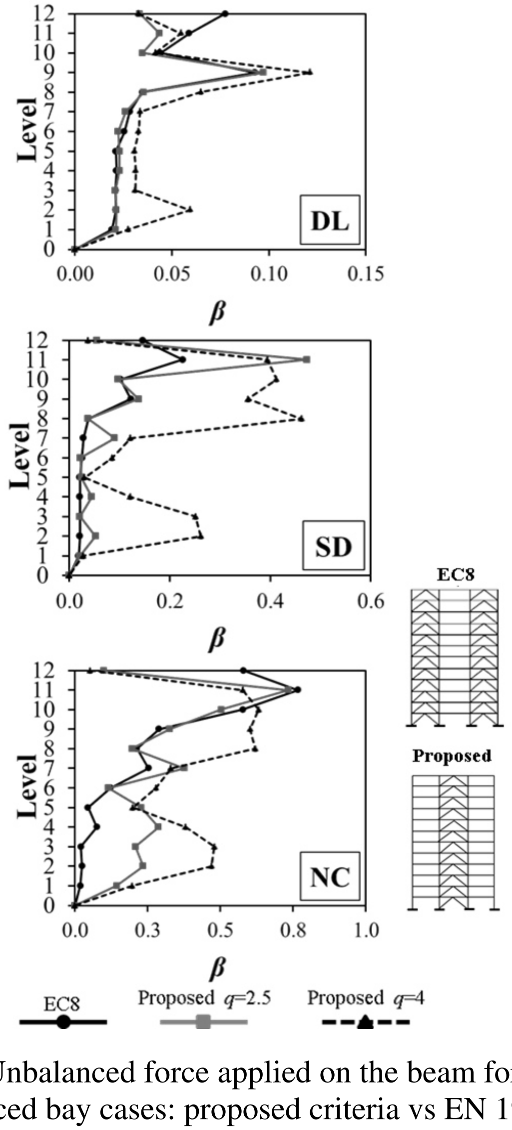

Figure 8.29 Unbalanced force applied on the beam for 12-storey – 1 braced bay cases: proposed criteria vs EN 1998.

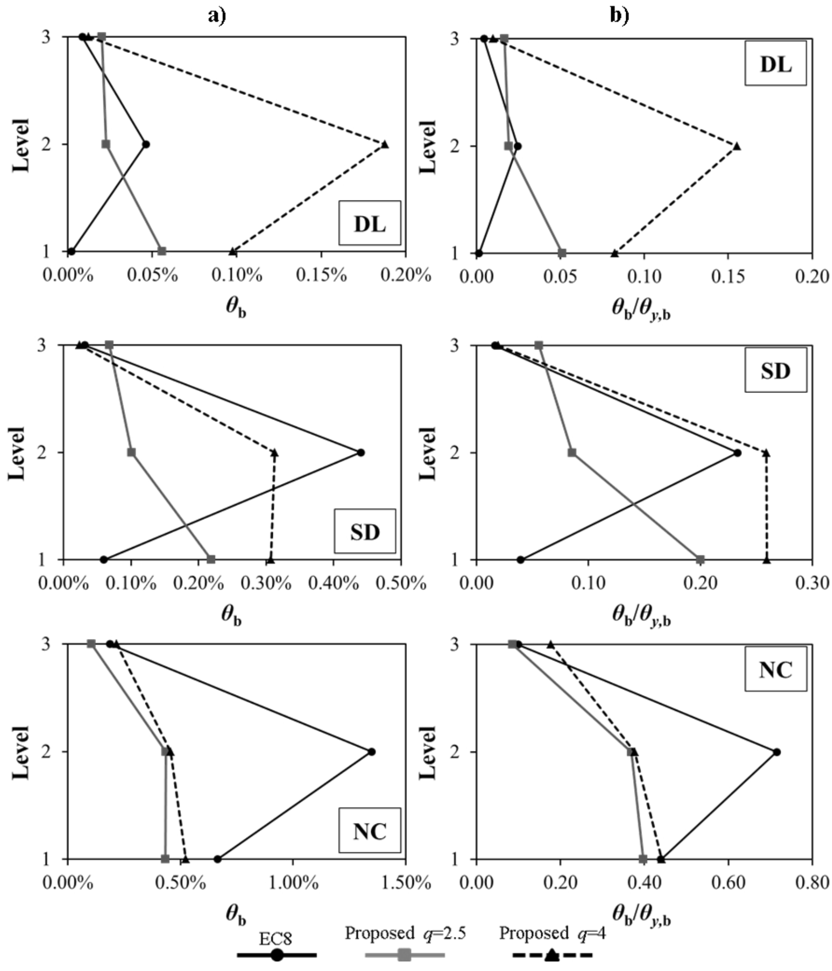

Figure 8.30 Beam chord rotation (a) and beam yielding (b) for 3-storey cases: proposed criteria vs EN 1998.

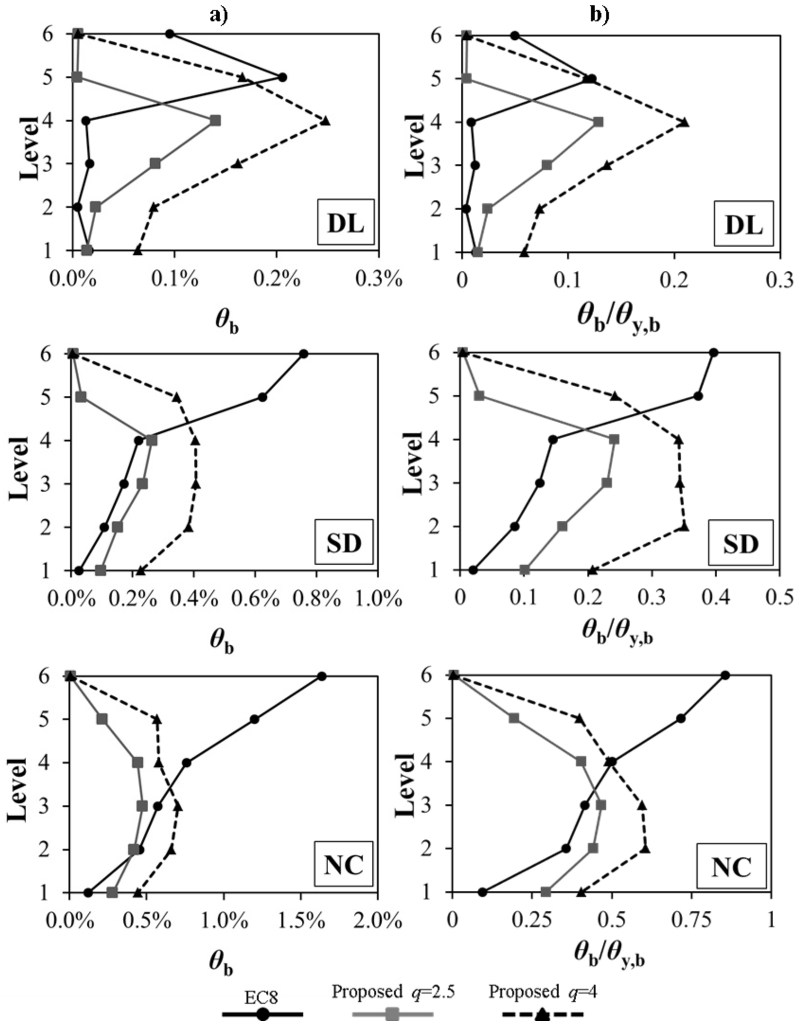

Figure 8.31 Beam chord rotation (a) and beam yielding (b) for 6-storey cases: proposed criteria vs EN 1998.

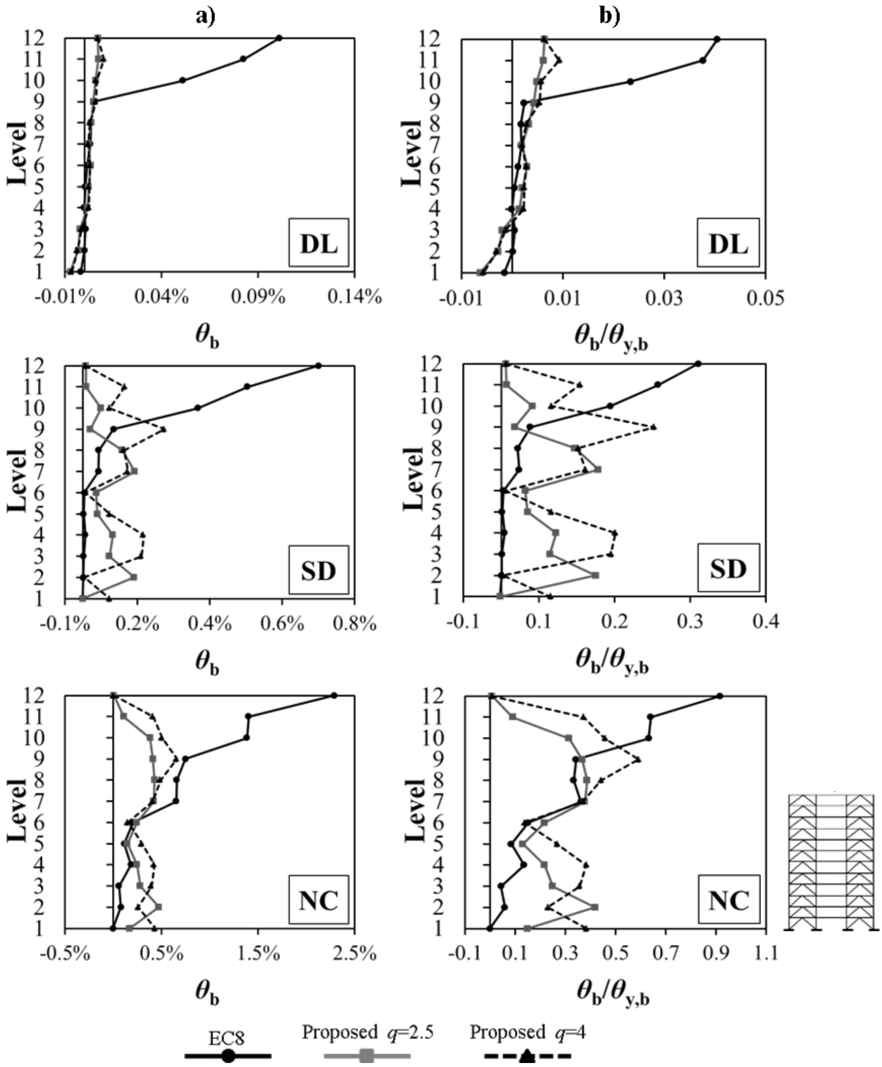

Figure 8.32 Beam chord rotation (a) and beam yielding (b) for 12-storey – 2 braced bays cases: proposed criteria vs EN 1998.

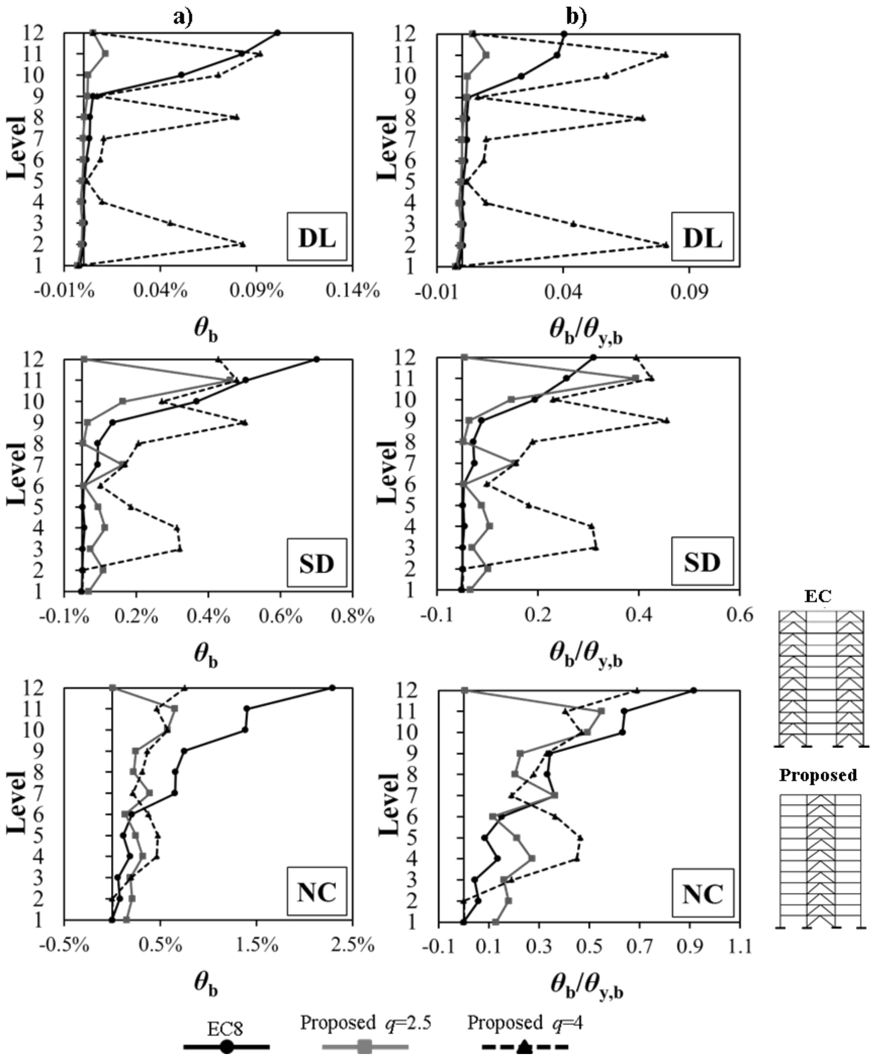

Figure 8.33 Beam chord rotation (a) and beam yielding (b) for 12-storey – 1 braced bay cases: proposed criteria vs EN 1998.

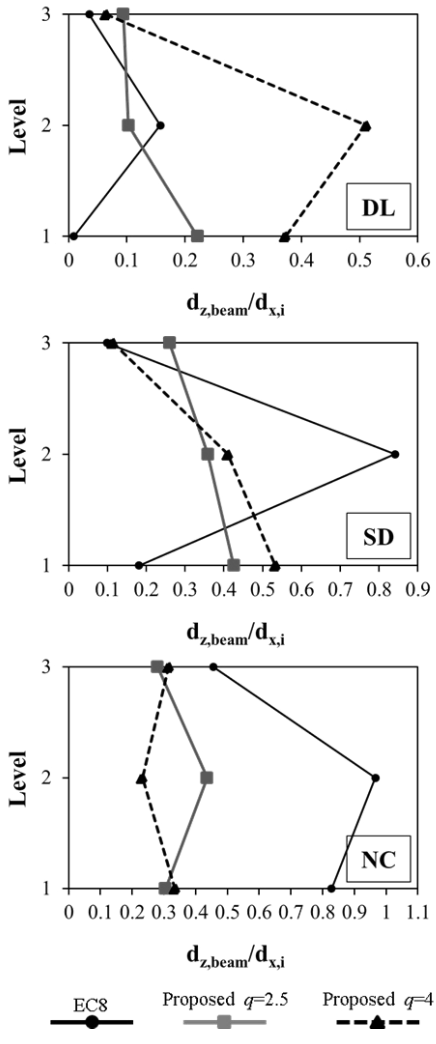

Figure 8.34 Beam vertical displacements-to-horizontal displacement ratio for 3-storey cases: proposed criteria vs EN 1998.

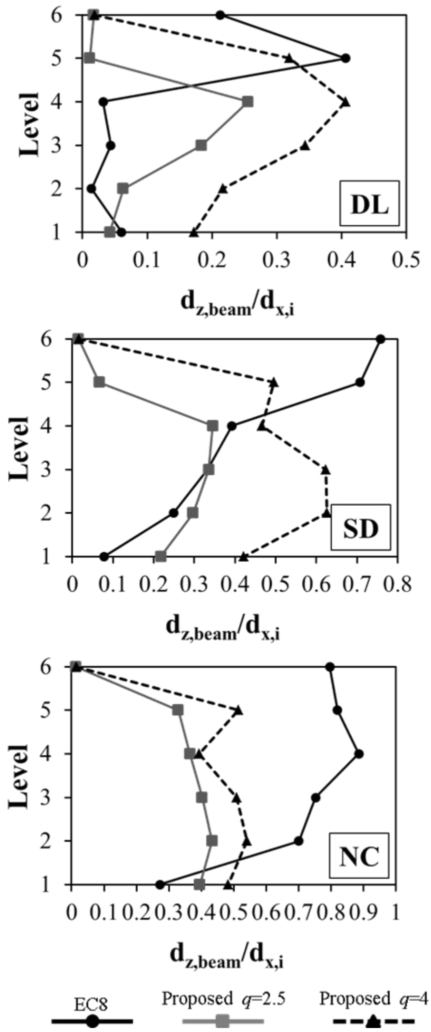

Figure 8.35 Beam vertical displacements-to-horizontal displacement ratio for 6-storey cases: proposed criteria vs EN 1998.

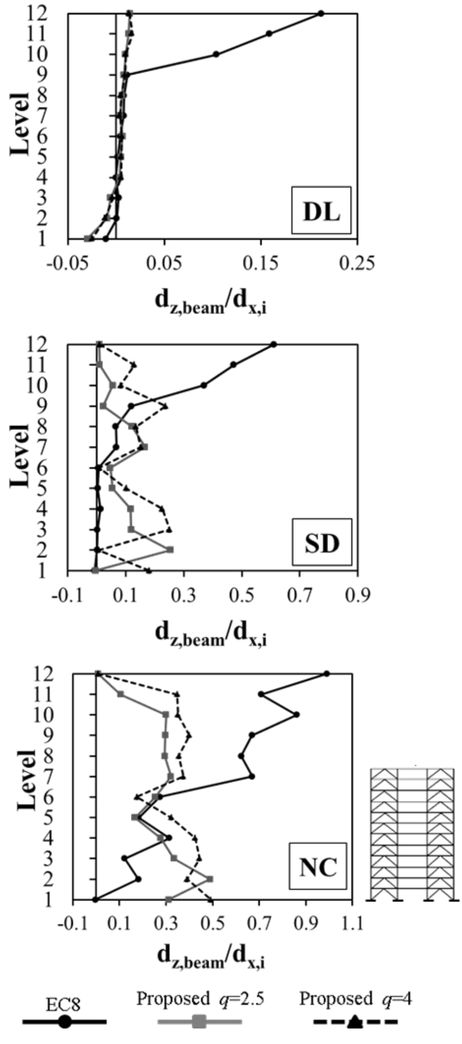

Figure 8.36 Beam vertical displacements-to-horizontal displacement ratio for 12-storey – 2 braced bays cases: proposed criteria vs EN 1998.

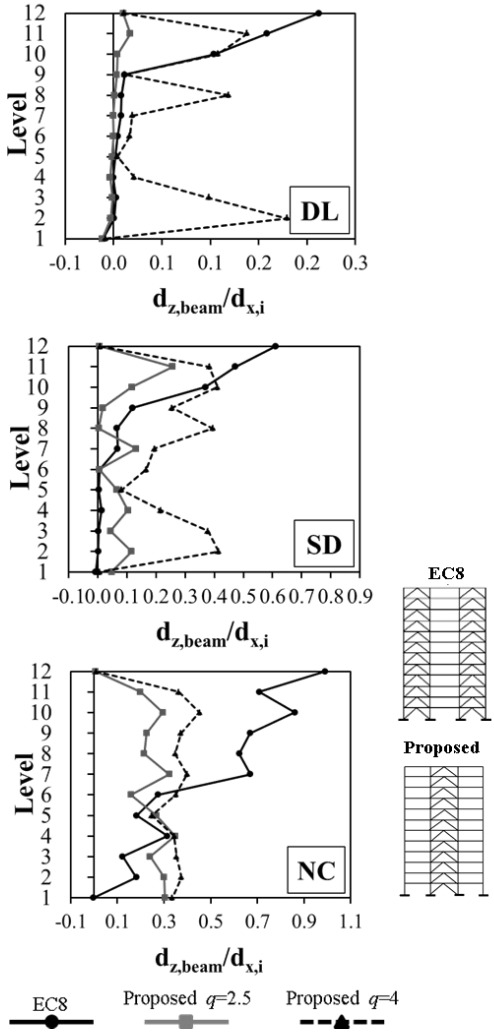

Figure 8.37 Beam vertical displacements-to-horizontal displacement ratio for 12-storey – 1 braced bay cases: proposed criteria vs EN 1998.

According to the proposed procedure, the requirement expressed by Eq. (8.2) is relaxed for low rise building up to three-storey frames and the required strength for bracings at the roof storey can be evaluated according to Eq. (8.3). As a consequence, in these cases the requirement on beam flexural stiffness (see Eq. (8.7)) must be applied also at the roof storey.

This different design rules is based on the remark that low rise building experience dynamic behavior that is generally not characterized by too pronounced cantilever shape. This is the reason why it was deemed unnecessary to restrain the bracings at the roof storey in the elastic range.

In order to clarify this aspect, Figures from 8.38 to 8.40 show the comparison between the response of three-storey buildings alternatively designed retaining (continuous lines in figures) or disregarding (dashed lines in figures) the requirement on the elastic bracings at the roof storey for the system designed assuming both q=2.5 (See Figs 8.38-8.40a), and q=4 (See Figs 8.38-8.40b).

No appreciably differences can be recognized in term of lateral stiffness (See Fig. 8.38); however, significant benefit can be recognized in terms of peak storey acceleration (See Fig. 8.39) disregarding the requirement on the elastic bracings (dashed lines) with smaller value of the ratio A/A_d due to the larger dissipative capacity provided by the yielding of braces (See Fig. 8.40).

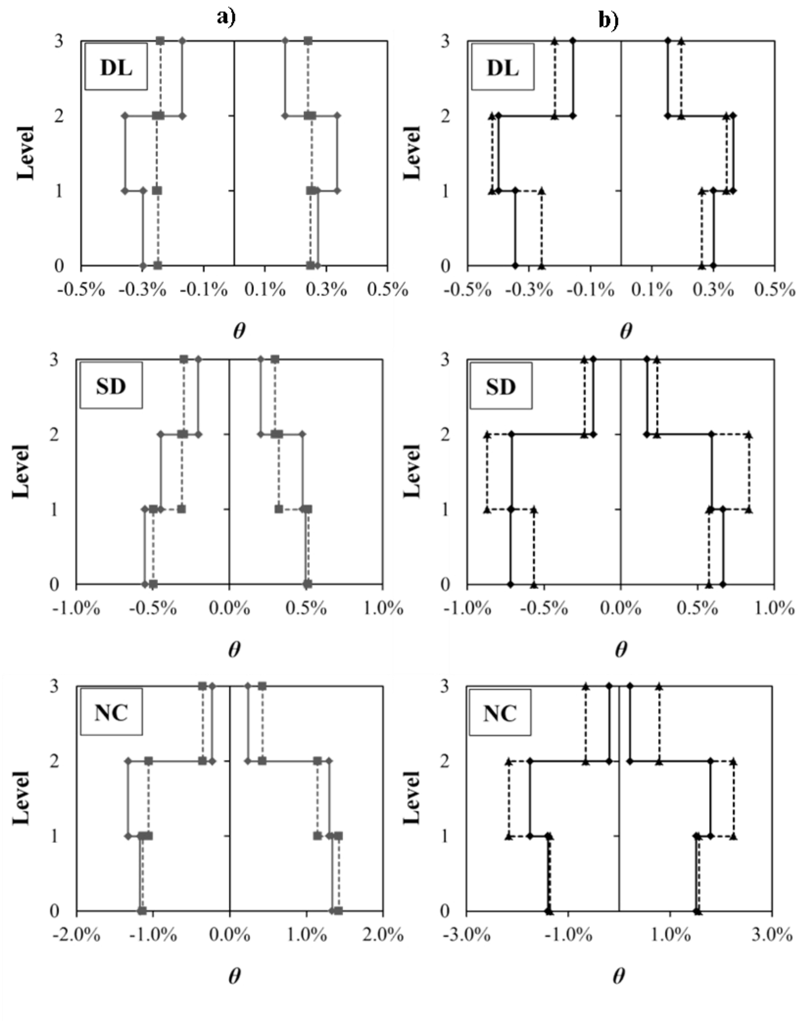

Figure 8.38 Interstorey drift transient (a) and residual (b) for 3-storey cases: the influence of requirement on elastic bracings at the roof storey.

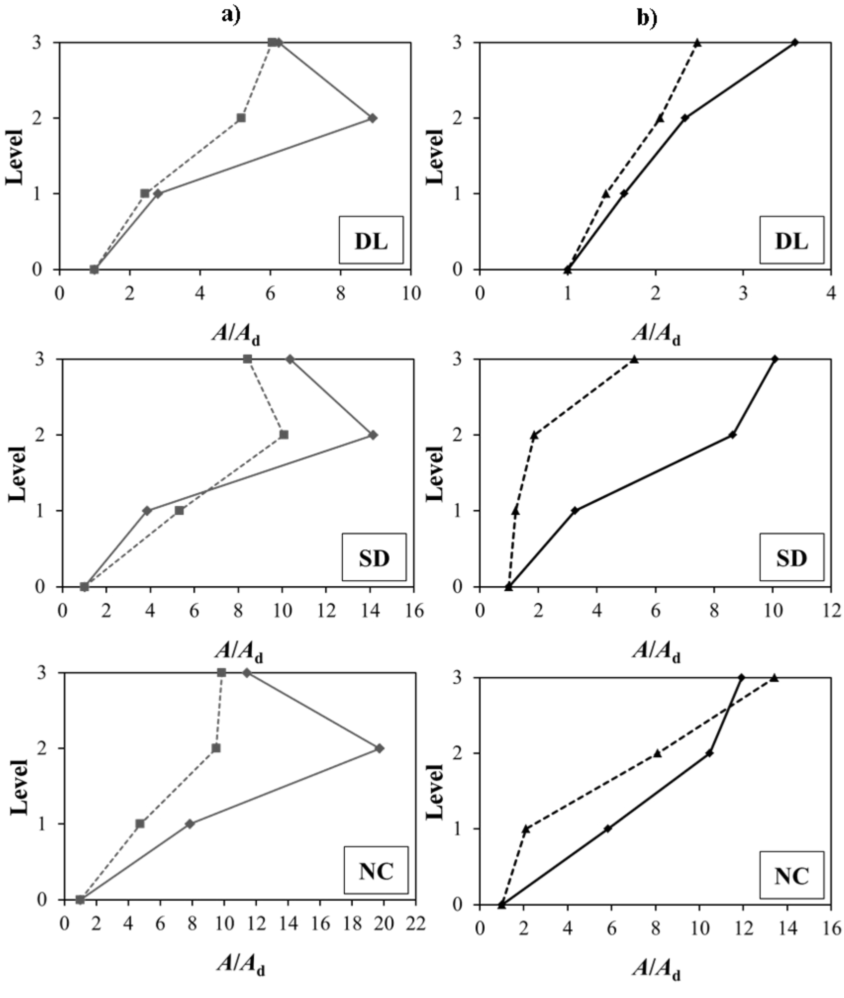

Figure 8.39 Peak storey acceleration for 3-storey cases: the influence of requirement on elastic bracings at the roof storey.

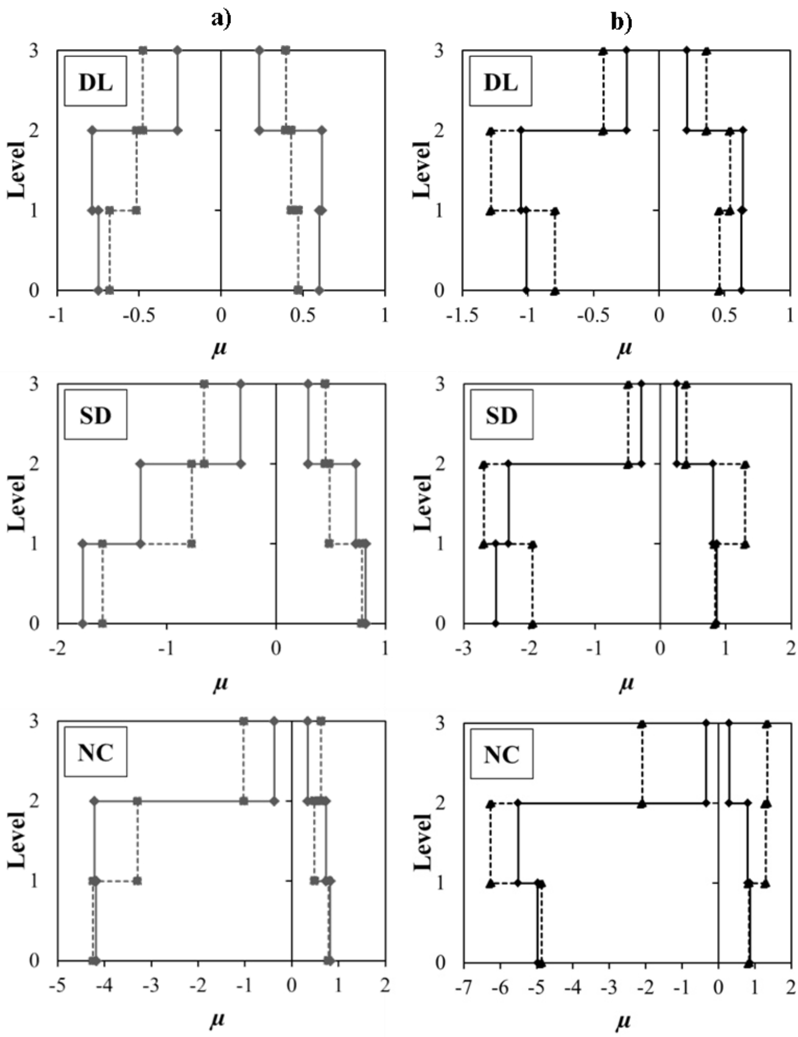

Figure 8.40 Braces ductility demand for 3-storey cases: the influence of requirement on elastic bracings at the roof storey.

8.3.2.2 *The influence of beam-to-column connections belonging to the braced bays*

A further set of nonlinear analyses was performed in order to assess the influence of the beam-to-column connections belonging to the braced bays.

Differently from European codes, AISC 341 provides a specific requirement for the beam-to-column connections in special concentrically braced bays, which should be moment-resisting type in order to increase the grade of redundancy of the system and to assure uniform distribution of plastic strain along the building height. Moreover, varying the type of the beam-to-column connections also allows obtaining different values of beam flexural stiffness at the same cross section.

In order to investigate these aspects, the degree of end fixity of the brace-intercepted beam was varied considering full-pinned restraints, semi-rigid restraints and full-fixed restraints as described in Section 8.3.1.

Figures from 8.41 to 8.43 show the influence of beam-to-column connections belonging to the braced bays on the response of six-storey frames designed according to both current codes and proposed design criteria.

Both interstorey drift ratios and braces ductility demand profiles clearly show that, assuming fixed connection allows obtaining more uniform distribution of damage along the building height, avoiding cantilever-shape behaviour.

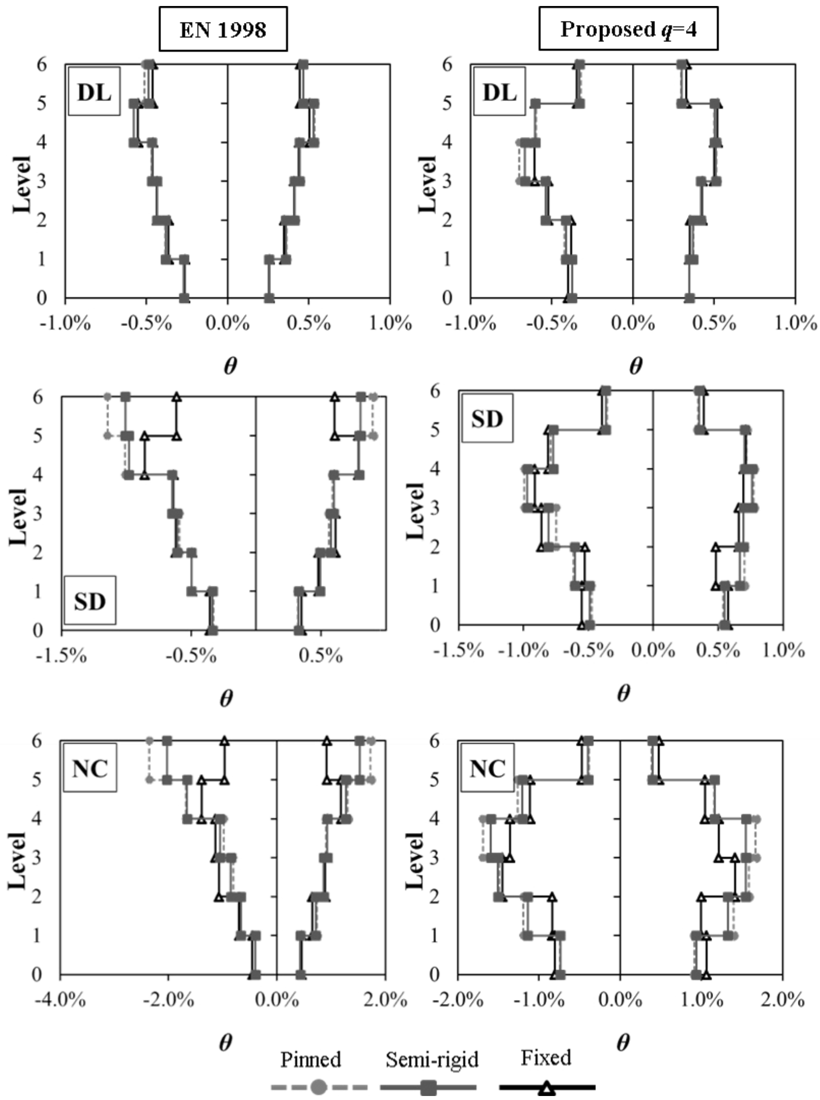

Figure 8.41 The influence of beam-to-column joint type belonging to the braced bays: transient interstorey drift ratios.

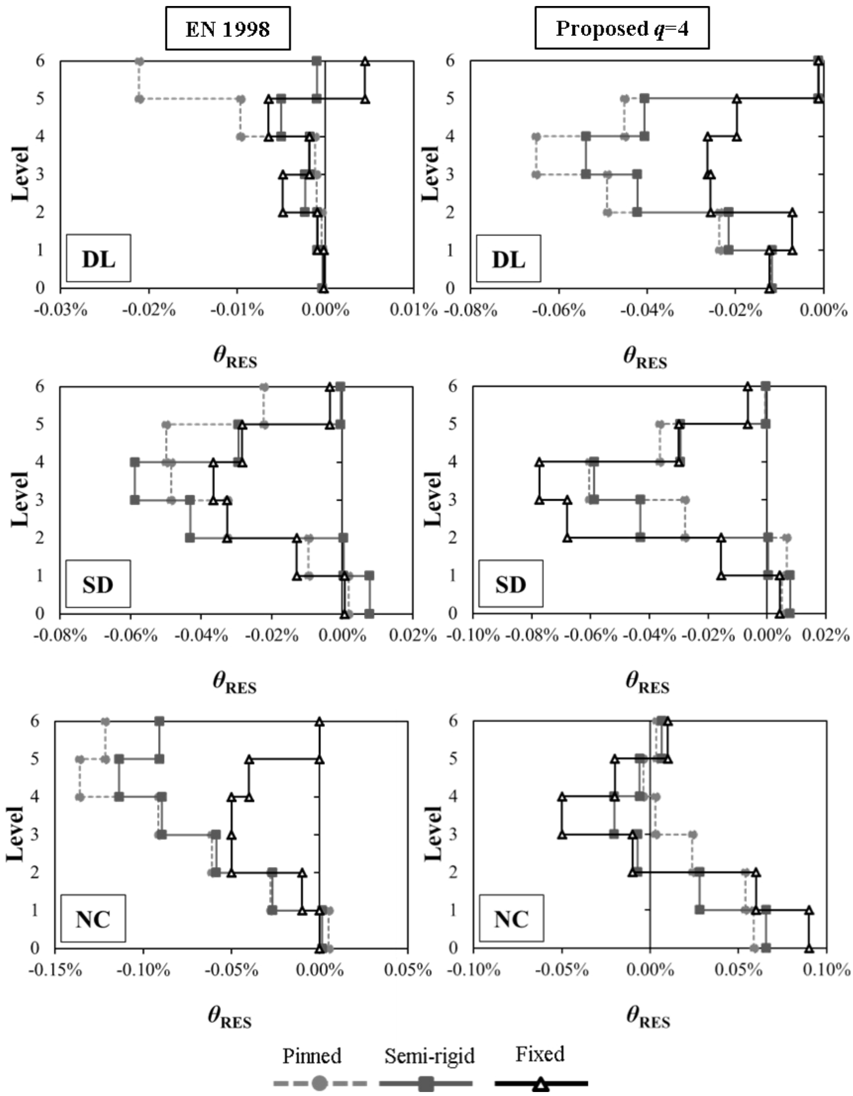

Figure 8.42 The influence of beam-to-column joint type belonging to the braced bays: residual interstorey drift ratios.

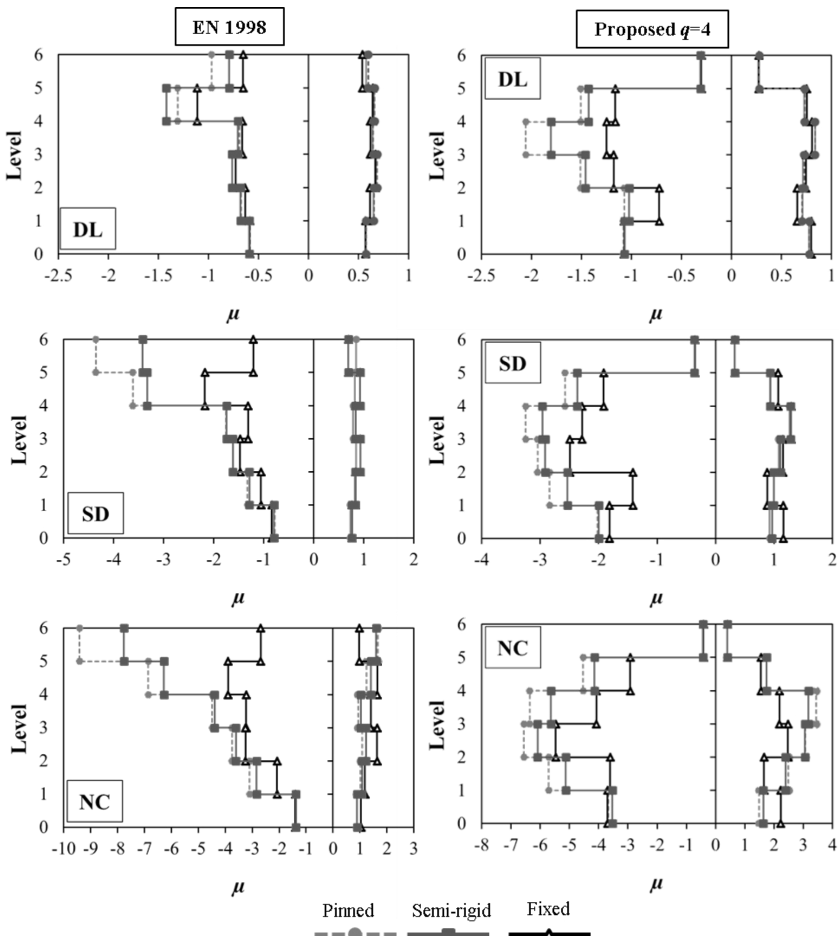

Figure 8.43 The influence of beam-to-column joint type belonging to the braced bays: braces ductility demand.

8.3.2.3 Building structures designed for high ductility class (DCH)

8.3.2.3.1 Designed structures

Structures for DCH were designed considering alternatively the behaviour factor q=4 and q=6.

Tables from 8.12 to 8.15 summarize the cross section properties of structural members of the three, six and twelve-storey buildings in both one and two braced bays configurations.

Figure 8.44 shows the value of the slenderness ratio $\bar{\lambda}$ of bracing members at each storey; the values of the normalized slenderness obtained for both q=4 and q=6 cases are also reported in Tables from 8.16 to 8.19.

Intermediate normalized slenderness can be recognized assuming q=4, with values ranging in [0.97, 1.00], [0.93, 1.18], [0.99, 1.47] and [0.83, 1.23] for low, medium and high rise buildings in two and one braced bays configuration, respectively. More slender braces can be recognized assuming q=6, with values ranging in [0.99, 1.28], [0.93, 1.49], [1.21, 1.89] and [0.99, 1.47] for low, medium and high rise buildings in two and one braced bays configuration, respectively.

Table 8.12 Cross section properties of structural members of 3-storey cases.

Storey	Columns		Beams		Braces (d x t)		Gravity members	
	q=4	q=6	q=4	q=6	q=4	q=6	Columns	Beams
	S355	S355	S355	S355	S235	S235	S355	S355
3	HE 220 B	HE 220 B	HE 340 A	IPE 400	168.3 x 4	139.7 x 4	HE 200 B	IPE 330
2	HE 260 B	HE 240 B	HE 360 A	IPE 400	168.3 x 6	168.3 x 4	HE 240 B	IPE 330
1	HE 260 B	HE 240 B	HE 400 B	IPE 450	177.8 x 8	177.8 x 5	HE 240 B	IPE 330

Table 8.13 Cross section properties of structural members of 6-storey cases.

Storey	Columns		Beams		Braces (d x t)		Gravity members	
	q=4	q=6	q=4	q=6	q=4	q=6	Columns	Beams
	S355	S355	S355	S355	S355	S355	S355	S355
6	HE 300 B	HE 260 A	HE 450 B	IPE 600	219.1 x 8	219.1 x 8	HE 260 A	IPE 330
5	HE 300 B	HE 260 A	HE 400 A	IPE 550	177.8 x 6	139.7 x 8	HE 260 A	IPE 330
4	HE 340 B	HE 280 B	HE 450 A	IPE 550	177.8 x 8	168.3 x 6	HE 280 B	IPE 330
3	HE 340 B	HE 280 B	HE 500 A	IPE 600	177.8 x 10	168.3 x 8	HE 280 B	IPE 330
2	HE 340 M	HE280 M	HE 500 B	IPE 600	177.8 x 12	168.3 x 8	HE 280 M	IPE 330
1	HE 340 M	HE280 M	HE 500 B	IPE 600	219.1 x 8	193.7 x 8	HE 280 M	IPE 330

Table 8.14 Cross section properties of structural members of 12-storey – 2 braced bays cases.

Storey	Columns		Beams		Braces (d x t)	
	q=4	q=6	q=4	q=6	q=4	q=6
	S355	S355	S355	S355	S355	S355
12	HE 300 B	HE 240 B	HE 450 A	HE 400 A	168.3 x 8	168.3 x 6
11	HE 300 B	HE 240 B	HE 360 A	HE 340 A	139.7 x 6	114.3 x 6.3
10	HE 300 B	HE 240 B	HE 400 A	HE 340 A	168.3 x 6	139.7 x 5
9	HE 400 B	HE 340 B	HE 400 A	HE 360 A	168.3 x 6.3	139.7 x 6
8	HE 400 B	HE 340 B	HE 450 A	HE 400 A	168.3 x 8	139.7 x 8
7	HE 400 B	HE 340 B	HE 450 A	HE 400 A	177.8 x 8	139.7 x 8
6	HE 400 M	HE 360 M	HE 500 A	HE 400 A	193.7 x 8	168.3 x 6
5	HE 400 M	HE 360 M	HE 500 A	HE 400 A	193.7 x 8	168.3 x 6
4	HE 400 M	HE 360 M	HE 500 A	HE 400 A	193.7 x 8	168.3 x 6
3	HD400x347	HE 450 M	HE 500 A	HE 400 A	193.7 x 8	168.3 x 6
2	HD400x347	HE 450 M	HE 500 B	HE 400 A	193.7 x 10	168.3 x 6.3
1	HD400x347	HE 450 M	HE 500 B	HE 500 A	219.1 x 8	168.3 x 8

*All gravity resistant beams are IPE 330

Table 8.15 Cross section properties of structural members of 12-storey – 1 braced bay cases.

Storey	*Columns*			*Beams*		*Braces (d x t)*	
	Gravity	*q*=4	*q*=6	*q*=4	*q*=6	*q*=4	*q*=6
	S355	*S355*	*S355*	*S355*	*S355*	*S355*	*S355*
12	HE 200 B	HE 400 B	HE 320 A	HE 450 B	HE 500 A	177.8 x 10	177.8 x 10
11	HE 200 B	HE 400 B	HE 320 A	HE 400 A	HE 360 A	168.3 x 6	139.7 x 6.3
10	HE 200 B	HE 400 B	HE 320 A	HE 450 A	HE 400 A	168.3 x 8	168.3 x 6
9	HE 220 B	HE 400 M	HE 360 B	HE 500 A	HE 450 A	193.7 x 8	168.3 x 8
8	HE 220 B	HE 400 M	HE 360 B	HE 500 A	HE 450 A	193.7 x 8	168.3 x 8
7	HE 220 B	HE 400 M	HE 360 B	HE 500 A	HE 450 A	219.1 x 8	177.8 x 8
6	HE 260 B	HD 400 x 347•/+	HE 360 M	HE 500 A	HE 500 A	219.1 x 8	177.8 x 10
5	HE 260 B	HD 400 x 347•/+	HE 360 M	HE 500 B	HE 500 A	244.5 x 8	177.8 x 10
4	HE 260 B	HD 400 x 347•/+	HE 360 M	HE 500 B	HE 550 A	244.5 x 8	177.8 x 12
3	HE 300 B	HD 400 x 421•/+	HD 400 x 347•/+	HE 500 B	HE 550 A	244.5 x 8	177.8 x 12
2	HE 300 B	HD 400 x 421•/+	HD 400 x 347•/+	HE 500 B	HE 550 A	244.5 x 8	177.8 x 12
1	HE 300 B	HD 400 x 421•/+	HD 400 x 347•/+	HE 550 B	HE 550 A	244.5 x 10	219.1 x 8

*All gravity resistant beams are IPE 330

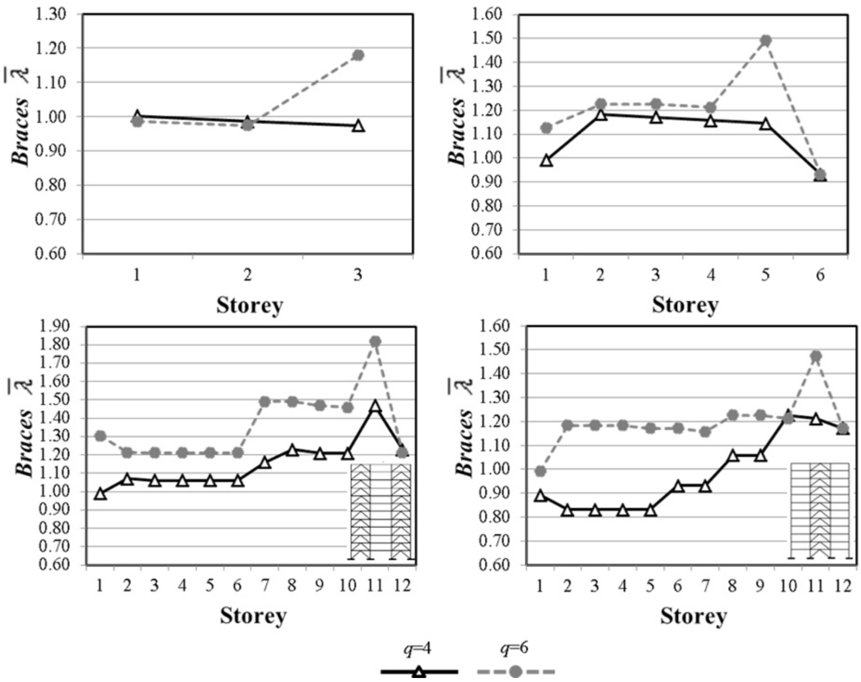

Figure 8.44 Normalized slenderness of braces at each storey.

Table 8.16 Slenderness ratios of diagonal members at each storey for the 3-storey cases.

	Brace normalized slenderness $\bar{\lambda}$	
Storey	q=4	q=6
3	0.97	1.18
2	0.99	0.97
1	1.00	0.99

Table 8.17 Slenderness ratios of diagonal members at each storey for the 6-storey cases.

	Brace normalized slenderness $\bar{\lambda}$	
Storey	q=4	q=6
6	0.93	0.93
5	1.14	1.49
4	1.16	1.21
3	1.17	1.23
2	1.18	1.23
1	0.99	1.13

Table 8.18 Slenderness ratios of diagonal members at each storey for the 12-storey – 2 braced bays cases.

	Brace normalized slenderness $\bar{\lambda}$	
Storey	q=4	q=6
12	1.23	1.21
11	1.47	1.82
10	1.21	1.46
9	1.21	1.47
8	1.23	1.49
7	1.16	1.49
6	1.06	1.21
5	1.06	1.21
4	1.06	1.21
3	1.06	1.21
2	1.07	1.21
1	0.99	1.30

Table 8.19 Slenderness ratios of diagonal members at each storey for the 12-storey – 1 braced bay cases.

Storey	Brace normalized slenderness $\bar{\lambda}$ q=4	q=6
12	1.17	1.17
11	1.21	1.47
10	1.23	1.21
9	1.06	1.23
8	1.06	1.23
7	0.93	1.16
6	0.93	1.17
5	0.83	1.17
4	0.83	1.18
3	0.83	1.18
2	0.83	1.18
1	0.89	0.99

Figure 8.45 reports the values of the beam-to-brace stiffness ratio K_F (see Eq. (5.1)) at each storey for the frames designed for high ductility class according to the proposed design rules, considering both q=4 and q=6.

It is trivial to observe that in both cases the values of the beam-to-brace stiffness ratio K_F significantly overcome the lower bound limit (K_F=0.2) stated by Eq. (8.7). This feature can be explained considering that assuming at design stage fixed restrained in both ends of brace-intercepted beams, allows obtaining significantly larger flexural stiffness four times larger respect the pinned-case, at the same cross section. As a consequence, differently from what observed in the DCM structures, smaller profiles can be used and the selection of beam cross sections is basically ruled by strength matters.

The values the beam-to-brace stiffness ratio K_F obtained for both q=4 and q=6 are also reported in Tables from 8.20 to 8.23, for all three, six and twelve-storey cases, respectively.

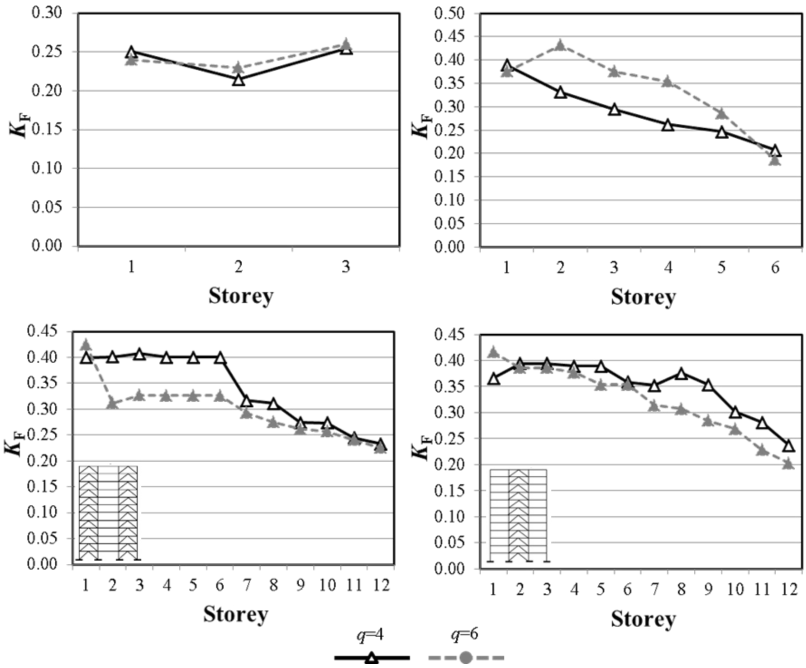

Figure 8.45 Beam-to-brace stiffness ratio at each storey.

Table 8.20 Beam-to-brace stiffness ratio at each storey for the 3-storey cases.

	Beam to brace stiffness ratio K_F	
Storey	q=4	q=6
3	0.25	0.26
2	0.21	0.23
1	0.25	0.24

Table 8.21 Beam-to-brace stiffness ratio at each storey for the 6-storey cases.

	Beam to brace stiffness ratio K_F	
Storey	q=4	q=6
6	0.21	0.19
5	0.25	0.29
4	0.26	0.35
3	0.29	0.38
2	0.33	0.43
1	0.39	0.38

Table 8.22 Beam-to-brace stiffness ratio at each storey for the 12-storey – 2 braced bays cases.

	Beam to brace stiffness ratio K_F	
Storey	q=4	q=6
12	0.23	0.23
11	0.24	0.24
10	0.27	0.26
9	0.27	0.26
8	0.31	0.27
7	0.32	0.29
6	0.40	0.33
5	0.40	0.33
4	0.40	0.33
3	0.41	0.33
2	0.40	0.31
1	0.40	0.42

Table 8.23 Beam-to-brace stiffness ratio at each storey for the 12-storey – 1 braced bay cases.

	Beam to brace stiffness ratio K_F	
Storey	q=4	q=6
12	0.24	0.20
11	0.28	0.23
10	0.30	0.27
9	0.35	0.28
8	0.38	0.31
7	0.35	0.31
6	0.36	0.35
5	0.39	0.35
4	0.39	0.38
3	0.39	0.39
2	0.39	0.39
1	0.37	0.42

8.3.2.3.2 Eigenvalue analyses

Figure 8.46 depicts the periods of vibration for the first (T_1) and the second (T_2) mode of vibration for all low, medium and high rise frames designed assuming both q=4 and q=6, while the relevant participating mass percentages ($M_{x,1}$ and $M_{x,2}$ respectively) are shown in Fig. 8.47. Either periods of vibration and participating mass percentages are even summarized in Tables from 8.24 to 8.27.

Slightly larger periods of vibration can be recognized assuming q=6, while appreciable differences can be noted in terms of participating mass percentages (see Fig. 8.47).

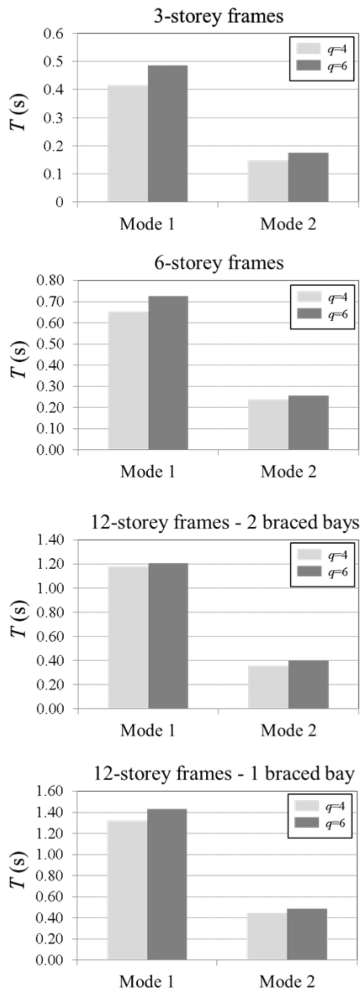

Figure 8.46 Periods of vibrations.

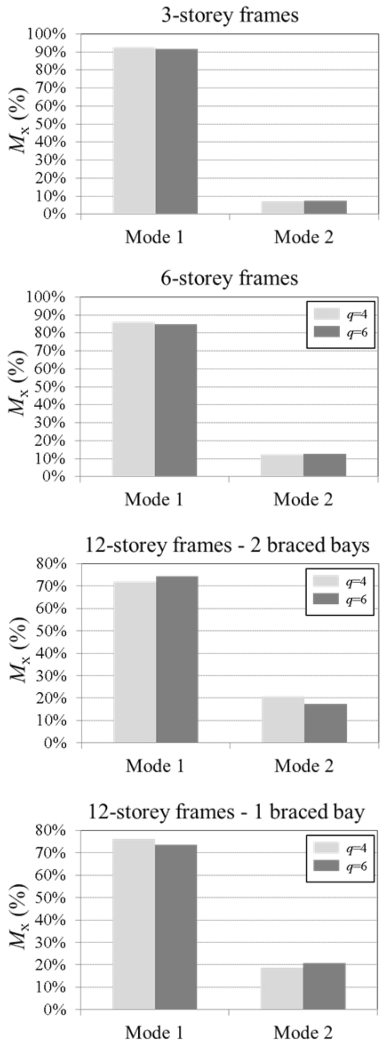

Figure 8.47 Participating mass percentages.

Table 8.24 Dynamic characteristics for the 3-storey cases.

Case	T_1 (sec)	T_2 (sec)	$M_{x,1}$ (%)	$M_{x,2}$ (%)
q=4	0.42	0.15	92.74%	7.09%
q=6	0.49	0.18	91.72%	7.27%

Table 8.25 Dynamic characteristics for the 6-storey cases.

Case	T_1 (sec)	T_2 (sec)	$M_{x,1}$ (%)	$M_{x,2}$ (%)
q=4	0.65	0.24	86.16%	12.15%
q=6	0.73	0.26	84.99%	12.64%

Table 8.26 Dynamic characteristics for the 12-storey – 2 braced bays cases.

Case	T_1 (sec)	T_2 (sec)	$M_{x,1}$ (%)	$M_{x,2}$ (%)
q=4	1.18	0.36	72.11%	20.82%
q=6	1.21	0.40	74.45%	17.36%

Table 8.27 Dynamic characteristics for the 12-storey – 1 braced bay cases.

Case	T_1 (sec)	T_2 (sec)	$M_{x,1}$ (%)	$M_{x,2}$ (%)
q=4	1.32	0.45	76.17%	18.67%
q=6	1.43	0.49	73.65%	20.85%

8.3.2.3.1 Nonlinear dynamic analyses

In this Section results from nonlinear analyses performed on building structures designed for DCH are presented and discussed: both global and local performance indicators were selected to evaluate the seismic response of all the examined frames; the monitored parameters for all limit states are summarized and described in Section 7.3.3.3.

Figures from 8.48 to 8.51depicts both transient (θ, see Fig. 8.48 to 8.51a) and residual (θ_{RES}, 8.48 to 8.51b) interstorey drift ratios for low, medium and high rise frames, related to the considered performance levels. The frames designed according to the proposed procedure exhibit adequate lateral stiffness, assuming both q=4 and q=6: all the examined frames exhibit satisfactorily performance at DL limit state according to the interstorey drift ratios limitation provided by EN 1998-1 for buildings having ductile non-structural elements and for buildings having non-structural elements fixed in a way so as not to interfere with structural deformations or without non-structural elements (namely 0.75% and 1%, respectively); moreover, relatively small residual interstorey drift ratio less than 0.3% and 0.2% for three and six and twelve-storey cases respectively can be recognized.

Figures from 8.52 to 8.55 show the profiles of peak storey accelerations for three, six and twelve-storey frames (in both two and one braced bays), respectively. Frames designed assuming q=4 are characterized by larger storey accelerations, whose peak average value (A) at SD limit state increases up to over 14 times, 6 times and 3 times the peak record acceleration (A_d) for the three and six-storey buildings and twelve-storey with two braced bay configurations, respectively. On the contrary, the significantly smaller average peak storey accelerations, with values of the ratio A/A_d close to the unit, can be recognized for frames designed assuming q=6, due to the larger dissipative capacity provided by the yielding of braces (see also Figs. from 8.56 to 8.58).

The peak storey accelerations reach smaller values for twelve storey frames in one braced bay configuration, exhibiting very small average peak storey accelerations, with values of the ratio A/A_d close to the unit, both assuming q=4 and q=6 (See Fig. 8.55)

Figures from 8.56 to 8.59 depict the braces ductility demand (μ) both in tension and in compression, for low, medium and high rise buildings, respectively. As it can be observed, assuming q=4 leads to slightly stiffer frames, basically characterized by limited damage in bracings under compression; on the other hand, also smaller plastic engagement is achieved under tension respect to the q=6 cases.

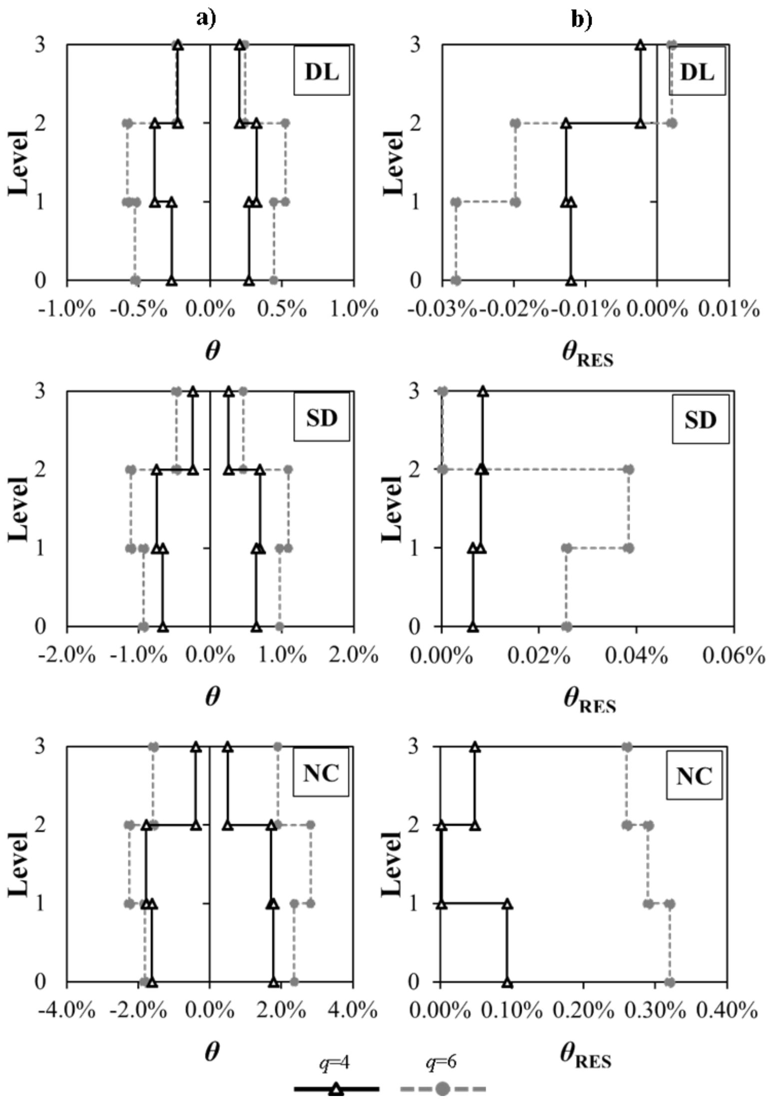

Figure 8.48 Interstorey drift transient (a) and residual (b) for 3-storey cases.

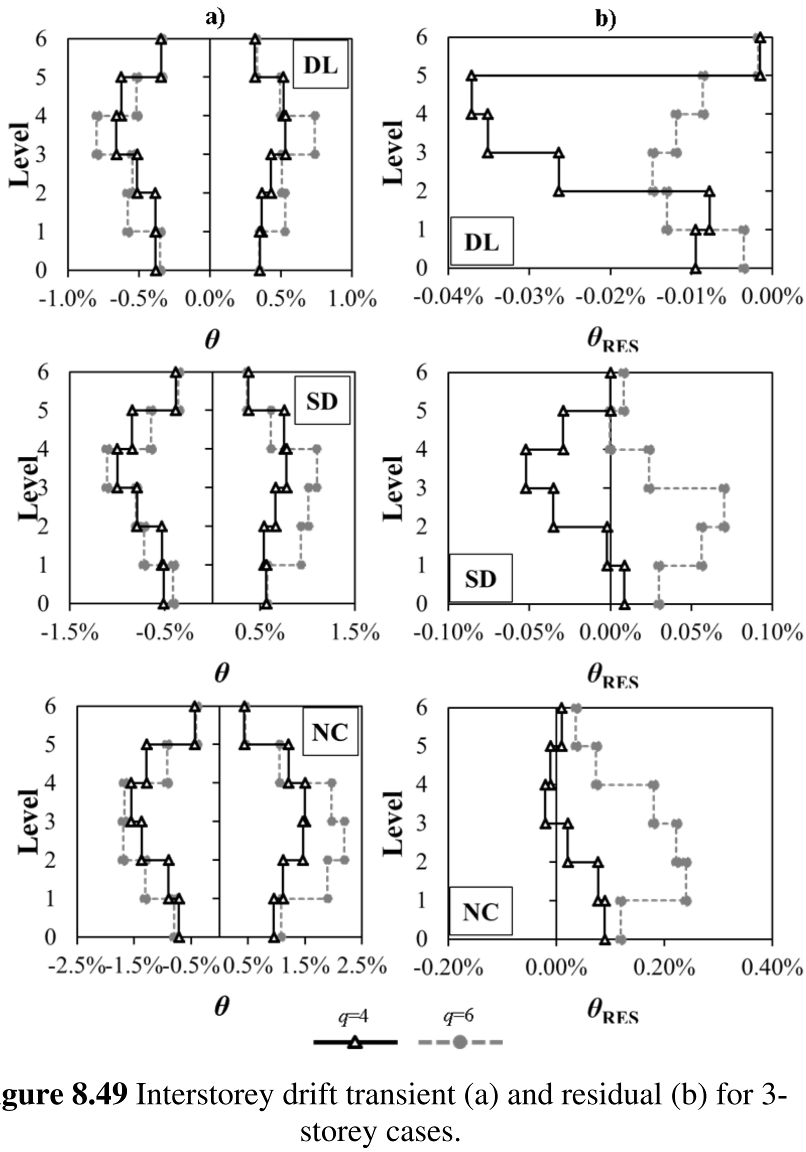

Figure 8.49 Interstorey drift transient (a) and residual (b) for 3-storey cases.

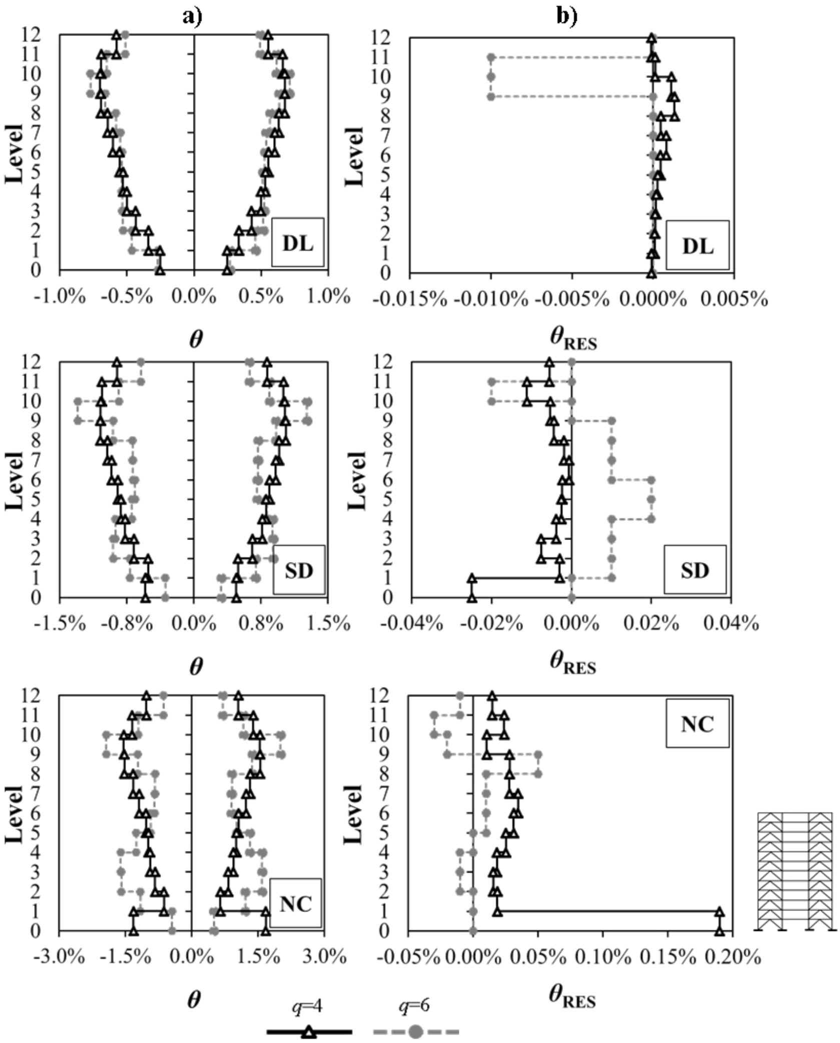

Figure 8.50 Interstorey drift transient (a) and residual (b) for 12-storey – 2 braced bays cases.

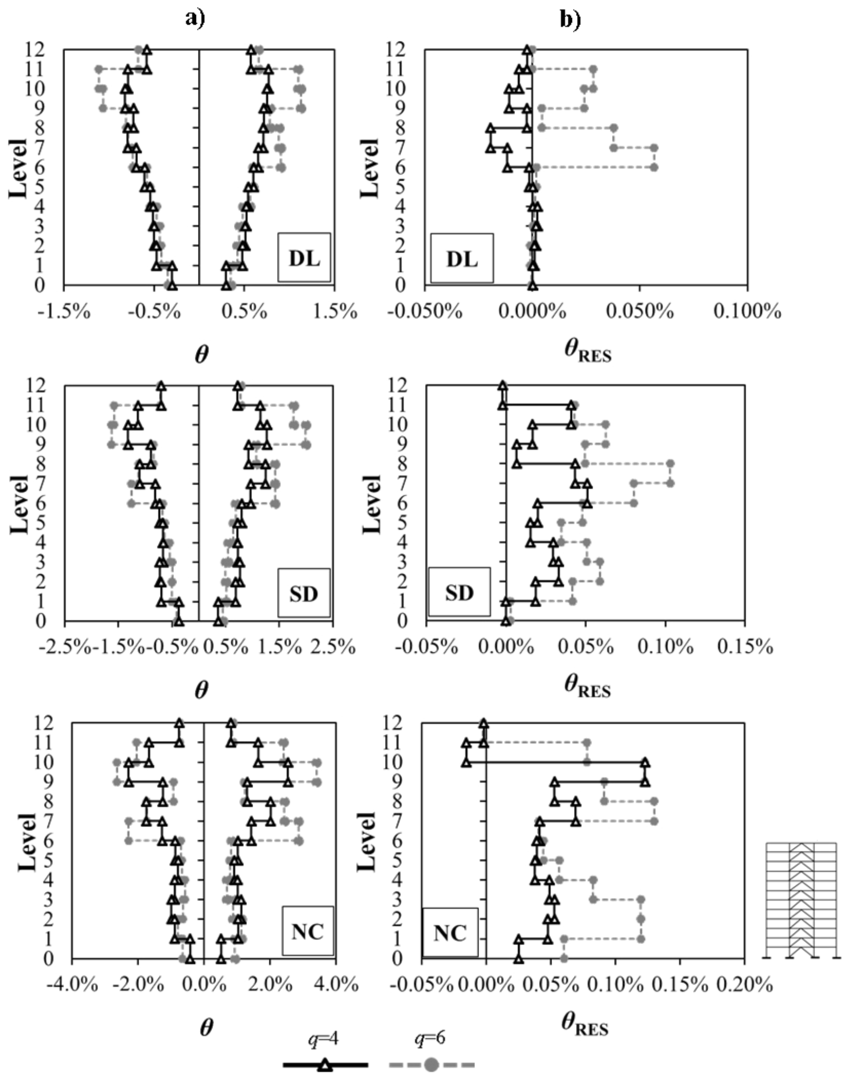

Figure 8.51 Interstorey drift transient (a) and residual (b) for 12-storey – 1 braced bay cases.

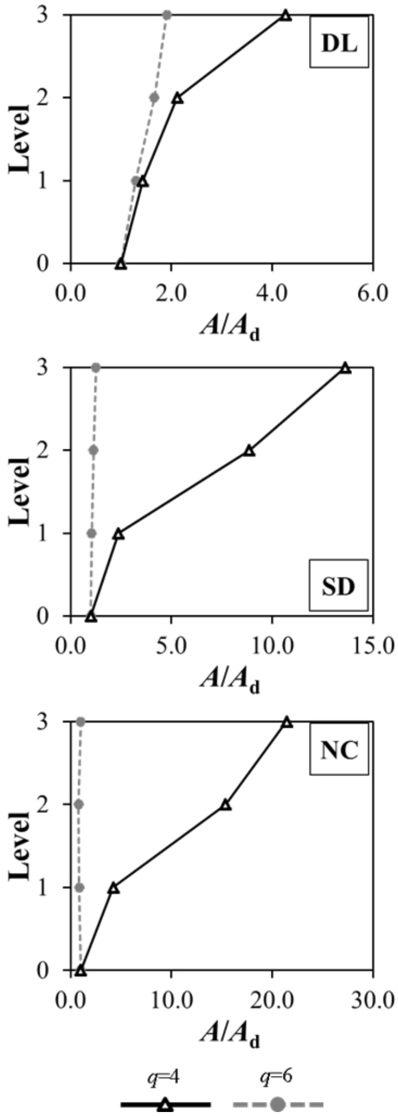

Figure 8.52 Peak storey acceleration for 3-storey cases.

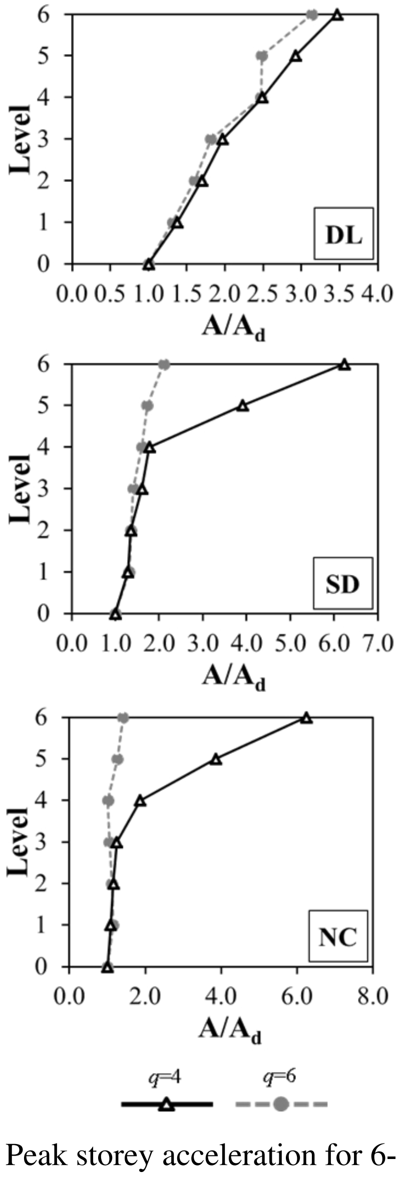

Figure 8.53 Peak storey acceleration for 6-storey cases.

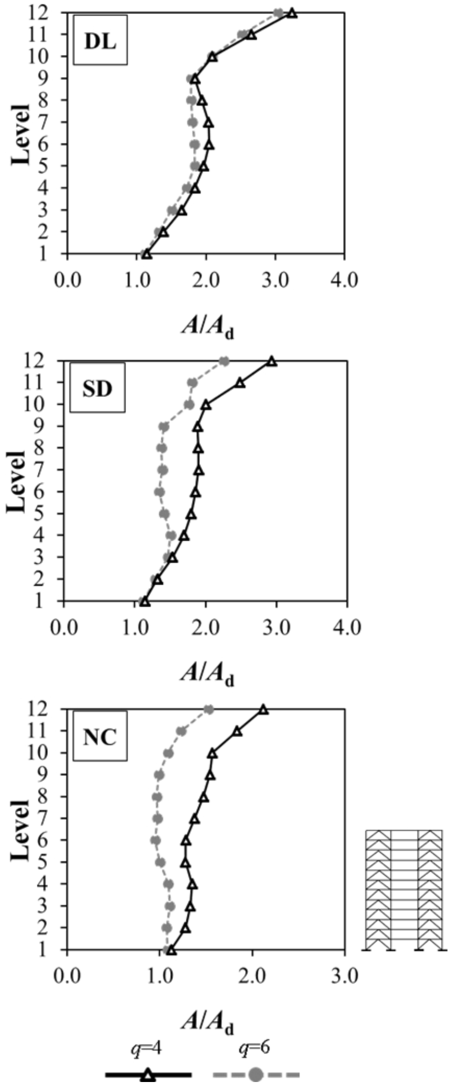

Figure 8.54 Peak storey acceleration for 12-storey – 2 braced bays cases.

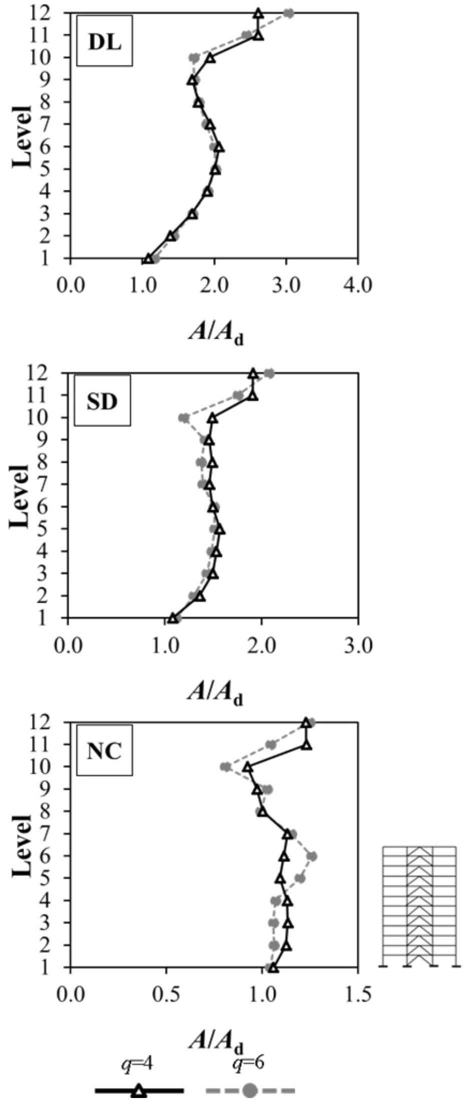

Figure 8.55 Peak storey acceleration for 12-storey – 1 braced bay cases.

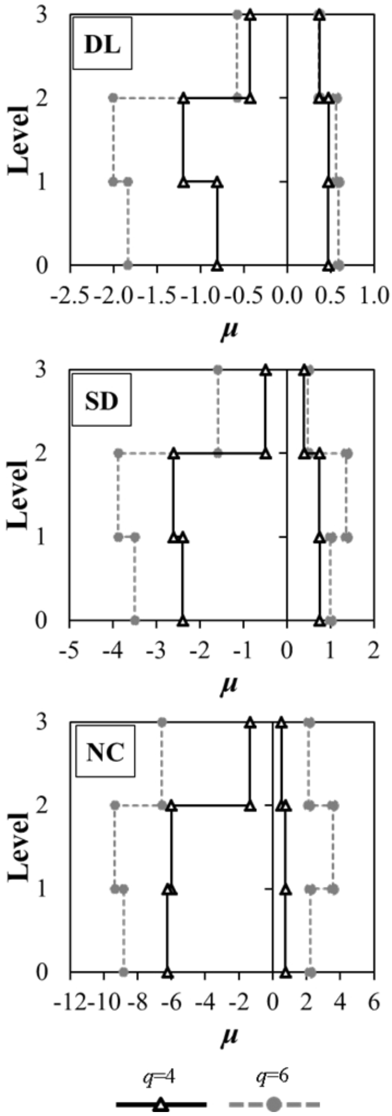

Figure 8.56 Braces ductility demand for 3-storey cases.

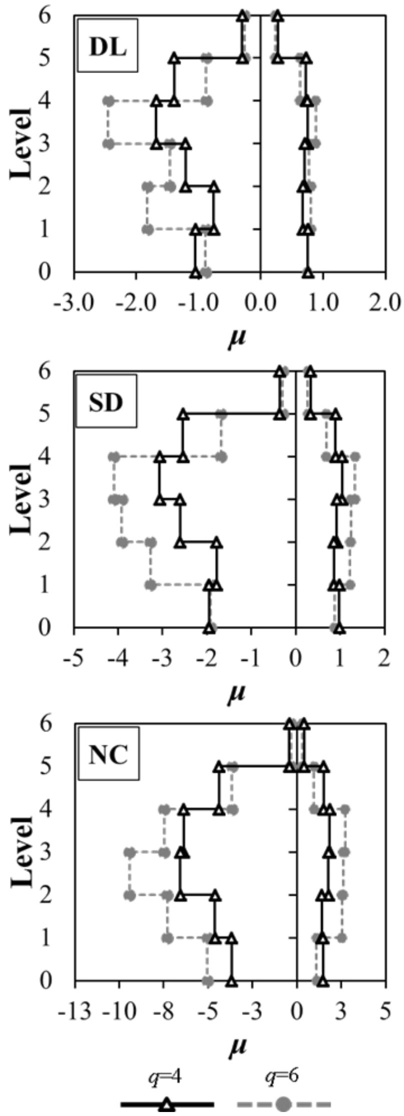

Figure 8.57 Braces ductility demand for 6-storey cases.

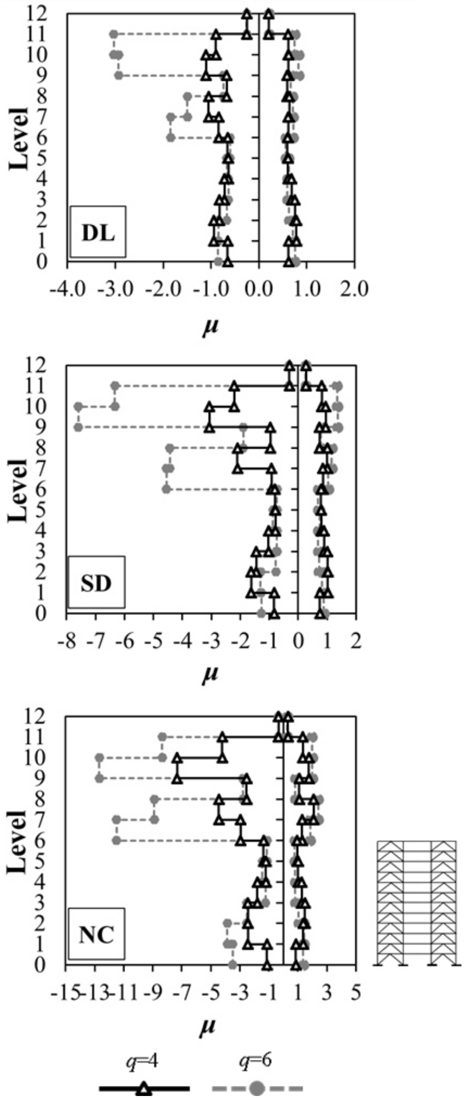

Figure 8.58 Braces ductility demand for 12-storey – 2 braced bays cases.

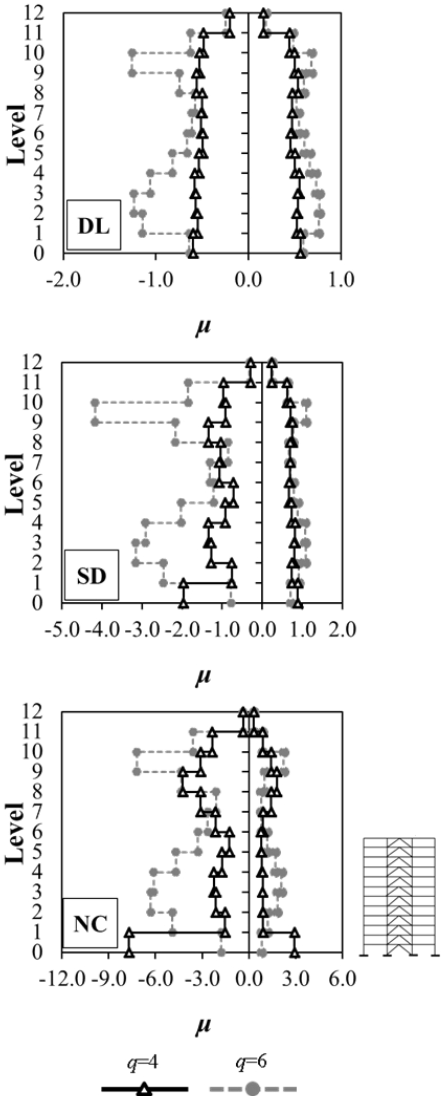

Figure 8.59 Braces ductility demand for 12-storey – 1 braced bay cases.

8.3.3 *Evaluation of behaviour factors*

According to Mazzolani and Piluso (1994) Salvitti and Elnashai (1996) and Elnashai and Broderick (1996) the actual behaviour factor is given as the ratio between the peak ground acceleration leading to accepted failure for the selected performance level (A_u) and the peak ground acceleration corresponding to the yielding of the frame (A_y). The values of A_y and A_u have been derived from incremental dynamic analyses. In this study the failure acceleration A_u is the minimum value corresponding to all possible theoretical states of collapse, as follows:

$$A_u = \min(A_c, A_{br}) \tag{8.11}$$

Where A_c corresponds to column buckling and A_{br} corresponds to bracing member attaining its maximum axial deformation.

With this regard, the axial deformation limit was defined by considering ductility capacity of bracing members as given by Goggins *et al* (2006); based on extensive experimental investigation on tubular profiles, Goggins *et al* (2006), provide simple linear relationships between ductility capacity and both global and local member slenderness. In the specific case the maximum ductility was obtained as function of the brace slenderness ratio, according to the following relationship:

$$\mu_\Delta = 26.2 \cdot \bar{\lambda} - 0.7 \quad (R^2{=}0.78) \tag{8.12}$$

It should be noted that the brace ductility expressed by Eq. (8.12) is intended as ductility capacity evaluated at the brace fracture. The maximum axial deformation at collapse for the brace under compression is calculated by simply assuming symmetrical cycle as:

$$\mu_{c,\mathrm{col}} = 0.5 \cdot \mu_{\Delta} \tag{8.13}$$

Moreover, the behaviour factors were evaluated by relating the axial deformation limitation to SD limit state; with this regard the maximum axial deformation at SD limit state was obtained as a fraction of maximum axial deformation at collapse as:

$$\mu_{c,\lim,\mathrm{SD}} = \frac{\Delta_{c,EC8-3,\mathrm{SD}}}{\Delta_{c,EC8-3,NC}}\mu_{c,\mathrm{col}} = \left(\frac{4}{6}\right)\mu_{c,\mathrm{col}} \tag{8.14}$$

Where the $\Delta_{c,EC8\text{-}3,SD}$ and $\Delta_{c,EC8\text{-}3,NC}$ are the axial shortening for SD an NC limit states as given by EC8-3, which correspond to $4\Delta_c$ and $6\Delta_c$ (where Δ_c is the buckling displacement of the brace).

8.3.3.1 Behaviour factor for structural buildings designed for DCM.

Figure 8.60 shows the values of behaviour factors evaluated for structures designed for medium ductility class; the results obtained for the frames designed according to proposed design criteria (assuming both q=2.5 and q=4) are compared with those obtained for EC8-compliant frames, by showing the average values of all the examined cases (namely including all low, medium and high rise buildings); in addition average plus and minus standard deviation values are shown to appreciate data dispersion.

By observing Fig. 8.60, it is trivial to recognize that the frames designed according to the proposed procedure exhibit significantly larger reserve of ductility respect to the EC8-compliant ones. In detail, average values of q factor equal to 2.65, 4.05 and 5.48 were calculated for EC8, proposed q=2.5 and q=4 – compliant frames, respectively. The largest values are recognized for frames designed according proposed criteria and assuming q=4. Moreover, results from nonlinear analyses confirm the effectiveness of assuming q=4 at design stage; indeed, values of behaviour factor larger than 4 are evaluated from dynamic nonlinear analyses, even calculating the behaviour factor as average value minus standard deviation.

However, it should be noted that in all examined cases, the state of collapse was always determined by brace under compression attaining its axial deformation limit; buckling of column is recognized in no case.

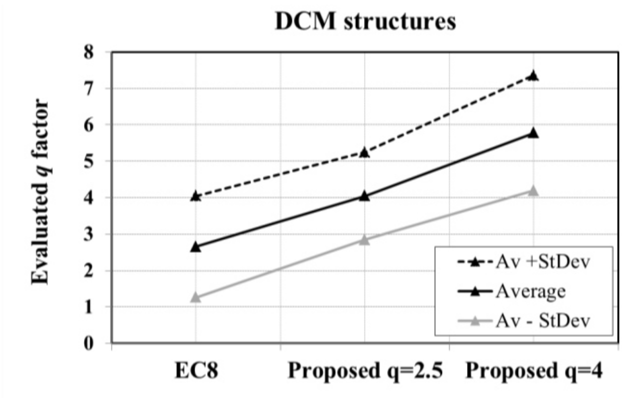

Figure 8.60 Behaviour factors evaluated for DCM cases.

In Fig. 8.61 the behaviour factors calculated from nonlinear dynamic analyses are shown for low, medium and high rise building separately. For frames designed according to current code, the largest *q* factor values are evaluated for three-storey frames, while similar value are assessed for six and twelve storey cases.

Conversely, for frames designed according to proposed design criteria the largest values are experienced by six-storey buildings that exhibit the most stable response. Twelve-storey frames exhibit the poorest ductility capacity, being the dynamic response of high-rise buildings much more affected by higher vibration modes.

Finally, IDA curves of structural buildings designed according to proposed criteria for DCM (namely assuming q=4) are compared with those obtained from frames designed according to current codes in Fig. 8.62; in detail the IDA curves are expressed in terms of A/A_g versus maximum roof displacement $d_{\max}$ for all three, six and twelve storey cases (in both two and one braced bay configurations) respectively.

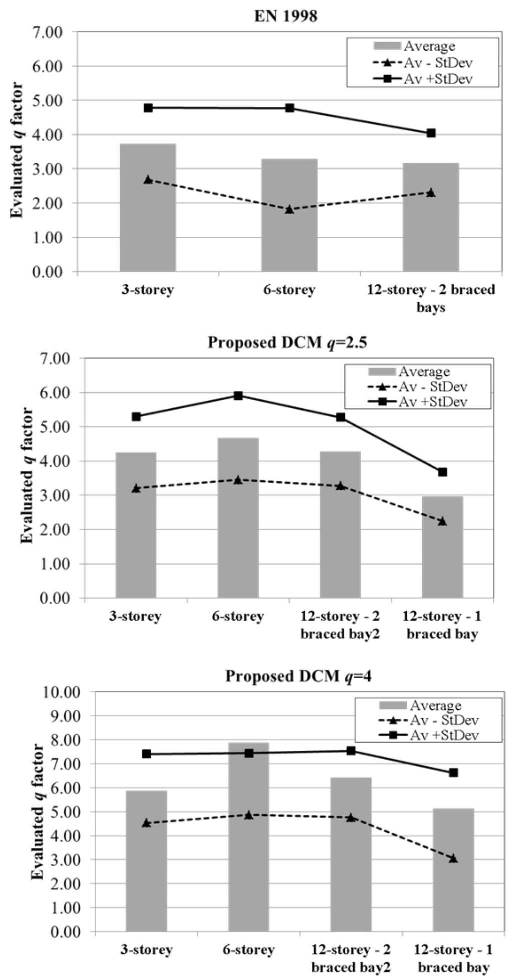

Figure 8.61 Behaviour factors evaluated for DCM cases: low, medium and high rise buildings.

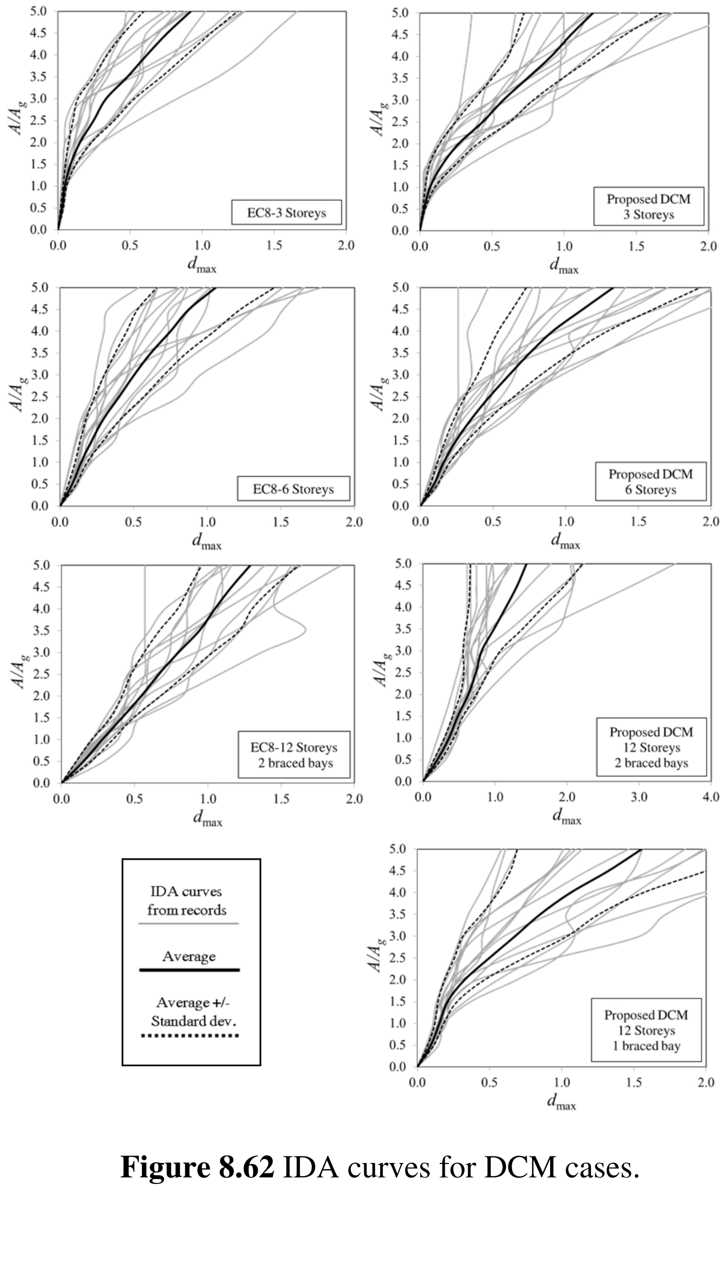

Figure 8.62 IDA curves for DCM cases.

8.3.3.2 Behaviour factor for structural buildings designed for DCH.

Figure 8.63 shows the values of behaviour factor evaluated for structures designed for high ductility class. The results obtained for the frames designed according to proposed design criteria (assuming both q=4 and q=6) are compared, by showing the average values of all the examined cases (namely including all low, medium and high rise buildings); in addition average plus and minus standard deviation values are shown to appreciate data dispersion.

Also for structures designed for DCH, the state of collapse was always determined by brace under compression attaining its axial deformation limit and buckling of column does not occur.

By observing Fig. 8.63, it is trivial to recognize that, even though frames designed assuming q=6 exhibit slightly larger deformability (See Section 8.3.2.3.1), larger behaviour factors can be obtained, with average value of 7.26) respect to the frames designed assuming q=4 with average value of 6.17).

In Fig. 8.64 the behaviour factor calculated from nonlinear dynamic analyses are shown for low, medium and high rise building separately. Similarly to what observed for structures in DCM (See Section 8.3.3.1) largest q factor values are evaluated for six-storey frames, while twelve-storey frames exhibit the poorest ductility capacity, being the dynamic response of high-rise buildings much more affected by higher vibration modes. Finally, IDA curves of structural buildings designed according to proposed criteria for DCH (namely assuming q=6) are shown in

Fig. 8.65, expressed in terms of A/A_g versus maximum roof displacement d_{max} for all three, six and twelve storey cases (in both two and one braced bay configurations) respectively.

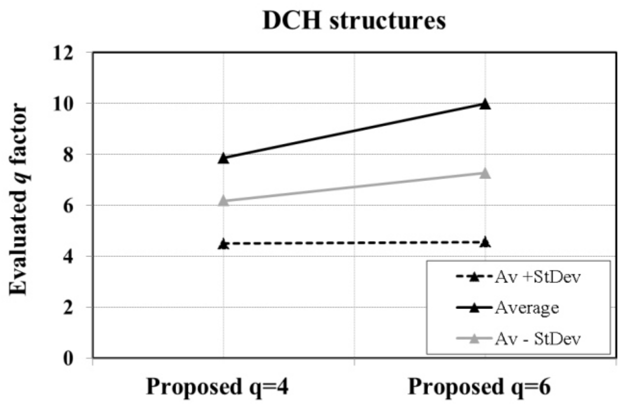

Figure 8.63 Behaviour factors evaluated for DCM cases.

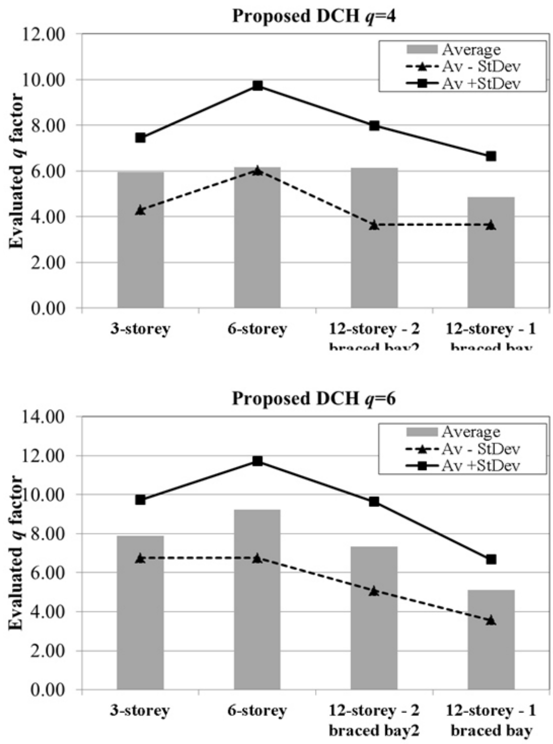

Figure 8.64 Behaviour factors evaluated for DCH cases: low, medium and high rise buildings.

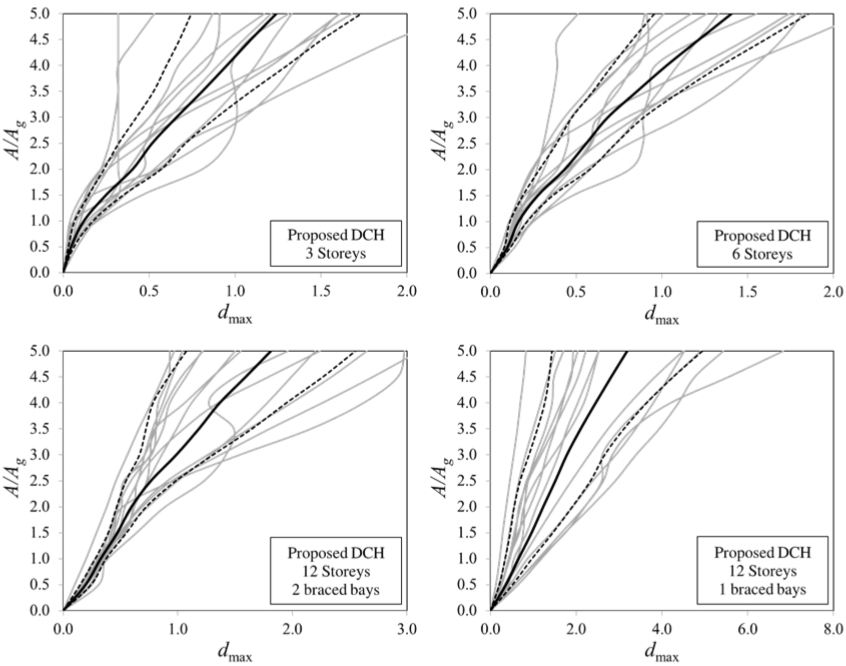

Figure 8.65 IDA curves for DCH cases.

8.4 CONCLUSIVE REMARKS

New design criteria for chevron concentrically braced frames have been proposed in this section, devoted to improve the ductility and the structural efficiency of this type of systems under severe earthquake.

Moreover, the possibility to design ductile chevron concentrically braced frames with reference to two ductility classes, namely medium ductility class (by assuming a behaviour factor equal to 4) and high ductility class (by assuming q=6) have been investigated.

An extensive numerical parametric study have been performed to validate the design assumptions and to verify the effectiveness of proposed design criteria. With this regard, low, medium and high rise residential buildings have been designed according to the proposed procedure and compared to the frames designed according to the requirement currently provided by EN-1998.

The interpretation of numerical results inferred the following remarks:

- Structures designed for DCM according to proposed design criteria exhibit good seismic performance, significantly improved respect to the frames designed according to current codes. Indeed, structures designed according to proposed procedure exhibit satisfactory lateral stiffness, with very uniform distribution of damage along the building height up to NC limit state. Moreover, significantly larger plastic engagement can be recognized in braces under tension, allowing stable and global plastic mechanism with improved dissipation capacity. As a consequence, also very small peak storey accelerations are recognized.

The evaluation of behaviour factors confirmed the effectiveness of assuming q=*4* at design stage.

- Additional requirement on beam-to-column joints belonging to the braced bays was investigated for structures designed for DCH. Results from analyses showed that having moment-resisting joins in the braced bays allows increasing the grade of redundancy and obtaining more uniform distribution of damage along the building height.
- Structures designed for DCH exhibit slightly larger deformability, but still satisfactorily performance; moreover incremental dynamic analyses showed very significant reserve of ductility with average values of behaviour factor larger than 6 in low and medium rise buildings. Slightly smaller values of behaviour factor were recognized for twelve-storey buildings, whose response is affected by higher vibration modes.
- The results from numerical analyses demonstrated that the frames design according to the proposed design rules exhibit improved seismic performance and energy dissipation capacity. Moreover, the possibility to design chevron concentrically braced frames for both medium and high ductility class seems to be confirmed.

8.5 REFERENCES

Elnashai A. S., Broderick B. M. (1996). Seismic response of composite frames II. Calculation of behaviour factors. *Engineering Structures* 18(9): 707-723.

Goggins JM, Broderick BM, Elghazouli AY, Lucas AS (2006) Behaviour of tubular steel members under cyclic axial loading. *Journal of Constructional Steel Research* 62. 121-31.

Mazzolani F.M., Piluso V. (1994) ECCS Manual on Design of Steel Structures in Seismic Zones. *Technical Committee 13 - Seismic Design*, Nº 76/1994. ECCS – European Convention for Constructional Steelwork

Salvitti L. M., Elnashai S., (1996) Evaluation of behaviour factors for RC buildings by nonlinear dynamic analyses.

Chapter IX
Conclusion

The research presented in this PhD thesis has been finalised to assess the effectiveness of current seismic design provisions and to propose new seismic design criteria for ductile and dissipative chevron concentrically braced frames. The whole activity was developed within the framework of the Working Group 2 (WG2) of CEN-TC250-SC8.

The main core of the thesis consists of a wide numerical investigations, constantly supported by a deepen theoretical study, devoted to characterize the seismic response of CCBs, by identifying the main structural parameters affecting the performance against lateral loads and to assess the effectiveness of codified design provisions with reference to both European and North-American framework of seismic standards.

New design criteria able to improve ductility and seismic performance against seismic action of chevron bracings, for next generation of Eurocodes, have been proposed and numerically validated.

In detail, the research activities have been focused on the following issues:

- The seismic design of steel buildings in the framework of EC8. With this regard, EN1998-1 (General rules, seismic actions and rules for buildings) has been examined with special focus on Section 6, which deals with the provisions for steel structures. However, in order to provide a comprehensive framework of seismic design of steel structures according to EC8, also few general aspects have been examined, covering material independent-rules as seismic performance levels, types of seismic action, and types of structural analysis.
- The framework of existing standard provisions for concentrically braced frames has been provided, by analysing the seismic design rules given by European and North-American standards. Both European and North-American (US and Canadian) codes adopt capacity design principles for CBFs, aimed at guaranteeing a similar seismic performance, namely restraining the dissipative behaviour into diagonal members and preventing the damage in the remaining structural elements. However, in order to achieve this purpose, European and North-American codes recommend some different requirements and design provisions. In the framework of European codes, the bracings in chevron configuration are expected

to provide smaller energy dissipation, respect to X-CBFs, and smaller behaviour factor are recommended. Conversely, in North-American seismic codes (CSA S16-0, 2009, FEMA P-750, 2009; AISC 341-10, 2010) analogous ductility and dissipation capacity is expected for concentrically braced frames regardless bracings configuration and the ductility class of the system is determined only by the requirements (more strict in higher ductility classes) to be met at design stage.

- The main issues related to the numerical modelling for seismic analyses of steel concentric bracings have been highlighted and examined. Physical-theory models (PTMs) of braces have been implemented using force-based (FB) elements with distributed or concentrated inelasticity and fibre discretization of the cross section; the accuracy of numerical prediction obtained using different assumptions for modelling parameters proposed in the literature have been examined, extending the analysis to further structural configurations and loading conditions. The examined parameters were the initial camber to trigger brace buckling, the type of material model, the type of force-based element, the number of integration points and the number of fibres to discretize the cross section.
- The influence of beam flexural stiffness on the seismic response of steel chevron concentrically braced frames has been investigated by performing a comprehensive numerical parametric study. In particular, the examined key parameter was the beam-to-brace stiffness ratio (K_F),

which was analysed varying both geometrical and mechanical parameters as the brace slenderness, the type of beam section (European IPE and HE hot-rolled profiles), the beam strength and stiffness, the span length, and the interstorey height.

The interpretation of numerical data showed that the stiffer is the brace-intercepted beam and the better is the achieved seismic performance and ductility capacity. Indeed, the higher the K_F value, the lower is the drift ratio for which yielding of braces under tension occurs. Moreover, results from both monotonic and cyclic analyses confirmed that for flexible beams the bracing members cannot yield in tension and at larger interstorey drift ratios both diagonal elements can be even subjected to compression.

The numerical analysis results allowed also developing empirical equations able to predict with satisfactory accuracy the brace ductility demand, also suitable as design aid to control the ductility demand of braces and the plastic mechanism at different performance levels.

- Conceptual design issues concerning the use of concentrically braced frames in seismic resistant steel building have been examined showing that, even though, chevron bracings are expected to provide smaller ductility and dissipation capacity respect to X-CBFs, they are generally more structural effective, considering the cost of fabrication and construction, the architectural advantages owing to the possibility of easily include opens (windows, doorways, etc.) in bracing bents and several geometrical features limiting the use of X-CBFs for storey height and span length dimensions commonly used in structural buildings.

In addition, the use of chevron bracings in dual-frames have been discussed. With this regard, the influence of joints behaviour on the overall response of steel multi-storey frames has been investigated and refined models, in which the moment-rotation behaviour of bolted end-plate moment resisting joints is specifically accounted for, have been developed. The proposed modelling assumption have been implemented to perform a set of non-linear dynamic analyses on few dual-frames taken as study cases in order to evaluate the influence of joints behaviour on the overall response. The numerical results suggested that semi-rigid connections can be used without affecting the overall response (provided that the deformability is correctly accounted for in the design) also reducing the constructional costs.

- The main technological aspects to be accounted for in the design of ductile concentrically braced frames have been briefly addressed, with special focus on the detailing of brace-to-brace, brace-to-beam/column, brace-to-beam mid-span and brace-to-column base connections.
- A parametric study devoted to assess the effectiveness of seismic design provisions and codified criteria given by both European (EN-1998) and North-American (AISC 341 and CSA S16-09) has been carried out. With this aim, a comprehensive set of non-linear dynamic analyses was has been performed on low, medium and high rise

residential buildings designed according to the examined codes. Moreover, further cases have been analyzed in order to evaluate the influence of some modifications applied to the requirements provided by EN-1998. Numerical results showed that EN 1998 leads to design stiffer system than those designed according to North-American codes. However, both CSA and AISC-compliant frames exhibit more uniform distribution of lateral displacements along the building height. Moreover, EC8-compliant frames show the smallest energy dissipation capacity with the most of bracing members behaving elastically in tension up to NC limit state and suffer very large storey accelerations.

All the frames, largely exceed the axial deformation capacity limitations provided by EN1998-3. Indeed, significantly larger engagement can be recognized at all the three considered limit states.

No improvement can be recognized in terms of energy dissipation capacity by applying the proposed revisions to EN-1998 design criteria; however, more uniform distribution of damage along the building height is obtained.

- New design criteria for chevron concentrically braced frames have been proposed. An extensive numerical parametric study have been performed to validate the design assumptions and to verify the effectiveness of proposed design criteria. In particular, the results of this study showed that it is possible to design ductile chevron concentrically braced frames with reference to two different performance levels and related ductility classes (namely medium ductility class by assuming a behaviour factor equal to 4 and high ductility class, by assuming q=6).

The results from numerical analyses demonstrated that the frames designed according to the proposed rules exhibit significantly improved seismic performance and energy dissipation capacity. Indeed, all the frames show satisfactory lateral stiffness with uniform distribution of deformations along the building height and plastic engagement of braces under tension noticeably increased.

The evaluation of behaviour factor confirmed that significantly larger dissipation capacity is achieved.